Spezifische Elektrolyteffekte in der Chromatographie von Biopharmazeutika

Dissertation
Judith Vajda

Darmstadt
03/13-07/16

TECHNISCHE UNIVERSITÄT DARMSTADT

Vom Fachbereich Chemie
der Technischen Universität Darmstadt

zur Erlangung des akademischen Grades eines
doctor rerum naturalium (Dr. rer. nat.)

genehmigte kumulative Dissertation

eingereicht von

Dipl. Biol. t.o. Judith Vajda
aus Böblingen

Referent: PD Dr. Egbert Müller
Ko-Referent: Prof. Dr. Jürgen Hubbuch

Tag der Einreichung: 4. Juli 2016
Tag der Disputation: 17. Oktober 2016

Darmstadt 2016

D17

"In science, the credit goes to the man who convinces the world,
not to whom the idea first occurs."

Sir Francis Darwin

Teile dieser Arbeit wurden im Rahmen des vom Bundesministerium für Bildung und Forschung geförderten Verbundprojektes „Optimierung der industriellen zellbasierten Herstellung von Influenzavakzinen (saisonal und pandemisch)“, Förderkennzeichen 0315640D, erstellt.

Danksagung

Mein herzlicher Dank gilt allen, ohne die die Anfertigung dieser Dissertation nicht möglich gewesen wäre. Er gilt insbesondere Herrn PD Dr. Egbert Müller, der nicht nur die Leitung dieser Arbeit übernommen hat, sondern auch stets ein guter Betreuer war. Die fachliche Diskussion unzähliger Ideen, Theorien und experimenteller Ergebnisse zu jedem Zeitpunkt der Arbeit trug maßgeblich zu ihrer Realisierung bei.

Bei Herrn Prof. Dr. Jürgen Hubbuch möchte ich mich besonders für die Übernahme des Zweitgutachtens und die Begleitung dieser Arbeit im Rahmen des Influenzaprojektes bedanken. Prof. Dr. Harald Kolmar und Prof. Dr. Heribert Warzecha danke ich für die Bereitschaft als Fachprüfer dieser Arbeit zu fungieren. Darüber hinaus bin ich Herrn Prof. Dr. Harald Kolmar für seine unermüdliche Hilfsbereitschaft bei der Einhaltung aller Formalien zu Dank verpflichtet. Und für interessante Seminare am Mittwochmorgen. Es gibt auch spannende Themen außerhalb des Tellerrands der Biochromatographie!

Der Tosoh Bioscience GmbH danke ich dafür, diese Doktorarbeit ermöglicht zu haben. Allen meinen Arbeitskollegen dort bin ich zu großem Dank für die kontinuierliche Unterstützung beim Spagat zwischen wissenschaftlichem Arbeiten und anderen Aufgaben verpflichtet. Im Besonderen gilt das für Dr. Werner Conze, Volker Nödinger, Achim Sprauer und Ariane Schütze. Darüber hinaus möchte ich mich bei Regina Römling, Maik Röhl, Dr. Elke Prohaska und Dr. Romain Dabre für die Diskussionsbereitschaft im Rahmen verschiedener Projekte bedanken. Den zum Praktikum oder der Abschlussarbeit bei uns im Labor tätigen Studenten, Dennis Weber, Dominik Brekel, Patrick Endres, Tanja Rathfelder, Angelika Wacker, Eva Bahret und Tim Frey danke ich für die Unterstützung bei der praktischen Umsetzung der Experimente.

Der IDT Biologika GmbH in Dessau-Roßlau danke ich für die großzügige Bereitstellung von H1N1 feedstream. Die Arbeit mit einem tatsächlichen Impfstamm stellt eine besondere Möglichkeit dar! Bei Dr. Boris Hundt bedanke ich mich für die Bereitschaft, auch im größten Stress wirklich alle Fragen zum Thema Influenza zu beantworten.

Abschließend möchte ich mich bei der großen Zahl von Menschen aus meinem privaten Umfeld bedanken, die mich über die ganze Zeit hinweg unterstützt und mir den Rücken freigehalten haben. Danke für Euer Verständnis und die Bereitschaft mit mir durch jedes Hoch und Tief dieser Arbeit zu gehen.

Publikationsliste

E. Müller, J. Vajda, D. Josic, T. Schröder, R. Dabre, T. Frey, Mixed electrolytes in hydrophobic interaction chromatography †, J. Sep. Sci. 36 (2013) 1327–1334. doi:10.1002/jssc.201200704.

J. Vajda, E. Mueller, E. Bahret, Dual salt mixtures in mixed mode chromatography with an immobilized tryptophan ligand influence the removal of aggregated monoclonal antibodies., Biotechnol. J. 9 (2014) 555–565. doi:10.1002/biot.201300230.

M. Franzreb, E. Müller, J. Vajda, Cost Estimation for Protein A Chromatography, BioProcess Inl 12(9). (2014) 44–52.

J. Vajda, W. Conze, E. Müller, Kinetic plots in aqueous size exclusion chromatography of monoclonal antibodies and virus particles., J. Chromatogr. A. 1426 (2015) 118–25. doi:10.1016/j.chroma.2015.11.057.

E. Müller, J. Vajda, Routes to improve binding capacities of affinity resins demonstrated for Protein A chromatography., J. Chromatogr. B. Analyt. Technol. Biomed. Life Sci. (2016). doi:10.1016/j.jchromb.2016.01.036.

J. Vajda, D. Weber, S. Stefaniak, B. Hundt, T. Rathfelder, E. Müller, Mono- and polyprotic buffer systems in anion exchange chromatography of influenza virus particles., J. Chromatogr. A. 1448 (2016) 73–80. doi:10.1016/j.chroma.2016.04.047.

J. Vajda, D. Weber, D. Brekel, B. Hundt, E. Müller, Size distribution analysis of influenza virus particles using size exclusion chromatography, J Chromatogr A: accepted for peer-review. (2016)

1. Poster und mündliche Konferenzbeiträge

J. Vajda, W. Conze, E. Müller, An orthogonal approach for mAb aggregate analysis. Poster auf der HPLC Konferenz in Anaheim, USA (2012).

J. Vajda, V. Pfennig, W. Conze, E. Müller, A toolbox of amino acids for mAb aggregate analysis. Poster auf der HPLC Konferenz in Amsterdam, Niederlande (2013).

J. Vajda, E. Bahret, E. Müller, Dual Salts in Mixed-Mode Chromatography and its Benefits for MAb Purification. Vortrag auf der PREP Konferenz in Boston, USA (2013).

H. Brück, J. Vajda, W. Conze, E. Müller, Analytical HIC for mAb Aggregate Analysis; How does the Salt Ion Type Influence the Selectivity?. Vortrag auf der ISPPP Konferenz in Boston, USA (2013).

W. Conze, J. Vajda, E. Müller, A Reflection on Speed and Efficiency of mAb SEC based on Kinetic Plots and Poppe Plots. Poster auf der HPLC Konferenz in New Orleans, USA (2014).

E. Müller, J. Vajda, L. Rulev, A. Wacker, Mechanistic investigations of IgG adsorption onto high capacity Protein A resins. Poster auf der Recovery Konferenz in Rostock, Deutschland (2014).

E. Müller, J. Vajda, Investigation of MAb Adsorption Phenomena to a new Protein A Resin. Vortrag auf der ISPPP Konferenz in Würzburg, Deutschland (2014).

J. Vajda, J.-F. Depoisier, R. Dabre, N. Fouque, K. Wilson, E. Müller, Development of an industrially relevant DSP platform process for a bispecific antibody, the κλ-body. Vortrag auf der HIC/RPC Konferenz in Sliema, Malta (2015)

J. Vajda, E. Müller, Binding properties of IVIG to a new type of anion exchanger at physiological pH. Poster auf der PPB Konferenz auf Sardinien, Italien (2015).

J. Vajda, W. Conze, P. Endres, E. Müller, Selectivity of a new type of preparative anion exchange resin for glycosylated proteins. Poster auf der PREP Konferenz in Philadelphia, USA (2015)

2. Zusammenfassung

Biopharmazeutika repräsentieren eine wachsende Gruppe von Arzneistoffen. Ihre Strukturen sind im Vergleich zu klassischen Pharmazeutika komplexer. Um die Verfügbarkeit von Biopharmazeutika für die Masse der Bevölkerung zu gewährleisten, sind kostengünstige, flexibel skalierbare Herstellungsverfahren unabdingbar. Die Produktion von Biopharmazeutika in Zellkultur leistet einen großen Beitrag hierzu, schafft jedoch auch neue Voraussetzungen für darauf die folgenden Aufreinigungsverfahren. Die Biochromatographie ist fester Bestandteil vieler Aufreinigungsverfahren. Während für die mAb Aufreinigung Chromatographie-Plattformen etabliert sind, stellt die Aufreinigung von Viruspartikeln aus Zellkultur eine neue Herausforderung dar. Das Spektrum der Kontaminanten in Zellkultur unterscheidet sich von dem in Eiern produziertem Virusmaterial. Die flüssige Phase in der Biochromatographie birgt dabei ein häufig vernachlässigtes Potential für die Optimierung von Plattformprozessen zur mAb- oder Viruspartikelaufreinigung. Hydrophobe Wechselwirkungen können durch verschiedene Salze und Dualsalze moduliert werden. Sie spielen in der hydrophoben Interaktionschromatographie, der ‚Mixed Mode' Chromatographie mit hydrophoben Kationenaustauschern und der Affinitätschromatographie eine Rolle. Die Kapazität für mAbs kann durch Optimierung des Adsorptionspuffers für alle genannten Modi um mindestens 30 % gesteigert werden. Ökonomisch am bedeutsamsten dürfte die Erhöhung der Bindekapazität eines hexameren Protein A Liganden um 100 % für einen mAb sein. Neben der Kapazität beeinflussen Elektrolyte die Selektivität in der Biochromatographie. Ein Gemisch aus Natriumchlorid und Natriumcitrat ermöglicht die Auflösung eines speziellen mAb-Monomers von seinen Aggregaten und weniger hydroben Isoformen auf einer Butyl-Säule, was in einem Standard Ammoniumsulfat-Gradienten nicht realisiert werden kann. Insbesondere die Verwendung von Dualsalzen steigert den erforderlichen Prozessentwicklungsaufwand. Miniaturisierte Parallelchromatographie erlaubt das deutlich schnellere Sichten eines großen Versuchsraumes bei vergleichsweise geringem Probenverbrauch. Dies ermöglicht eine umfassende und frühzeitige Methodenentwicklung. Ein weiterer Engpass in der Methodenentwicklung ist die begleitende Analytik, insbesondere in Hinblick auf Vakzine. Die Freigabe von Vakzinen basiert häufig auf Aktivitätstests. Der Hemagglutinations-Test ist weit verbreitet zur Analyse von Influenzavakzinen. Er beruht auf der Agglutination von roten Blutzellen und Viruspartikeln. Die Massekonzentration des Virus wird aus dem dazu erforderlichen, geschätzten Verhältnis von Erythrozyten zu Viruspartikeln berechnet. Der Test ist mit großen Standardabweichungen (bis zu einer log-Stufe) sowie hohem Arbeits- und Zeitaufwand verbunden. Im Rahmen dieser Dissertation wird das Potential untersucht, analytische Größenausschlusschromatographie als zusätzliche oder substituierende Analytik für Viruspartikel einzusetzen. Die Methode wird mit dem pandemischen Influenza A H1N1v 5258 Impfstamm, sowie den beiden Laborstämmen H1N1 Puerto Rico/8/34 und H3N2 Aichi/2/68 evaluiert. H1N1v 5258 wird im industriellen Maßstab in Zellkultur vermehrt. Die Proben der Laborstämme sind aufgereinigt und stammen aus embryonierten Hühnereiern. Reproduzierbare und hinreichend vollständige Wiederfindungsraten werden für 100 mM Natriumphosphat-Puffer, pH 7.0 mit Zusatz von 200 mM Natriumchlorid erzielt. Die Retention aller Virusproben stimmt überein, was die Universalität der Methode bestätigt. Die Hemagglutinations-Analyse aller Fraktionen der analytischen Größenausschlusschromatographie ergibt, dass ungefähr 50 % der Virusaktivität durch Virusfragmente verursacht wird. Dies bedeutet, dass die gängige Massekonzentrationsberechnung falsch positive Ergebnisse erzielt. Analytische Größenausschlusschromatographie als ergänzende Analytik in Forschung, Entwicklung und Qualitätskontrolle erscheint daher empfehlenswert. In der Prozessentwicklung ermöglicht die gezeigte Methode zur analytischen Größenausschlusschromatographie die Quantifizierung ganzer Viruspartikel in 20 Minuten. Entgegen bisheriger Annahmen sind vergleichsweise hohe Flussraten in der Größenausschlusschromatographie von Influenzaviruspartikeln förderlich. Niedrige Flüsse und lange Verweilzeiten beeinflussen die Polydispersität der Viruspartikel Proben. Die Stabilität der Viruspartikel wird auch durch verschiedene Elektrolyte beeinflusst. Natriumphosphat erweist sich als wirkungsvoll, insbesondere während der Anionenaustauschchromatographie mit einem Polyamin-Liganden. Die Kapazität des Polyamin-Anionenaustauschers ist je nach Pufferbedingungen bis zu 6,4-mal höher als für ein Harz mit immobilisiertem, quaternärem Ammonium-Liganden. Natriumphosphat-Puffer wirkt sich positiv auf die Bindekapazitäten beider Harze für Viruspartikel aus, was dem Verhalten von Proteinen widerspricht. Möglicherweise beruht diese Kapazitätserhöhung auf einem Pseudoaffinitätsmechanismus des Polyamin-Liganden mit dem viralen Protonenkanal M2. Um eine Wiederfindung des Viruspartikels vom Polyamin-Adsorber zu erzielen, ist die Verwendung von Natriumphosphat-Puffer gegenüber Tris/HCl-Puffer und Natriumchlorid zur Elution vorteilhaft. Andere polyvalente Anionen wie Citrat wirken sich ebenfalls positiv auf die Wiederfindung der Viruspartikel aus. Polyvalente Anionen beeinflussen die erzielte DNA-Abreicherung jedoch nachteilig. Die durch polyvalente Ionen verursachten Effekte hinsichtlich der Anionenaustauschchromatographie von

Influenzaviruspartikeln beruhen wahrscheinlich auf der höheren Avidität, der vergleichsweise höheren eingetragenen Ionenstärke und der Quervernetzung der Polyamin-Liganden.

3. Abstract

Biopharmaceuticals represent a growing class of drug substances. Their structures are more complex in comparison to classical pharmaceuticals. Cost-effective and flexibly scalable production processes are indispensable to ensure availability for a majority of the population. Production of biopharmaceuticals in cell culture contributes immensely to this. However, it also creates new conditions for the subsequent purification processes. Biochromatography is an inherent component of many downstream processes. While chromatography platforms for mAb purification are well established, purification of virus particles from cell culture represents a new challenge. The cell culture derived contaminant spectrum differs from egg produced virus material. The liquid phase in biochromatography holds a frequently neglected potential in optimization of platform processes for mAb and virus particle purification. Hydrophobic interactions can be modulated by different salts and dual salt mixtures. They play a role in hydrophobic interaction chromatography, mixed mode chromatography with hydrophobic cation exchangers, and affinity chromatography. Capacity of all mentioned modes for mAb can be increased by at least 30 %, optimizing the adsorption buffer. The increase of binding capacity of a hexameric protein A ligand for a mAb by 100 % might be the economically most significant achievement. Besides capacity, different electrolytes affect selectivity of biochromatography. A mixture of sodium chloride and sodium citrate allows for resolution of a particular mAb monomer from its aggregates and less hydrophobic isoforms on a butyl column, which cannot be realized in a standard ammonium sulfate gradient. Especially, the use of dual salts increases the efforts required in process development. Miniaturized parallel chromatography enables significantly faster screening of a large design space at comparatively low sample consumption. This facilitates a comprehensive and early method development. Another bottleneck in method development is the accompanying analytics, in particular regarding vaccines. Release of vaccines is frequently based on activity assays. The hemagglutination assay is widely applied for the analysis of influenza vaccines. It is based on agglutination of red blood cells with virus particles. The mass concentration of viruses is calculated using therefore required, estimated ratio of erythrocytes to virus particles. The assay is afflicted with high standard deviations (up to one order of magnitude), and excessive work and time. In the context of this thesis, the potential of analytical size exclusion chromatography as an additional or substituting analysis has been investigated for virus particles. The method is evaluated with the pandemic influenza A H1N1v 5258 vaccine strain, as well as with the two lab strains H1N1 Puerto Rico/8/34 and H3N2 Aichi/2/68. H1N1 5258 is propagated in cell culture on industrial scale. Samples of the two laboratory strains originate from embryonated chicken eggs and are purified. Reproducible and sufficiently complete recoveries are achieved in 100 mM sodium phosphate buffer, pH 7.0 with addition of 200 mM sodium chloride. Retention of all virus samples coincides, which confirms the universality of the method. Hemagglutination analysis of all fractions from size exclusion chromatography indicates that roughly 50 % of the virus activity is based on virus fragments. This means that the commonly applied mass concentration calculation leads to false positive results. Hence, analytical size exclusion chromatography seems advisable as a complementary analysis in research, development, and quality control. The presented analytical size exclusion chromatography method provides quantification of whole virus particles in process development within 20 minutes. In contrast to previous assumptions, comparatively high flow rates in size exclusion chromatography of influenza virus particles are beneficial. Low flow rates and extended residence times affect the polydispersity of the virus particle samples. Stability of virus particles is further impacted by several electrolytes. Sodium phosphate proofs to be efficient, particularly during anion exchange chromatography with a polyamine ligand. Capacity of the polyamine anion exchanger is up to 6.4 times higher, compared to a resin with an immobilized quaternary ammonium ligand and depending on the conditions. Sodium phosphate buffer supports binding capacity of both resins for virus particles, which contradicts the behavior of proteins. This might be due to a pseudo affinity mechanism, involving the polyamine ligand and the viral proton channel M2. Sodium phosphate buffer is beneficial for achieving virus recovery from the polyamine adsorber, compared to Tris/HCl buffer and sodium chloride for elution. Other polyvalent anions, such as citrate, improve virus particle recovery, as well. However, polyvalent anions adversely influence DNA removal. Effects of polyvalent ions regarding anion exchange chromatography of influenza virus particles are probably due to a higher avidity, a comparatively greater contribution to ionic strength, and cross-linking of the polyamine ligand.

4. Inhaltsverzeichnis

5. Einführung

Biopharmazeutika sind biologische, medizinische Wirkstoffe, die vielfältigen Einsatz in der Therapie schwerwiegender Krankheiten finden. Sie werden mit Hilfe von (gentechnisch veränderten) Zellen oder Organismen hergestellt. Schätzungen zur Folge wird der weltweite Umsatz mit verschreibungspflichtigen Pharmazeutika bei einer angenommenen durchschnittlichen jährlichen Wachstumsrate von 4.8% im Jahr 2020 etwa 1 Billion US-$ betragen [1]. Etwa 46 % des Verkaufsvolumens der 100 umsatzstärksten pharmazeutischen Produkte dürfte dann durch nur 42 biopharmazeutische Produkte erzielt werden [1]. Biopharmazeutika bilden eine diverse Gruppe: Peptide, (Glyco-) Proteine und Ribonucleinsäuren. Die Produktion der Biopharmaka erfolgt über die zelleigenen Synthesewege. Die biotechnologische Herstellung ermöglicht die Ausbildung komplexer Strukturen wie Viruspartikel. Wichtige biopharmazeutische Produkte sind zum Beispiel Insulin, virale Impfstoffe und monoklonale Antikörper (engl. monoclonal antibodies, mAb). 2015 betrugen allein die Einnahmen mit Humira®, einem mAb-Präparat, 14 Mrd. US-$ [2]. Dagegen lag der weltweite Umsatz des gesamten Influenzavakzin-Marktes in diesem Zeitraum nach Schätzungen des Pharmaherstellers CSL bei vergleichsweise bescheidenen 4 Mrd. US-$ [3]. Es ist jedoch eine steigende wirtschaftliche Bedeutung von Vakzinen gegenüber anderen (Bio-)Pharmazeutika zu erwarten. Die Weltgesundheitsorganisation (WHO) prognostiziert jährliche Wachstumsraten von 10 – 15 % für den gesamten Vakzin-Sektor bis 2018 [4]. Ecker et al. erwarten im gleichen Zeitraum eine durchschnittliche jährliche Wachstumsrate von 8 % für mAbs [5]. Infolgedessen scheinen Biopharmazeutika, insbesondere Vakzine, ein interessanter Wachstumsmarkt mit guten Chancen zu sein.

5.1. Monoklonale Antikörper

Verschiedene Immunglobulin (Ig) Typen und Subtypen sind als Arzneistoffe zugelassen. Neben dem hauptsächlich verwendeten IgG1 und IgG2 werden IgM, IgA und IgE in Therapie und Diagnostik eingesetzt. Dabei wird der Begriff mAb oft einem monoklonalen IgG gleichgesetzt. IgG besteht aus je zwei über Disulfidbrücken verknüpfte, 25 kDa leichte und 50 kDa schwere Ketten. Die schweren Ketten sind in der Gelenkregion ebenfalls über Disulfidbrücken miteinander verknüpft und glycosyliert. Der Fc-Teil wird durch die zusammengelagerten, schweren Ketten gebildet. Die variablen Domänen jeder Kette enthalten in einem regulären IgG Molekül je drei komplementaritätsbestimmende Regionen (engl. complimentary determining region, CDR). Der schematische Aufbau eines IgG ist in Abbildung 1dargestellt.

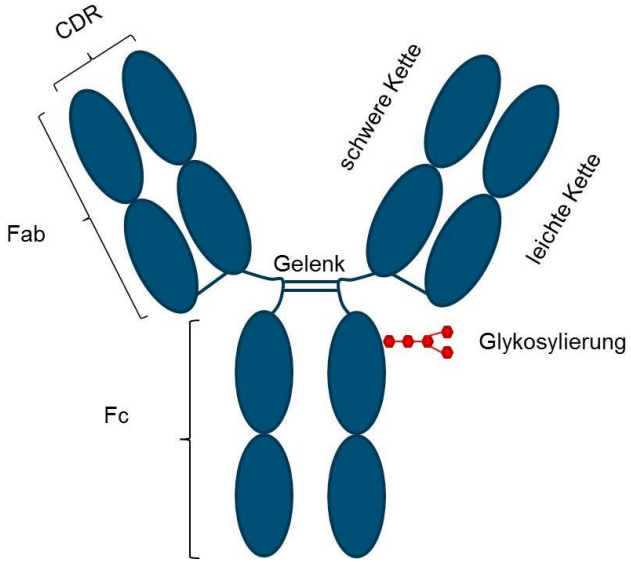

Abbildung 1: Schematische Darstellung eines IgG1. Leichte und schwere Kette, sowie die beiden schweren Ketten sind über Disulfidbrücken miteinander verbunden.

Seit der Entwicklung der Hybridoma-Technologie [6] durch Köhler und Mihlstein ermöglicht eine Reihe weiterer Entwicklungen die Produktion von mAbs im industriellen Maßstab bei bestmöglicher Patientensicherheit. MAbs stammen im Gegensatz zu polyklonalen Antikörpern von einem gemeinsamen

Zellklon ab. Ein Antikörper produzierender B-Zell Lymphozyt wird mit einer Myelomzelle fusioniert. Die entstehende, immortalisierte Zelllinie exprimiert Antikörper. Ursprünglich wurden murine mAbs entwickelt, die bei längerfristiger Anwendung im Menschen Immunreaktionen hervorrufen können. Aus diesem Grund wurde zunächst der Anteil des Mausproteins reduziert und in chimären mAbs mit einem humanen Fc-Teil kombiniert. Solche chimären mAbs können weiterhin Immunreaktionen hervorrufen, was als Antrieb zur Entwicklung von humanisierten und humanen mAbs diente. Humanisierte mAbs beinhalten nur noch einige Aminosäuren murinen Ursprungs in der variablen Domäne des mAbs. Die beste therapeutische Verträglichkeit besteht jedoch für vollständig humane mAbs. Eine schematische Grafik von murinem, chimärem, humanisiertem und humanem IgG ist in Abbildung 2 dargestellt. Die Herkunft des mAbs kann über die Nomenklatur ausgedrückt werden. Der seit 1986 zugelassene Muromonab-CD3, der unter dem Handelsnamen Orthoclone OKT3® vertrieben wird, ist ein muriner mAb. Adalimumab, das TNF-α neutralisierende Humira®, ist ein humaner mAb, der 2002 zugelassen wurde. Bis zu 63 % der behandelten Patienten entwickeln eine Immunreaktion gegen Orthoclone, wohingegen nur 12 % der mit Adalimumab medikamentierten Patienten eine Immunantwort entwickeln [7][8].

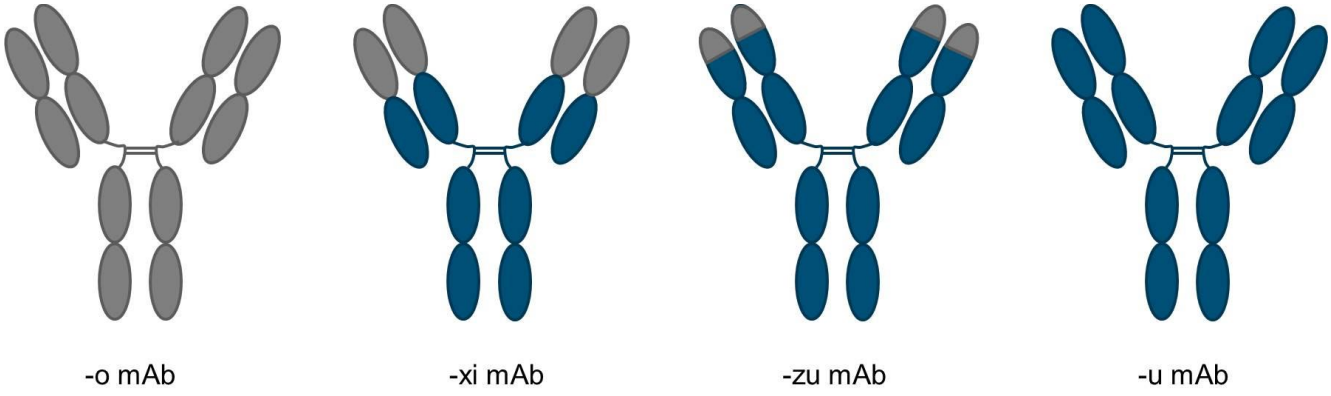

Abbildung 2: Murines, chimäres, humanisiertes und humanes IgG. Der murine Proteinanteil ist grau eingefärbt, der Humane blau. MAbs aus diesen vier Kategorien beinhalten die dargestellten Endungen in ihrem Namen. Der Handelsname kann von diesem Muster abweichen.

Monoklonales Immunglobulin G wird im industriellen Maßstab oft in Zellen aus Ovarien des Chinesischen Hamsters *Cricetulus griseus* (engl. Chinese hamster ovary cells, CHO-Zellen) exprimiert. CHO-Zellen erlauben eine über Monate hinweg stabile und hohe Expression von mAbs [9]. Zelllinienentwicklung und Fermentation werden unter dem Begriff des „Upstream Processings" zusammengefasst. Zum darauffolgenden „Downstream Processing" gehören die primäre Ernte des sekretierten mAbs, die Aufreinigung und die Formulierung des Endpräparates. Durch die Verwendung moderner Zellkulturtechnologie sind mAb-Konzentrationen höher als 5 g/L keine Besonderheit mehr [10]. Dadurch lastet ein höherer Optimierungsdruck auf den Aufreinigungsschritten. Bis zu 80 % der Herstellungskosten für einen mAb entfallen auf das Downstream Processing [11][12]. Bei der primären Ernte werden Zellfragmente durch Zentrifugation und Tiefenfiltration abgetrennt. Die weitere Aufreinigung basiert häufig auf 3 Chromatographieschritten, die als Plattformen aufgebaut sind. Protein A Chromatographie steht als elegante „Capturing" Methode zur Entfernung eines Großteils der prozessinduzierten Verunreinigungen zur Verfügung. Die erreichten Produktreinheiten nach Protein A sind größer als 98 %, wobei insbesondere Wasser, Wirtszellproteine und DNA entfernt werden [10]. Die potentielle Virusabreicherung durch Protein A liegt zwischen 1-3.5 log-Stufen [13][14]. Das aufkonzentrierte Produkt wird nach einer sauren Inkubation zur Inaktivierung behüllter Viren weiter aufgereinigt. Aggregations- und Fragmentationsprodukte des mAbs werden mit Kationenaustauschchromatographie (CEX), hydrophober Interaktionschromatographie (HIC) oder Mixed Mode Chromatographie (MXC) abgetrennt. Der darauffolgende Chromatographieschritt zur Entfernung von verbleibender Wirtszell-DNA, Endotoxinen, Wirtszellproteinen und ausgewaschenem Protein A basiert oft auf Anionenaustauschchromatographie (AEX). Die verschiedenen Chromatographiemodi können sowohl im Binde- und Elutionsmodus, als auch im Durchfluss betrieben werden. Mit Ausnahme der AEX, erniedrigen Durchfluss Schritte jedoch die Virusabreicherung des Gesamtprozesses [15]. Vor der Formulierung erfolgt ein Nanofiltrationsschritt um die Virussicherheit zu gewährleisten. Alternative Prozessvarianten kombinieren CEX und HIC, wie zum Beispiel in Abbildung 3 dargestellt.

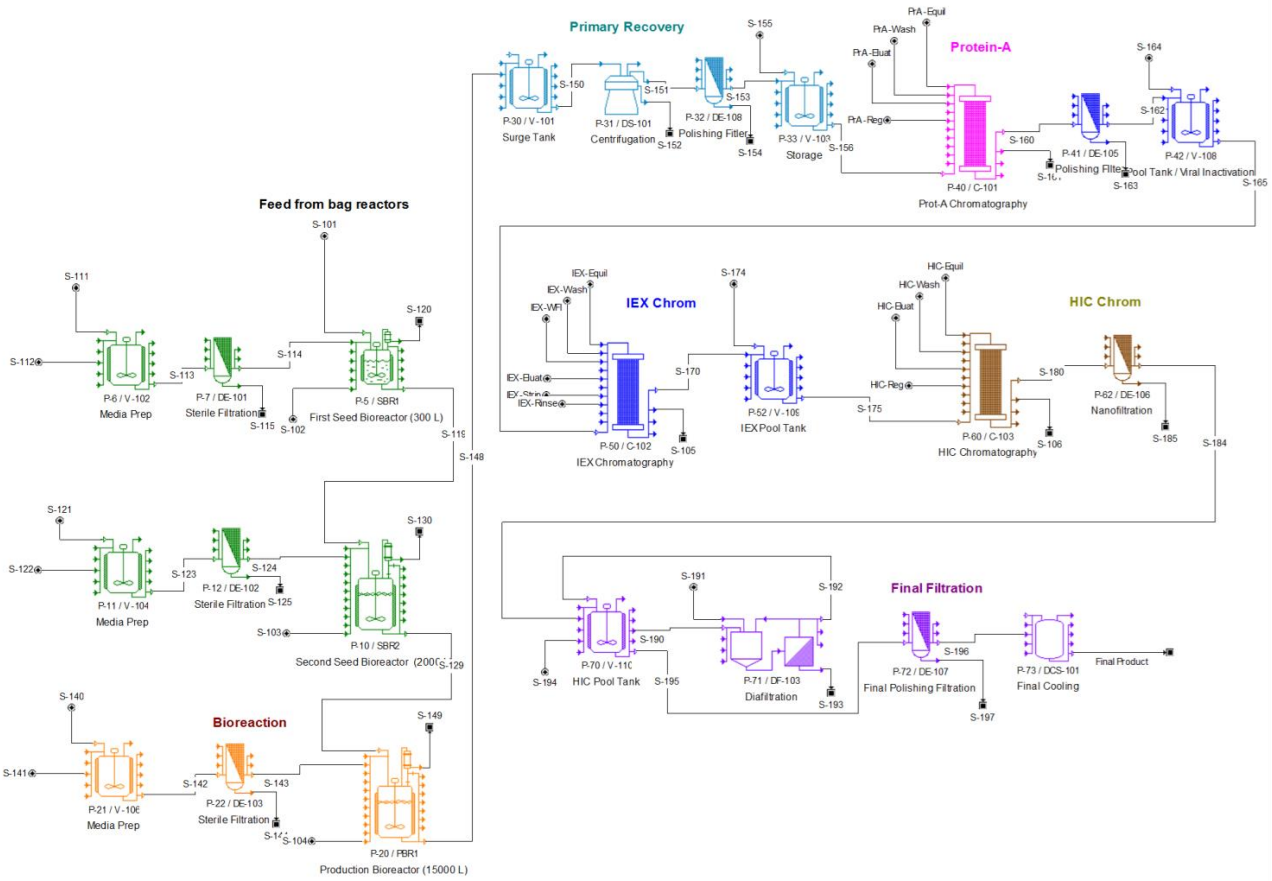

Abbildung 3: Flussschema eines mAb Produktionsprozesses. Nach der Fermentation im Bioreaktor wird der mAb geerntet. Nach Klärfiltration und Zentrifugation wird ein Großteil der Verunreinigungen durch Protein A Chormatographie abgetrennt. Bei einem Standardplattform-Prozess folgen zwei weitere Chromatographieschritte zur weiteren Reinigung. Insbesondere die Abreicherung von produktabgeleiteten Kontaminanten, die einen F_c-Teil enthalten, obliegt diesen Schritten. Grafik wurde erstellt mit SuperPro Designer®, Itelligen Inc. [16]. ©2014 BioProcess International, genehmigter Nachdruck.

Die Entfernung von mAb-Aggregaten kann sich als problematisch erweisen. Aggregationsprodukte sind ebenso vielfältig wie die Bedingungen, die zur mAb-Aggregation führen. Aggregation kann kovalent oder nicht-kovalent, reversibel oder irreversibel sein [17]. Verschiedene Faktoren begünstigen die Aggregation. Zu diesen gehören unter anderem Edelstahloberflächen [18], Flüssigkeits-Luft Interphasen [19], Scherkräfte und saure Inkubation [20], Sorption an und Desorption von Protein A [21], sowie Frier- und Tauprozesse [22]. Dabei bilden sich Dimere und Multimere mit höherem Molekulargewicht. Aggregate müssen während des Aufreinigungsprozesses entfernt werden, da sie potentiell immunogen sind und die Aktivität des Biopharmazeutikums verändern können [20]. Die geforderte Obergrenze für den Aggregatgehalt liegt bei < 1 % und die Einhaltung dieses Grenzwertes bestimmt in vielen Fällen über die Implementation eines dritten Chromatographieschrittes [23]. Die Abreicherung von Aggregaten kann verhältnismäßig einfach durch Größenausschlusschromatographie (SEC) bewerkstelligt werden. Dieses Verfahren ist jedoch aufgrund der niedrigen Beladungen wenig produktiv [23][24]. Effizientere Alternativen bieten CEX, HIC und MXC. Eine ladungsdiskriminierende Trennung von mAb-Monomer und Aggregaten, wie sie in der CEX erfolgt, kann sich anspruchsvoll gestalten. Die isoelektrischen Punkte von Monomer und Aggregaten sind mitunter sehr ähnlich. In solchen Fällen kann die Aggregatentfernung durch HIC vorgenommen werden. Aggregate erfahren eine höhere Retention an HIC Phasen, als das jeweilige mAb-Monomer. Dynamische Bindekapazitäten von stationären Phasen zur HIC sind niedriger, als die Kapazitäten von oberflächenmodifizierten Kationenaustauschern. Pfropfpolymerisation und andere Oberflächenmodifikationen erhöhen die Hydrophilie der stationären Phase zum Ionenaustausch und erleichtern den Massentransfer [25][26]. Eine Erhöhung der Hydrophilie widerspricht dem Sorptionsprozess der HIC und wirkt sich negativ auf die Kapazität solcher Medien aus. Um Hydrophobizität weiterhin als Selektivitätskriterium nutzen zu können und gleichzeitig hohe Bindekapazitäten zu erzielen, werden seit einigen Jahren vermehrt hydrophobe Kationenaustauscher zur Aggregatentfernung eingesetzt [27].

5.2. Influenza

Influenza A, B und C Viren gehören zur Familie der *Orthomyxoviridae*. Seit kurzem wird die Existenz eines Influenza D Taxons [28] vermutet. Influenza A und ein Influenza B Virusstamm sind humanpathogen [29]. Es handelt sich um behüllte Einzelstrang-RNA Viren, die ca. 100 nm groß sind. Ihre Replikation benötigt keine reverse Transkription, wie zum Beispiel beim HI-Virus. Die RNA von Influenza liegt unterteilt in acht Segmenten vor, was die Rekombination bei Mehrfachinfektionen erleichtert [30]. Abbildung 4 zeigt eine schematische Darstellung eines Influenza A Viruspartikels. Die Oberflächenproteine Hämagglutinin und Neuraminidase sind in der Membran verankert. Das Transmembranprotein M2 dient zur Regulation des pH-Wertes. Das Matrixprotein M1 kleidet die Membran von innen aus. Die drei Polymeraseproteine PA, PB1 und PB2 sitzen endständig auf dem Ribonucleoprotein.

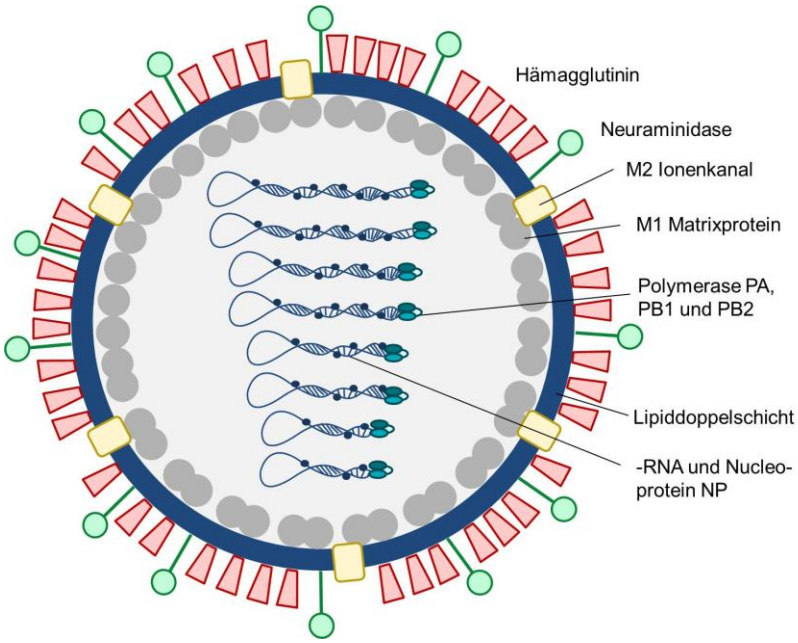

Abbildung 4: Influenza A Viruspartikel. Die Oberflächenproteine Hämagglutinin und Neuraminidase sind in der Lipidhülle verankert, die von innen mit dem Matrixprotein M1 ausgekleidet ist. Der Ionenkanal M2 ist ein Transmembranprotein. Die Polymerase Proteine PA, PB1 und PB2 sitzen endständig auf den acht Einzelstrang RNA Segmenten, die mit Nucleoproteinen besetzt sind.

Influenza A Viren können nicht nur Menschen infizieren, sondern auch andere Säugetierspezies, wie z.B. echte Schweine (*Suidae*), oder aviane Arten [31]. Verschiedene Faktoren begünstigen die Ausbreitung und Veränderung von Influenza. Zu diesen gehören die Massentierhaltung, sehr enger Kontakt des Menschen mit den betroffenen, domestizierten und wilden Tierarten und mangelnde Hygiene. Dies führt dazu, dass vor allem in den Schwellenländern Asiens aber auch Afrikas sich immer wieder neue Virusstämme bilden, deren pandemische oder epidemische Verbreitung sich zu einer globalen Bedrohung ausbilden kann [32][33][34][35].

Die Wahl des zur Vermehrung notwendigen, spezifischen Wirtszellorganismus eines Influenza A Virus wird hauptsächlich von Hemagglutinin bestimmt [35]. Innerhalb der Nomenklatur für die verschiedenen Influenza A Virustypen wird Hemagglutinin als H abgekürzt und mit der jeweiligen Nummer eines der 17 Hemagglutinin Typen bezeichnet. Pro-Hemagglutinin beinhaltet eine monobasische Spaltungsstelle (ein Arginin). Es muss nach der Transkription in der Wirtszelle durch extrazelluläre Serin Proteasen in zwei Untereinheiten gespalten werden, die sich dann zu einem Homotrimer anordnen. Darüber hinaus gibt es Hemagglutinine, die über eine polybasische Spaltungsstelle verfügen. Die Spaltung des Hemagglutinin Pro-Proteins mit polybasischen Spaltungsstellen kann durch intrazelluläre, ubiquitäre subtilisinartige Proteasen erfolgen. Solche Virusstämme haben eine erhöhte Pathogenität [33][35]. Hemagglutinin bindet Sialinsäure auf den Wirtszellen. Humane Sialinsäure ist größtenteils α-2,6 glycosidisch gebunden, wohingegen die Sialinsäuren auf der Oberfläche von avianen Epithelzellen des Darms bevorzugt α-2,3 glycosidisch gebunden

sind. Dies stellt eine Infektions-Barriere für aviane und humane Influenzaviren dar [34][32][33][35]. Die meisten der kürzlich humanadaptierten H5, H7 und H9 Subtypen tragen Mutationen in der Bindungsstelle für Sialinsäure [35]. Hauptinfektionsort im Menschen ist der respiratorische Trakt, während bei Vögeln hauptsächlich das Darmepithel betroffen ist. Tracheale Epithelzellen in Schweinen tragen α-2,3 und α-2,6 glycosidisch gebundene Sialinsäure, was den speziesübergreifenden Antigen-Shift vereinfacht [36][32][33]. Nachdem das Virus an die Oberfläche der Zelle gebunden hat, wird es von der Zelle durch Endozytose aufgenommen. Auf dem Weg zum Lysosom wird das Endosom angesäuert, was zu einer Konformationsänderung des Hemagglutinins führt. Ein Teil des Hemagglutinin Proteins verankert sich in der endosomalen Membran, was die Fusion der Virusmembran mit der endosomalen Membran einleitet. Die Virus-RNA wird ins Zytosol entlassen und gelangt in den Nucleus. Dort findet die Polymeristation in +RNA statt, auf deren Grundlage die Transkription der Virusproteine basiert [35].

Die Konformationsänderung des Hemagglutinins ist pH-abhängig und ist neben der Spezifität des Hemagglutinins entscheidend für die Pathogenität des Viruses. Der dafür notwendige pH liegt zwischen 5.0 und 6.0. Erfolgt die Konformationsänderung schon durch eine verhältnismäßig geringe Erhöhung der H^+ Konzentration, so ist das Virus weniger stabil in Gewässern, die als einer der Infektionsorte, hauptsächlich für aviane Stämme gelten [32]. Ein zu wenig pH-empfindliches Hemagglutinin kann die Fusion von Virusmembran und endosomaler Membran nicht vermitteln, sodass es zum lysosomalen Abbau des Viruspartikels kommt. Abbildung 5 zeigt eine vereinfachte Darstellung des Replikationszykluses von Influenza A.

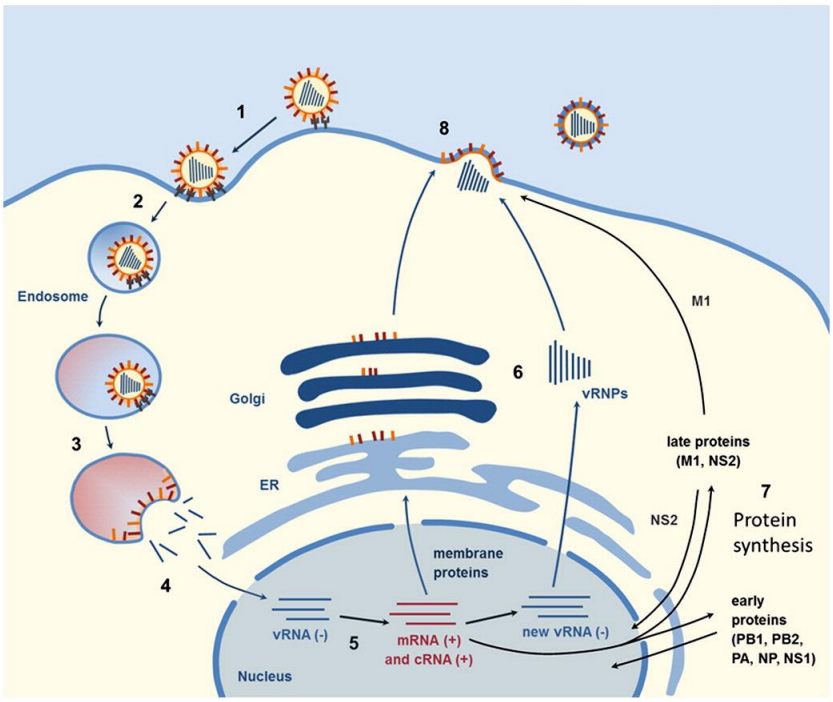

Abbildung 5: Replikation eines Influenza A Virus. (1) Das Virus dockt über Hemagglutinin an die Zelle an und (2) wird endosomal aufgenommen. (3) Auf dem Weg zum Lysosom wird das Vesikel angesäuert, die Membranen fusionieren und (4) die virale RNA gelangt über das Zytosol in den Nukleus. (5) Nach der Transkription in mRNA werden (6) Hämagglutinin und Neuraminidase am endoplasmatischen Reticulum translatiert. (7) Die viralen Polymerasen und das Nucleoprotein werden zytosolisch translatiert und polymerisieren virale RNA. M1 wird zeitlich versetzt im Zytosol translatiert. (8) Ein neues Viruspartikel schnürt sich ab, das sich durch Neuraminidase von der Zelle lösen kann. Nachdruck aus Biochimica et Biophysica Acta, 1838(4), Mair et al., Receptor binding and pH stability — How influenza A virus hemagglutinin affects host-specific virus infection, Seite 1156. © 2013 mit Genehmigung von Elsevier B.V.

Aufgrund der durch Hemagglutinin vermittelten pH-Sensitivität des Viruspartikels kommt einem weiteren Protein, dem M2 Protein, eine zentrale Bedeutung bei der Stabilisierung der Viruspartikel zu. M2 ist ein Transmembranprotein und ein Ionenkanal, der den Protonenflux über die Virusmembran reguliert [37]. In physiologischer Umgebung lagert M2 Kalium- oder Natriumionen ein. Polyamine wie Spermidin binden mit hoher Affinität an M2 und inhibieren den Ionenkanal. In Anwesenheit von physiologischen Natriumkonzentrationen, liegt die notwendige Polyaminkonzentration bei 100 – 500 µM, in Abwesenheit von

Natriumionen sinkt die benötigte Polyaminkonzentration um den Faktor 10^2-10^3 [38]. Eine Blockade des M2 Kanals kann therapeutisch genutzt werden: Amantadin oder 1-Adamantanamin ist ein mit einer Aminogruppe substituiertes Cycloalkan, das als Virostatikum bei Influenza A Infektionen eingesetzt werden kann [32]. Mutationen im M2-Gen lassen die Therapie mit Amantadinen unwirksam werden: Influenza A/Puerto Rico/8/34 (H1N1) ist Amantadin resistent [39]. Neuraminidasehemmer wie Oseltamivir®, die das Ablösen der Viruspartikel von der Zelle, das sogenannte „Budding" unterdrücken, haben eine breitere Wirksamkeit. Sie wirken gegen Influenza A und B und nur wenige Stämme haben dagegen Resistenzen entwickelt [32].

In der vorliegenden Arbeit werden drei verschiedene Influenza A Stämme verwendet: H1N1v 5258, H1N1 Puerto Rico/8/34 und H3N2 Aichi/2/68. Ersterer wurde in Madin-Darby Rindernieren (engl. Madin-Darby Bovine Kidney, MDBK) Zellen vermehrt [40] und mit β-Propriolacton inaktiviert. H1N1 Puerto Rico/8/34 und H3N2 Aichi/2/68 sind aus einer Produktion in embryonierten Hühnereiern stammende Laborstämme und sind durch Formalin inaktiviert.

5.2.1. Virale Impfstoffe

Virale Impfstoffe bilden eine diverse Gruppe innerhalb der Biopharmazeutika. Die Entdeckung einer Impfwirkung gegen Pocken im Jahr 1796 durch die Immunisierung mit Kuhpocken wird heute oft Edward Jenner zugeschrieben. Tatsächlich war Jenner der Erste, der die Immunisierung durch Impfung wissenschaftlich untersucht und beschrieben hat [41]. Die Immunisierung durch Variolation wurde in Afrika und Asien allerdings schon lange praktiziert, bevor sie im 18. Jahrhundert in Europa bekannt wurde [42]. Impfungen stellen auch heute eine wichtige Möglichkeit zur Eindämmung viral verursachter Krankheiten dar [43]. Eine Influenzainfektion beispielsweise kann am effektivsten durch Impfung verhindert werden [44]. Neben der saisonalen Influenza stellen pandemisch auftretende Influenzawellen, wie zuletzt die landläufig als Schweinegrippe bezeichnete Infektion mit H1N1, eine Gefahr dar.

Neben der Verwendung ähnlicher, für den Menschen weniger gefährlicherer Viren [42] zur Impfung können attenuierte Viruspartikel [45], inaktivierte Viruspartikel [46], virale Partikel ohne Erbgut (sogenannte „virus like particles", VLP) [47] oder einzelne Virusproteine zur Impfung verwendet werden. Letztere können entweder als Spaltvakzin [48] oder als eine Kombination rekombinant produzierter Proteine [49] dargereicht werden. Konjugation von Antigenen an ein Trägerprotein kann die Wirksamkeit verbessern [50]. DNA-Impfstoffe bilden eine weitere Gruppe, bei der die Impfantigene erst durch die Zellen des Impfkandidaten translatiert werden [51]. VLPs, wie zum Beispiel Gardasil® gegen das humane Papillomvirus, eignen sich für nicht kultivierbare Viren und bergen in Bezug auf eine Infektion ein geringeres Risiko als Lebend- oder Todimpfstoffe [47]. Letztere werden seit Jahrzenten zum Schutz gegen Influenza eingesetzt [33]. Der Impfschutz gegen Influenza basiert auf der Bildung von Antikörpern, unter anderem gegen die Kopfstruktur von Hemagglutinin, das in neutralisiertem Zustand nicht an Sialinsäure binden kann. Der antikörpervermittelte Schutz beschränkt sich in den meisten Fällen auf einen speziellen Virus Subtyp [52].

Die von der europäischen Pharmacopoeia spezifizierten Anforderungen an trivalente, auf ganzen Viruspartikeln basierende Influenza Impfstoffe umfassen den DNA-Gehalt, den Protein-Gehalt und eine Massevorgabe für die enthaltenen Hemagglutinine. Eine Impfdosis muss mindestens 15 µg und maximal 100 µg Hemagglutinin jedes Stammes enthalten. Der Gesamt-Proteingehalt darf 300 µg nicht überschreiten. Die limitierende DNA-Konzentration liegt bei 10 ng pro Dosis [53][54].

5.2.2. Produktion von Influenzapartikeln

Seit den 1940iger Jahren werden Influenzaviruspartikel in sterilen, befruchteten Hühnereiern vermehrt [55][33]. Bei dieser Vorgehensweise liegen 6 Monate zwischen Beginn und Ende einer Produktionskampagne [29]. Die Produktion einer Impfdosis kann bis zu zwei Eier erfordern [46]. Im Falle einer Pandemie ist jedoch die schnelle und flexible Skalierbarkeit eines Produktionsprozesses wichtig, um ausreichende Mengen eines Impfstoffes zur Verfügung stellen zu können. Neben den langen Vorlaufzeiten ergeben sich bei einigen Virusstämmen besondere Einschränkungen, die sich aus dem avianen Reservoir für Influenza ableiten. Das landläufig auch als Vogelgrippe bezeichnete H5N1, und einige andere ursprünglich aviane Influenzastämme, töten Hühnerembryonen, sodass die Ausbeuten aus Ei-basierter Produktion niedrig sind [33][56]. Ein weiterer Nachteil der auf Eier basierenden Produktion sind im Ei enthaltene Antigene, die

abgereichert werden müssen. Allergische Reaktionen gegen Ovalbumin und andere Proteine des Hühnereiweißes in Folge von Impfungen mit in Hühnerei produzierten Viren stellen ein klinisches Problem dar [57][43]. Des Weiteren konnte ein Drift der Influenza-Antigene für die Vermehrung in Eiern nachgewiesen werden. Verschiedenen Untersuchungen zur Folge bieten Influenza Impfstoffe aus Säugetierzellen einen gleichwertig wirksamen oder besseren Schutz gegen eine Infektion [58][59][60][61]. Ein vereinfachtes Flussschema eines Ei-basierten Produktionsprozessen ist in Abbildung 6 dargestellt. Viruspartikel können durch Dichtegradientenzentrifugation aus Allantoisflüssigkeit aufgereinigt werden [62]. Abbildung 7 beinhaltet einen vereinfachten Ablauf eines auf Zellkultur basierten Verfahrens.

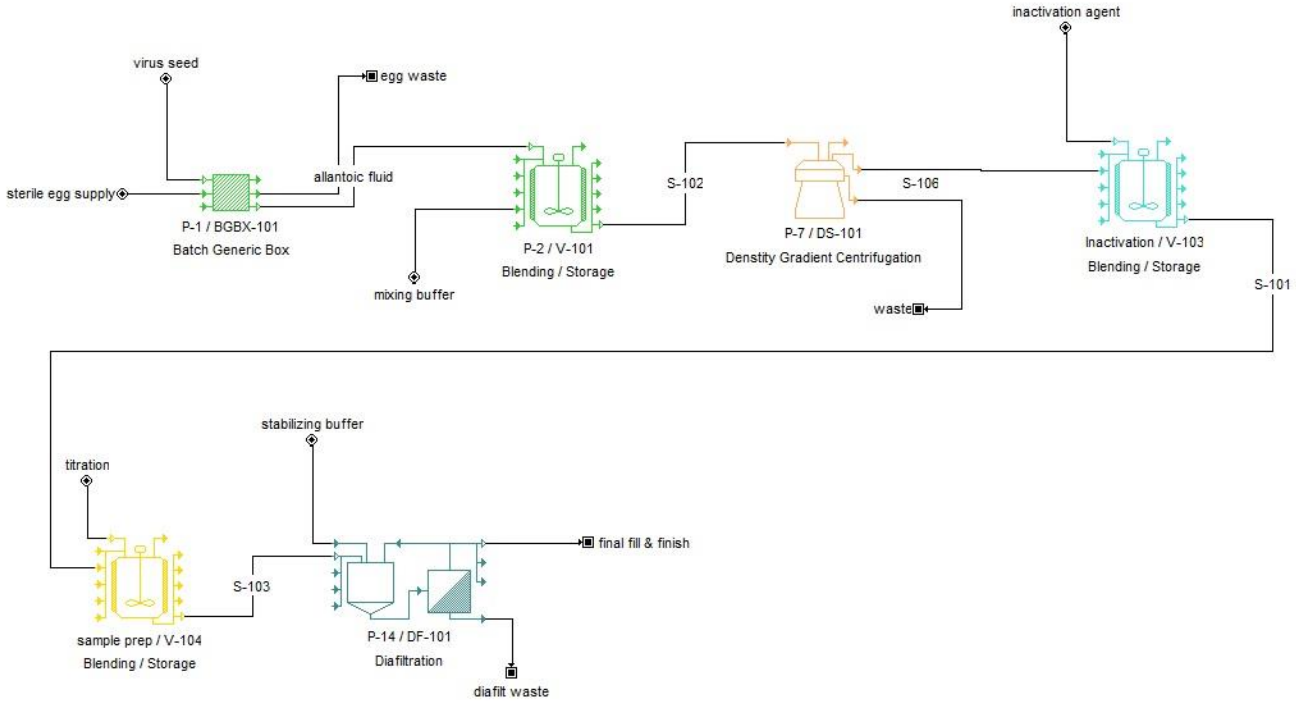

Abbildung 6: Schematische Darstellung eines konventionellen Produktionsprozesses für ganze Influenzaviruspartikel zur Vakzinherstellung. Die Viruspartikel werden in sterilen, embryonierten Hühnereiern vermehrt. Der Dichtegradientenzentrifugation zur Aufreinigung folgen Inaktivierung und Filtration. Abbildung wurde erstellt mit SuperPro Designer®, Itelligen Inc.

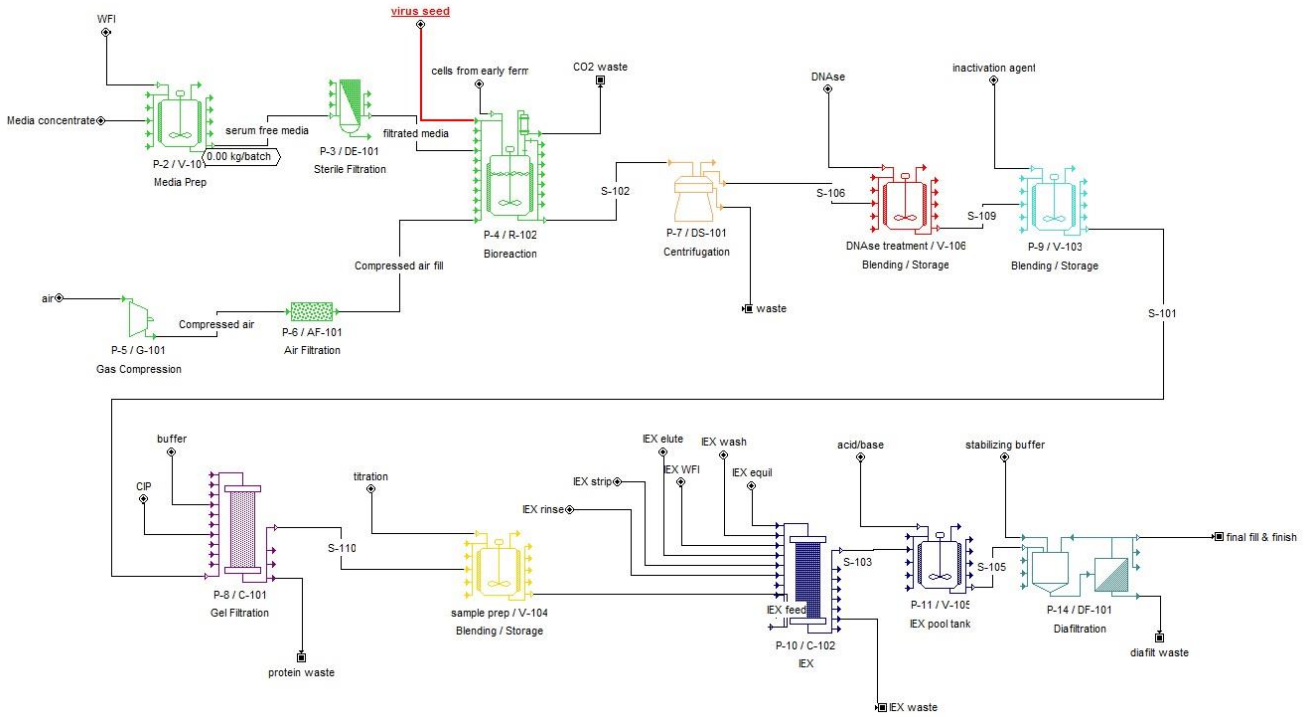

Abbildung 7: Vereinfachtes Flussschema eines Produktionsprozessen für auf ganzen Influenzaviruspartikeln basierte und in Zellkultur vermehrte Vakzine. Die Produktion in Säugetierzellen erfordert Anpassungen der Aufreinigungsschritte. Abbildung in Anlehnung an [55][63], erstellt mit SuperPro Designer®, Itelligen Inc.

In zellkulturbasierten Verfahren wird Influenza beispielsweise in MDBK [40], Madin-Darby Kaninchennieren (engl. Madin-Darby Canine Kidney, MDCK) [57] oder Vero Monkey Zellen [46] vermehrt. Das früher zur Zellkultivierung notwendige Serum kann durch definierte Medien ersetzt werden [46], was das Risiko einer möglichen Kontamination durch Prionen [57] und andere adjuvant wirkende Substanzen [61] reduziert, sowie die Kosten der Fermentation senkt. Die Zellen in Kultur werden nach erfolgreicher Vermehrung mit dem Virus angeimpft. Einige Stunden bis Tage nach der Infektion können die Viren im Überstand geerntet werden. Die Inaktivierung erfolgt beispielsweise durch Formaldehyd oder β-Propriolacton [29]. Die inaktivierende Wirkung von β-Propriolacton wird größtenteils durch Reaktion mit Aminosäureresten wie Cystein oder Methionin erzielt [64]. Hemagglutinin verliert in Folge der Alkylierung durch β-Propriolacton seine Fähigkeit die Fusion von Viruspartikelmembran und endosomaler Membran zu vermitteln [65]. Im Gegensatz zur Behandlung mit β-Propriolacton ist die Hemagglutination (HA) durch Inkubation mit Formaldehyd weniger stark beeinträchtigt [66]. Beide Agenzien schränken die Vermittlung einer Kreuzimmunität im Vergleich zu mit γ-Strahlen behandelten Influenzaviruspartikeln ein [67].

Die Vermehrung von Influenzaviruspartikeln in Zellkultur impliziert Anpassungen des Aufreinigungsverfahrens. Angewandte Methoden zur Aufreinigung sollen skalierbar sein, um die Flexibilität des gesamten Produktionsprozesses zu gewährleisten. Die Abreicherung der Wirtszell-DNA stellt bei zellkulturbasierten Prozessen hohe Anforderungen an den Aufreinigungsprozess [63] und kann den Einsatz von Nucleasen erfordern [44]. Darüber hinaus ist eine generelle Optimierung bezüglich der Wirtschaftlichkeit und des Durchsatzes wünschenswert. Traditionellerweise werden Influenzaviruspartikel durch Dichtegradienten-Zentrifugation, Ammoniumsulfat-Fällung, Calciumphosphat-Präzipitation oder SEC aufgereinigt [68]. Weitere, chromatographiebasierte Verfahren sind AEX [63], und Affinitätschromatographie (AFC) [54][69][70][71]. Ein zentrales Problem sind die im Vergleich zu typischen Proteinprozessen niedrigen Wiederfindungsraten.

SEC ist eine vergleichsweise schonende Methode für die Viruspartikelreinigung, da die Partikel geringem osmotischem Stress und niedrigen Scherkräften ausgesetzt sind [72]. Aufgrund der Größe von Influenzaviruspartikeln ist der für die SEC erforderliche Methodenentwicklungsaufwand vergleichsweise

gering. Ein Hauptnachteil der SEC ist die geringe Effizienz im Vergleich zu adsorptiven Chromatographiemodi. In der Praxis kann sich auch die Skalierbarkeit einer präparativen Säule zur SEC als problematisch erweisen. Das Verhältnis von Betthöhe zu Säulendurchmesser ist größer als bei adsorptiven Medien. Produktionsgebäude lassen im Regelfall eine Vergrößerung der Säulenstandfläche besser zu, als eine Raumerhöhung. Kontinuierliche Verfahren, wie die Simulated Moving Bed (SMB) Chromatographie können die Effizienz der SEC steigern und reduzieren das Volumen der einzelnen Säulen. Die Anwendung eines SMB Verfahrens kann die Ausbeute für Adenovirus 5 bei gleichbleibender DNA- und Wirtszellproteinreinheit von 57 % auf 86 % steigern [73]. Die Wiederfindungsrate für Hemagglutinin und Neuraminidase in präparativen SEC Versuchen mit Sepharose 2B und in MDCK Zellen produzierten Influenzapartikeln betrug 70 % [43]. In einem alternativen SEC Capturing Verfahren konnte 85 % der HA-Aktivität nach Aufreinigung mit Sepharose 4FF wiedergefunden werden [63]. Ein Nachteil von kontinuierlichen Prozessen ist die Notwendigkeit einer komplexen Regelung. Solche Prozesse werden daher häufig als Risiko in Bezug auf die Virussicherheit eingestuft [74].

Weniger komplex in Betrieb, Wartung und Validierung bei gleichzeitig gesteigerter Produktivität sind Batch-Chromatographieverfahren, die auf adsorptiven Medien basieren. Zu kontinuierlichen SEC Reinigungen vergleichbare Wiederfindungsraten werden in der AEX mit Sepharose Q XL erreicht [63]. AFC und AEX sind chromatographische Verfahren mit höherer Produktivität. In der Literatur finden sich verschiedene Liganden und stationäre Phasen zur AFC von Influenzaviruspartikeln [54][69][70][71]. Die Produktivität eines Aufreinigungsverfahrens wird nachhaltig von der Kapazität des Aufreinigungsmediums für das Produkt bestimmt. Die Kapazität von Zn^{2+} Metallaffinitätschromatographie-Membranen für Influenza A liegt bei 15.36 kHAU/cm² [71]. Sulfatierte Membranen und Q-Typ Membranen erreichen eine Kapazität von 18 kHAU/cm² [75] und 5,2 kHAU/cm² [76].

Die hochspezifischen Wechselwirkungen eines Affinitätsliganden erweisen sich für das Capturing von Viruspartikeln als problematisch, da sich diese durch einen stetigen Antigen-Drift und –Shift der Bindung durch einen Affinitätsliganden entziehen. Sorption an die stationäre Phase eines Ionenaustauschers basiert auf ionischen Wechselwirkungen. Der isoelektrische Punkt der meisten Influenzaviruspartikel liegt bei pH 5. Ergebnissen aus Experimenten mit proteinbeschichteten Nanopartikeln von Kalashnikova et al. zur Folge, könnte die Adsorption von Viruspartikeln an Ionenaustauscher und AFC-Medien durch die Oberflächenproteine dominiert sein [77]. Aus diesem Grund bietet sich AEX zum Capturing von Influenzaviruspartikeln an. Moderne AEX Harze haben Proteinbindekapazitäten >100 mg/mL. Oberflächentechnologien wie die Pfropfpolymerisation und hohe Ionenaustauschkapazitäten gewährleisten vergleichsweise hohe Bindekapazitäten und eine gewisse Salztoleranz. Die zu erwartende Kapazität für Viruspartikel ist jedoch mindestens um Faktor 10 geringer [78]. Aufgrund der unzureichenden Porengröße steht in den meisten Fällen nur die äußere Oberfläche zur Adsorption von großen Viruspartikeln zur Verfügung. Weitere Vorteile von Ionenaustauschchromatographie (IEX) sind die vergleichsweise hohen Flussraten und die daraus resultierende kürzere Prozessdauer.

Medien mit beschränktem Porenzugang, sogenannte „restricted access media“ (RAM), binden Verunreinigungen wie Wirtszell-Proteine. Für die größeren Influenzapartikel sind die in den Poren befindlichen Ladungen sterisch nicht zugänglich. RAM-Medien werden im Durchfluss betrieben. Die volumenbezogen größte Verunreinigung, das Wasser, wird durch Chromatographie im Negativmodus nicht abgereichert. Konvektive Medien wie Membranen oder Monolithen bilden einen weiteren Ansatz. Die Aufreinigung von Baculoviren aus Zellkultur mit Monolithen zur AEX kann im Labormaßstab realisiert werden [79].

Die prozessentwicklungsbegleitende Analytik stellt eine Hürde bei der Optimierung von Aufreinigungsprozessen da. Der derzeit einzige, validierte Test zur Quantifizierung von Hemagglutinin in humanen Influenza Impfstoffdosen ist die zeitintensive einfache radiale Immunodiffusion (SRID) [80][81]. In Wissenschaft, Forschung und zur Freigabe von tierischen Impfstoffen wird Influenza seit mehr als einem halben Jahrhundert durch die Agglutination von Erythrozyten quantifiziert [82]. Die HA erfordert durchschnittlich einen Viruspartikel pro Erythrozyt [83]. Nachteile des HA-Assays sind ein vergleichsweise hoher Arbeitsaufwand und eine Standardabweichung im Bereich von 20 % bis hin zu einer log-Stufe. Eine HA-Aktivität von 1 HAU/100 µL entspricht näherungsweise einer Massekonzentration von 3.24 ng/mL [63]. Antikörperbasierte Nachweise wie der enzymgekoppelte Immunosorptions-Nachweis (ELISA) oder Oberflächenplasmonresonanz können aufgrund der Virusvariabilität in den meisten Fällen nur spezifisch für

einen Stamm genutzt werden. Elektronenmikroskopie kann neben dem Nachweis von Viruspartikeln auch zur strukturellen Analyse von Influenzapartikeln herangezogen werden [83][84], ist jedoch vergleichsweise teuer und erfordert einen hohen Aufwand zur Probenvorbereitung [81]. Die Quantifizierung von Hemagglutinin durch Umkehrphasenchromatographie ist vielversprechend. Allerdings führt β-Propriolacton, das zur Virusinaktivierung eingesetzt wird, zu einer Retentionsverschiebung [85]. Eine alternative Hochdruckflüssigchromatographie (HPLC) Methode, deren Quantifizierungsgrenze (LOQ) mit 10^9-10^{11} Partikeln/mL vergleichsweise hoch ist, basiert auf AEX [86]. Die verschiedenen Methoden beruhen auf einer Quantifizierung der Aktivität oder des Antigengehaltes, was Vergleiche erschwert. Aktivitätsbasierende Nachweise sind zudem anfällig gegenüber Interferenzen. Calciumionen führen beispielsweise in Anwesenheit von Amyloidproteinen zu falsch positiven Ergebnissen des HA-Assays [87]. Ein analytischer Nachweis, der unabhängig von der Probenmatrix Aufschluss über die Größenverteilung und Aktivität einer Probe gibt, könnte die Entwicklung neuer Aufreinigungsstrategien für Influenzaviruspartikel unterstützen.

5.3. Biochromatographie

Die Chromatographie ist ein Trennverfahren, das auf der Verteilung von Stoffen in verschiedenen Phasen beruht. Die meisten biochromatographischen Verfahren basieren auf einer flüssigen und einer festen Phase. Die biologische Aktivität von Biopharmaka kann durch den Einsatz von wässrigen Lösemitteln in Kombination mit hydrophilen stationären Phasen erhalten werden. Stationäre Phasen zur Biochromatographie verfügen idealerweise über folgende Eigenschaften: hohe Selektivität und Bindekapazität, einen hohen Massentransfer, wenige unspezifische Wechselwirkungen, Inkompressibilität, hohe chemische Stabilität (die Immobilisierung des Liganden eingeschlossen), nicht-toxische Auswaschungsprodukte, hohe Wiederverwendbarkeit, gute Sanitisierbarkeit und einen günstigen Preis [88]. Solche Materialeigenschaften finden sich bei Vertretern von natürlichen und synthetischen Polymeren, anorganischen Verbindungen und Verbundmaterialien. Zu den am häufigsten verwendeten Basismaterialen in der Biochromatographie gehören Sepharosen, Polymethacrylatharze und Silicagele. Das Einbringen von Hydroxy- oder Diolgruppen an der Oberfläche der stationären Phasen erhöht die Hydrophilie und minimiert sekundäre Wechselwirkungen.

Stationäre Phasen zur SEC bilden im Idealfall keine Wechselwirkungen mit den Analyten aus. Eine Trennung wird über die Porengröße der stationären Phase bestimmt. SEC ist eine der am häufigsten verwendeten Methoden zur Analytik von Proteinen [89][20][90] und zur präparativen Aufreinigung von Viruspartikeln [63][91][73]. Selektivitätskriterium in der SEC ist der hydrodynamische Radius der zu trennenden Moleküle. Große Moleküle haben keinen oder nur eingeschränkten Zugang zu den Poren der stationären Phase und eluieren zuerst. Kleinere Moleküle müssen eine größere Wegstrecke in der Säule zurücklegen, da sie Zugang zu fast allen Poren der stationären Phase haben. Auf dieser Grundlage eluieren Moleküle in der Reihenfolge absteigender Größe von der Säule. Mit Hilfe einer Kalibration kann das Molekulargewicht von Molekülen aus derselben Molekülklasse bestimmt werden.

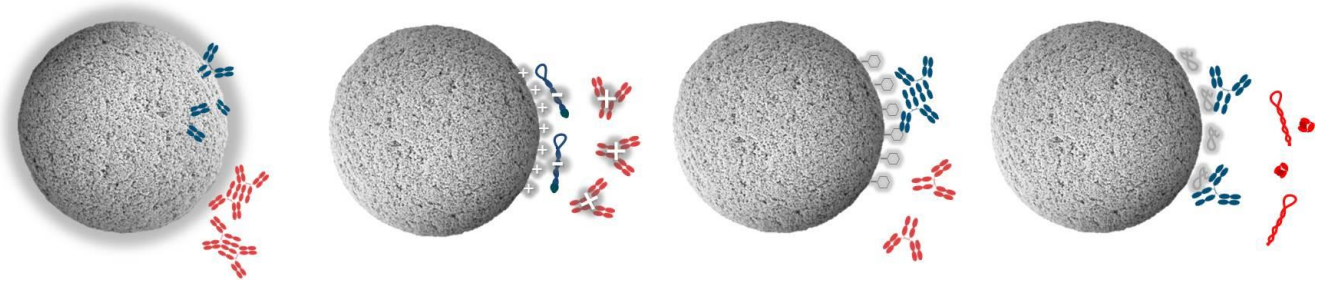

Abbildung 8: Schematische Darstellung verschiedener Chromatographiemodi von links nach rechts: SEC, IEX, HIC und Protein A AFC. Rot markierte Analyten erfahren eine geringere Retention als blau markierte Analyten.

Einige weitere Medien, wie Hydroxyapatit oder Silicagele zur Umkehrphasenchromatographie, kommen ohne Liganden aus, gehören aber zu den adsorptiven Chromatographiemodi. Im Regelfall wird die Retention eines Adsorbaten an der stationären Phase durch die Wahl des Liganden dominiert. Zur Funktionalisierung der Basismatrix können hydrophobe, hydrophile, ionische, mixed mode oder Affinitätsliganden immobilisiert werden. Ein Schema der in der Biochromatographie häufig eingesetzten Modi ist in Abbildung 8 dargestellt. Typische Liganden für die Biochromatographie, ihre zu Grunde liegenden Wechselwirkungen und Applikationsbeispiele für Biopharmazeutika sind in Tabelle 1 aufgelistet. In den letzten Jahren wurden

vermehrt multimodale Liganden und Harze entwickelt und kommerzialisiert. Mehrheitlich handelt es sich um Liganden, die hydrophobe mit ionischen Wechselwirkungen kombinieren. Sie versprechen eine erhöhte Selektivität und/oder Kapazität gegenüber Liganden, die nur eine primäre Wechselwirkung anbieten.

Tabelle 1: Häufig in der Biochromatographie eingesetzte Liganden und deren primäre Wechselwirkungen mit verschiedenen Biopharmazeutika.

Ligand	Wechselwirkung	Modus	Applikationsbeispiel
-	-	SEC	Vakzine, mAb-Aggregat Analytik
Protein A	IgG1,IgG2, IgG4	AFC	mAb Capturing
Sulfopropyl	elektrostatisch	CEX	Insulin, mAb Capturing/ Abreicherung von Aggregaten
Carboxymethyl	elektrostatisch	CEX	Abreicherung von mAb- Aggregaten
Quaternäres Ammonium	elektrostatisch	AEX	Enzyme, Vakzine
Diethyl Aminoethyl	elektrostatisch	AEX	Faktor VIII
Butyl	hydrophob	HIC	Abreicherung von mAb-Aggregaten, bi-spezifische mAbs
Phenyl	hydrophob	HIC	Abreicherung von mAb-Aggregaten
Polypropylenglycol	hydrophob	HIC	Abreicherung von mAb-Aggregaten, konjugierte mAbs
Tryptophan	elektrostatisch/hydrophob	MXC	Abreicherung von mAb-Aggregaten, bi-spezifische mAbs

In der IEX werden geladene Moleküle in einer Niedrigsalzumgebung auf eine gegennamig geladene stationäre Phase durch elektrostatische Wechselwirkungen adsorbiert. Die selektive Elution erfolgt in der Reihenfolge aufsteigender Nettoladung im ansteigenden Salzgradienten. Alternativ zum Leitfähigkeitsgradienten kann ein pH-Gradient angelegt werden. Beim sogenannten „Chromatofocusing" wird die Nettoladung des Adsorbaten durch die pH-Umgebung moduliert [92]. Die verschiedenen Adsorbaten eluieren an ihrem jeweiligen isoionischen Punkt. Für einige Applikationen ist die Trennschärfe des Chromatofocusings im Vergleich zu einem Leitfähigkeitsgradienten höher. Die überwiegende Mehrheit der auf IEX basierenden Prozesse beruht jedoch aufgrund der einfacheren Realisierung auf einem Leitfähigkeitsgradienten. Auf der Grundlage des „Steric Mass Action Models" (dt. sterisches Massenwirkungsmodel) von Brooks und Cramer kann nicht jede ionische Gruppe auf der Geloberfläche oder dem Analyten an der Wechselwirkung teilnehmen [93]. Infolgedessen führt eine Erhöhung der Ionenaustauschkapazität nach Überschreiten eines Sättigungswertes zu keiner signifikanten Steigerung der Bindekapazität. Polymermodifikationen zur Hydrophilierung der stationären Phase und Tentakelbildung für eine bessere sterische Zugänglichkeit erweisen sich als wirkungsvoller [94]. Beide Faktoren führen zu einer erhöhten Salztoleranz der Medien bei der Proteinbindung. Sie lassen eine quantitative Proteinadsorption in Gegenwart von 20-50 mM Pufferkonzentrationen zu. Weitere Strategien zur Steigerung der Salztoleranz von IEX-Medien beinhalten die Erhöhung der Hydrophobizität des Liganden und die Verwendung polyvalenter Liganden. Letzteres führt zu einer Erhöhung der Ladungsdichte, nicht notwendigerweise aber zu einer Erhöhung der Ionenaustauschkapazität.

Vergleichsweise geringe Kapazitäten werden in der HIC erreicht [95]. Die Retention wird durch die Hydrophobizität und die adiabatische Kompressibilität (Flexibilität) eines Analyten bestimmt. Letztere wird unter anderem über die Größe des Analyten beeinflusst [96]. Phenyl-Liganden können darüber hinaus π-π Wechselwirkungen eingehen. Die Selektivität der HIC ist orthogonal zur IEX [97]. Prominente Anwendungsfelder sind die Entfernung von hydrophoben Aggregationsprodukten [15][95][98] oder die

Trennung von Antikörper Derivaten, die mit Chemotherapeutika konjugiert sind [99][100]. Hohe Konzentrationen von kosmotropen Salzen vermitteln die Adsorption durch präferentielle Hydratation [101][102] und eine hohe Oberflächenspannung [103] der flüssigen Phase. Der Übergang in die flüssige Phase bei Verringerung der Salzkonzentration erfolgt in der Reihenfolge aufsteigender Hydrophobizität. Die Hydrophobizität eines Moleküls wird auch über dessen Nettoladung beeinflusst. In Folge wird meist ein pH Wert nahe des isoelektrischen Punktes eines Adsorbaten zur HIC gewählt. Bei Annäherung an den isoelektrischen Punkt steigt die Anzahl der frei werdenden Wassermoleküle [104]. Die Adsorption von mAb-Aggregaten an ein hydrophobes Harz kann beispielsweise über den pH moduliert werden [98]. Hydrophobe Wechselwirkungen basieren auf einer Erhöhung der Freiheitsgrade des Wassers in der flüssigen Phase, was eine Erhöhung der Entropie des Systems bedeutet. Dem zur Folge kommt der Temperatur als weiterer Einflussgröße, neben pH und Leitfähigkeit, eine besondere Rolle im Hinblick auf die Retention zu. Darüber hinaus erlaubt die Verwendung von verschiedenen Elektrolyten und dualen Salzpuffern die Kapazität eines Mediums zur HIC zu modulieren [105]. Weitere Details werden in Kapitel 5.4 erläutert.

Liganden, die elektrostatische und hydrophobe Wechselwirkungen anbieten, erscheinen vor dem Hintergrund steigender Anforderungen an die ökonomische Effizienz eines biochromatographischen Prozesses sinnvoll. Die hohe Kapazität und Wiederfindung, sowie der vergleichsweise schnelle Massentransfer von Liganden zur IEX können auf diese Weise mit der hohen Selektivität von hydrophoben Liganden kombiniert werden. Neben der Komplexität der Wechselwirkungen nimmt aber auch die Komplexität der Einfluss nehmenden Parameter zu. Trennungen können über pH, Leitfähigkeit, Temperatur, das verwendete Salz und Additive moduliert werden. Dies eröffnet ein großes Optimierungspotential zur erfolgreichen Realisierung einer Trennung, birgt aber auch einen hohen Aufwand in der Methodenentwicklung. Die Übergänge zwischen Einzelmodus-Chromatographie und Dualmodus-Chromatographie sind fließend. Unerwünschte sekundäre Wechselwirkungen lassen sich nur begrenzt und in Abhängigkeit des speziellen Adsorbaten in Kombination mit einer bestimmten Basismatrix vermeiden. Die dynamische Bindekapazität für das hydrophobe Peptid Insulin erreicht beispielsweise einen maximalen Wert bei einer definierten Quervernetzung eines Sulfopropyl-Ionenaustauschers [106]. Neben den dominierenden elektrostatischen Wechselwirkungen, dürfte hydrophobe Interaktion zur Adsorption beitragen. Je größer die Anzahl der beteiligten Wechselwirkungen, desto selektiver wird eine stationäre Phase. Pseudo-Affinitätsmedien und echte Affinitätsmedien wie Protein A wechselwirken über komplexe, hochspezifische Interaktionen mit dem Adsorbaten und ermöglichen eine vergleichsweise hohe Reinheit des Produktes in einem Chromatographieschritt. Ein Nachteil von Affinitätsmedien ist der oft hohe Preis pro produzierter Einheit des Produktes [16]. Die kommerziell bedeutendste Klasse der Affinitätsmedien sind Protein A Chromatographiemedien [107]. Diese und andere Affinitätsmedien zur Aufreinigung von Antikörpern und daraus abgeleiteten Molekülen erhalten ihre Funktionalisierung durch immobilisierte Proteinliganden. Die Proteinliganden sind zum Teil bakteriellen Ursprungs und potentiell immunogen.

Neben den hauptsächlich eingesetzten porös partikulären stationären Phasen gibt es Monolithen, Membranen und nicht-poröse, partikuläre Medien. Sie erzielen dank ihres schnellen Massentransfers hohe Auflösungen bei kurzen Trennzeiten [108] und eignen sich für den Einsatz in der Analytik. Der Massentransport in konvektiven Medien ist nahezu diffusionsunabhängig, was auch bei großen Biopharmazeutika wie Viruspartikeln die Anwendung von hohen Flussraten zulässt [109]. Monolithen haben eine makroporöse Struktur, die im Vergleich zu nichtporösen Medien eine größere Oberfläche darstellt. Die Kapazität von partikulär porösen Medien ist aufgrund der noch größeren Oberfläche dieser Medien der Kapazität von Monolithen überlegen [24]. Die Skalierbarkeit von Monolithen kann ein weiteres Problem im Produktionsmaßstab darstellen. Partikuläre Medien können zu Bettvolumen von 1000 L und größer gepackt werden. Kommerziell erhältliche Monolithen haben momentan ein Bettvolumen < 10 L [79]. Die Nachteile von Membranadsorbern sind ein höherer Preis und eine geringere Oberfläche pro Volumeneinheit [108]. Beides wirkt sich negativ auf die Wirtschaftlichkeit des Prozessschrittes aus.

5.3.1. Leistungsparameter für chromatographische Trennungen: die theoretische Bodenhöhe

Die Trennung von großen Biopharmazeutika wie Viruspartikeln oder IgM in porös-partikulären Medien muss bei vergleichsweise niedrigen Flussraten realisiert werden, da der Massentransport innerhalb der Poren auf Diffusion beruht. Die Abhängigkeit von volumetrischer Flussrate u und der theoretischen Bodenhöhe H_t kann empirisch durch die van Deemter Gleichung (Gleichung 1) beschrieben werden [110]. In einer starken Vereinfachung wird eine näherungsweise laminare Flussverteilung angenommen. Die Eddy Diffusion A ist

eine für die jeweiligen Prozesskomponenten flussunabhängige Konstante. Die Wanderungsgeschwindigkeit verschiedener Moleküle in der Säule hängt unter anderem von der Position ihres Massenmittelpunktes im Flussprofil ab. Unter Annahme eines laminaren Flussprofils ist die Wanderungsgeschwindigkeit an Oberflächen geringer als im Zentrum des Flussprofils. Der Einfluss der longitudinalen Diffusion *B* nimmt bei steigender Flussrate ab, da die Moleküle weniger Gelegenheit haben, parallel zur Flussrichtung zu diffundieren. Der Massentransfer-Widerstand *C* beschreibt den Widerstand der Moleküle, sich (im Gegensatz zu Massepunkten) gleichmäßig zu verteilen und nimmt mit steigender Flussrate zu. Der Massentransfer-Widerstand umfasst die Verteilung im Zwischenkornvolumen und Porenvolumen. Die SEC stellt einen Sonderfall dar. Die nicht-adsorptive Trennung beruht hauptsächlich auf der Diffusion in und aus der Pore, die in diesem Fall den Massentransferwiderstand bildet. Zweitrangige Beiträge werden durch hydrodynamische Effekte im Zwischenkornvolumen erzeugt. Der Trennvorgang an adsorptiven Medien beinhaltet ebenfalls den Massentransfer in die stagnierende Flüssigphase in den Poren [111]. Zusätzlich bildet der Massentransfer an den Liganden ein weiteres Selektivitätskriterium. Nicht-poröse Medien bilden einen weiteren Sonderfall ohne Massentransferwiderstand durch das Porenvolumen.

$$H_t = A + \frac{B}{u} + C \cdot u \qquad \text{(Gleichung 1)}$$

Verschiedene Weiterentwicklungen der ursprünglichen van Deemter Gleichung beziehen die Diffusivität des Analyten und die Größe der verwendeten Partikel mit ein [112]. Eine Normierung der Bodenhöhe (Gleichung 2) und der Flussrate (Gleichung 3) gegenüber dem Diffusionskoeffizienten *D* des Analyten und der Partikelgröße d_p der stationären Phase lässt Vergleiche zwischen verschiedenen Säulen und Analyten zu [113].

$$h = \frac{H_t}{d_p} \qquad \text{(Gleichung 2)}$$

$$v = \frac{u \cdot d_p}{D} \qquad \text{(Gleichung 3)}$$

Die reduzierte van Deemter Gleichung (Gleichung 4) korreliert die auf die Partikelgröße normierte Bodenhöhe *h* mit der reduzierten Flussrate *v*.

$$h = A + \frac{B}{v} + C \cdot v \qquad \text{(Gleichung 4)}$$

Für vergleichsweise große und sehr große Analyten postulierten Knox, Parcher und Giddings eine Kopplung von Massentransfer-Widerstand und Eddy Diffusion (Gleichung 5) [114][115]. Der Kopplungsterm A_C beschreibt die kombinierten Effekte von Massentransfer und Eddy Diffusion.

$$h = \frac{B}{v} + A_C \cdot v^n \qquad \text{(Gleichung 5)}$$

Die Bandenverbreiterung aufgrund der Eddy Diffusion nimmt für sehr große Moleküle ab. Die große sphärische Ausbreitung führt zu einer zentrumsnahen Lokalisierung des Massenmittelpunktes im Flussprofil. Die engere Verteilung der Wandergeschwindigkeiten beruht auf der Zugänglichkeit der verschiedenen Flussströme für große Analyten. Insbesondere bei hohen Flussraten erweist sich dieses empirische Konzept als bedeutsam [115]. Allen Konzepten zur Korrelation von Bodenhöhe und Flussrate gemein ist die Annahme eines Analyten, dessen Diffusivität unabhängig von den angewendeten Parametern konstant ist. Die Diffusivität eines Biopharmazeutikums kann durch Aggregation, Degradation oder sphärische Deformation verändert werden. Solche Veränderungen sind auch die Grundlage von slalomchromatographischen Effekten. Dieser, auf hydrodynamischen Einflüssen basierende Trennprozess selektiert Analyten reziprok zur SEC [116].

5.3.2. Leistungsparameter für chromatographische Trennungen: Auflösung

Neben der Bodenhöhe, beziehungsweise der dazu inversen Bodenzahl *N*, bildet die Auflösung ein weiteres wichtiges Qualitätskriterium für die chromatographische Trennung von Biopharmazeutika. Die Peakschärfe von Biopharmazeutika ist im Regelfall geringer als die von klassischen pharmazeutischen Wirkstoffen wie Aspirin. Eine Analytik von Aspirin mittels Umkehrphasenchromatographie kann in 2 Minuten realisiert werden [117]. Die kleine Molekülgröße führt zu einer hohen Diffusivität und erlaubt schnelle Trennungen bei geringer Bandenverbreiterung. Ein weiterer Punkt ist die Stabilität solcher Moleküle. Sie tolerieren hohe Drücke und Reibungswärme, wie sie durch hohe Flussraten und kleine Partikelgrößen induziert werden. Letzteres steigert die Trennleistung bei konstanter Säulenlänge. Biopharmazeutika sind vergleichsweise polydispers und fragil. Sie weisen eine komplexe Struktur auf. Eine Vielzahl von Isoformen führt zu einer Peakverbreiterung. Reibungswärme und daraus entstehende laterale Temperaturgradienten [118] beeinflussen die Trennung stärker, da die Diffusivität großer Biopharmazeutika geringer ist. Als Folge davon sind Basislinientrennungen meist nur mit langsameren linearen Flussraten und kleinen Partikeln zu realisieren. Der Auflösung R_s (Gleichung 6) kommt in der Chromatographie von Biopharmazeutika eine wichtige Rolle als Qualitätskriterium für eine Trennung zu [111]:

$$R_s = \frac{2(V_{R2} - V_{R1})}{W_{B1} + W_{B2}} \qquad \text{(Gleichung 6)}$$

Wobei V_R das Elutionsvolumen des jeweiligen Analyten ist und W_B die Peakbreite bei 50 % der Peakhöhe. Für adsorptive Medien gilt dabei weiterhin eine Abhängigkeit von *N* sowie der Retention (Gleichung 7):

$$R_s = \frac{\Delta k' \sqrt{N}}{4(1 + k')} \qquad \text{(Gleichung 7)}$$

Neben *N* ist die Auflösung zweier Analyten abhängig vom Retentionsfaktor *k'* (Gleichung 8):

$$k' = \frac{t_R - t_0}{t_0} \qquad \text{(Gleichung 8)}$$

SEC Trennungen sind im Idealfall frei von Wechselwirkungen, wodurch die Adsorptionsenthalpie ΔH der Gibbs'schen Enthalpie ΔG (Gleichung 9) gleich null ist:

$$\Delta G = \Delta H - T\Delta S = RT \cdot ln(k) \qquad \text{(Gleichung 9)}$$

Es verbleiben die Entropie ΔS und die universelle Gaskonstante R=8,31 J mol^{-1} K^{-1}. Für den Verteilungskoeffizienten K_D ergibt sich demnach aus der Gibbs'schen Enthalphie (Gleichung 10):

$$ln(K_D) = {}^{-\Delta S}/_{R} \qquad \text{(Gleichung 10)}$$

Die Temperatur *T* hat dennoch praktische Relevanz in der SEC. Sie beeinflusst die Viskosität des Eluenten und die Diffusionsgeschwindigkeit der Analyten und dadurch indirekt die Trennung [90].

5.4. Elektrolyte in der Biochromatographie

5.4.1. Wechselwirkungen von gelösten Ionen

Die Wechselwirkungen von niedrig konzentrierten Ionen in unendlicher Lösung werden durch die Debye-Hückel Theorie beschrieben. In realen Lösungen ziehen sich gegennamige Ladungen an und gleichnamig geladene Moleküle stoßen sich ab. Verantwortlich dafür sind Coulomb Wechselwirkungen. Die potentielle Energie E_{pot} zweier Punktladungen q, ergibt sich aus ihrer gegenseitigen Entfernung r und der Permittivität des Vakuums ε_0 (Gleichung 11). Durch Austausch von ε_0 gegen die Permittivität eines beliebigen Mediums, kann E_{pot} auch in anderen Medien berechnet werden [119].

$$E_{pot} = \frac{q_1 q_2}{4\pi\varepsilon_0 r} \qquad \text{(Gleichung 11)}$$

Coulomb Wechselwirkungen verschiedener, gelöster Ionen werden durch das Lösemittel als Dielektrikum abgeschwächt. Die thermische Bewegung führt anders als im Salzgitter, zu einer Überlappung der Ionenwolken. Als Folge ergibt sich eine Diskrepanz zwischen der Aktivität der gelösten Ionen und der molaren Konzentration. Die Ionenaktivität $\alpha\pm$ nach Debye-Hükel kann für Salzkonzentrationen < 0.1 M näherungsweise beschrieben werden (Gleichung 12)[119]:

$$log(\alpha_{\pm}) = -\frac{A_D|z_+ z_-|\sqrt{I}}{1 + B_D\sqrt{I}} + C_D I \qquad \text{(Gleichung 12)}$$

In wässrigen Lösungen bei 25 °C ist A_D = 0.509, B_D und C_D sind empirische Parameter. Die Valenz z eines Ions beeinflusst die Ionenstärke I eines Elektrolyten in Lösung. I ist proportional zur Summe aus den Produkten der Valenzen z und der Konzentrationen c der gelösten Ionen (Gleichung 13)[120]:

$$I = {}^1\!/_2 \sum_i z_i^2 \cdot c_i \qquad \text{(Gleichung 13)}$$

Experimentell zugänglich ist nur die Aktivität aller Ionen in Lösung, weshalb die Valenz der Ionen eine Rolle spielt. Der Radius, in dem die Nettoladung eines Zentralions und der umgebenden Ionen um das 1/e-fache abfällt, heißt Debye-Länge δ. Die Umgebung eines Ions durch eine statistisch gesehen größere Anzahl von gegennamigen Ladungen führt zur Ladungsabschirmung innerhalb der Debye-Länge. Dieses Prinzip ist auch auf in Elektrolytlösungen solvatisierte Partikel und Proteine anwendbar. Elektrolyte haben wesentlichen Einfluss auf die lokale Ionenumgebung eines solvatisierten Partikels. Neben der Debye-Länge bilden die Lage der Stern-Schicht und der Scherebene (Abbildung 9) charakteristische Größen.

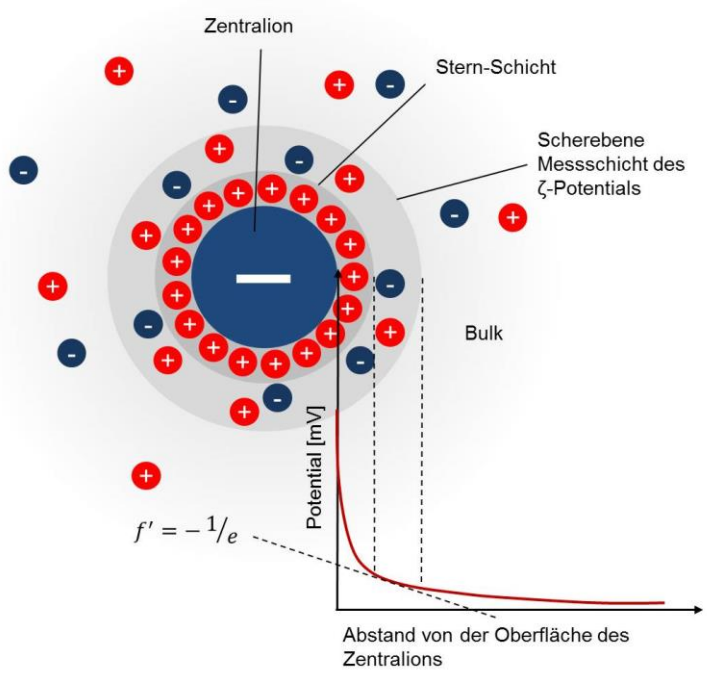

Abbildung 9: Schematische Darstellung eines netto negativ geladenen Zentralions in einer Salzlösung. Das Zentralion ist von einer primären Schicht von Gegenionen umgeben (Stern-Schicht). Um diese liegt eine diffuse Schicht von Kationen und Anionen, die mit dem Zentralion wandern und die von Bulk-Wasser und gelösten Ionen umgeben ist.

Die Stern-Schicht ist die primäre Schicht aus Gegenionen um das zentrale Ion. Die Scherebene bildet die Grenzschicht zwischen allen mit dem Zentralion wandernden Ionen und dem Bulk-Wasser. An ihr wird das ζ-Potential gemessen, welches experimentell zugänglich ist. Die Partikelbewegung im elektrischen Wechselfeld wird mittels dynamischer Lichtstreuung gemessen.

Bei der Solvatisierung eines Proteins wird für die Beschreibung durch die Debye-Hückel Theorie vereinfachend angenommen, dass Wechselwirkungen mit kurzer Reichweite und Änderungen des Dipolmoments nicht signifikant sind. Für die Abhängigkeit der Debye-Länge δ vom Aktivitätskoeffizienten einer Elektrolytlösung ergibt sich (Gleichung 14)[119]:

$$\delta = -\frac{N_A|z_+ \cdot z_-|e^2}{8\pi\varepsilon\varepsilon_0 RT \cdot ln(\alpha_\pm)} \qquad \text{(Gleichung 14)}$$

N_A ist die Avogadro-Konstante, e die Elementarladung. Die Debye-Länge δ nimmt mit zunehmender Ionenstärke des Solvents ab. Änderungen in der Debye-Länge führen zu Konsequenzen für die Löslichkeit eines Moleküls. 1924 (nur ein Jahr nach Publikation der Debye-Hückel Theorie) erkannte Wagner, dass die Gegenwart von Ionen die Luft-Wasser Interphase polarisiert, und so zu einer Oberflächenspannung führt [121][122]. Aufgrund der verschiedenen Dielektrizitätskonstanten von Wasser und Luft ergeben sich Spiegelladungen, die in Größe und Ladung mit denen der Ionen übereinstimmen und zu repulsiven Wechselwirkungen führen [122]. Die Oberflächenspannung einer Lösung hängt dabei von der Konzentration und dem gelösten Salz ab. Das molare Oberflächenspannungsinkrement für ein Salz kann zur Berechnung der Oberflächenspannung herangezogen werden. Melander und Horvarth postulierten eine logarithmische Korrelation zwischen der Löslichkeit L eines Proteins und der Konzentration c eines gelösten Salzes und der Oberflächenspannung γ (Gleichung 15)[123][124]:

$$log\frac{L}{L_0} = \delta + E_\gamma + F_c \qquad \text{(Gleichung 15)}$$

L_o ist die Löslichkeit eines Proteins in reinem Wasser, E die intrinsische Aussalzungskonstante und F das Protein Dipolmoment. Die intrinsische Aussalzungskontante E beschreibt den hydrophoben Beitrag an der Proteinlöslichkeit. In der Biochromatographie erweist sich die Debye-Hückel Theorie häufig als unzureichend, da oft hochkonzentrierte, komplexe Salzmischungen eingesetzt werden. Staby und Mollerup entwickelten knapp zwei Jahrzehnte nach Melander und Horvarth eine abgewandelte Beschreibung, die auf der Änderung der Proteinaktivität durch gelöste Elektrolyte basiert [125][96].

5.4.2. Wechselwirkungen zwischen Kolloidpartikeln

Die Wechselwirkungen zwischen zwei Kolloidpartikeln können durch die DLVO Theorie beschrieben werden [126]. Die DLVO Theorie ist ein von Derjaguin, Landau, Verwey und Overbeek entwickeltes Konzept, das Einflüsse der elektrischen Doppelschicht und van der Waals Wechselwirkungen zusammenfasst [119]. Van der Waals Wechselwirkungen umfassen Keesom (Dipol-Dipol), Dipol induzierte, und London Wechselwirkungen (zwischen zwei induzierten Dipolen). Die elektrische Doppelschicht und van der Waals Wechselwirkungen haben Einfluss auf die Stabilität von Partikeln in Lösung. Die DLVO Theorie ist sowohl auf die Homoaggregation als auch die Heteroaggregation anwendbar. Die elektrischen Doppelschichten können sich überlappen. Als Folge verlieren abstoßende elektrostatische Wechselwirkungen ihre Wirkung und die Partikel aggregieren auf Grundlage von van der Waals Wechselwirkungen. Alternativ kann es beispielsweise zur Adsorption an Oberflächen kommen. Die potentielle Energie zweier gelöster Kolloidteilchen errechnet sich aus der Summe von abstoßenden und anziehenden Wechselwirkungen (Gleichung 16). Die beiden Partikelzentren befinden sich im Abstand r zueinander, während die Oberflächen den Abstand s zueinander haben. Der Partikelradius r_{rad}, die Dicke der elektrischen Doppelschicht r_D und die beiden Konstanten A_{DLVO} und B_{DLVO} gehen in die näherungsweise Berechnung mit ein [119].

$$E_{pot} = +\frac{A_{DLVO}(r_{rad})^2\zeta^2}{r}e^{-s/r_D} - \frac{B_{DLVO}}{s} \qquad \text{(Gleichung 16)}$$

Die DLVO Theorie berücksichtigt jedoch keine ionenspezifische Wirkungen, wie zum Beispiel Hofmeister-Effekte [120]. So ist eine rationale und universelle Erklärung für die Interaktion von verschiedenen Proteinen in verschiedenen Elektrolytlösungen nicht bekannt [127].

Insbesondere in der präparativen Biochromatographie ist die Verwendung von Elektrolyten mit hohem LD_{50} wichtig. Vorzugsweise werden Elektrolyte verwendet, die in vergleichsweise hohen Konzentrationen Bestandteil des Blutes sind und/oder gut vom Stoffwechsel abgebaut werden können. Die eingesetzten Salze dienen zur Stabilisierung der Biopharmazeutika während des Aufreinigungsprozesses und in der Formulierung. Darüber hinaus erfordern klassische, adsorptive Biochromatographieschritte eine Verschiebung der Gleichgewichtskonstante für die Verteilung des Analyten zwischen stationärer und flüssiger Phase. In der HIC vermitteln hohe Salzkonzentrationen die Adsorption des Analyten an die stationäre Phase. Niedrige bis moderate Puffersalzkonzentrationen gewährleisten einen definierten pH, der die Adsorption und Desorption an und von IEX und Affinitätsmedien regulieren kann. Hohe Salzkonzentrationen führen zur Verdrängung von ionischen Adsorbaten von einer gegennamig geladenen Chromatographiematrix.

Häufig eingesetzte Salze sind Phosphat, Acetat, Histidin, Arginin, Tris(hydroxymethyl)-aminomethan (Tris), Malat und Natriumchlorid [128][129]. Salze beeinflussen die Hydratation eines Moleküls [101]. Die Struktur eines Biopharmazeutikums wird durch hydrophobe und elektrostatische Wechselwirkungen, Wasserstoffbrückenbindungen und van der Waals Interaktionen beeinflusst. Kauzman war 1959 der Erste, der hydrophoben Wechselwirkungen die größte Bedeutung zuschrieb [130][131]. Die Funktion eines Biomoleküls steht in Zusammenhang mit seiner Struktur, sodass verschiedene Elektrolyte einen direkten Einfluss auf die Aktivität eines Biopharmazeutikums haben. Neben ihrer Verträglichkeit mit dem Produkt und dem Einsatz in der Therapie darf die Wirtschaftlichkeit verschiedener Elektrolyte nicht vernachlässigt werden. Die Produktion im großen Maßstab erfordert große Mengen verschiedener Elektrolyte. Dabei spielen nicht nur Beschaffung und Entsorgung der entsprechenden Puffer eine Rolle. Standzeiten, Materialbeschaffenheit und Arbeitsaufwand, die durch etwaige Pufferwechsel entstehen, müssen in eine Gesamtbetrachtung einbezogen werden. Kombinierte Puffersysteme und polyvalente Pufferionen können je nach Bedarf des jeweiligen Aufreinigungsschrittes über einen breiten pH Bereich näherungsweise linear titriert werden. Polyvalente Ionen erlauben die Ausbildung von van der Waals Wechselwirkungen bei

niedrigeren Konzentrationen als monovalente Ionen. Dies geht aus der empirischen Schulze-Hardy Regel hervor, die besagt, dass Flokkulation bevorzugt durch Gegenionen mit hoher Ladungsnummer induziert wird [119]. Solche Ionen führen zu einer Verringerung der Debye-Länge (Gleichung 14). Für $\delta << r_{rad}$ entsteht ein sekundäres Minimum für die potentielle Energie bei mittelweiten Partikelabständen (Gleichung 16). Die Dielektrische Doppelschicht verhindert die Flokkulation in diesem Fall nicht. Jedoch werden Van der Waals Wechselwirkungen in Bezug auf Protein-Protein und Protein-Oberflächen Wechselwirkungen häufig zu viel Bedeutung beigemessen [132]. Ein weiterer Effekt ergibt sich aus der Ausbildung von Salzbrücken und einer höheren Avidität. Die Quervernetzung von auf Tentakeln immobilisierten Liganden durch Salzbrücken führt zu einer kompakteren Struktur der polymeren Oberflächenbeschichtung [133]. Als Folge ist die Zugänglichkeit der Liganden eingeschränkt.

5.4.3. Elektrolyte in der Anionenaustauschchromatographie

Um in der IEX hohe Bindekapazitäten durch schnellen Massentransfer zu erzielen, sollte der zur Adsorption verwendete Puffer ein kleines, monovalentes Gegenion zur stationären Phase bilden. Unter der Annahme eines stöchiometrischen Austausches von anorganischen Gegenionen durch Biopharmazeutika ist eine rasche Diffusion der Salzionen vorteilhaft für die Ausbildung des Gleichgewichtes. Chromatographie ist ein dynamischer Prozess und hohe Flussraten sind erstrebenswert im Hinblick auf die Dauer des Prozesses. In Folge ergibt sich eine Differenzierung zwischen Pufferionen für die CEX und die AEX. Für die CEX von Biopharmazeutika verwendete Puffersalze sind üblicherweise Natriumphosphat, Natriumcitrat und Natriumacetat. AEX wird häufig in Tris/HCl- und Bis-Tris-Puffern durchgeführt. Die Verwendung von gegennamig geladenen Pufferionen kann pH-Schwankungen beim Wechsel der Flüssigphase induzieren [134]. Insbesondere schwache Ionenaustauscher sind von solchen Effekten betroffen [135]. Die Elution erfolgt durch den stöchiometrischen Austausch mit anorganischen Ionen. Im Regelfall wird ein Natriumchlorid Gradient angewendet, aber auch andere Salze können ohne Änderung der Selektivität verwendet werden. Das Elutionsprofil aggregathaltiger mAb Proben von einem Kationenaustauscher ist unabhängig von der Verwendung von Natriumchlorid, Kaliumchlorid oder Natriumsulfat zur Elution [136]. Natriumchlorid erlaubt den Einsatz von 4 M wässrigen Lösungen. In der Praxis genügen im Regelfall 1-2 M konzentrierte Lösungen.

5.4.4. Elektrolyte in der hydrophoben Interaktionschromatographie

Die Löslichkeit der meisten Biopharmazeutika in Natriumchlorid ist vergleichsweise gut. Eine Einordnung verschiedener Salze in Bezug auf die Löslichkeit verschiedener Biopharmazeutika kann durch das Oberflächenspannungsinkrement vorgenommen werden [123]. Gemäß der „Solvophobic Theory“ ergibt sich aus dem Oberflächenspannungsinkrement auch die Retention in der HIC [103]. Dieser Ansatz wurde von Staby und Mollerup auf den Aktivitätskoeffizienten von Proteinen in Elektrolytlösungen erweitert. Das Modell erlaubt valide Vorhersagen für die Retention von Lysozym in Ammoniumsulfat-Lösungen [125][137]. Einen (historisch deutlich älteren) alternativen Ansatz bildet die Hofmeister-Reihe. Die Klassifizierung von Salzen im Hinblick auf ihr Potential zur Präzipitation und Denaturierung von Proteinen wurde Ende des 19. Jahrhunderts von S. Lewith, einem Schüler Franz Hofmeisters, und später von Franz Hofmeister selbst vorgenommen [138]. Die nach Hofmeister benannte Reihe ordnet Kationen und Anionen in Reihenfolge der zur Präzipitation erforderlichen Konzentration. Es handelt sich um eine rein empirische Einteilung und die Position einzelner Ionen kann für verschiedene Proteine variieren. Eine exemplarische Hofmeister-Reihe ist in Tabelle 2 dargestellt [137].

Tabelle 2: Hofmeister-Reihe für verschiedene Anionen und Kationen. Einige der aufgeführten Ionen, wie zum Beispiel Thiocyanat, finden kaum Einsatz in der Biochromatographie.

Anionen	PO_4^{3-}	SO_4^{2-}	CH_3COOH^-	Cl^-	Br^-	NO_3^-	ClO_4^-	I^-	SCN^-
Kationen	NH_4^+	Rb^+	K^+	Na^+	Cs^+	Li^+	Mg_2^+	Ca_2^+	Ba_2^+

Ionen die in vergleichsweise geringer Konzentration zur Protein Präzipitation führen, heißen kosmotrop und sind in Tabelle 2 links aufgeführt. Kosmotrope Ionen werden vorzugsweise für die Fällung und Adsorption

von Biopharmazeutika an hydrophobe Chromatographiemedien verwendet. Das Standardsalz in der HIC ist Ammoniumsulfat in natriumphosphatgepufferter Lösung. Ammoniumsulfat ist gut in wässrigen Puffern löslich, hat einen hohen Aussalzungseffekt, eine gute Stabilität und ist kostengünstig [139]. Mittig stehende, neutrale Ionen sind beispielsweise Chlorid und Natrium. Neben dem Einsatz in der IEX werden neutrale Ionen häufig zur mAb Elution von Protein A Adsorbern eingesetzt. Die erzielten Reinheitsgrade sind meist geringfügig höher, als bei Verwendung von kosmotropen Elutionspuffern wie Natriumcitrat [107]. Chaotrope Ionen wie Calcium, Magnesium und Iodid haben einsalzende Eigenschaften und führen in hohen Konzentrationen zur Denaturierung von Proteinen. Collins konnte unter anderem durch SEC und Jones-Dole B Koeffizienten Messungen zeigen, dass kleine Ionen mit hoher Ladungsdichte, wie Sulfat, Phosphat, Carboxylat, Natrium und Fluorid stark hydriert werden und demnach kosmotrop wirken. Dementgegen sind große, monovalente Ionen mit niedriger Ladungsdichte, wie Ammonium, Chlorid, Kalium und die positiv geladenen Seitenketten von Aminosäuren schwach hydriert und agieren chaotrop. Betrachtet man die Ionen als Sphären mit zentraler Punktladung, so überwiegen ab einer gewissen Größe die Wasserstoffbrückenbindungen gegenüber der Wechselwirkung zwischen Ionen und Wassermolekülen [140]. Eine konzeptionelle Erfassung der Abweichungen zwischen den Messdaten von Collins (oder ähnlichen, messbaren Größen) und der in Tabelle 2 dargestellten Hofmeister-Reihe existiert bis heute nicht. Individuelle Effekte für einzelne, gelöste Proteine steigern die Komplexität noch erheblich.

Neben der Hofmeister-Reihe, die für hohe Salzkonzentrationen gilt, gibt es eine Reverse Hofmeister-Reihe. Sie ist für niedrige Ionenkonzentrationen gültig und beruht auf Interaktionen von polarisierbaren Anionen mit Proteinen. In Folge wird die Nettoladung von Proteinen gesenkt, wodurch diese eher präzipitieren. In Gegenwart von höheren Konzentrationen steigt die Nettoladung durch Co-Interaktion von Kationen und weiteren Anionen [141].

Die Diskrepanz der Hofmeister-Reihe zu der Einordnung verschiedener Salze über deren jeweilige Oberflächenspannungsinkremente ist zum Teil erheblich. Magnesiumchlorid beispielsweise hat ein Oberflächenspannungsinkrement von 3.15 x 10^3 dyn g cm^{-1} mol^{-1}, wohingegen das wesentlich kosmotropere Ammoniumsulfat ein Oberflächenspannungsinkrement von 2.16 x 10^3 dyn g cm^{-1} mol^{-1} hat [142]. Ursache des verschiedenartigen Verhaltens von Proteinen und Partikeln in Salzlösungen ist die präferentielle Hydratation. Kosmotrope Salzionen werden von der unmittelbaren Umgebung der gelösten Moleküle ausgeschlossen, was ihre Löslichkeit in Wasser senkt. Chaotrope Salzionen wechselwirken mit den gelösten Molekülen und fördern deren Löslichkeit in polarer Umgebung. Bei der Adsorption eines Analyten an einen HIC Adsorber werden in Gegenwart von kosmotropen Ionen mehr Wassermoleküle frei [104]. Arakawa und Timasheff zeigten, dass das Oberflächenspannungsinkrement zweiwertiger Kationen nicht als Indikator für die präferentielle Interaktion herangezogen werden kann, wie es für Natriumsalze möglich ist [143]. In der HIC muss weiterhin die präferentielle Interaktion der Ionen mit dem Adsorber berücksichtigt werden [144][137]. Bulk-Wassereffekte wurden lange Zeit ebenfalls für Unterschiede zwischen chaotropen und kosmotropen Salzen verantwortlich gemacht. Demnach führen kosmotrope Ionen in Lösung zu einer stärkeren Strukturierung des Bulk-Wassers, was eine Fällung und das Herauslösen von Biopharmazeutika aus den Wasserstrukturen begünstigt. Einige neue Publikationen stellen diesen Effekt jedoch in Frage [145]. Spektroskopische Experimente konnte keinen Einfluss auf die Orientierung von Bulk-Wassermolekülen nach Zugabe von chaotropen und kosmotropen Salzen nachweisen [146].

5.4.5. Präferentielle Interaktion von Zwitterionen

Präferentielle Hydratation wird weiterhin für bestimmte Effekte in der Chromatographie mit zwitterionischen Elektrolyten verantwortlich gemacht. Folgt einer HIC eine IEX, so ist im Regelfall eine Senkung der Leitfähigkeit des feedstreams erforderlich. Dies kann zum Beispiel über einen Diafiltrationsschritt erzielt werden. Durch das Umspülen einer HIC Säule in einen glycinhaltigen Puffer nach dem Adsorptionsschritt kann die Probenelution durch ein Absenken der Glycinkonzentration herbeigeführt werden [24].

Eine weitere Aminosäure, Arginin, findet vielfältigen Einsatz in der Biochromatographie, insbesondere in der Aufreinigung und der Analytik von mAbs. Die Wiederfindung von mAbs und polyklonalen Antikörpern von AFC Säulen kann durch einen Argininzusatz gesteigert werden und das eluierte Produkt enthält weniger Aggregationsprodukte [147][148]. Der Zusatz von Arginin in der HIC steigert die Wiederfindungsrate des Produktes [149]. In der SEC wird Arginin dem Eluenten zugesetzt, um unspezifische Wechselwirkungen mit der stationären Phase zu unterbinden [150][151][90].

5.4.6. Elektrolyte können die Doppelschichtausbildung unterstützen

Ein weiterer, pufferspezifischer Effekt ist die Ausbildung von Doppelschichten des Adsorbaten auf der Oberfläche der stationären Phase. Doppelschichten können durch sehr hohe Konzentrationen der zu adsorbierenden Moleküle induziert werden. Solche Adsorptionsisothermen zeigen ein zweites Sättigungsplateau. Chen und Cramer fanden eine signifikante Erhöhung der Bindekapazität für große Proteine und verschiedene HIC Adsorber nach Überschreiten einer bestimmten Salzkonzentration [152]. Der vorgeschlagene Mechanismus beinhaltet die Ausbildung einer Doppelschicht, wie sie auch für BSA und HIC-Sepharosen unter Überladungsbedingungen vorgeschlagen wird [153].

5.4.7. Dualsalzsysteme und Polysalzsysteme

Die Vorteile der Verwendung von verschiedenen Einzelpuffern zur Proteinbiochromatographie werden seit Jahrzehnten genutzt. Das Verhalten von Puffermischungen ist jedoch vergleichsweise unzulänglich beschrieben, und dessen Abschätzungen beruhen auf verschiedenen empirischen Vorhersagen [126]. Ein Grund dürfte die steigende Komplexität solcher Dual- oder Polysalzsyteme sein, die den Screening Aufwand erheblich steigert. Seit einiger Zeit ermöglichen parallelchromatographiegestützte Systeme ein deutlich schnelleres Screening. Die Miniaturisierung bis zum 50 µl Säulenmaßstab erfordert eine geringere Probenmenge pro Lauf. Gleichzeitig ist der Kostendruck auf Aufreinigungsverfahren von Biopharmazeutika gewachsen. Um komplexe Biopharmazeutika einem breiten Patientenkreis zugänglich zu machen, dürfen die Kosten für das Gesundheitssystem nicht zu hoch werden. Dies gilt insbesondere für Vakzine, die durch die WHO auch in Schwellenländern verteilt werden. Durch die Einführung von Biosimilars, wird dieses Ziel adressiert, was den Kostendruck auf die Herstellung des primären Produktes weiter verstärkt. Eine Steigerung der Produktivität durch den Einsatz komplexerer Puffersysteme bedeutet daher einen großen Vorteil.

Die Entwicklung einer von der Puffersubstanz unabhängigen Analytik für Vakzine, wie sie für mAbs Verwendung findet, könnte diese Entwicklung weiter begünstigen.

6. Hervorzuhebende Ergebnisse

6.1. Einfluss von dualen Salzgemischen auf hydrophobe Wechselwirkungen

Salze beeinflussen die Oberflächenspannung der flüssigen Phase sowie die elektrische Doppelschicht eines gelösten Moleküls. Unterschiede zwischen einzelnen Salzen hinsichtlich ihrer Eigenschaften hydrophobe Interaktionen zu unterstützen sind bekannt und in der Literatur beschrieben [138][123][103][140]. Einflüsse von dualen Salzgemischen auf hydrophobe Interaktionen sind weniger gut untersucht und fanden erst in jüngerer Vergangenheit Beachtung. Die Anwendung miniaturisierter Hochdurchsatz-Verfahren in der Chromatographie als bewährter Standard ermöglicht es, die Komplexität eines Versuchsraumes zu erhöhen. Die notwendigen Experimente können schneller umgesetzt und in einigen Fällen durch mathematische Modelle (Design of Experiments, DoE) reduziert werden. In einer 2009 von Senczuk et al. veröffentlichten Publikation wird die Erhöhung von dynamischen Bindekapazitäten in der HIC durch kosmotrope Dualsalzgemische beschrieben [105]. Das vorgeschlagene Konzept beruht auf der Löslichkeitsvermittlung durch den Einsatz verschiedener Salze, was eine Erhöhung der Oberflächenspannung in der flüssigen Phase zulässt. In der vorliegenden Arbeit wurde die Verwendung von Dualsalzgemischen, bestehend aus kosmotropen und chaotropen Salzen, hinsichtlich ihres Einsatzes in der reinen HIC und der hydrophoben IEX untersucht. Kapazitäten von rein hydrophoben Medien für mAb werden durch die Verwendung von kosmotrop-chaotropen Dualsalzgemischen erhöht [124]. Die durchschnittlich erzielten Kapazitätszuwächse sind niedriger als bei Verwendung von rein kosmotropen Dualsalzgemischen. Die Löslichkeitsvermittlung durch das chaotrope Salz dürfte die Bindung an den hydrophoben Adsorber beeinflussen. Ein entscheidendes Argument für den Einsatz von kosmotrop-chaotropen Dualsalzgemischen in der HIC ist die Modulierbarkeit der Selektivität von HIC Adsorbern. Während rein kosmotrope Dualsalzgemische keinen Einfluss auf die Selektivität einer HIC Trennung haben [105], erlaubt die Verwendung von chaotrop-kosmotropen Dualsalzgemischen eine Modulation der Selektivität. In Abbildung 10 ist dieser Effekt für die Trennung verschiedener Standardproteine auf HIC Adsorbern mit variierender Hydrophobizität dargestellt [154].

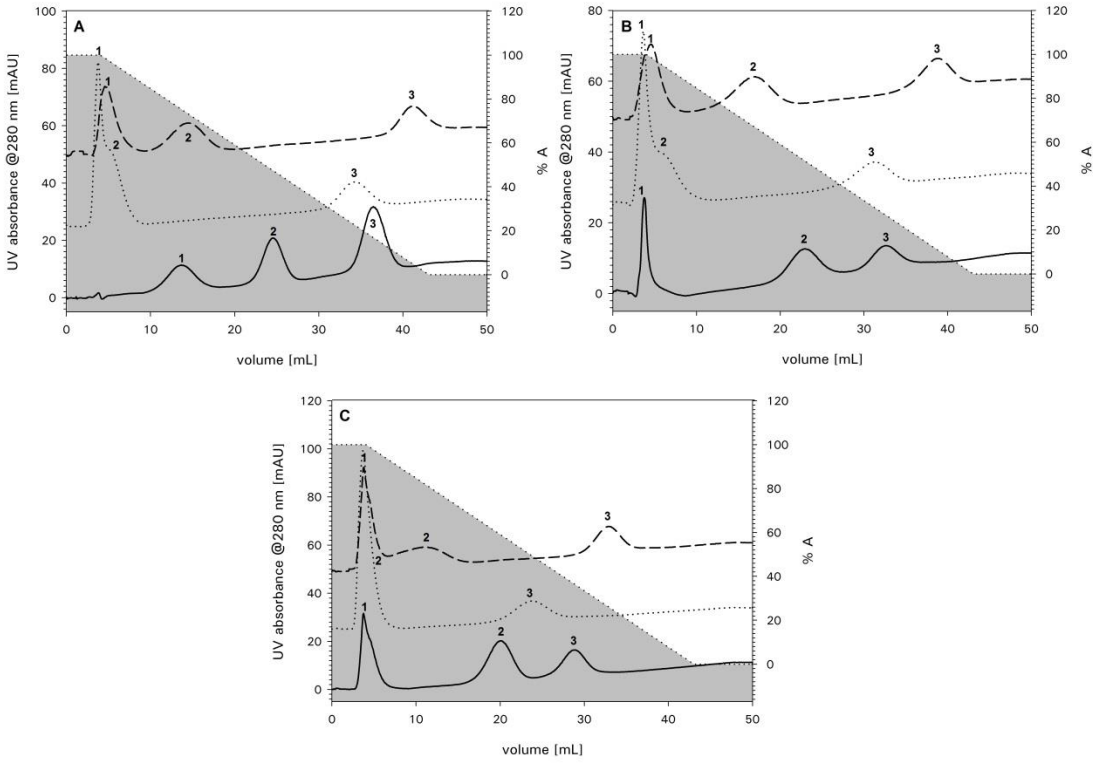

Abbildung 10: Selektivität von TOYOPEARL Butyl-600M (A), TOYOPEARL Phenyl-600M (B) und TOYOPEARL PPG-600M (C) für Cytochrom C (1), Ribonuclease A (2) und Lyoszym (3). Die Trennungen wurden in verschiedenen Adsorptionspuffern realisiert. 1,8 M Ammoniumsulfat (—), 1,0 M Ammoniumsulfat + 1,0 M Natriumacetat (···) und 1,0 M Natriumsulfat + 1,0 M Natriumchlorid (---) wurden in 100 mM Natriumphosphat-Puffer, pH 7.0 gelöst. Genehmigter Nachdruck aus [154]. © Tosoh Bioscience GmbH.

Industriell bedeutsamer ist die Trennung von mAbs und mAb-Aggregaten. Die Auflösung von mAb-Monomeren, Dimeren und Trimeren in der HIC kann durch die Verwendung von verschiedenen, chaotrop-kosmotropen Dualsalzgemischen moduliert werden. Die erzielten Effekte sind vergleichsweise weniger deutlich, als für die Trennung von Standardproteinen, können in manchen Fällen aber das Unterschreiten des kritischen Aggregatgehaltes sicherstellen. Im analytischen Maßstab ist der Effekt verschiedener Puffersysteme aufgrund der höheren Auflösung besser zu sehen. Abbildung 11 A zeigt eine Trennung von mAb und mAb-Aggregaten in einer natriumphosphatgepufferten Ammoniumsulfat-Lösung. Trennungen in Natriumchlorid, Natriumcitrat, sowie einem Gemisch beider Salze sind in Abbildung 11 B dargestellt [155]. Chaotrope Salze scheinen eine differenzierte Löslichkeitsvermittlung herbeizuführen. Diese beruht wahrscheinlich auf ohnehin vorhandenen Unterschieden der Analyten und führt lediglich zu einer Erhöhung der Trennschärfe. Eine Umkehr der Elutionsreihenfolge konnte in den durchgeführten Experimenten nicht beobachtet werden. Während kosmotrope Ionen von der Oberfläche von Proteinen ausgeschlossen werden, könnten chaotrope Ionen die Löslichkeit von Analyten mit möglichst ähnlicher Größe und Jones-Dole B Koeffizienten steigern [140]. Auf dieser Grundlage würden chaotrope Ionen bevorzugt mit kleineren und hydrophoberen Analyten präferentiell interagieren und deren Löslichkeit in Wasser vergleichsweise stärker steigern.

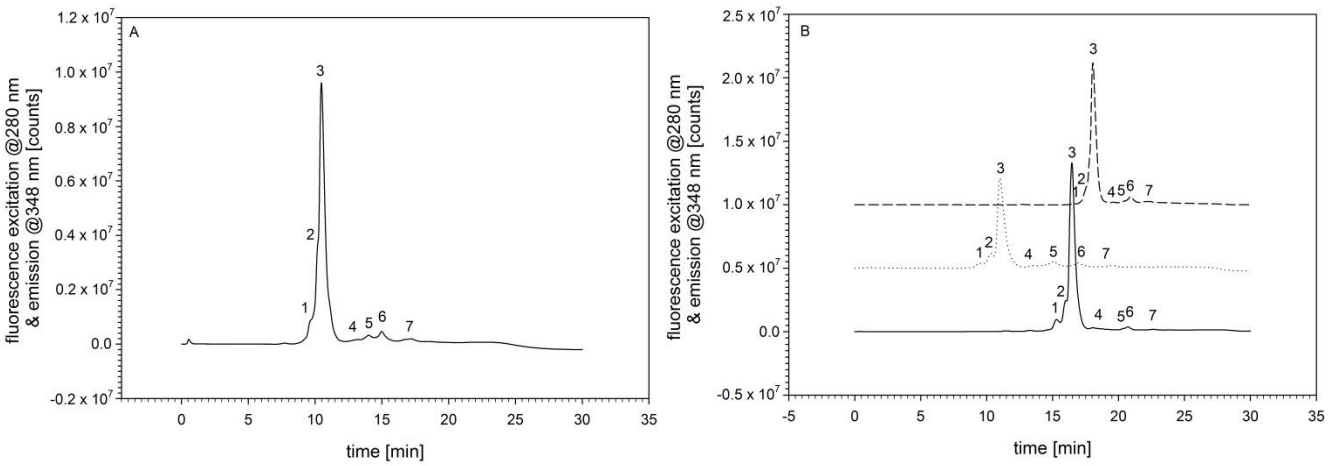

Abbildung 11: Analytische HIC mit TSKgel Butyl-NPR zur Trennung von mAb-Monomeren und mAb-Aggregaten. Die Trennung im Ammoniumsulfat-Gradienten (A) erzielt keine Auflösung der monomeren Isoformen 1 und 2 vom Hauptpeak (3). In (B) wurden zur Adsorption 3,0 M Natriumchlorid (···), 1 M Natriumcitrat (--) sowie 3,0 M Natriumchlorid + 0,25 M Natriumcitrat (—) in 100 mM Natriumphosphat-Puffer, pH 7,0 verwendet. Peak 3 repräsentiert den Hauptanteil der mAb-Monomere. Monomere Isoformen bilden wahrscheinlich Peak 1 und 2. Nachfolgende Peaks repräsentieren Aggregate und hydrophobere Varianten. Die Selektivität der Trennung verschiebt sich. Zusatz von Natriumcitrat erzielt vergleichsweise schlechtere Auflösungen für Peak 5 und 6, sowie für Peak 2 und 3. Peak 1 und 2, sowie 4 und 5 werden besser aufgelöst. Abbildung umfasst in [155][156] vorgestellte Daten.

Pufferbedingte Kapazitätssteigerungen und Selektivitätsänderungen beschränken sich nicht auf rein hydrophobe Adsorber. Die Trennung von mAb-Monomeren und mAb-Aggregaten mit hydrophoben Kationenaustauschern wird durch elektrostatische und hydrophobe Wechselwirkungen erzielt. Die Kapazität von TOYOPEARL MX-Trp-650M, einem hydrophoben CEX-Medium, für mAb erhöht sich um bis zu 125 % bei Verwendung eines Natriumacetat-Puffers, gegenüber einem Natriumcitrat-Puffer [157]. Die Verwendung eines kosmotroperen Puffers unterstützt hydrophobe Wechselwirkungen stärker als Natriumacetat. Die mit Natriumcitrat erzielten Kapazitäten für zwei verschiedene mAbs liegen im Bereich von HIC Kapazitäten. Ein kleinerer Beitrag von hydrophoben Wechselwirkungen zur Proteinadsorption scheint vorteilhaft für das Erreichen hoher Bindekapazitäten zu sein. Neben der Kapazität ist auch die Selektivität des Gels für die mAb-Aggregatabreicherung in Natriumacetat-Puffer höher, als in Natriumcitrat-Puffer [157]. Die schwachen, durch Natriumacetat verursachten hydrophoben Wechselwirkungen sind ausreichend, um die Trennschärfe des hydrophoben CEX Adsorbers gegenüber einem schwachen CEX-Medium zu erhöhen. Ein zu starker Beitrag hydrophober Wechselwirkungen, wie durch kosmotropere Salze gefördert, führt zu Verlusten der Trennschärfe. Die Verwendung verschiedener Puffersysteme mit hydrophoben CEX Adsorbern eröffnet Optimierungspotential hinsichtlich des universellen Gebrauchs von hydrophoben Kationenaustauschern. MAbs unterscheiden sich stark in ihrer Hydrophobizität. Um eine ausgewogene Kombination von hydrophoben und elektrostatischen Wechselwirkungen zu erzielen, können verschiedene hydrophobe Kationenaustauscher verwendet werden. Die Liganden der vergleichsweise wenigen kommerzialisierten

hydrophoben CEX-Medien unterscheiden sich in ihrer Hydrophobizität. Die geringe Anzahl von zur Verfügung stehenden Medien erlaubt keine kontinuierliche Einstellung der Hydrophobizität, wie sie in Kombination mit verschiedenen Puffersystemen und Dualsalzsystemen erreicht werden kann.

Hydrophobe Wechselwirkungen tragen auch zur Adsorption in der AFC bei. Die Adsorption und Desorption von mAbs an Protein A wird unter anderem durch die Protonierung von Histidingruppen in der Bindungsstelle von Protein A beeinflusst [14]. Ein Absenken des pHs der flüssigen Phase führt zur Protonierung von Histidin, wodurch der mAb eluiert werden kann. Die Verwendung von 100 mM Natriumphosphat-Puffer gegenüber 20 mM Natriumphosphat-Puffer erhöht die dynamische Kapazität von TOYOPEARL AF-rProtein A HC-650F (Abbildung 12) [107]. Die funktionelle Gruppe des Harzes ist eine hexamere Protein A Untereinheit. Ein solcher Effekt kann mit einem Tetramer-Liganden derselben Protein A Untereinheit nicht reproduziert werden. Adsorptionsisothermen mit 2 Sättigungsplateaus unter Verwendung von moderaten Natriumphosphat- und hohen mAb-Konzentrationen lassen auf eine Doppelschichtbildung schließen. Gleichzeitig führen kosmotrope Elutionspuffer zu einer Verringerung der Wirtszellproteinabreicherung.

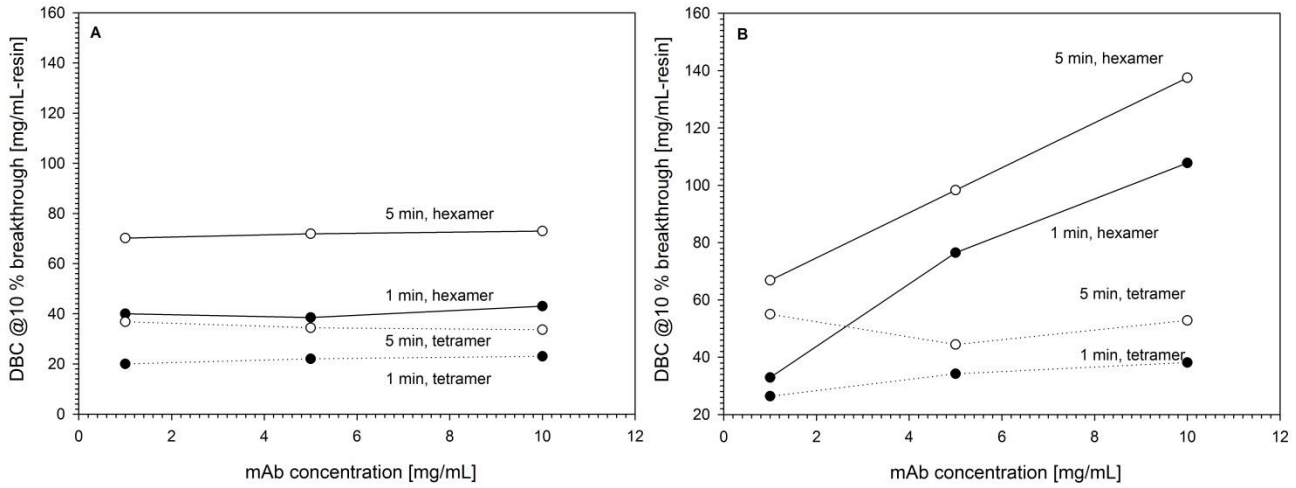

Abbildung 12: Dynamische Bindekapazitäten bei 10 % Durchbruch von TOYOPEARL AF-rProtein A HC-650F (Hexamer) und TOYOPEARL AF-rProtein A-650F (Tetramer). Die Darstellung beinhaltet Daten für 5 min Verweilzeit (°) und 1 min Verweilzeit (•). Kapazitäten wurden in 20 mM (A) und 100 mM (B) Natriumphosphat-Puffer, pH 7,0, gemessen. Die Kapazität von TOYOPEARL AF-rProtein A HC-650F steigt in 100 mM Natriumphosphat-Puffer für ansteigende mAb-Konzentrationen. Nachdruck aus J Chormatogr B, 1021, Müller, E.; Vajda, J., Routes to improve binding capacities of affinity resins demonstrated for Protein A chromatography, Seiten 159-168. © 2016 mit Genehmigung von Elsevier B.V.

6.2. Salze in der Anionenaustauschchromatographie

Salzspezifische Effekte in der IEX sind weniger komplex als in der HIC. Die Elution von Analyten erfolgt durch einen stöchiometrischen Austausch von Ladungen. Dennoch wird die Bindung eines Proteins von der Wahl des Pufferions beeinflusst. Dies ist der Diffusionsgeschwindigkeit verschiedener Ionen in Lösung und deren Bindungsavidität zur stationären Phase geschuldet. Letzteres betrifft vor allem Liganden, deren Salztoleranz durch Polyvalenz erzeugt wird. Die dynamische Bindekapazität verschiedere AEX-Medien für bovines Serumalbumin ist in Tris/HCl-Puffer entsprechend mehr als doppelt so hoch als in Natriumphosphat-Puffer (Abbildung 13 A). Von diesem Verhalten abweichende Ergebnisse wurden für Viruspartikel von zwei verschiedenen H1N1 Stämmen gefunden. Die Kapazitäten von TOYOPEARL GigaCap Q-650M und TOYOPEARL NH2-650F für H1N1v 5258 sind unbeeinflusst oder höher in Natriumphosphat-Bindepuffer (Abbildung 13 B). Dieses, gegenüber Proteinen, widersprüchliche Verhalten ist teilweise den Größenverhältnissen von Gelpartikeln und Viruspartikeln geschuldet. Proteine sind deutlich kleiner und dringen diffusionsgetragen auch in den Porenraum der Partikel ein. Ein langsames Ablösen von Gegenionen von der stationären Phase kann dazu führen, dass das Protein, bevor es zur Adsorption kommt, seine räumliche Nähe zum Liganden verlässt. Größere Viruspartikel diffundieren langsamer und das Ablösen von großen und polyvalenten Gegenionen ist relativ gesehen schneller. Es ist zudem fraglich, ob Viruspartikel

aufgrund ihrer Größe Zugang zum Porenraum haben. An der äußeren Oberfläche von Gelpartikeln wird die Fortbewegung von gelösten Salzen und Analyten durch Konvektion dominiert.

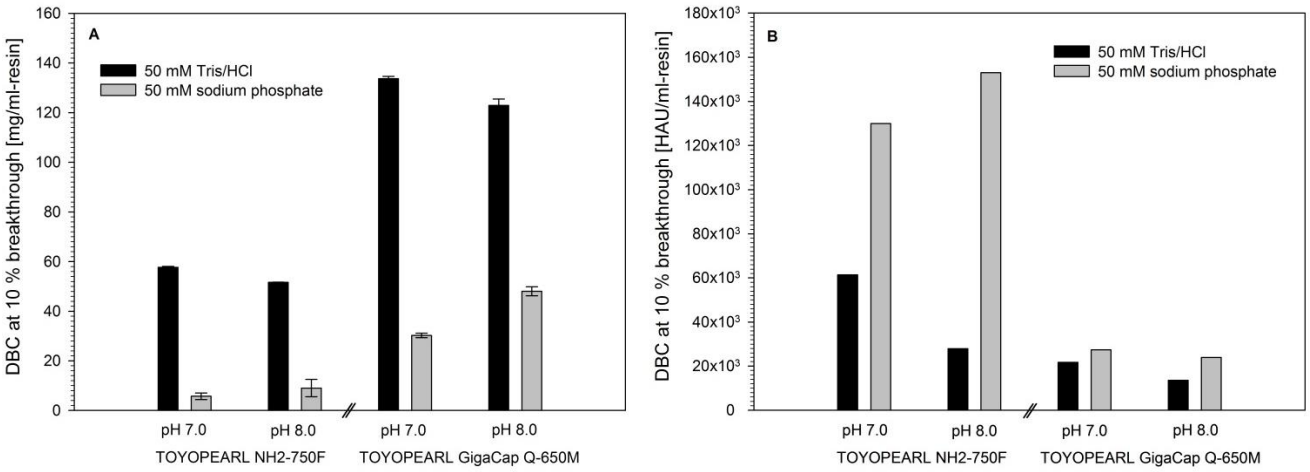

Abbildung 13: Dynamische Bindekapazitäten bei 10 % Durchbruch von TOYOPEARL GigaCap Q-650M und TOYOPEARL NH2-750F für BSA (A) und H1N1v 5258 (B). Die Kapazitäten für BSA wurden über die Absorption @280 nm bestimmt, H1N1 Kapazitäten über die HA-Aktivität der Durchflussfraktionen. Vergleichsweise höhere Kapazitäten für BSA werden mit TOYOPEARL GigaCap Q-650M in Tris/HCl-Puffer (schwarze Balken) erzielt. Für H1N1v 5258 erzielt TOYOPEARL NH2-750F in Natriumphosphat-Puffer vergleichsweise höhere Kapazitäten. Veränderte Abbildung aus [158]. Von Elsevier B.V. unter einer CC-BY-NC-ND Lizenz publizierte Daten.

TOYOPEARL NH2-750F hat höhere Kapazitäten als TOYOPEARL GigaCap Q-650M. Dies dürfte zum einen durch die Poren- und Partikelgröße bedingt sein, zum anderen durch die Struktur des Liganden. Das Polyamin-Gel hat Poren >100 nm, die zum Teil für kleinere Viruspartikel zugänglich sein dürften. Die Porengröße des nicht polymermodifizierten Basis Gels, aus dem TOYOPEARL GigaCap Q-650M hergestellt wird, beträgt 100 nm. Die durchschnittliche Partikelgröße von TOYOPEARL NH2-750F liegt bei 45 µm, im Gegensatz zu 75 µm für TOYOPEARL GigaCap Q-650M. Die äußere Oberfläche von TOYOPEARL NH2-750F ist vergleichsweise größer. Die Struktur des Polyamin-Liganden dürfte darüber hinaus zu den vergleichsweise hohen Kapazitäten beitragen.

Patch-Clamp Experimente mit liposomalen, M2 tragenden Partikeln ergaben eine hohe Affinität für die Bindung von hydrophoben Aminen und Polyaminen, wie Spermidin und Putrescin, an den M2 Ionenkanal [159]. Dies lässt auf eine Pseudoaffinitätsbindung an TOYOPEARL NH2-750F schließen. Versuche die Bindung kompetitiv durch Spermidin zu hemmen, führten zu einem gänzlichen Aktivitätsverlust der Viruspartikel, sodass keine Aussage möglich ist.

Die Kapazität beider Gele in Natriumphosphat-Puffer für H1N1v 5258 ist bis zu 6,4-fach höher [158]. Insbesondere TOYOPEARL NH2-750F hat eine höhere Kapazität in Natriumphosphat-Puffer. Natriumphosphat ist kosmotroper als Tris/HCl und unterstützt zusätzliche hydrophobe Wechselwirkungen. Präferentielle Interaktionen mit Natrium- und Phosphationen beeinflussen die elektrische Doppelschicht der Viruspartikel, sodass van der Waals Interaktionen zur Adsorption beitragen können.

Die Wiederfindung von Viruspartikeln wird ebenfalls durch die Verwendung von Natriumphosphat-Puffer positiv beeinflusst. Hsu et. al wiesen nach, dass Oberflächenbeschichtungen aus hydrophoben Polykationen inaktivierend auf Influenza wirken. Die Viruspartikel verlieren ihre sphärische Gestalt, brechen auf und virale RNA tritt aus den Partikeln aus [160]. Dieser Mechanismus scheint auch in der Chromatographie mit dem hydrophoben Polyamin-Liganden zum Tragen zu kommen. Die Viruspartikel Wiederfindung von diesem Gel ist mit Ausnahme der Elution durch polyvalente Puffer, vernachlässigbar. Natriumcitrat und Natriumphosphat begünstigen die Wiederfindung. Dieser Effekt dürfte auf der höheren Avidität von Citrat und Phosphat beruhen. Eine weitere Steigerung der Viruspartikel Wiederfindung kann durch die Adsorption in Natriumphosphat-Puffer gegenüber einer Adsorption in Tris/HCl erzielt werden. Natriumionen besetzen in physiologischer Umgebung den M2 Ionenkanal, was zu einer Stabilisierung der Viruspartikel führen könnte. Ein Zusammenhang zwischen der vorgeschlagenen Pseudoaffinitätsbindung an TOYOPEARL NH2-

750F und der Wiederfindung liegt nahe, da die Wiederfindung von TOYOPEARL GigaCap Q-650M von der Wahl des Bindepuffers weniger stark beeinträchtigt ist.

Die Wiederfindungen erscheinen durchweg niedrig im Vergleich zu Wiederfindungsraten von typischen AEX Schritten zur Aufreinigung von Proteinen. Ebenfalls auffällig ist die hohe Diskrepanz zwischen den einzelnen Wiederfindungsraten, die durch SEC und den HA-Assay ermittelt wurden. Diese Phänomene sowie Wiederfindungsraten >100 % werden in Kapitel 6.3, dem Ergebnisteil für die analytische SEC erläutert. Vergleichswerte aus der Literatur basieren in den meisten Fällen auf dem HA-Assay. Aus diesem Grund wird eine Einordnung der Wiederfindungsraten auf Grundlage der HA-Assay basierenden Wiederfindungsraten vorgenommen. Opitz et al. erzielten eine Wiederfindungsrate von 67,6 ± 9,8 % in der Elutionsfraktion von Cellufine™ Sulfate, einem Pseudoaffinitätsgel für die Isolierung von Influenzaviruspartikeln aus Zellkulturüberstand oder Hühnerei. Die verbleibende Virusaktivität wurde im Durchfluss wiedergefunden [69]. Bei einem AEX Schritt zur Reinigung von H1N1 PR/8/34 mit Sepharose Q XL nach SEC konnten >80 % der Virusaktivität wiedergefunden werden [63]. Nicht-adsorptive Chromatographieschritte erzielen nicht notwendigerweise eine höhere Wiederfindung. Ergebnissen von Weigel et al. zur Folge, liegt die HA-Aktivität von verschiedenen Influenza A und B Viruspartikeln nach DNase-Behandlung und Durchflusschromatographie mit DEAE Sepharose FF zwischen 96 % und 99 % [44]. Die Wiederfindung eines auf Sepharose 2B basierenden SEC Schrittes für equine Influenzapartikel liegt bei 37,8 % [43]. Durchschnittlich 85 % der HA-Aktivität von H1N1 PR/8/34 wurden nach einer präparativen SEC mit Sepharose 4FF wiedergefunden [63]. Die im Rahmen dieser Dissertation durchgeführten Experimente erzielten Wiederfindungsraten von bis zu 50,0 % für TOYOPEARL NH2-750F und 251,6 % für TOYOPEARL GigaCap Q-650M [158]. Unter Berücksichtigung des eigentlichen Zieles, eine Methode zur Prozessentwicklung für Viruspartikel zu etablieren und den Einfluss verschiedener Puffer und Elektrolyte auf die AEX zu untersuchen, sind die ermittelten Wiederfindungsraten akzeptabel.

Die Abreicherung von Wirtszellproteinen und DNA kann im Kontext der durchgeführten Versuche nur vergleichend betrachtet werden. Weitere Schritte zur Prozessoptimierung, wie die Entwicklung eines Gradienten und eine größere Skalierung der Säulen sind notwendig, um reelle Trennungen zu erzielen. Dennoch zeigt ein Vergleich der DNA-Wiederfindungsraten, dass polyvalente Ionen für die Elution von DNA vorteilhaft sind. Dies wirkt sich negativ auf die Reinheit des Viruseluates aus und dürfte durch die größere Avidität dieser Ionen bedingt sein. Der Wahl des Bindepuffers kommt nur geringe Bedeutung zu. Die DNA-Abreicherung durch beide Chromatographieharze in Natriumphosphat-Eluaten liegt unabhängig vom Bindepuffer bei 90% [158]. Dementgegen sind die Proteinabreicherungsraten höher für die Adsorption in Natriumphosphat-Puffer. Die Kapazität von AEX Harzen für Proteine in Natriumphosphat-Puffer ist niedriger als in Tris/HCl-Puffer. Darüber hinaus wurde die Proteinabreicherung mittels analytischer SEC bestimmt. Dabei kann nicht zwischen Wirtszellproteinen und Virusfragmenten unterschieden werden. Dies unterstützt die Hypothese, dass Natriumphosphat-Puffer zur Stabilität von Viruspartikeln beiträgt.

Entgegen der gängigen Praxis bezüglich der Pufferwahl für die AEX eignet sich Natriumphosphat-Puffer zur AEX von Viruspartikeln. Im Hinblick auf ein möglichst wirtschaftliches Verfahren entfällt durch die Verwendung von Phosphat-Puffer ein Prozessschritt zum Pufferwechsel, wie zum Beispiel ein Diafiltrationsschritt. Kapazität, Reinheit und Wiederfindung sind vergleichsweise robust gegenüber Änderungen im getesteten pH Bereich. Die angewendete, miniaturisierte Parallelchromatographie auf einem Pipettierroboter erlaubt ein vergleichsweise schnelles Sichten verschiedener Bedingungen und die Automatisierung des arbeits- und zeitintensiven HA-Assays. Obwohl dieser Ansatz aus der Prozessentwicklung für therapeutische Proteine hinreichend bekannt ist und erfolgreich eingesetzt wird, wurde die Anwendung der Methode auf Viruspartikel (nach jetzigem Kenntnisstand) zuvor nicht publiziert. Die Stabilität von Viruspartikeln und Erythrozyten gegenüber Scherkräften setzt eine Anpassung des Pipettiervorgangs voraus. Unter Berücksichtigung dieser Einschränkung erlaubt die miniaturisierte Parallelchromatographie eine erhebliche Steigerung des Durchsatzes bei geringerem Probenverbrauch und ermöglicht eine reelle Prozessentwicklung, wie sie für die Aufreinigung von Viruspartikeln (bisher) wenig üblich ist.

6.3. Analytische Größenausschlusschromatographie

Die effiziente Entwicklung eines Aufreinigungsverfahrens erfordert eine schnelle und zuverlässige, qualitative und quantitative Analytik von Ausgangsstoffen und Produkten eines Prozessschrittes. Die SEC, die zu diesem Zweck für die Analytik von Proteinen verwendet wird, kann auch zur Analytik von Viruspartikeln angewendet werden. Influenzaviruspartikel haben einen durchschnittlichen Durchmesser 100 nm. Die Porengröße einer stationären Phase sollte 3-10 mal so groß sein wie ein Analyt [110]. Gemäß dieser Annäherung läge die erforderliche Porengröße bei 300-1000 nm. Die Trennung von H1H1v 5258, H1N1 PR/8/34 und H3N2 Aichi/2/68 von Wirtszellproteinen und anderen Verunreinigungen kann mit TSKgel G6000PWxl realisiert werden. Quecksilberporosimetrie ergab eine mittlere Porengröße von 250 nm mit einer Verteilung, die sich von 100 - 1000 nm erstreckt [161]. Die Identifikation des Viruspeaks erfolgte durch eine für den hochmolekularen Teil fortgeführte Kalibrationskurve für Proteine auf dieser Säule. Das Molekulargewicht des Proteinanteils am Virus beträgt 26600 kDa [63][30]. Die Verfügbarkeit ähnlich großer, monodisperser Proteine ist stark eingeschränkt. Das Elutionsvolumen aller Viruspartikel beträgt (unter den gegebenen Bedingungen) 9 mL. Die in dieser Arbeit verwendeten Laborstämme H1H1 PR/8/34 und H3N2 Aichi/2/68 wurden beide in embryonierten Hühnereiern vermehrt, H1N1v 5258 in MDBK Zellen. Unterschiede ergeben sich auch durch die verschiedenen Inaktivierungsagenzien. Darüber hinaus sind H1N1 Puerto Rico/8/34 und H3N2 Aichi/2/68 über Dichtegradientenzentrifugation aufgereinigt und aufkonzentriert. Die SEC mit TSKgel G6000PWxl zeigt, dass in allen Proben niedermolekulare Substanzen enthalten sind. Die nicht vorgereinigte Probe von H1N1v 5258 enthält einen vergleichsweise hohen Anteil an niedermolekularen, ultraviolette Strahlung absorbierenden Komponenten. Neben Viruspartikelfragmenten dürften auch Wirtszellproteine darunter sein. In einem semi-präparativen Ansatz wurden 1 mL Fraktionen der durch SEC getrennten Virusproben gesammelt. Die HA-Aktivität der einzelnen Fraktionen wurde mit dem HA-Assay bestimmt. Abbildung 14 stellt die Ergebnisse dar. Die Fraktionen zwischen 8 und 10 mL Elutionsvolumen weisen die höchste HA-Aktivität auf, was die Identifikation dieses Peaks durch Kalibration bestätigt. Über 50 % der insgesamt widergefundenen HA-Aktivität befinden sich in den Fraktionen, die nach 10 mL und später eluieren.

Die HA-Aktivität der aufsummierten Fraktionen stimmt gut mit den injizierten HA-Aktivitäten überein. Etwaige Verluste von Virusmaterial durch sekundäre Wechselwirkungen sind unter den angewandten Bedingungen vernachlässigbar. Von 3.9 log HAU H1N1v 5258 können 4.1 log HAU in den Fraktionen wiedergefunden werden. Von PR/8/34 wurden 5.4 log HAU injiziert. Die Aufsummierung der SEC Fraktionen ergibt 5.2 log HAU. Für H3N2 Aichi/2/68 ergibt sich eine vergleichsweise größere Differenz in der Massenbilanz. Von den applizierten 5.4 log HAU werden 4.8 log HAU wiedergefunden. Die Abweichungen der Wiederfindungsraten sind höchstwahrscheinlich durch die Schwankungen des HA-Assays und durch dessen diskretes Format bedingt. Aktivitätsverluste können sich auch durch den Verlust der Randfraktionen ergeben, deren Aktivität möglicherweise unterhalb des LOD des Assays liegt. Die Ergebnisse deuten darauf hin, dass niedrige Ausbeuten in der präparativen SEC von Influenzaviruspartikeln durch eine fragmentierte Probe zu Stande kommen können. Die wiedergefundene HA-Aktivität im Viruspeak eines präparativen SEC Schrittes für equine Influenzaviren liegt beispielsweise bei 37,4 % [43].

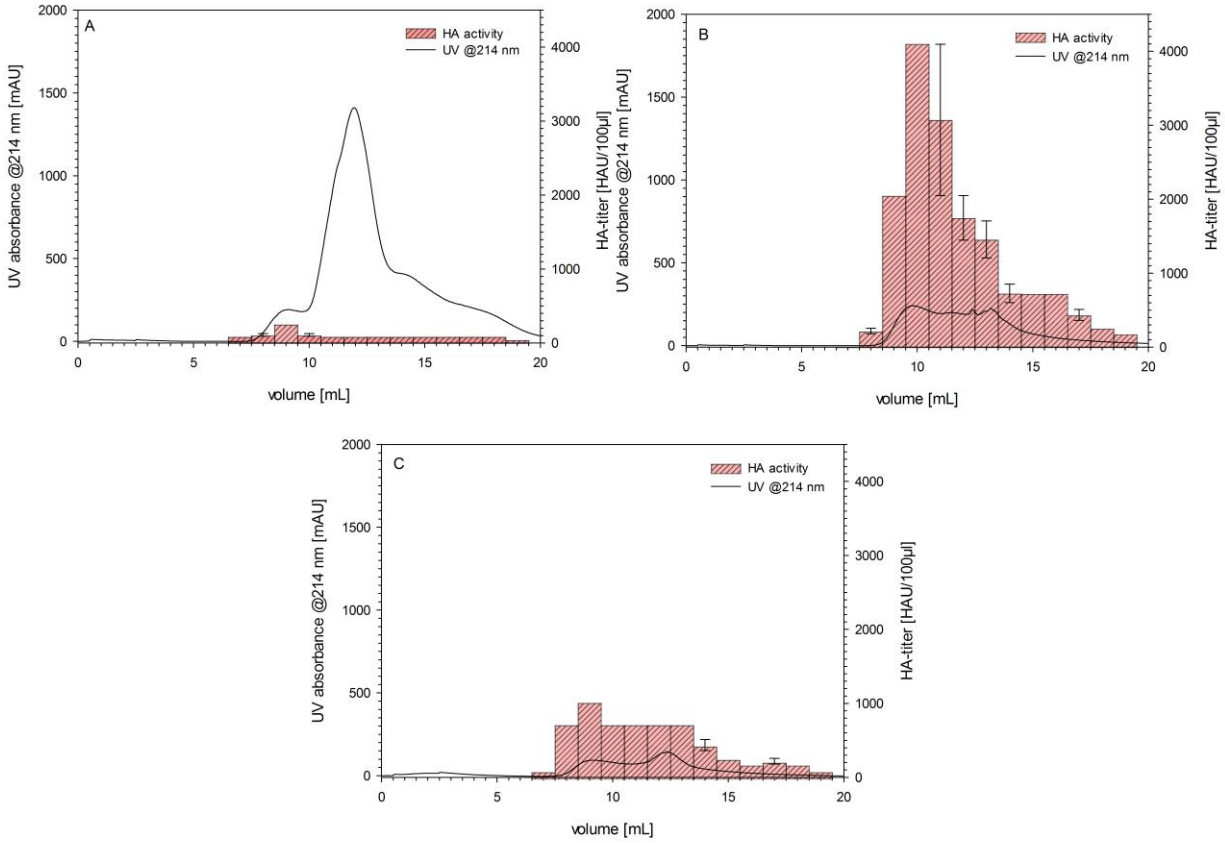

Abbildung 14: SEC Chromatogramme von H1N1v 5258 (A), H1N1 PR/8/34 (B) und H3N2 Aichi/2/68 (C) auf TSKgel G6000PWxl. Die HA-Aktivität der gesammelten Fraktionen wird durch die roten Balken dargestellt. Die höchste HA-Aktivität ist jeweils dem Virusmonomer, das zwischen 8 und 10 min eluiert, zuzuschreiben. Über 50 % der HA-Aktivität befinden sich in den später eluierenden Fraktionen. Veränderte Abbildung aus [161].

In Bezug auf die Quantifizierung von Influenzaviruspartikeln durch den HA-Assay erklärt dies Wiederfindungsraten >100 % und einen Teil der hohen Schwankungen dieses Assays. Einzelne Hemagglutinin Proteine führen nicht zur Quervernetzung mit Erythrozyten. Jedoch verfügen Viruspartikelfragmente diesen Ergebnissen zur Folge eine nicht zu vernachlässigende HA-Aktivität. Viruspartikelfragmentation erhöht die Anzahl der HA-induzierenden Moleküle. Bei einem stöchiometrischen Verhältnis von einem Erythrozyt pro Viruspartikel oder Viruspartikelfragment führt Viruspartikelfragmentation zu falsch positiven Ergebnissen. Viruspartikelaggregation könnte zu einer Abnahme der HA-Aktivität führen. Solche potentiell falsch negativen HA-Aktivitäten sind als besonders kritisch einzustufen. Die Größe eines Pathogens stellt einen Schlüsselreiz für das menschliche Immunsystem dar [162], wodurch eine Potenzierung der Immunantwort in Folge der Impfung möglich wäre. Neben der Größenverteilung einer Viruspartikelprobe kann die Aktivität der Oberflächenproteine durch verschiedene Prozessbedingungen variieren. Inaktivierungsagenzien verändern die HA-Aktivität von Influenza [66]. Die Behandlung von H1N1v 5258 mit Triton X-100 führt zu einer Fragmentation der Viruspartikel. Bei Anwendung niedriger Konzentrationen des Detergens wird die HA-Aktivität erhöht. Dementgegen führt die Inkubation von H1N1v 5258 bei >50 °C ebenfalls zur Fragmentation und einem Verlust der HA-Aktivität. Diese Ergebnisse unterstreichen die Empfehlung der Europäischen Arzneimittel-Agentur EMA, Influenzaviruspartikel und Formulierungen auf ihren Aggregatgehalt hin zu untersuchen [163]. Den Ergebnissen dieser Arbeit zur Folge ermöglicht SEC eine schnelle und automatisierbare Analytik der Größenverteilung von Influenzaviruspartikeln [161].

Die angewandten Flussraten in der SEC von Viruspartikeln haben einen wesentlich Einfluss auf die Analytik. Proteine, wie zum Beispiel mAbs, diffundieren langsamer als klassische pharmazeutische Wirkstoffe. Da die Retention in der SEC auf der Diffusion in der stagnierenden Flüssigphase beruht, profitieren größenausschlusschromatographische Proteintrennungen von vergleichsweise niedrigen Flussraten. Aus den van Deemter Kurven für mAb-Monomere und mAb-Dimere (Abbildung 15 A & B) ist eine Erhöhung dieser Flussratenabhängigkeit für die größeren Dimere ersichtlich. Vor diesem Hintergrund sollten die Flussraten zur Trennung von Viruspartikeln noch weiter herabgesetzt werden, da diese aufgrund ihrer Größe eine geringere Diffusivität als Proteine haben. Die van Deemter Kurven (Abbildung 15 C) für Viruspartikel auf TSKgel G6000PW, TSKgel G6000PWxl und TSKgel G-DNA-PW zeigen ein abweichendes Verhalten [112].

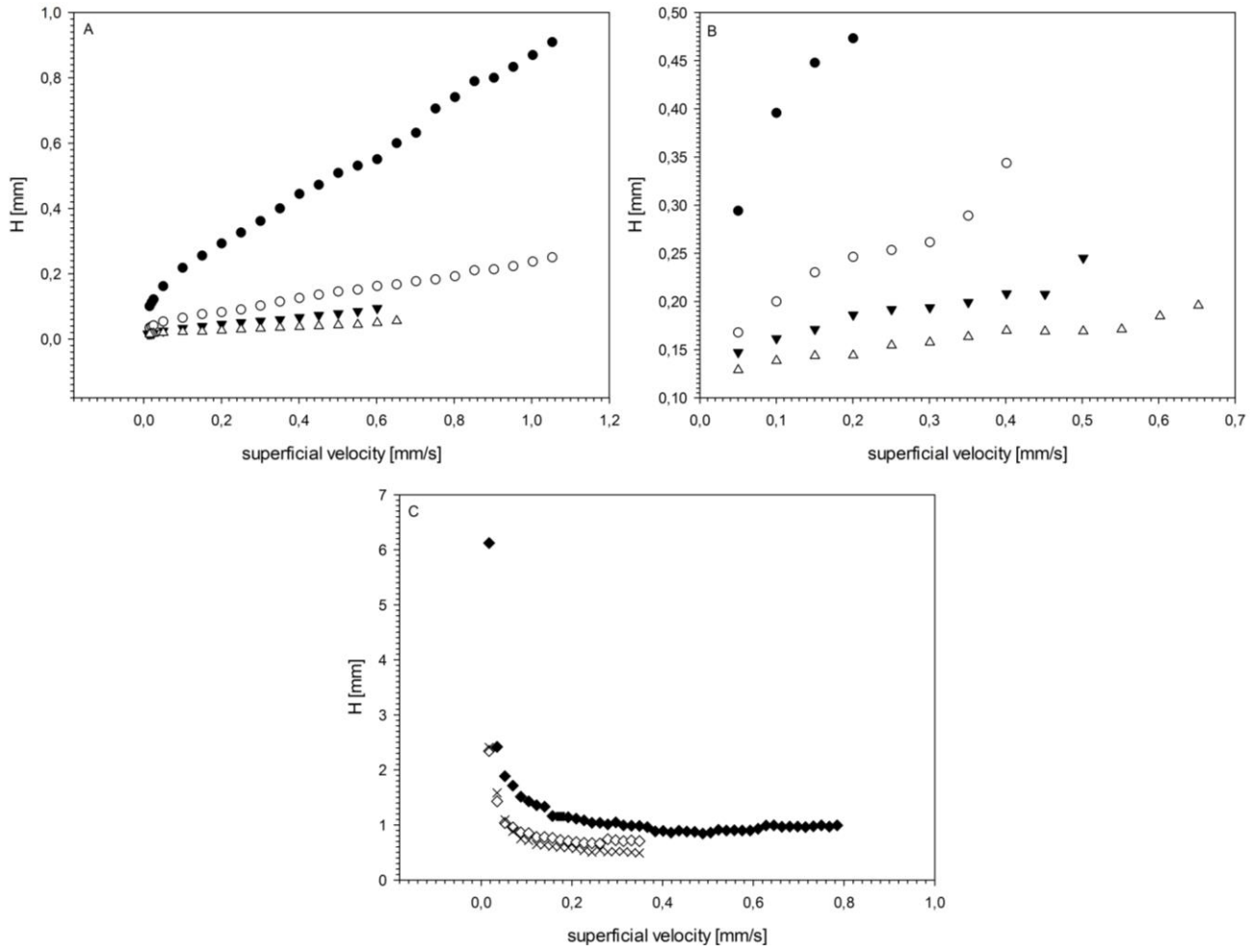

Abbildung 15: van Deemter Kurven für mAb-Monomer (A), mAb-Dimer (B) und H1N1v Viruspartikel (C). Die Trennungen wurden auf verschiedenen Partikelgrößen realisiert: 10 µm (•), 5 µm (°), 4 µm (▼), 2 µm (Δ), 17 µm (♦), 13 µm (◊) und 10 µm(x). Geringfügig veränderter Graph aus [112]. Von Elsevier B.V. unter einer CC-BY-NC-ND Lizenz publizierte Daten.

Ähnlich wie die van Deemter Kurven für niedermolekulare Substanzen steigen die Bodenhöhen für sehr langsame Flussraten an. Anders als bei niedermolekularen Substanzen kann dieses Verhalten aber nicht auf die verhältnismäßig hohe, longitudinale Diffusion zurückgeführt werden. Wahrscheinlicher erscheint eine zunehmende Viruspartikelpolydispersität. Die sehr langsamen Flussraten führen zu Analysezeiten über 6 h. Das Viruspartikel ist in dieser Zeit Druck und der Raumtemperatur ausgesetzt. Für moderate und hohe Flussraten ist der Anstieg der Bodenhöhe, wie er für mAbs und niedermolekulare Substanzen beobachtet werden kann, vergleichsweise gering. Ursache hierfür dürfte die Kopplung von Massentransfer und Eddy Diffusion sein [114][113]. Für die Analytik von Influenzaviruspartikeln mit diesen Säulen ergibt sich dadurch ein von gängigen Annahmen abweichendes Bild. Die Analytik der Influenzaviruspartikel profitiert von Flussraten im Bereich von 0.7 – 1.0 mL/min. Demgegenüber sind die theoretischen Bodenhöhen für mAb und mAb-Dimere desto niedriger, je langsamer die angewendete Flussrate ist. Dies gilt für TSKgel G3000SW, TSKgel G3000SWxl, TSKgel SuperSW3000 und TSKgel UP-SW3000. Alle Säulen zur mAb-

Analytik haben 25 nm Poren und unterscheiden sich in ihrer Partikelgröße. Ein differenziertes Bild kann durch den Vergleich der Trennungen in kinetischen Plots gewonnen werden. Die notwendige Zeit zum Erreichen eines theoretischen Bodens kann als Parameter zum Leistungsvergleich verschiedener Säulen herangezogen werden. Poppe Plots sind eine Form kinetischer Plots. Poppe Plots für mAb und Influenzaviruspartikel sind in Abbildung 16 dargestellt.

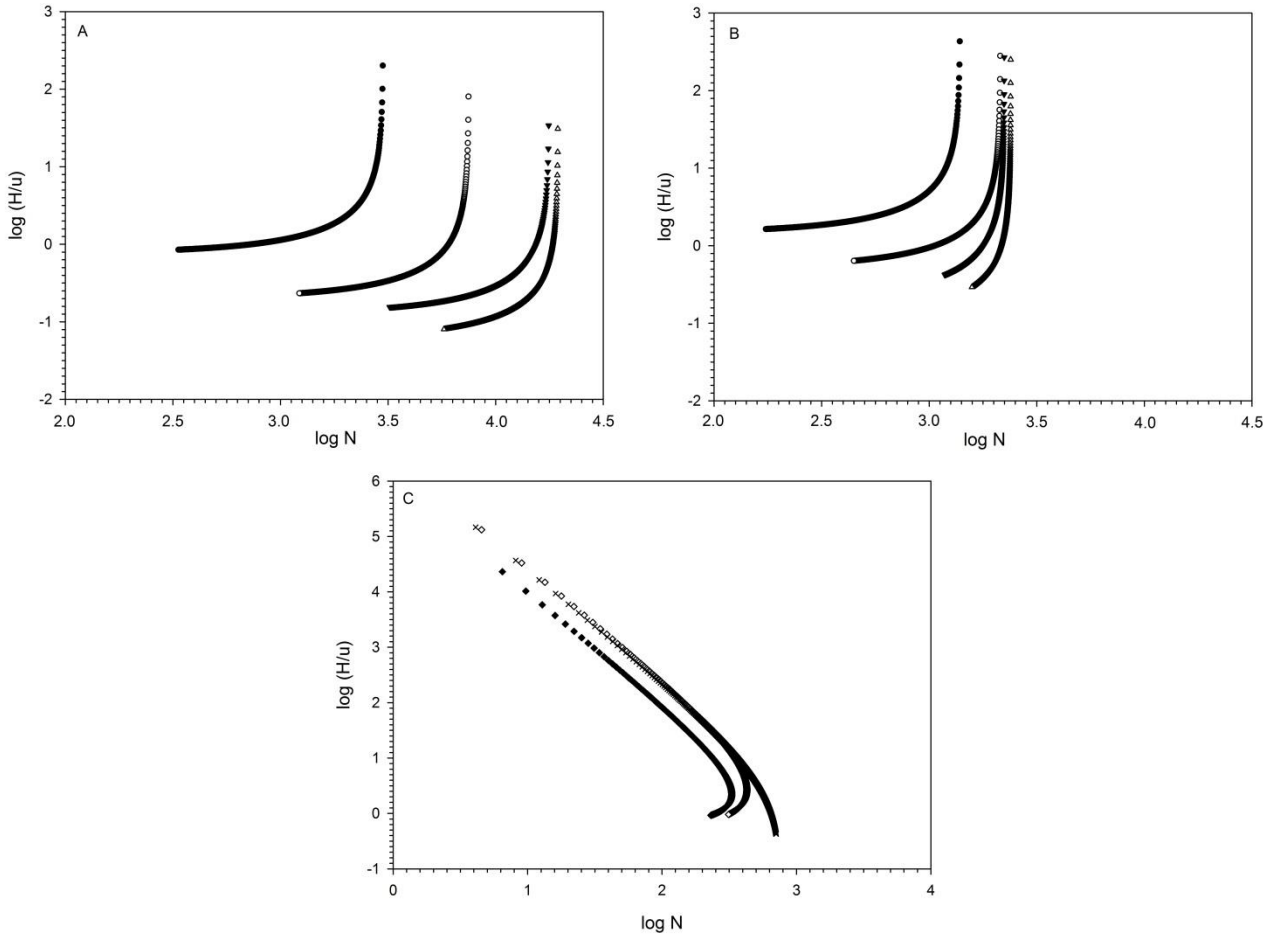

Abbildung 16: Poppe Plots für mAb-Monomere (A), mAb-Dimere (B) und H1N1v Viruspartikel (C). Poppe Plots sind für jeweils verschiedene Partikelgrößen dargestellt: 10 µm (•), 5 µm (°), 4 µm (▼), 2 µm (Δ), 17 µm (♦), 13 µm (◊) und 10 µm(x). Veränderter Graph aus [112]. Von Elsevier B.V. unter einer CC-BY-NC-ND Lizenz publizierte Daten.

Ein wichtiger, in den Poppe Plots ersichtlicher Aspekt bei der SEC von verschiedenen Biopharmazeutika ist, dass die Größe des Analyten die optimale Partikelgröße beeinflusst [112]. MAbs haben eine durchschnittliche Größe von 5 nm. Die maximale Bodenzahl für mAb-Monomere nimmt mit abnehmender Partikelgröße bis hin zu 2 µm Partikeln zu. Bei den größeren mAb-Dimeren wird die Bodenzahl durch die Verwendung von 2 µm Partikeln anstatt von 4 µm Partikeln kaum positiv beeinflusst. Ein weiterer Anstieg der Partikelgröße auf 5 oder 10 µm führt jedoch zu einem Abfall der Bodenzahlen. Dieser Trend wird durch die Viruspartikel fortgesetzt. Die erreichten Bodenzahlen von 10 µm und 13 µm Partikeln sind nahezu gleich. 17 µm Partikel führen zu einer niedrigeren Bodenzahl.

Neben der Bodenhöhe ist die Auflösung ein wichtiger Parameter zur Abschätzung der Trennleistung einer Säule. In der Biochromatographie kommt der Auflösung eine ebenso wichtige Rolle zu, wie der Bodenzahl. Die Verlässlichkeit und Genauigkeit einer Aggregatanalytik und Produktquantifizierung beruht auf der vollständigen Auflösung des Zielpeaks von anderen Peaks. Die Auflösung von mAbs und mAb-Aggregaten, sowie die Auflösung von Viruspartikeln und niedermolekularen Komponenten verändern sich in Abhängigkeit vom Fluss. Die zum Erreichen eines theoretischen Bodens notwendige Zeit korreliert nichtlinear mit der Auflösung [112].

7. Ausblick

Im Rahmen dieser Arbeit wurde der Einfluss chaotrop-kosmotroper Dualsalzgemische auf hydrophobe Wechselwirkungen zur Biochromatographie untersucht. Hydrophobe Wechselwirkungen spielen nicht nur in der HIC, sondern auch in der MXC mit hydrophoben Kationenaustauschern und in der AFC eine Rolle. In den beiden letztgenannten Modi wurde verschiedenen Elektrolyten bisher wenig Bedeutung beigemessen. Die Kapazität und Selektivität aller genannten Modi kann unter Beachtung des verwendeten Puffers gesteigert und moduliert werden. Verantwortlich ist die differenzierte Löslichkeitsvermittlung. Eine Berücksichtigung von pufferspezifischen Effekten in der Entwicklung von AFC und MXC könnte die Produktivität zukünftiger Aufreinigungsprozesse erheblich steigern. In Ermangelung einer systematischen Beschreibung für dualsalzinduzierte Effekte könnten diese auf Grundlage empirischer Experimente zum Einsatz kommen. Dies ist für Aufreinigungsprobleme sinnvoll, die anderweitig nicht gelöst werden können. In solchen Fällen kann miniaturisierte Parallelchromatographie einen wertvollen Beitrag dazu leisten, die Prozessentwicklungsdauer möglichst gering zu halten.

Die Nutzung miniaturisierter Parallelchromatographie und der zugehörigen Laborinfrastruktur zur Entwicklung von Aufreinigungsprozessen für auf ganzen Viruspartikeln basierende Vakzine dürfte das Prozessverständnis weiter vorantreiben. Aus der Proteinchromatographie bekannte Effekte verschiedener Puffersystem können dabei nicht ohne weiteres übernommen und angewendet werden. Um die Pseudoaffinitätsbindung von Influenza A Viruspartikeln an TOYOPEARL NH2-750F genauer zu untersuchen, sollten weitere Virusstämme hinzugezogen werden. Aufgrund der weiten Verbreitung von Viroporinen könnten auch andere Viren über eine Pseudoaffinitätschromatographie mit TOYOPEARL NH2-750F oder strukturverwandten Liganden aufgereinigt werden. Einflüsse durch verschiedene Inaktivierungsmethoden, und die dabei eingeführten Veränderungen der viralen Oberflächenproteine, sollten untersucht werden. Versuche bezüglich der Universalität von durch polyvalente Ionen vermittelten Effekten können zu einer weiteren Differenzierung des Verhaltens von Viruspartikeln in der Chromatographie beitragen. Die Entwicklung von Plattformverfahren setzt ein breiteres Verständnis für das Verhalten von Viruspartikeln in der Chromatographie voraus.
Ein zusätzlicher Aspekt ergibt sich aus der Notwendigkeit der Virusabreicherung in Proteinaufreinigungsprozessen. Die vorgeschlagene Pseudoaffinität des Polyamin-Liganden könnten zur Abreicherung behüllter Viren genutzt werden.

SEC ermöglicht eine schnelle und automatisierbare Analytik in der Entwicklung von Aufreinigungsschritten für Influenzaviruspartikel. Im Vergleich zum gängigen HA-Assay wird SEC weniger durch Interferenzen von verschiedenen Elektrolyten beeinflusst. Trotzdem sollte die SEC mit aktivitätsbasierten Assays kombiniert werden, um eine vollständige Aussage über den Viruspartikelgehalt und dessen Aktivität treffen zu können. Die Anwendbarkeit auf weitere Viruspartikel bleibt zu überprüfen.

8. Anhang

8.1. Literaturverzeichnis

[1] EvaluatePharma, World Preview 2015, Outlook to 2020, 2015. http://info.evaluategroup.com/rs/607-YGS-364/images/wp15.pdf.

[2] Statista, AbbVie's revenue from top product Humira from 2011 to 2015 (in million U.S. $), (2016). http://www.statista.com/statistics/318206/revenue-of-humira/ (accessed March 29, 2016).

[3] M. Tirell, The $1.6 billion business of flus, CNBC Homepage. (2015). http://www.cnbc.com/2015/10/19/ (accessed June 14, 2016).

[4] I. Miloud Kaddar, WHO, Global Vaccine Market Features and Trends, Geneva, 2008. http://who.int/influenza_vaccines_plan/resources/session_10_kaddar.pdf.

[5] D.M. Ecker, S.D. Jones, H.L. Levine, The therapeutic monoclonal antibody market., MAbs. 7 (2015) 9–14. doi:10.4161/19420862.2015.989042.

[6] M. Tomita, K. Tsumoto, Hybridoma technologies for antibody production., Immunotherapy. 3 (2011) 371–80. doi:10.2217/imt.11.4.

[7] J.A. Kimball, D.J. Norman, C.F. Shield, T.J. Schroeder, P. Lisi, M. Garovoy, et al., The OKT3 Antibody Response Study: a multicentre study of human anti-mouse antibody (HAMA) production following OKT3 use in solid organ transplantation., Transpl. Immunol. 3 (1995) 212–21. http://www.ncbi.nlm.nih.gov/pubmed/8581409 (accessed February 2, 2016).

[8] J.C. Almagro, W.R. Strohl, Antibody Engineering: Humanization, Affinity Maturation and Selection Techniques, in: Z. An (Ed.), Ther. Monoclon. Antibodies - From Bench to Clin., John Wiley & Sons, Hoboken, 2009: pp. 311–334.

[9] M.L. Kennard, D.L. Goosney, D. Monteith, L. Zhang, M. Moffat, D. Fischer, et al., The generation of stable, high MAb expressing CHO cell lines based on the artificial chromosome expression (ACE) technology., Biotechnol. Bioeng. 104 (2009) 540–53. doi:10.1002/bit.22406.

[10] A. a. Shukla, J. Thömmes, Recent advances in large-scale production of monoclonal antibodies and related proteins, Trends Biotechnol. 28 (2010) 253–261. doi:10.1016/j.tibtech.2010.02.001.

[11] A.C.A. Roque, C.R. Lowe, M.A. Taipa, Antibodies and genetically engineered related molecules: production and purification., Biotechnol. Prog. 20 (2004) 639–54. doi:10.1021/bp030070k.

[12] A.M. Azevedo, P. a J. Rosa, I.F. Ferreira, J. de Vries, T.J. Visser, M.R. Aires-Barros, Downstream processing of human antibodies integrating an extraction capture step and cation exchange chromatography, J. Chromatogr. B Anal. Technol. Biomed. Life Sci. 877 (2009) 50–58. doi:10.1016/j.jchromb.2008.11.014.

[13] S. Lute, L. Norling, M. Hanson, R. Emery, D. Stinson, K. Padua, et al., Robustness of virus removal by protein A chromatography is independent of media lifetime, J. Chromatogr. A. 1205 (2008) 17–25. doi:10.1016/j.chroma.2008.07.094.

[14] S. Vunnum, G. Vedantham, B. Hubbard, Protein A based Affinity Chromatography, in: U. Gottschalk (Ed.), Process Scale Purif. Antibodies, John Wiley & Sons, Hoboken, 2009: pp. 79–99.

[15] A. a. Shukla, B. Hubbard, T. Tressel, S. Guhan, D. Low, Downstream processing of monoclonal antibodies-Application of platform approaches, J. Chromatogr. B Anal. Technol. Biomed. Life Sci. 848 (2007) 28–39. doi:10.1016/j.jchromb.2006.09.026.

[16] M. Franzreb, E. Müller, J. Vajda, Cost Estimation for Protein A Chromatography, BioProcess Inl 12(9). (2014) 44–52.

[17] S. Amin, G. V. Barnett, J.A. Pathak, C.J. Roberts, P.S. Sarangapani, Protein aggregation, particle formation, characterization & rheology, Curr. Opin. Colloid Interface Sci. 19 (2014) 438–449. doi:10.1016/j.cocis.2014.10.002.

[18] J.S. Bee, M. Davis, E. Freund, J.F. Carpenter, T.W. Randolph, Aggregation of a monoclonal antibody induced by adsorption to stainless steel., Biotechnol. Bioeng. 105 (2010) 121–9. doi:10.1002/bit.22525.

[19] J.S. Bee, J.L. Stevenson, B. Mehta, J. Svitel, J. Pollastrini, R. Platz, et al., Response of a concentrated monoclonal antibody formulation to high shear., Biotechnol. Bioeng. 103 (2009) 936–43. doi:10.1002/bit.22336.

[20] M. Vázquez-Rey, D.A. Lang, Aggregates in monoclonal antibody manufacturing processes., Biotechnol. Bioeng. 108 (2011) 1494–508. doi:10.1002/bit.23155.

[21] P. Gagnon, R. Nian, D. Leong, A. Hoi, Transient conformational modification of immunoglobulin G during purification by protein A affinity chromatography, J. Chromatogr. A. 1395 (2015) 136–142. doi:10.1016/j.chroma.2015.03.080.

[22] L.A. Kueltzo, W. Wang, T.W. Randolph, J.F. Carpenter, Effects of solution conditions, processing parameters, and container materials on aggregation of a monoclonal antibody during freeze-thawing., J. Pharm. Sci. 97 (2008) 1801–12. doi:10.1002/jps.21110.
[23] S. Aldington, J. Bonnerjea, Scale-up of monoclonal antibody purification processes, J. Chromatogr. B Anal. Technol. Biomed. Life Sci. 848 (2007) 64–78. doi:10.1016/j.jchromb.2006.11.032.
[24] P. Gagnon, Technology trends in antibody purification, J. Chromatogr. A. 1221 (2012) 57–70. doi:10.1016/j.chroma.2011.10.034.
[25] E. Müller, Comparison between mass transfer properties of weak-anion-exchange resins with graft-functionalized polymer layers and traditional ungrafted resins., J. Chromatogr. A. 1006 (2003) 229–40. doi:10.1016/S0021-9673(03)00555-7.
[26] A.M. Lenhoff, Protein adsorption and transport in polymer-functionalized ion-exchangers., J. Chromatogr. A. 1218 (2011) 8748–59. doi:10.1016/j.chroma.2011.06.061.
[27] P. Gagnon, IgG aggregate removal by charged-hydrophobic mixed mode chromatography., Curr. Pharm. Biotechnol. 10 (2009) 434–9. http://www.ncbi.nlm.nih.gov/pubmed/19519420 (accessed March 5, 2016).
[28] B.M. Hause, E.A. Collin, R. Liu, B. Huang, Z. Sheng, W. Lu, et al., Characterization of a novel influenza virus in cattle and Swine: proposal for a new genus in the Orthomyxoviridae family., MBio. 5 (2014) e00031–14. doi:10.1128/mBio.00031-14.
[29] C. Gerdil, The annual production cycle for influenza vaccine., Vaccine. 21 (2003) 1776–9. http://www.ncbi.nlm.nih.gov/pubmed/12686093 (accessed January 15, 2016).
[30] P. Palese, Orthomyxoviridae, in: D.M. Knipe, P.M. Howley, D.E. Griffin, R.A. Lamb, M.A. Martin, B. Roizman, et al. (Eds.), Fields Virol., Lippincott Wiliams & Wilkins, Philadelphia, 2007: pp. 1647–1689.
[31] R.G. Webster, W. Bean, O. Gorman, T. Chambers, Y. Kawaoka, Evolution and ecology of influenza A viruses., Microbiol. Rev. 56 (1992) 152–179.
[32] S.S.Y. Wong, K. Yuen, Avian Influenza Virus Infections in Humans, CHEST Glob. Med. 129 (2006) 156–168. doi:10.1378/chest.130.1.261.
[33] G. Neumann, T. Noda, Y. Kawaoka, Emergence and pandemic potential of swine-origin H1N1 influenza virus, Nature. 459 (2009) 931–939. doi:10.1038/nature08157.Emergence.
[34] Y. Watanabe, M.S. Ibrahim, K. Ikuta, Evolution and control of H5N1, EMBO Rep. 14 (2013) 1–6. doi:10.1038/embor.2012.212.
[35] C.M. Mair, K. Ludwig, A. Herrmann, C. Sieben, Receptor binding and pH stability - how influenza A virus hemagglutinin affects host-specific virus infection., Biochim. Biophys. Acta. 1838 (2014) 1153–68. doi:10.1016/j.bbamem.2013.10.004.
[36] T. Ito, J.N.S.S. Couceiro, S. Kelm, L.G. Baum, S. Krauss, M.R. Castrucci, et al., Molecular Basis for the Generation in Pigs of Influenza A Viruses with Pandemic Potential, J. Virol. 72 (1998) 7367–7373. http://jvi.asm.org/content/72/9/7367.short (accessed January 11, 2016).
[37] S. Grambas, M.S. Bennett, A.J. Hay, Influence of amantadine resistance mutations on the pH regulatory function of the M2 protein of influenza A viruses, Virology. 191 (1992) 541–549. doi:10.1016/0042-6822(92)90229-I.
[38] T.I. Lin, H. Heider, C. Schroeder, Different modes of inhibition by adamantane amine derivatives and natural polyamines of the functionally reconstituted influenza virus M2 proton channel protein., J. Gen. Virol. 78 (Pt 4) (1997) 767–74. doi:10.1099/0022-1317-78-4-767.
[39] M.R. Castrucci, Y. Kawaoka, Reverse genetics system for generation of an influenza A virus mutant containing a deletion of the carboxyl-terminal residue of M2 protein., J. Virol. 69 (1995) 2725–8. http://www.pubmedcentral.nih.gov/articlerender.fcgi?artid=188964&tool=pmcentrez&rendertype=abstract.
[40] B. Hundt, N. Mölle, S. Stefaniak, R. Dürrwald, J. Weyand, Large pilot scale cultivation process study of adherent MDBK cells for porcine Influenza A virus propagation using a novel disposable stirred-tank bioreactor, BMC Proc. 5 (2011) P128. doi:10.1186/1753-6561-5-S8-P128.
[41] S. Riedel, Edward Jenner and the history of smallpox and vaccination., Proc. (Bayl. Univ. Med. Cent). 18 (2005) 21–5. http://www.pubmedcentral.nih.gov/articlerender.fcgi?artid=1200696&tool=pmcentrez&rendertype=abstract (accessed January 3, 2015).
[42] a M. Behbehani, The smallpox story: life and death of an old disease., Microbiol. Rev. 47 (1983) 455–509.
[43] D.P. Nayak, S. Lehmann, U. Reichl, Downstream processing of MDCK cell-derived equine influenza virus., J. Chromatogr. B. Analyt. Technol. Biomed. Life Sci. 823 (2005) 75–81.

doi:10.1016/j.jchromb.2005.05.022.
[44] T. Weigel, T. Solomaier, A. Peuker, T. Pathapati, M.W. Wolff, U. Reichl, A flow-through chromatography process for influenza A and B virus purification, J. Virol. Methods. 207 (2014) 45–53. doi:10.1016/j.jviromet.2014.06.019.
[45] C.D. O'Donnell, L. Vogel, Y. Matsuoka, H. Jin, K. Subbarao, The matrix gene segment destabilizes the acid and thermal stability of the hemagglutinin of pandemic live attenuated influenza virus vaccines., J. Virol. 88 (2014) 12374–84. doi:10.1128/JVI.01107-14.
[46] O. KISTNER, Development of a mammalian cell (Vero) derived candidate influenza virus vaccine, Vaccine. 16 (1998) 960–968. doi:10.1016/S0264-410X(97)00301-0.
[47] L. Santi, Z. Huang, H. Mason, Virus like particles production in green plants, NIH Public Access. 40 (2009) 66–76. doi:10.1016/j.ymeth.2006.05.020.Virus.
[48] K. McKeage, Inactivated quadrivalent split-virus seasonal influenza vaccine (Fluarix® quadrivalent): a review of its use in the prevention of disease caused by influenza A and B., Drugs. 73 (2013) 1587–94. doi:10.1007/s40265-013-0114-3.
[49] E.S. Sedova, D.N. Shcherbinin, a I. Migunov, I. a Smirnov, D.I. Logunov, M.M. Shmarov, et al., Recombinant influenza vaccines., Acta Naturae. 4 (2012) 17–27. doi:10.1186/1471-2334-11-233.
[50] J.O. Josefsberg, B. Buckland, Vaccine process technology, Biotechnol. Bioeng. 109 (2012) 1443–1460. doi:10.1002/bit.24493.
[51] B. Ferraro, M.P. Morrow, N.A. Hutnick, T.H. Shin, C.E. Lucke, D.B. Weiner, Clinical applications of DNA vaccines: current progress., Clin. Infect. Dis. 53 (2011) 296–302. doi:10.1093/cid/cir334.
[52] G.W. Carnell, F. Ferrara, K. Grehan, C.P. Thompson, N.J. Temperton, Pseudotype-Based Neutralization Assays for Influenza: A Systematic Analysis, Front. Immunol. 6 (2015) 1–17. doi:10.3389/fimmu.2015.00161.
[53] European Pharmacopoeia 5.0, 2005.
[54] L. Opitz, J. Salaklang, H. Büttner, U. Reichl, M.W. Wolff, Lectin-affinity chromatography for downstream processing of MDCK cell culture derived human influenza A viruses., Vaccine. 25 (2007) 939–47. doi:10.1016/j.vaccine.2006.08.043.
[55] E. Milián, A. a Kamen, Current and Emerging Cell Culture Manufacturing Technologies for Influenza Vaccines, 2015 (2015).
[56] L. Widjaja, N. Ilyushina, R.G. Webster, R.J. Webby, Molecular changes associated with adaptation of human influenza A virus in embryonated chicken eggs., Virology. 350 (2006) 137–45. doi:10.1016/j.virol.2006.02.020.
[57] Y. Genzel, I. Behrendt, S. König, H. Sann, U. Reichl, Metabolism of MDCK cells during cell growth and influenza virus production in large-scale microcarrier culture., Vaccine. 22 (2004) 2202–8. doi:10.1016/j.vaccine.2003.11.041.
[58] J.M. Wood, J.S. Oxford, U. Dunleavy, R.W. Newman, D. Major, J.S. Robertson, Influenza A (H1N1) vaccine efficacy in animal models is influenced by two amino acid substitutions in the hemagglutinin molecule., Virology. 171 (1989) 214–21. http://www.ncbi.nlm.nih.gov/pubmed/2741341 (accessed January 29, 2016).
[59] K. Nerome, H. Kumihashi, R. Nerome, Y. Hiromoto, Y. Yokota, R. Ueda, et al., Evaluation of immune responses to inactivated influenza vaccines prepared in embryonated chicken eggs and MDCK cells in a mouse model., Dev. Biol. Stand. 98 (1999) 53–63; discussion 73–4. http://www.ncbi.nlm.nih.gov/pubmed/10494959 (accessed January 29, 2016).
[60] O. Kistner, P.N. Barrett, W. Mundt, M. Reiter, S. Schober-Bendixen, G. Eder, et al., A novel mammalian cell (Vero) derived influenza virus vaccine: development, characterization and industrial scale production., Wien. Klin. Wochenschr. 111 (1999) 207–14. http://europepmc.org/abstract/med/10226351 (accessed January 29, 2016).
[61] J.A. Tree, C. Richardson, A.R. Fooks, J.C. Clegg, D. Looby, Comparison of large-scale mammalian cell culture systems with egg culture for the production of influenza virus A vaccine strains, Vaccine. 19 (2001) 3444–3450. doi:10.1016/S0264-410X(01)00053-6.
[62] R. Levy, Z. Zakay-Rones, Preparation and evaluation of a zonal purified influenza vaccine gripax, J. Med. Virol. 10 (1982) 265–272. doi:10.1002/jmv.1890100406.
[63] B. Kalbfuss, M. Wolff, R. Morenweiser, U. Reichl, Purification of Cell Culture-Derived Human Influenza A Virus by Size-Exclusion and Anion-Exchange Chromatography, Biotechnol. Bioengeneering. 96 (2007) 932–944. doi:10.1002/bit.
[64] J.P. Uittenbogaard, B. Zomer, P. Hoogerhout, B. Metz, Reactions of??-propiolactone with nucleobase analogues, nucleosides, and peptides: Implications for the inactivation of viruses, J. Biol. Chem. 286

(2011) 36198–36214. doi:10.1074/jbc.M111.279232.
[65] P. Bonnafous, M.-C.C. Nicolaï, J.-C.C. Taveau, M. Chevalier, F. Barrière, J. Medina, et al., Treatment of influenza virus with Beta-propiolactone alters viral membrane fusion, Biochim. Biophys. Acta - Biomembr. 1838 (2014) 355–363. doi:10.1016/j.bbamem.2013.09.021.
[66] M. Jonges, W.M. Liu, E. van der Vries, R. Jacobi, I. Pronk, C. Boog, et al., Influenza virus inactivation for studies of antigenicity and phenotypic neuraminidase inhibitor resistance profiling., J. Clin. Microbiol. 48 (2010) 928–40. doi:10.1128/JCM.02045-09.
[67] Y. Furuya, M. Regner, M. Lobigs, A. Koskinen, A. Müllbacher, M. Alsharifi, Effect of inactivation method on the cross-protective immunity induced by whole "killed" influenza A viruses and commercial vaccine preparations., J. Gen. Virol. 91 (2010) 1450–60. doi:10.1099/vir.0.018168-0.
[68] C.B. Reimer, R.S. Baker, T.E. Newlin, M.L. Havens, R.M. Van Frank, W.O. Storvick, et al., Comparison of techniques for influenza virus purification., J. Bacteriol. 92 (1966) 1271–2. http://www.pubmedcentral.nih.gov/articlerender.fcgi?artid=276412&tool=pmcentrez&rendertype=abstract (accessed January 22, 2016).
[69] L. Opitz, S. Lehmann, A. Zimmermann, U. Reichl, M.W. Wolff, Impact of adsorbents selection on capture efficiency of cell culture derived human influenza viruses., J. Biotechnol. 131 (2007) 309–17. doi:10.1016/j.jbiotec.2007.07.723.
[70] L. Opitz, A. Zimmermann, S. Lehmann, Y. Genzel, H. Lübben, U. Reichl, et al., Capture of cell culture-derived influenza virus by lectins: strain independent, but host cell dependent., J. Virol. Methods. 154 (2008) 61–8. doi:10.1016/j.jviromet.2008.09.004.
[71] L. Opitz, J. Hohlweg, U. Reichl, M.W. Wolff, Purification of cell culture-derived influenza virus A/Puerto Rico/8/34 by membrane-based immobilized metal affinity chromatography., J. Virol. Methods. 161 (2009) 312–6. doi:10.1016/j.jviromet.2009.06.025.
[72] C.C. Loa, T.L. Lin, C.C. Wu, T. a. Bryan, H.L. Thacker, T. Hooper, et al., Purification of turkey coronavirus by Sephacryl size-exclusion chromatography, J. Virol. Methods. 104 (2002) 187–194. doi:10.1016/S0166-0934(02)00069-1.
[73] P. Nestola, R.J.S. Silva, C. Peixoto, P.M. Alves, M.J.T. Carrondo, J.P.B. Mota, Adenovirus purification by two-column, size-exclusion, simulated countercurrent chromatography., J. Chromatogr. A. 1347 (2014) 111–21. doi:10.1016/j.chroma.2014.04.079.
[74] C.A. Challener, Viral Clearance Challenges in Bioprocessing. Challenges remain for virus removal and validation, BioPharm Int Vol27 issue11. (2014). http://www.biopharminternational.com/viral-clearance-challenges-bioprocessing (accessed February 1, 2016).
[75] L. Opitz, S. Lehmann, U. Reichl, M.W. Wolff, Sulfated membrane adsorbers for economic pseudo-affinity capture of influenza virus particles., Biotechnol. Bioeng. 103 (2009) 1144–54. http://www.ncbi.nlm.nih.gov/pubmed/19449393 (accessed January 29, 2016).
[76] B. Kalbfuss, M. Wolff, L. Geisler, A. Tappe, R. Wickramasinghe, V. Thom, et al., Direct capture of influenza A virus from cell culture supernatant with Sartobind anion-exchange membrane adsorbers, J. Memb. Sci. 299 (2007) 251–260. doi:10.1016/j.memsci.2007.04.048.
[77] I. V. Kalashnikova, N.D. Ivanova, T.G. Evseeva, a. Y. Menshikova, E.G. Vlakh, T.B. Tennikova, Study of dynamic adsorption behavior of large-size protein-bearing particles, J. Chromatogr. A. 1144 (2007) 40–47. doi:10.1016/j.chroma.2006.10.060.
[78] E.I. Trilisky, a. M. Lenhoff, Sorption processes in ion-exchange chromatography of viruses, J. Chromatogr. A. 1142 (2007) 2–12. doi:10.1016/j.chroma.2006.12.094.
[79] P. Gerster, E.-M. Kopecky, N. Hammerschmidt, M. Klausberger, F. Krammer, R. Grabherr, et al., Purification of infective baculoviruses by monoliths., J. Chromatogr. A. 1290 (2013) 36–45. http://www.ncbi.nlm.nih.gov/pubmed/23587319 (accessed January 15, 2016).
[80] T.S.J.L.S.B.S. Pincus, Release and Stability Testing Programs for a Novel Virus-Like Particle Vaccine, (n.d.). http://www.biopharminternational.com/release-and-stability-testing-programs-novel-virus-particle-vaccine (accessed January 15, 2016).
[81] C.M. Thompson, E. Petiot, A. Lennaertz, O. Henry, A. a Kamen, Analytical technologies for influenza virus-like particle candidate vaccines: challenges and emerging approaches., Virol. J. 10 (2013) 141. doi:10.1186/1743-422X-10-141.
[82] G.K. Hirst, the Quantitative Determination of Influenza Virus and Antibodies By Means of Red Cell Agglutination., J. Exp. Med. 75 (1942) 49–64. doi:10.1084/jem.75.1.49.
[83] H.B. DONALD, A. ISAACS, Counts of influenza virus particles., J. Gen. Microbiol. 10 (1954) 457–64. doi:10.1099/00221287-10-3-457.
[84] A. Isaacs, H.B. Donald, Particle counts of haemagglutinating viruses., J. Gen. Microbiol. 12 (1955)

241–7. doi:10.1099/00221287-12-2-241.
[85] J.C. Kapteyn, A.M. Porre, E.J.P. de Rond, W.B. Hessels, M.A. Tijms, H. Kessen, et al., HPLC-based quantification of haemagglutinin in the production of egg- and MDCK cell-derived influenza virus seasonal and pandemic vaccines., Vaccine. 27 (2009) 1468–77. doi:10.1016/j.vaccine.2008.11.113.
[86] J. Transfiguracion, A.P. Manceur, E. Petiot, C.M. Thompson, A. a Kamen, Particle quantification of influenza viruses by high performance liquid chromatography, Vaccine. 33 (2015) 78–84. doi:10.1016/j.vaccine.2014.11.027.
[87] H. Hamazaki, Calcium-mediated hemagglutination by serum amyloid P component and the inhibition by specific glycosaminoglycans, Biochem. Biophys. Res. Commun. 150 (1988) 212–218. doi:10.1016/0006-291X(88)90507-4.
[88] A. Jungbauer, Chromatographic media for bioseparation, J. Chromatogr. A. 1065 (2005) 3–12. doi:10.1016/j.chroma.2004.08.162.
[89] R.D. Ricker, L.A. Sandoval, Fast, reproducible size-exclusion chromatography of biological macromolecules., J. Chromatogr. A. 743 (1996) 43–50. http://www.ncbi.nlm.nih.gov/pubmed/8817873 (accessed September 3, 2015).
[90] P. Hong, S. Koza, E.S.P. Bouvier, Size-Exclusion Chromatography for the Analysis of Protein Biotherapeutics and their Aggregates., J. Liq. Chromatogr. Relat. Technol. 35 (2012) 2923–2950. doi:10.1080/10826076.2012.743724.
[91] M. Potschka, Size exclusion chromatography of DNA and viruses: properties of spherical and asymmetric molecules in porous networks, Macromolecules. 24 (1991) 5023–5039. doi:10.1021/ma00018a008.
[92] C.M. Li, T. William Hutchens, Chromatofocusing., Methods Mol. Biol. 11 (1992) 237–48. doi:10.1385/0-89603-213-2:237.
[93] C.A. Brooks, S.M. Cramer, Steric mass-action ion exchange: Displacement profiles and induced salt gradients, AIChE J. 38 (1992) 1969–1978. doi:10.1002/aic.690381212.
[94] E. Müller, Polymere Oberflächenbeschichtungen - eine Methode zur Herstellung von Trägermaterialien für die Biochromatographie, Otto-von-Guericke Universität Magdeburg, 2003.
[95] J. Chen, J. Tetrault, A. Ley, Comparison of standard and new generation hydrophobic interaction chromatography resins in the monoclonal antibody purification process, J. Chromatogr. A. 1177 (2008) 272–281. doi:10.1016/j.chroma.2007.07.083.
[96] B.C.S. To, A.M. Lenhoff, Hydrophobic interaction chromatography of proteins. I. The effects of protein and adsorbent properties on retention and recovery, J. Chromatogr. A. 1141 (2007) 191–205. doi:10.1016/j.chroma.2006.12.020.
[97] E. Haimer, A. Tscheliessnig, R. Hahn, A. Jungbauer, Hydrophobic interaction chromatography of proteins IV. Kinetics of protein spreading, J. Chromatogr. A. 1139 (2007) 84–94. doi:10.1016/j.chroma.2006.11.003.
[98] S. Ghose, Y. Tao, L. Conley, D. Cecchini, Purification of monoclonal antibodies by hydrophobic interaction chromatography under no-salt conditions., MAbs. 5 795–800. doi:10.4161/mabs.25552.
[99] A.E. Albers, A.W. Garofalo, P.M. Drake, R. Kudirka, G.W. de Hart, R.M. Barfield, et al., Exploring the effects of linker composition on site-specifically modified antibody–drug conjugates, Eur. J. Med. Chem. 88 (2014) 3–9. doi:10.1016/j.ejmech.2014.08.062.
[100] M.R. Leanna, C.L. Becker, Antibody drug conjugate (adc) purification, WO2014152199 A1, 2014. http://www.google.com/patents/WO2014152199A1?cl=en (accessed March 4, 2016).
[101] T. Arakawa, Thermodynamic analysis of the effect of concentrated salts on protein interaction with hydrophobic and polysaccharide columns., Arch. Biochem. Biophys. 248 (1986) 101–5. http://www.ncbi.nlm.nih.gov/pubmed/3729409 (accessed March 4, 2016).
[102] T.W. Perkins, D.S. Mak, T.W. Root, E.N. Lightfoot, Protein retention in hydrophobic interaction chromatography: Modeling variation with buffer ionic strength and column hydrophobicity, J. Chromatogr. A. 766 (1997) 1–14. doi:10.1016/S0021-9673(96)00978-8.
[103] W.R. Melander, D. Corradini, C. Horváth, Salt-mediated retention of proteins in hydrophobic-interaction chromatography. Application of solvophobic theory., J. Chromatogr. 317 (1984) 67–85. doi:10.1016/S0021-9673(01)91648-6.
[104] F. Xia, D. Nagrath, S.M. Cramer, Effect of pH changes on water release values in hydrophobic interaction chromatographic systems, J. Chromatogr. A. 1079 (2005) 229–235. doi:10.1016/j.chroma.2005.04.005.
[105] A.M. Senczuk, R. Klinke, T. Arakawa, G. Vedantham, Y. Yigzaw, Hydrophobic interaction chromatography in dual salt system increases protein binding capacity., Biotechnol. Bioeng. 103 (2009)

930–5. doi:10.1002/bit.22313.
[106] K. Toshito, H. Yoshimi, S. Emi, S. Kouji, Y. Mitoma, Optimization of Cation-Exchange Resin for Insulin Purification, in: ISPPP, 2002: p. Poster.
[107] E. Müller, J. Vajda, Routes to improve binding capacities of affinity resins demonstrated for Protein A chromatography., J. Chromatogr. B. Analyt. Technol. Biomed. Life Sci. (2016). doi:10.1016/j.jchromb.2016.01.036.
[108] T.M. Przybycien, N.S. Pujar, L.M. Steele, Alternative bioseparation operations: Life beyond packed-bed chromatography, Curr. Opin. Biotechnol. 15 (2004) 469–478. doi:10.1016/j.copbio.2004.08.008.
[109] P. Gagnon, The Emerging Generation of Chromatography Tools for Virus Purification, Suppl. BioProcess Intl. (2008) 24–30.
[110] G. Carta, A. Jungbauer, Protein Chromatography: Process Development and Scale-Up, Wiley-VCH Verlag, Weinheim, 2010.
[111] A. Striegel, J. Kirkland, W. Yau, D. Bly, Modern Size-Exclusion Liquid Chromatography Practice of Gel Permeation and Gel Filtration Chromatography, 2nd ed., John Wiley & Sons, Hoboken, 2009.
[112] J. Vajda, W. Conze, E. Müller, Kinetic plots in aqueous size exclusion chromatography of monoclonal antibodies and virus particles, J. Chromatogr. A. 1426 (2015) 118–125. doi:10.1016/j.chroma.2015.11.057.
[113] S.T. Popovici, W.T. Kok, P.J. Schoenmakers, Band broadening in size-exclusion chromatography of polydisperse samples, J. Chromatogr. A. 1060 (2004) 237–252. doi:10.1016/j.chroma.2004.05.099.
[114] J.H. Knox, J.F. Parcher, Effect of the column to particle diameter ratio on the dispersion of unsorbed solutes in chromatography, Anal. Chem. 41 (1969) 1599–1606. doi:10.1021/ac60281a009.
[115] S.T. Popovici, P.J. Schoenmakers, Fast size-exclusion chromatography--theoretical and practical considerations., J. Chromatogr. A. 1099 (2005) 92–102. doi:10.1016/j.chroma.2005.08.071.
[116] J. Hirabayashi, N. Ito, K. Noguchi, K. Kasai, Slalom chromatography: size-dependent separation of DNA molecules by a hydrodynamic phenomenon, Biochemistry. 29 (1990) 9515–9521. doi:10.1021/bi00493a004.
[117] D.R. Heidemann, E.S. Schulenberg, W.H. Smith, Determination of aspirin and salicylic acid by reverse-phase liquid chromatography., J. Assoc. Off. Anal. Chem. 70 964–6. http://www.ncbi.nlm.nih.gov/pubmed/3436909 (accessed February 17, 2016).
[118] I. Halász, R. Endele, J. Asshauer, Ultimate limits in high-pressure liquid chromatography, J. Chromatogr. A. 112 (1975) 37–60. doi:10.1016/S0021-9673(00)99941-2.
[119] P. Atkins, J. De Paula, Atkin's Physical Chemistry, Oxford University Press, Oxford, 2006.
[120] C. Pfeiffer, C. Rehbock, D. Hu, C. Carrillo-carrion, D.J. De Aberasturi, V. Merk, et al., Interaction of colloidal nanoparticles with their local environment : the (ionic) nanoenvironment around nanoparticles is different from bulk and determines the physico-chemical properties of the nanoparticles, J R Soc Interfaces. 11 (2014) 1–13. doi:10.1098/rsif.2013.0931.
[121] C. Wagner, Die Oberflächenspannung verdünnter Elektrolytlösungen, Phys. Zeitschrift. 25 (1924) 474–477.
[122] Y. Levin, Interfacial tension of electrolyte solutions, J. Chem. Phys. 113 (2000) 9722–9726. doi:10.1063/1.1321043.
[123] W. Melander, C. Horváth, Salt effect on hydrophobic interactions in precipitation and chromatography of proteins: an interpretation of the lyotropic series., Arch. Biochem. Biophys. 183 (1977) 200–215. doi:10.1016/0003-9861(77)90434-9.
[124] E. Müller, J. Vajda, D. Josic, T. Schröder, R. Dabre, T. Frey, Mixed electrolytes in hydrophobic interaction chromatography ☥, J. Sep. Sci. 36 (2013) 1327–1334. doi:10.1002/jssc.201200704.
[125] A. Staby, J. Mollerup, Solute retention of lysozyme in hydrophobic interaction perfusion chromatography, J. Chromatogr. A. 734 (1996) 205–212. doi:10.1016/0021-9673(95)01161-7.
[126] W. Kunz, P. Lo Nostro, B.W. Ninham, The present state of affairs with Hofmeister effects, Curr. Opin. Colloid Interface Sci. 9 (2004) 1–18. doi:10.1016/j.cocis.2004.05.004.
[127] J. Zhang, Protein-Protein Interactions in Salt Solutions, Protein-Protein Interact. - Comput. Experimantal Tools. (2012) 359–76. doi:10.5772/2679.
[128] A.K. Banga, Therapeutic Peptides and Proteins: Formulation, Processing, and Delivery Systems, Third Edition, CRC Press, 2015. https://books.google.com/books?id=cnF3CAAAQBAJ&pgis=1 (accessed February 18, 2016).
[129] S.M. Carl, D.J. Lindley, G.T. Knipp, K.R. Morris, E. Oliver, G.W. Becker, et al., Pharmaceutical Manufacturing Handbook, John Wiley & Sons, Hoboken, 2008.
[130] W. KAUZMANN, Some factors in the interpretation of protein denaturation., Adv. Protein Chem. 14

(1959) 1–63. http://www.ncbi.nlm.nih.gov/pubmed/14404936 (accessed January 9, 2016).
[131] K.M. Biswas, D.R. DeVido, J.G. Dorsey, Evaluation of methods for measuring amino acid hydrophobicities and interactions, J. Chromatogr. A. 1000 (2003) 637–655. doi:10.1016/S0021-9673(03)00182-1.
[132] C.M. Roth, B.L. Neal, A.M. Lenhoff, Van der Waals interactions involving proteins., Biophys. J. 70 (1996) 977–87. doi:10.1016/S0006-3495(96)79641-8.
[133] A. Wasserman, Mechanochemistry, in: Unsolved Probl. Polym. Sci. A Compil. Essays Prep. Dir. Mater. Process. Aeronaut. Syst. Div. Air Force Syst. Command. Wright-Patterson Air Force Base, Ohio, National Academies, WASHINGTON, D. C., 1962: p. 168f. https://books.google.com/books?id=-z8rAAAAYAAJ&pgis=1 (accessed February 18, 2016).
[134] A. Jungbauer, R. Hahn, Methods in Enzymology - Ion Exchange Chromatography, in: R.R. Burgess, M.P. Deutscher (Eds.), Guid. to Protein Purif., 2nd ed., Academic Press, San Diego, 2009: pp. 349–370. https://books.google.com/books?id=f6Lp4yna4hoC&pgis=1 (accessed March 30, 2016).
[135] T.M. Pabst, G. Carta, pH transitions in cation exchange chromatographic columns containing weak acid groups., J. Chromatogr. A. 1142 (2007) 19–31. doi:10.1016/j.chroma.2006.08.066.
[136] V. Kumar, A.S. Rathore, Two-stage chromatographic separation of aggregates for monoclonal antibody therapeutics, J. Chromatogr. A. 1368 (2014) 155–162. doi:10.1016/j.chroma.2014.09.077.
[137] M.E. Lienqueo, A. Mahn, J.C. Salgado, J. a. Asenjo, Current insights on protein behaviour in hydrophobic interaction chromatography, J. Chromatogr. B Anal. Technol. Biomed. Life Sci. 849 (2007) 53–68. doi:10.1016/j.jchromb.2006.11.019.
[138] W. Kunz, J. Henle, B.W. Ninham, "Zur Lehre von der Wirkung der Salze" (about the science of the effect of salts): Franz Hofmeister's historical papers, Curr. Opin. Colloid Interface Sci. 9 (2004) 19–37. doi:10.1016/j.cocis.2004.05.005.
[139] a. M. Azevedo, P. a J. Rosa, I.F. Ferreira, M.R. Aires-Barros, Integrated process for the purification of antibodies combining aqueous two-phase extraction, hydrophobic interaction chromatography and size-exclusion chromatography, J. Chromatogr. A. 1213 (2008) 154–161. doi:10.1016/j.chroma.2008.09.115.
[140] K.D. Collins, Ions from the Hofmeister series and osmolytes: Effects on proteins in solution and in the crystallization process, Methods. 34 (2004) 300–311. doi:10.1016/j.ymeth.2004.03.021.
[141] M. Boström, D.F. Parsons, A. Salis, B.W. Ninham, M. Monduzzi, Possible origin of the inverse and direct Hofmeister series for lysozyme at low and high salt concentrations., Langmuir. 27 (2011) 9504–11. doi:10.1021/la202023r.
[142] J.A. Queiroz, C.T. Tomaz, J.M. Cabral, Hydrophobic interaction chromatography of proteins., J. Biotechnol. 87 (2001) 143–59. http://www.ncbi.nlm.nih.gov/pubmed/11278038 (accessed March 4, 2016).
[143] T. Arakawa, S.N. Timasheff, Mechanism of protein salting in and salting out by divalent cation salts: balance between hydration and salt binding., Biochemistry. 23 (1984) 5912–23. http://www.ncbi.nlm.nih.gov/pubmed/6525340 (accessed March 4, 2016).
[144] F. Xia, D. Nagrath, S. Garde, S.M. Cramer, Evaluation of selectivity changes in HIC systems using a preferential interaction based analysis., Biotechnol. Bioeng. 87 (2004) 354–63. doi:10.1002/bit.20120.
[145] Y. Zhang, P.S. Cremer, Interactions between macromolecules and ions: the Hofmeister series, Curr. Opin. Chem. Biol. 10 (2006) 658–663. doi:10.1016/j.cbpa.2006.09.020.
[146] A.W. Omta, M.F. Kropman, S. Woutersen, H.J. Bakker, Negligible effect of ions on the hydrogen-bond structure in liquid water., Science. 301 (2003) 347–9. doi:10.1126/science.1084801.
[147] T. Arakawa, J.S. Philo, K. Tsumoto, R. Yumioka, D. Ejima, Elution of antibodies from a Protein-A column by aqueous arginine solutions, Protein Expr. Purif. 36 (2004) 244–248. doi:10.1016/j.pep.2004.04.009.
[148] D. Ejima, R. Yumioka, K. Tsumoto, T. Arakawa, Effective elution of antibodies by arginine and arginine derivatives in affinity column chromatography., Anal. Biochem. 345 (2005) 250–7. doi:10.1016/j.ab.2005.07.004.
[149] K. Tsumoto, D. Ejima, K. Nagase, T. Arakawa, Arginine improves protein elution in hydrophobic interaction chromatography. The cases of human interleukin-6 and activin-A, J. Chromatogr. A. 1154 (2007) 81–86. doi:10.1016/j.chroma.2007.02.061.
[150] D. Ejima, R. Yumioka, T. Arakawa, K. Tsumoto, Arginine as an effective additive in gel permeation chromatography., J. Chromatogr. A. 1094 (2005) 49–55. doi:10.1016/j.chroma.2005.07.086.
[151] R. Yumioka, H. Sato, H. Tomizawa, Y. Yamasaki, D. Ejima, Mobile phase containing arginine provides more reliable SEC condition for aggregation analysis., J. Pharm. Sci. 99 (2010) 618–20.

doi:10.1002/jps.21857.
[152] J. Chen, S.M. Cramer, Protein adsorption isotherm behavior in hydrophobic interaction chromatography, J. Chromatogr. A. 1165 (2007) 67–77. doi:10.1016/j.chroma.2007.07.038.
[153] M.A. Esquibel-King, A.C. Dias-Cabral, J.A. Queiroz, N.G. Pinto, Study of hydrophobic interaction adsorption of bovine serum albumin under overloaded conditions using flow microcalorimetry, J. Chromatogr. A. 865 (1999) 111–122. doi:10.1016/S0021-9673(99)01118-8.
[154] J. Vajda, T. Frey, E. Müller, R. Römling, Application note: Mixed Electrolytes in Hydrophobic Interaction Chromatography, (2013) 1–2. http://www.separations.eu.tosohbioscience.com/literature/advanced-literature-search?LiteratureType=Application Note.
[155] J. Vajda, W. Conze, E. Müller, Mab Aggregate detection – analytical HIC as an orthogonal chromatographic approach, (2012) Poster at HPLC conference.
[156] H. Brück, J. Vajda, W. Conze, E. Müller, Analytical HIC for mAb Aggregate Analysis; How Does the Salt Ion Type Influence the Selectivity?, (2013) Oral Conference Contribution, ISPPP.
[157] J. Vajda, E. Mueller, E. Bahret, Dual salt mixtures in mixed mode chromatography with an immobilized tryptophan ligand influence the removal of aggregated monoclonal antibodies., Biotechnol. J. 9 (2014) 555–565. doi:10.1002/biot.201300230.
[158] J. Vajda, D. Weber, S. Stefaniak, B. Hundt, T. Rathfelder, E. Müller, Mono- and polyprotic buffer systems in anion exchange chromatography of influenza virus particles., J. Chromatogr. A. 1448 (2016) 73–80. doi:10.1016/j.chroma.2016.04.047.
[159] T.I. Lin, H. Heider, C. Schroeder, Different modes of inhibition by adamantane amine derivatives and natural polyamines of the functionally reconstituted influenza virus M2 proton channel protein., J. Gen. Virol. 78 (Pt 4) (1997) 767–74. http://www.ncbi.nlm.nih.gov/pubmed/9129648 (accessed January 13, 2016).
[160] B.B. Hsu, S. Yinn Wong, P.T. Hammond, J. Chen, A.M. Klibanov, Mechanism of inactivation of influenza viruses by immobilized hydrophobic polycations., Proc. Natl. Acad. Sci. U. S. A. 108 (2011) 61–66. doi:10.1073/pnas.1017012108.
[161] J. Vajda, D. Weber, D. Brekel, B. Hundt, E. Müller, Size distribution analysis of influenza virus particles using size exclusion chromatography, J Chromatogr A Accept. Peer-Review. (2016).
[162] N.K. Jerne, Paper 36 Waiting for the End, in: I. Levkovits (Ed.), Portrait Immune Syst. Sci. Publ. N K Jerne, 2nd ed., World Scientific Pub Co Inc, 1996: p. 480.
[163] European Medicines Agency, Guideline on Influenza Vaccines – Quality Module, 2014. http://www.ema.europa.eu/docs/en_GB/document_library/Scientific_guideline/2014/06/WC500167817.pdf.

8.2. Abbildungsverzeichnis

8.3. Abkürzungsverzeichnis

A. Eddy Diffusion
A_C. *Kopplungsterm Eddy Diffusion und Massentransfer Widerstand*
A_{DLVO}. *Konstante zur Beschreibung der potentiellen Energie nach der DLVO Theorie*
AEX. *anion exchange chromatography, Anionenaustausch Chromatographie*
AFC. *affinity chromatography, Affinitätschromatographie*
B. longitudinale Diffusion
B_{DLVO}. *Konstante zur Beschreibung der potentiellen Energie nach der DLVO Theorie*
c. Konzentration
C. Massentransfer Widerstand
CD. *Cluster of Differentiation, Unterscheidungsgruppe*
CDR. *complimentary determining region, Komplementaritäts bestimmende Region*
CEX. *cation exchange chromatography, Kationenaustauschchromatographie*
CHO. *Chinese Hamster Ovary, Ovarien des chinesischen Hamsters*
D. Diffusionskoeffizient
DLVO. *Derjaguin, Landau, Verwey, Overbeek*
DNA. *deoxyribonucleic acid, Desoxyribonukleinsäure*
DoE. *Design of Experiments*
d_p. *Partikelgröße*
e. Elementarladung
E. intrinsische Aussalzungskonstante
ELISA. *enzyme linked immunosorbent assay, enzymgekoppelter Immunosorptions-Nachweis*
EMA. *European Medicines Agency, Europäische Arzneimittel-Agentur*
E_{pot}. *potentielle Energie*
F. Protein Dipolmoment
Fc. *crystallizable fragment, kristallisierbares Fragment*
γ. *Oberflächenspannung*
H. *Hemagglutinin*
HA. *Hemagglutination*
HIC. *hydrophobic interaction chromatography, Hydrophobe Interaktionschromatographie*
HI-Virus. *human immunodefficiency virus, humanes Immundefizienz-Virus*
HPLC. *high pressure liquid chromatography, Hochdruckflüssigchromatographie*
H_t. *theoretische Bodenhöhe*
I. Ionenstärke
IEX. *ion exchange chromatography, Ionenaustauschchromatographie*
Ig. *Immunglobulin*
k'. Retentionsfaktor
K_D. *Verteilungskoeffizient*
L. Löslichkeit eines Proteins
L_0. *Löslichkeit eines Proteins in Wasser*
LOQ. *limit of quantification, Quantifizierungsgrenze*
mAb. *monoclonal antibody, monoklonaler Antikörper*
MDBK. *Madin-Darby Bovine Kidney, Madin Darby Rinder Niere*
MDCK. *Madin-Darby Canine Kidney, Madin-Darby Kaninchenniere*
MXC. *mixed mode chromatography, Mixed Mode Chromatographie*
N. Bodenzahl
N_A. *Avogadro-Konstante*
pH. *potentia hydrogenii*
q. Punktladung
r. Entfernung
RAM. *restricted access media, Medien mit eingeschränktem Zugang*
r_D. *Dicke der elektrischen Doppelschicht*
RNA. *Ribonukleinsäure*
r_{rad}. *Partikelradius*
R_s. *Auflösung*
s. Abstand zweier Partikeloberflächen voneinander
SEC. *size exclusion chromatography, Größenausschlusschromatographie*
SMB. *Siumulated Moving Bed*
SRID. *single radial immunodiffusion, einfache radiale Immunodiffusion*
T. Temperatur
TNF. *Tumor Nekrose Faktor*
Tris. *Tris(hydroxymethyl)-aminomethan*
u. volumetrische Flussrate
V_R. *Elutionsvolumen*
W_B. *Peakbreite auf halber Höhe*
WHO. *World Health Organization, Weltgesundheitsorganisation*
z. Valenz
$\alpha_{\pm}$. *Ionenaktivität*
δ. Debye-Länge
ΔG. *Gibbs'sche Enthalpie*
ΔH_A. *Adsorptionsenthalpie*
ΔS. *Entropie*
ε_0. *Permittivität des Vakuums, auch: elektrische Feldkonstante oder Dieelektrizitätskonstante des Vakuums*

9. Kumulativer Teil

9.1. Mixed electrolytes in hydrophobic interaction chromatography

Autoren: Egbert Müller[1], Judith Vajda[1], Djuro Josic[2], Tim Schröder[3], Romain Dabre[1], Tim Frey[4]

Institutionen:
[1]Tosoh Bioscience GmbH, Zettachring 6, 70567 Stuttgart, Deutschland
[2]Rohde Island Hospital, The Coro Center for Cancer Research and Development, Providence, RI, USA
[3]Atoll GmbH, Ettishoferstraße 10, 88250 Weingarten, Deutschland
[4]Otto von Guericke-University Magdeburg, Institute for Process Engineering, Magdeburg, Germany

DOI: 10.1002/jssc.201200704

Online veröffentlicht am 25.März 2013

keywords: Dual salts, Hydrophobic interaction, Modulation, Salt mixtures

Egbert Müller[1]
Judith Vajda[1]
Djuro Josic[2]
Tim Schröder[3]
Romain Dabre[1]
Tim Frey[4]

[1]TOSOH Bioscience GmbH, Stuttgart, Germany
[2]Rhode Island Hospital, The Coro Center for Cancer Research and Development, Providence, RI, USA
[3]Atoll GmbH, Weingarten, Germany
[4]Otto von Guericke-University Magdeburg, Institute for Process Engineering, Magdeburg, Germany

Received July 29, 2012
Revised January 19, 2013
Accepted January 21, 2013

Research Article

Mixed electrolytes in hydrophobic interaction chromatography†

An essential part of the modulation of protein-binding capacity in hydrophobic interaction chromatography is the buffer-salt system. Besides using "single" electrolytes, multicomponent electrolyte mixtures may be used as an additional tool. Both the protein solubility and the binding capacity depend on the position of a salt in the so-called Hofmeister series. Specific interactions are observed for an individual protein-salt combination. For salt mixtures, selectivity, recovery, and binding capacity do not behave like for the single salts that are positioned in between the two mixed components in the Hofmeister series, as the continuous correlation would suggest. Thus, finding strategies for mixed salts could potentially lead to improved capacities in hydrophobic interaction chromatography. Mixtures of ammonium sulfate, sodium citrate, sodium sulfate, sodium chloride, sodium acetate, and glycine were used to investigate the binding capacities for lysozyme and a monoclonal antibody on various hydrophobic resins. Resin capacity for two investigated proteins increases when mixtures consisting of a chaotropic and a kosmotropic salt are applied. It seems to be related to the rather basic isoelectric points of the proteins.

Keywords: Dual salts / Hydrophobic interaction / Modulation / Salt mixtures
DOI 10.1002/jssc.201200704

1 Introduction

Hydrophobic interaction chromatography (HIC) is frequently used for the purification and analytical characterization of proteins [1, 2]. This chromatographic mode relies on interactions between hydrophobic patches on the protein's surface with immobilized hydrophobic ligands [3]. The specific interaction is influenced by the addition of highly concentrated electrolytes and additives. In contrast to other chromatographic modes, the salt type and potential additives can be varied in a wide range. This offers additional modulation opportunities for the separation of proteins [4].

Some additives like alcohols and polymers greatly impact the protein solubility as well as adsorption to HIC media [5]. They can either increase or decrease the binding capacity and their use may lead to an increase in recovery. Ammonium sulfate is frequently employed for protein precipitation and HIC, because it is readily soluble at high concentrations. Further, it precipitates proteins at high pH and it is available at relatively high purity and in large quantities [6]. Several other salts like sodium citrate, sodium phosphate, or sodium chloride provide an alternative. In contrast to single salt applications, electrolyte mixtures have rarely been adopted [7, 8]. One reason might be the increased complexity in multicomponent electrolyte mixtures. So far, there is no distinct description of the dependence of binding capacity of salt mixtures in HIC. It seems to be a difficult task to find an appropriate mixture without extensive testing. Recently, developed robotic high throughput systems have emerged to be a tremendous help for method development, enabling many parallel tests in a short time. However, some empirically derived classification criteria for the characterization of salt mixtures and their influence on capacity of different HIC resins would be helpful. The most prominent example for salt classification is the Hofmeister series [9]. Salts are therewith classified as "kosmotropic" or "chaotropic". Kosmotropic salts are usually employed for precipitation of proteins. In contrast, chaotropic salts support protein solubilization. In HIC, mainly kosmotropic salts are used, because they convey the interaction between protein and resin thereby increasing the binding capacity. The Hofmeister series may vary from different proteins [10]. Further, the relative salting out effectiveness also depends on the isoelectric point of a certain protein and the experimentally applied pH value [11].

The most adequate way to represent the Hofmeister series is the use of either surface tension or its specific value, the surface tension increment [8, 12]. The surface tension increment (σ) is equal the relative surface tension normalized to salt molality ($\sigma = (\gamma - \gamma_0)/m$, where γ_0 is the water surface tension). The surface tension increment is often a

Correspondence: Dr. Egbert Müller, TOSOH Bioscience GmbH, Zettachring 6, 70567 Stuttgart, Germany
E-mail: egbert.mueller@tosoh.com
Fax: 00497111325789

Abbreviations: HIC, hydrophobic interaction chromatography; **HTS**, high throughput system

†This paper is included in the virtual special issue Monoliths available at the Journal of Separation Science website.

linear function of the salt molality. According to the theory of Melander and Horvath [12], the logarithm of the solubility (S) of a protein is proportional to the salt molality (m) and the surface tension (γ). Based upon these assumptions the following equation can be derived:

$$\log S/S_0 = A + B \cdot \gamma + C \cdot m \quad (1)$$

The decimal logarithm of the protein solubility is thus proportional to the surface tension of the salt solution and the salt molality (A is mostly the electrostatic Debye term, B is the intrinsic salting-out constant, C is the protein dipole moment, and S_0 is the protein solubility in pure water). A similar equation as (1) was derived for the capacity factor (k) of a protein on a solid phase by Fasnaugh and Regnier (E, F, and G are constants that corresponds to A, B, and C in Eq. (1) and k_0 is the protein capacity factor with pure water as eluant) [13]:

$$\log k/k_0 = E + F \cdot \gamma + G \cdot m \quad (2)$$

Theoretically, a higher retention for proteins on HIC resins can only be expected for salts with a high surface tension or surface tension increment and at elevated salt concentrations. The relationship (2) is derived for the linear part of the isotherm and might not be generally applicable for the nonlinear range at higher loadings, but it can be used as a first approximation for prediction of the relationship of dynamic-binding capacity and the salt type used for single salt solutions.

Mixing salts with high and low surface tension or salts positioned at the opposite ends of the Hofmeister series, respectively, seems to be senseless. An increase in capacity would only be expected if different kosmotropic salts were mixed. Due to superpositioning of the single surface tensions, such a combination shall result in a higher overall surface tension.

The correctness of this hypothesis was recently demonstrated by Senczuk [7]. By mixing citrate and phosphate an increase up to 100% in dynamic-binding capacity of the resin was achieved for several mAbs. Following this hypothesis, mixing citrate (as a kosmotropic salt) with chloride as a rather chaotropic salt should result in a decrease of surface tension and an increase in protein solubility. Consequently, binding capacity of HIC is expected to decrease. For analytical HIC with proteins, El Rassi et al. [8] have already demonstrated that salt gradients with paired kosmotropic and chaotropic salts result in an augmented retention of basic proteins, while the retention of acidic proteins declines or remains unchanged. This is in contrast to the expected assumption of decreasing the retention or binding capacity due to the addition of a chaotropic salt to a salt with a high surface tension, regardless of the kind of investigated protein. It seems that the model of a linear relationship between the logarithm of retention and surface tension (Eq. (2)) cannot be extended to the salt mixtures. In order to investigate this effect, we selected two model proteins: lysozyme and a humanized IgG1 monoclonal antibody. The solubilities and binding capacities of these proteins were determined for single salts and salt mixtures.

Table 1. Specification of various Toyopearl® HIC gels

Resin	Mode	Particle size [μm]	Pore size [nm]	Mean-binding capacity [mg/mL]
Toyopearl® Butyl-600M	HIC	65	75	50 ± 10 (human γ-globulin)
Toyopearl® Phenyl-600M	HIC	65	75	>25 (human γ-globulin)
Toyopearl® PPG-600M	HIC	65	75	>25 (human γ-globulin)

All static-binding capacities were determined in 20 mM sodium phosphate buffer pH 7 containing 1 M ammonium sulfate and with protein concentration of 1 mg/mL at room temperature.

2 Materials and methods

2.1 Reagents

All salts and hen egg white lysozyme were purchased from Sigma-Aldrich (Munich, Germany). The humanized IgG1 monoclonal antibody was kindly provided by Boehringer Ingelheim (Biberach, Germany).

2.2 Resins

The following resins were used for the capacity determinations:

(1) Toyopearl® Phenyl-600M.
(2) Toyopearl® Butyl-600M.
(3) Toyopearl® PPG-600M.

All resins were supplied by Tosoh Bioscience (Stuttgart, Germany).

Table 1 summarizes the most important properties that are provided by the supplier. The Butyl resin is considered to be purely hydrophobic whereas the PPG (poly propylen glycol) resin is a more polar-hydrophobic resin due to the ether bridges. Due to the hydroxyl group, Phenyl's aromatic ring has a polar character trait. According to the values in Table 1 Toyopearl® Phenyl-600M resin offers the highest binding capacity for standard proteins. All resins have the same pore size and are thus not different in respect to mass transfer resistance.

2.3 Dynamic-binding capacities

The dynamic-binding capacities were determined using an Akta Explorer HPLC (GE Healthcare, Uppsala, Sweden).

The solubility measurements of the mAb were performed using a Tecan EVO 200 (Tecan, Switzerland) robotic HTS system from Atoll (Weingarten, Germany).

2.4 Dynamic-binding capacity evaluation of HIC resins

The capacity determinations for lysozyme were performed using Omnifit glass columns 18 mm × 6.6 mm id (DIBA Industries, UK). The bed volume was adjusted to 1 mL. To maintain pH, 20 mM phosphate buffer was used. The pH was adjusted to 7.0, after all other compounds have been added. Each stock solution was diluted with a 20-mM sodium phosphate buffer to a concentration of 1 mg/mL. The columns were loaded with a linear flow rate of 150 cm/h. Salt concentrations corresponding to 90% of the maximum salt concentration were the protein is still soluble were employed. The dynamic capacity was determined at 10% breakthrough. Due to limited availability, the binding capacities for mAb were determined on a 100 µL RoboColumn MediaScout® (Atoll Weingarten, Germany). The columns were equilibrated with 10 column volumes of starting buffer at a flow rate of 150 cm/h and the sample was subsequently loaded applying the same linear flow rate. Fractions of 277 µL were collected on an UV readable plate (Tecan). UV absorption measurements were performed using an automated Tecan system. The RSD of the dynamic-binding capacity measurement (triplet analysis) was 11%.

2.5 Solubility measurements of proteins

The solubility of lysozyme was determined manually by preparing the relevant salt mixtures containing the protein in concentration of 1 mg/mL and pH 7 in small Erlenmeyer flasks. All experiments were performed at room temperature. The turbidity was determined by photometrical absorbance measurements at 620 nm.

The measurements of the mAb solubility were performed in 96-well micro titer plates with an optical reader at 620 nm by recording the absorbance. Fifty microliters of the 5 mg/mL mAb solution were placed into each well. x µL single stock electrolyte solution or a mixture of different salt stock solutions and y µL of dilution buffer were mixed to fulfill the required final concentration. The total volume in each well was adjusted to 250 µL. A 20 mM phosphate buffer, pH 7 (adjusted with concentrated phosphoric acid) was used for dilution. The salt stock solutions were: 5 M sodium chloride, 3.75 M ammonium sulfate, 4.5 M sodium acetate, 1.5 M sodium sulfate, 3 M glycine, 1.5 M sodium citrate. The pH was adjusted to 7.

3 Results and discussions

3.1 Determination of the salt concentration for lysozyme

Beginning with ammonium sulfate, we performed screening for the salt concentration in the directions of highest binding capacity for lysozyme (2.2 M, see Table 5). The final salt concentration was found to be about 90% of the lysozyme solubility limiting concentration.

The first experiments, for dual salts, were performed using salt combinations containing 1 M ammonium sulfate and 1 M of a second salt. In the next step, we used 1:1 combinations of other salts. In some experiments, lysozyme could not be dissolved. In this case, salt concentrations were synchronistic reduced by 0.1 M steps. If lysozyme was soluble, the salt concentrations were increased, by use of same steps.

3.2 Salt mixtures used for MAb

Following results obtained in lysozyme experiments, the initial salt concentration was set to 90% of the amount tolerated by the protein. In contrast to the experience with lysozyme, we found higher binding capacities for more asymmetrical mixtures (unequal molar). In order to optimize the binding capacities, we focused on such complex mixtures using the Tecan robotic system.

3.3 Single salt solutions and number of salt mixtures

Six different salts were selected for this study: trisodium citrate, sodium acetate, ammonium sulfate, sodium sulfate, sodium chloride, and glycine. These salts are frequently used for HIC or multimodal applications [1]. In total, 21 salt systems were evaluated regarding binding capacity for lysozyme and six single salts and three salt mixtures were evaluated for the mAb.

3.4 Surface tension increments as classification criteria

As described by Eqs. (1) and (2), the protein solubility S and the capacity factor k are functions of the surface tension increments of the salt. The values of the surface tension increment of the six salts applied in this study, obtained from literature, were used to arrange them in descending order [12, 14]. (Of citrate only the potassium value was available):

Potassium citrate	3.17 kg/s²mol
Sodium sulfate	2.73 kg/s²mol
Ammonium sulfate	2.16 kg/s²mol
Sodium chloride	1.64 kg/s²mol
Sodium acetate	0.94 kg/s²mol
Glycine	0.92 kg/s²mol

Based upon these values, the six salts may be arranged into the following groups:

(1) Salts with high surface tension (>2 kg/s²mol, sodium citrate, sodium sulfate, ammonium sulfate).
(2) Salts with low surface tension (<2 kg/s²mol, sodium chloride, sodium acetate, glycine).

There is a discrepancy in classification of sodium acetate in the literature. The Hofmeister series considers it to be a kosmotropic salt whereas it is a more chaotropic salt according to it is low surface tension [15]. We used the latter classification in the current study.

3.5 Protein-binding capacities for lysozyme and mAb for single salt solutions

The protein-binding capacities for the six single salts were determined as described in the experimental section. The maximum dynamic-binding capacities for the single salt solutions for Toyopearl® Phenyl-600M, PPG-600M, and Butyl-600M are presented in Fig. 1A. High-binding capacities (about 50 mg/mL for lysozyme, see Fig. 1) were achieved for sodium sulfate, ammonium sulfate, and trisodium citrate applying 2 M or lower salt concentrations, consistent with the predictions obtained from Eq. (2). The salts characterized by low surface tensions, such as sodium chloride, glycine, and sodium acetate show different behavior compared to the salts with high surface tensions. Competitive capacities could only be observed for salt concentrations much more elevated than for the high surface tension salts. For instance, the binding capacity obtained when applying 4 M sodium chloride is about 30 mg/mL for the Toyopearl® Phenyl-600M resin, whereas the binding capacity for Toyopearl® Phenyl-600M at 1.5 M sodium sulfate is 50 mg lysozyme/mL resin.

For the single salts, the dynamic-binding capacities as a function of surface tension show a similar trend for the mAb and lysozyme, despite the mAb-binding capacities are generally lower (see Fig. 1B). The highest binding capacities (up to 20 mg mAb/mL) were found for Phenyl-600 and Butyl-600 in ammonium sulfate and sodium sulfate. In contrast to lysozyme, higher binding capacity (17 mg/mL) was also found for glycine. This might be the result of a particular interaction between this amino acid and the mAb [16].

3.6 Binding capacities for lysozyme in electrolyte mixtures (dual salt mixtures)

The mixtures of the six salts can be set up into three groups based on their surface tension (see Table 2).

3.6.1 Binding capacities for lysozyme in salt mixtures of electrolytes exhibiting high surface tension

The dynamic-binding capacities for Toyopearl® Butyl-600M, Toyopearl® Phenyl-600M, and Toyopearl® PPG-600M resins using salt combinations out of group 1 (high–high) and 3 (low–low) are shown in Fig. 2. The dynamic-binding capacities for a combination of high surface tension salts are low compared to the ones achieved for pure electrolytes. Low solubility of the protein in mixed electrolyte solutions seems to be the major problem. The maximum-binding capacity that could be achieved for the sodium sulfate–sodium citrate system is about 25 mg lysozyme/mL resin for PPG-600M. Mixing two kosmotropic salts did generally not allow achieving much higher lysozyme-binding capacities on that resin than the ones observed for pure ammonium sulfate with nearly 50 mg/mL (see Fig. 1A).

Table 2. Salt combinations

	Na3 citrate	Na_2SO_4	Na acetate	NaCl	Glycine
$(NH_4)_2SO_4$	High–high	High–high	High–low	High–low	High–low
Na3 citrate		High–high	High–low	High–low	High–low
Na_2SO_4			High–low	High–low	High–low
Na acetate				Low–low	Low–low
NaCl					Low–low

The various salt combinations can be grouped into three classes according to their surface tension: there is one group consisting of two high surface tension salts, one of a high and a low surface tension salt and a third group that is built up of low surface tension salts in combination with low surface tension salts.

3.6.2 Binding capacities for lysozyme in salt mixtures of electrolytes with low surface tension

As demonstrated in Fig. 2, the possible maximum-binding capacities are <20 mg/mL when 1:1 salt mixtures with low surface tension were applied. It might be possible to get slightly higher binding capacities for these mixtures by increasing the individual salt concentrations up to the solubility limit, but this is without practical importance, because there is a certain risk of protein precipitation or unfolding when working without a safety margin.

3.6.3 Binding capacities for lysozyme in salt mixtures between electrolytes of low and high surface tension

Three subgroups are possible:

(1) Subgroup with sodium acetate addition.
(2) Subgroup with sodium chloride addition.
(3) Subgroup with glycine addition.

For the first subgroup, the maximum-binding capacity for lysozyme was determined to be 62 mg/mL on Toyopearl® Phenyl-600M resin, using a 1:1 M mixture with sodium sulfate and sodium acetate. A variety of results is presented in Fig. 3.

In the group of sodium chloride addition, maximum-binding capacities were determined to be 55 and 43 mg/mL on Toyopearl® Phenyl-600M. These values can be achieved with a mixture containing 1 M ammonium sulfate and 1 M sodium chloride and a mixture of 0.9 M sodium citrate and 0.9 M sodium chloride, respectively.

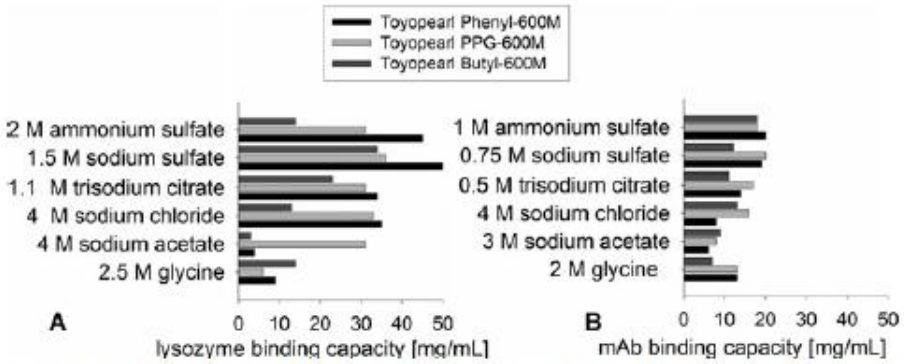

Figure 1. (A) Dynamic lysozyme-binding capacities for Toyopearl® Phenyl-600M, Toyopearl® Butyl-600M, and Toyopearl® PPG-600M (protein concentration 1 mg/mL, room temperature, pH 7) for single salt solutions at a concentration 10% below the solubility limit. (B) Dynamic mAb-binding capacities for Toyopearl® Phenyl-600M, Toyopearl® Butyl-600M, and Toyopearl® PPG-600M (protein concentration 1 mg/mL, room temperature, pH 7) for single salt solutions at a concentration 10% below the solubility limit.

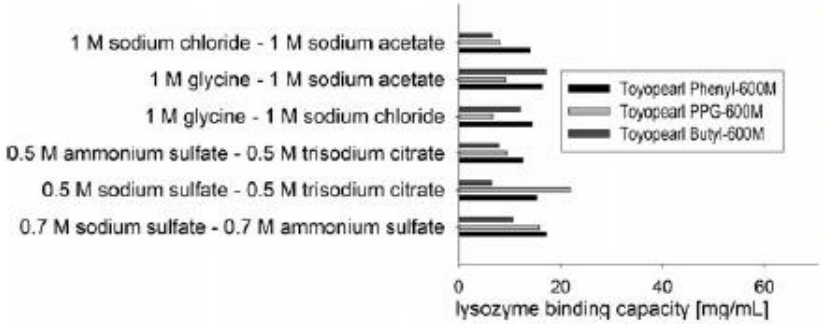

Figure 2. Dynamic lysozyme-binding capacities for Toyopearl® Phenyl-600M, Toyopearl® Butyl-600M, and Toyopearl® PPG-600M (protein concentration 1 mg/mL, room temperature, pH 7) for either mixtures of the three kosmotropic salts (ammonium sulfate, sodium sulfate, and sodium citrate) or mixtures of the three chaotropic salts (sodium chloride, glycine, sodium acetate), respectively.

In the group of glycine addition, a dynamic-binding capacity of 39 mg/mL is found for a mixture of 1 M sodium sulfate and 1 M glycine on Toyopearl® Phenyl-600M.

Results for the salt mixtures with the highest binding capacities are summarized in Table 3. The binding capacity for 2 M ammonium sulfate was used as a reference value. An increase in binding capacity of 37% compared to the ammonium sulfate system was found when a mixture of sodium sulfate and sodium acetate was used. The binding capacities for the three other salt pairs used in these experiments are comparable to the capacity in a 2 M ammonium sulfate solution. Exceptionally, Toyopearl® Butyl-600M resin shows a dramatic rise in binding capacity (more than two times, see Table 3) an ammonium sulfate–glycine mixture was applied.

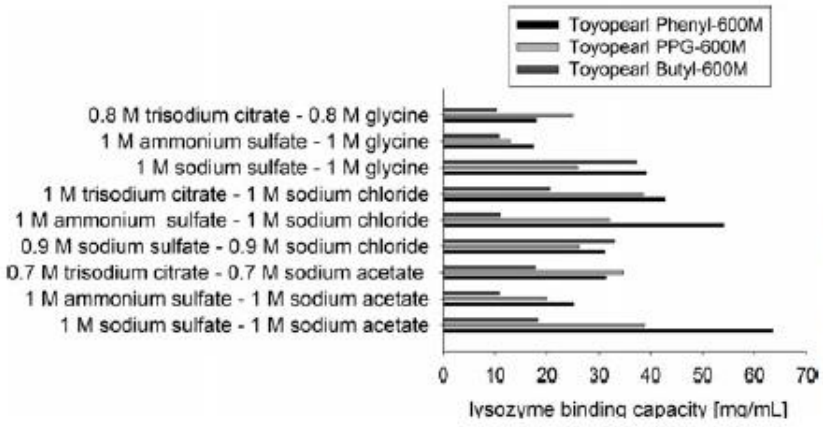

Figure 3. Dynamic lysozyme-binding capacities for Toyopearl® Phenyl-600M, Toyopearl® Butyl-600M, and Toyopearl® PPG-600M (protein concentration 1 mg/mL, room temperature, pH 7). The applied salt mixtures contain one chaotropic and one kosmotropic salt.

Table 3. Dynamic-binding capacities of Toyopearl® HIC resins for lysozyme in ammonium sulfate and optimal binary salt mixtures

	Toyopearl ® Phenyl-600M, binding capacity [mg/mL]	Toyopearl® PPG-600M, binding capacity [mg/mL]	Toyopearl® Butyl-600M, binding capacity [mg/mL]
2 M ammonium sulfate	46 (100%)	30 (100%)	15 (100%)
1 M sodium sulfate–1 M sodium acetate	63 (137%)	39 (130%)	18 (120%)
1 M ammonium sulfate–1 M sodium chloride	54 (117%)	31 (103%)	10 (67%)
0.9 M trisodium citrate–0.9 M sodium chloride	43 (93%)	38 (127%)	20 (133%)
1 M ammonium sulfate–1 M glycine	40 (87%)	25 (83%)	32 (213%)

Each number in brackets represents the capacity increase (decrease) in comparison to the 2 M ammonium sulfate-binding capacity.

Table 4. Dynamic-binding capacities of Toyopearl® HIC resins for mAb in ammonium sulfate and optimal binary salt mixtures

	Toyopearl® Phenyl-600M, binding capacity mAb [mg/mL]	Toyopearl® Butyl-600M, binding capacity mAb [mg/mL]	Toyopearl® PPG-600M, binding capacity mAb [mg/mL]
1 M ammonium sulfate	20 (100%)	18 (100%)	18 (100%)
1.7 M sodium chloride–0.7 M ammonium sulfate	25 (125%)	15 (83%)	30 (167%)
1.3 M sodium chloride–0.6 M sodium sulfate	20 (100%)	12 (67%)	25 (139%)
1.2 M glycine–0.6 M ammonium sulfate	21 (105%)	12 (67%)	25 (139%)

Each number in brackets represents the capacity increase (decrease) in comparison to the 1 M ammonium sulfate-binding capacity

This might be due to the fact that glycine is the only zwitterion beyond the employed electrolytes. For this reason, the higher degree of ligand hydrophobicity of the butyl resin might be necessary for any significant effect in dynamic-binding capacity emerging, emphasizing the specific importance of the electrolyte-protein-ligand interplay.

3.7 Binding capacities for mAb in dual salt systems

The mAb capacity determinations include a reduced set of experiments. Based upon the assumption that lysozyme and mAb are both positively charged at pH 7, we limited ourselves to the combinations in highest capacity for lysozyme:

(1) Ammonium sulfate–chloride.
(2) Sodium citrate–sodium chloride.
(3) Sodium sulfate–glycine.

Specific surface interactions with anions might potentially happen. However, the influence on binding capacity should be similar for both proteins. As previously discussed, Fasnaugh and Regnier [13] found similar trends in retention behavior of basic proteins in analytical chromatography for salt mixtures of kosmotropic and chaotropic salts.

The results for the three salt pairs are summarized in Table 4. After optimization of the salt concentrations, capacities are increased by 50% (from 20 to 30 mg/mL for the mAb) for the sodium citrate–sodium chloride salt system compared to 1 M ammonium sulfate that is 90% of the solubility limiting salt concentration (Table 5). Interestingly, a shift in the most appropriate resin type for mAb binding is observed. From an overall point of view, the binding capacity increases for the three resins for the single salt solutions starting with Butyl-600M via PPG-600M to Phenyl-600M. This behavior changes for dual salt systems: PPG-600M > Phenyl-600M > Butyl-600M. Consequently, the more polar resin types seem to have a more favorable behavior in mixed salt systems. Regarding a possible strategy for the salt screening in a mixed salt approach, we suggest to halve the amount of high surface tension salt that is applied for a single salt approach. This allows at the addition of at least the same quantity of low surface tension salt or even more. Expanding the screening beyond this rule of thumb is elaborate and may require extended testing. Hence, the described approach seems to be promising, especially in terms of time efficiency. The increasing binding capacity for dual salt mixtures cannot be explained by the increase or decrease in conductivities. The overall conductivities of the "best" dual salt mixtures are lower than the conductivities of the corresponding high surface tension single salts, due to the fact that a part of the multivalent salt (sulfate) was partly replaced by a monovalent salt (chloride). However, we achieved the opposite results for citrate, as it possesses a lower conductivity than chloride.

Table 5. Limiting salt concentrations for solubility of lysozyme and mAb

Salt	Salt concentration for lysozyme [M]	Salt concentration for mAb [M]
Ammonium sulfate	2.2	1.1
Sodium sulfate	1.7	0.8
Trisodium citrate	1.2	0.6
Sodium chloride	4.4	4.4
Sodium acetate	4.4	3.3
Glycine	2.8	2.2

1 mg/mL protein concentration, room temperature, pH 7.

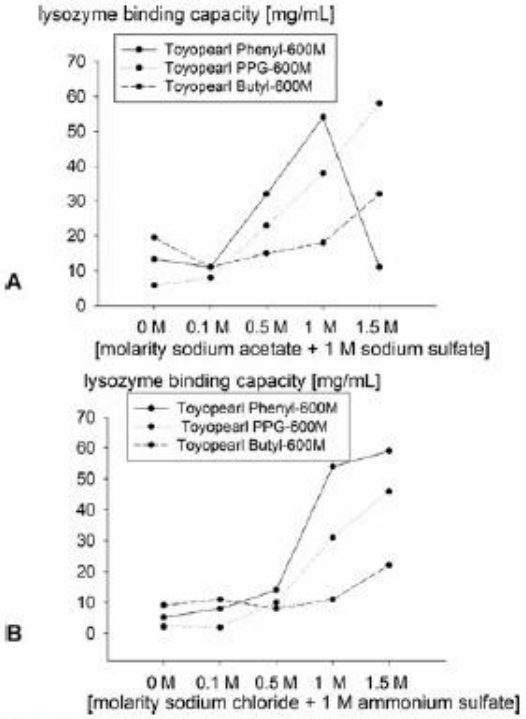

Figure 4. Concentration dependency of the lysozyme-binding capacity for Toyopearl® Phenyl-600M, Toyopearl® Butyl-600M, and Toyopearl® PPG-600M (protein concentration 1 mg/mL, room temperature, pH 7) in a binary salt mixture. (A) Capacities for the binary salt mixture sodium sulfate and sodium acetate. The concentration of sodium sulfate was 1 M, while the sodium acetate concentration was gradually increased. (B) Capacities for the binary salt mixture ammonium sulfate and sodium chloride. The concentration of ammonium sulfate was set to a constant value of 1 M, while the sodium chloride concentration was gradually increased.

3.8 Resin-binding capacity as a function of concentration of the added second electrolyte

Figure 4A shows a plot of the dynamic-binding capacity of lysozyme versus the concentration of sodium acetate added to sodium sulfate. The binding capacities were determined for a 1 M sodium sulfate solution with increasing amount of sodium acetate up to 1.5 M. It can be concluded from the experimental data that an addition of >0.5 M sodium acetate is necessary to achieve an increase in binding capacity. The increase in binding capacity can only be explained as a specific effect of the salt mixture that increases the protein solubility and increases the interaction with the HIC resin. Binding capacities as a function of the acetate content showed different results for the tested resins. For the Phenyl resin, the binding capacity reaches a maximum when 1 M sodium acetate is applied, and it is decreasing at higher concentrations. The binding capacity for the PPG resin is steadily increasing and reaches a maximum at a concentration of 1.5 M sodium acetate, closed to the solubility limit of the protein. Deviating maximum binding capacities for different resins can be interpreted as a change in solution polarity. As demonstrated in Fig. 4B), maximum-binding capacity was observed for the system ammonium sulfate and sodium chloride at a sodium chloride concentration of 1.5 M. From the obtained results, we conclude that the dual salt system affects both dynamic-binding capacity and the preferred ligand polarity, as capacity for the different ligands do not alter in parallel.

4 Concluding remarks

Compared to the single salt solutions, similar or higher dynamic-binding capacities can be achieved for salt mixtures of chaotropic and kosmotropic. This contradicts the common opinion in the literature [7]. For lysozyme and mAb appropriate concentrations of the salt with the low surface tension to be added is around 1 M whereas the concentration of salt with the high surface tension depends on the solubility of the protein. In addition to the already described salt system sodium sulfate–sodium acetate [17], the salt combinations of sodium citrate–sodium chloride, ammonium sulfate–sodium chloride, and ammonium sulfate–glycine lead to the most promising results regarding increase in resin capacity. Binding capacity increases by 30–50% are possible for all investigated HIC resins. In fact, the increased binding capacity seems to be a result of overall salt concentration. Hence, the chaotropic salt mediates solubility. We suggest a supercritical state of the protein solution that will be repealed as soon as it gets in touch with an accessible hydrophobic surface. Following this assumption, we suppose that the degree of solubility mediation needed depends on the amino acid composition of a specific protein. For the presented work, the mAb seems to require a higher degree of solubility mediation, which might also be due to the fact that in terms of molecular weight it is approximately tenfold larger than lysozyme. The resin ranking according to binding capacity alters when a chaotropic salt is added. This shift depends on the molar fraction and the type of the chaotropic salt. So far, it seems like screening mixed salts would need to include various ligand polarities, rather focusing on more polar stationary phases for the inorganic salts. Glycine as a zwitterion has to be considered with retention in this context. Also, further investigations are necessary in order to elucidate the influence of multi salt systems on the recovery and selectivity of proteins.

The authors have declared no conflict of interest.

5 References

[1] Aguilar, M. I., Hearn, M. T. W, in: Hearn, M. T. W. (Ed.), *HPLC of Proteins, Peptides and Polynucleotides*, Wiley-VCH, Weinheim 1991, pp. 247–275.

[2] Eriksson, K.-J., in: Janson, J.-C. (Ed.), *Protein Purification*, Wiley & Sons, Hoboken, New Jersey 2011, pp. 165–183.

[3] Deitcher, R. W., *J. Chromatogr. A* 2010, *1272*, 199–208.

[4] Machold, C., Deinhofer, K., Hahn, R., Jungbauer A., *J. Chromatogr. A* 2002, *972*, 3–19.

[5] Arakawa, T., Kita, E., Ejima, D., Gagnon, P., *Protein Pept. Lett.* 2008, *12*, 544–555.

[6] Harris, E. L. V., in: Harris, E. L. V., Angal, S. (Eds.), *Protein Purification Methods – A Practical Approach*, IRL Press, Oxford 1992, pp. 149–163.

[7] Senczuk, A., Klinke, R., Arakawa, T., *Biotechnol. Bioeng.* 2009, *103*, 930–935.

[8] El Rassi, Z., de Ocampo, L. F., Bacolod, M. D., *J. Chromatogr. A* 1990, *499*, 141–152.

[9] Hofmeister, F., *Arch. Exp. Pathol. Physiol.* 1888, *24*, 247–260.

[10] Baldwin, R. L., *Biophys. J.* 1996, *71*, 2056–2063.

[11] Boström, M., Tavares, F.J., Finet, S., Skouri-Panet, F., Tardieu, A., Ninham, F. W., *J. Biophys. Chem.* 2005, *3*, 217–224.

[12] Melander, W., Horvath, C., *Arch. Biochem. Biophys.* 1977, *183*, 200–215.

[13] Fasnaugh, J. L., Regnier, F. E., *J. Chromatogr. A* 1986, *359*, 131–146.

[14] Weissenborn, P. K., Pugh, R. J., *J. Colloid Interface Sci.* 1996, *184*, 550–563.

[15] Broering, J. M., *PhD Thesis*, Georgia Institute of Technology, Atlanta, GA 2006.

[16] Gagnon, P. S., *European Patent Application EP 1711512*.

[17] Senczuk, A., *European Patent Application EP 1711512*.

9.2. Dual salt mixtures in mixed mode chromatography with an immobilized tryptophan ligand influence the removal of aggregated monoclonal antibodies

Autoren: Judith Vajda[1], Eva Bahret[2], Egbert Müller[1]

Institutionen:
[1]Tosoh Bioscience GmbH, Zettachring 6, 70567 Stuttgart, Deutschland
[2] Hochschule Furtwangen University, Villingen-Schwenningen, Germany

DOI: 10.1002/biot.201300230

Online veröffentlicht am 14.Januar 2014

keywords: Dual salts, Dynamic binding capacity, mAb aggregate removal, Mixed mode chromatography, Tryptophan

Biotechnology Journal
www.biotechnology-journal.com

Biotechnol. J. 2014, 9, 555–565

DOI 10.1002/biot.201300230

Research Article

Dual salt mixtures in mixed mode chromatography with an immobilized tryptophan ligand influence the removal of aggregated monoclonal antibodies

Judith Vajda[1], *Egbert Mueller*[1] *and Eva Bahret*[2]

[1] Tosoh Bioscience GmbH, Stuttgart, Germany
[2] Hochschule Furtwangen University, Villingen-Schwenningen, Germany

In downstream processing of monoclonal antibodies, proper aggregate removal is crucial. Mixed mode ligands such as immobilized tryptophan have been developed to satisfy the need for efficient removal of antibody aggregates. However, method development for mixed mode applications is complicated, since protein binding and elution can be modulated by an increased set of parameters. In the current study, we investigate the effect of different dual salt mixtures on mixed mode chromatography using TOYOPEARL MX-Trp-650M resin, with respect to the dynamic binding capacity, resolution and monomer purity of two different humanized immunoglobulins. Binding capacities varying by more than 50% were observed for different salt mixtures. Furthermore, antibody monomer and aggregate resolution deviated by 30% for different salt mixtures and linear gradient elution. Similar trends were obtained using an immobilized carboxymethyl ligand for the same set of experiments, but the overall resolution was lower. Less kosmotropic salt systems emphasize the electrostatic binding of the relatively hydrophobic mAbs and reduce hydrophobic attraction to a selectivity-determining constraint. Kosmotropic salts such as citrate appear to cause dominating hydrophobic interactions in protein adsorption that hinder electrostatic protein-ligand interactions. This effect may depend on the ionic and hydrophobic site distribution of a protein. The data presented here are important for the further improvement of downstream processing of therapeutic monoclonal antibodies.

Received	12 JUN 2013
Revised	29 NOV 2013
Accepted	09 DEC 2013
Accepted article online	14 JAN 2014

Keywords: Dual salts · Dynamic binding capacity · mAb aggregate removal · Mixed mode chromatography · Tryptophan

1 Introduction

Recently, mixed mode chromatography has gained popularity. In particular, stationary phases combining hydrophobic and ionic interactions appear to provide solutions to complex separation challenges, such as those found in the production processes for pharmaceutically active proteins, e.g. monoclonal antibodies (mAbs) [1]. The two sets of major interactions involved in the process of binding and elution lead to an increased number of parameters affecting the chromatographic purification [2], compared to traditional ion exchanger chromatography (IEX) and hydrophobic interaction chromatography (HIC). Mixed mode chromatography cannot be considered a novel technique, as the first stationary phases intentionally designed for HIC were prone to electrostatic interactions [3]. While the electrostatic repulsion or attraction was at that time undesirable, now the specifically designed and dedicated mixed mode ligands are promising tools for the separation of proteins. For this system, the two differing single mode selectivities are combined in one ligand [4]. Among proteins, mAbs are a potential target for mixed mode separations, as these molecules themselves offer a

Correspondence: Judith Vajda, Tosoh Bioscience GmbH, Zettachring 6, 70567 Stuttgart, Germany
E-mail: judith.vajda@tosoh.com

Abbreviations: **CV**, column volume; **DBC_{10}**, dynamic binding capacity at 10% breakthrough; **HIC**, hydrophobic interaction chromatography; **IEX**, ion exchange chromatography; **mAb**, monoclonal antibody; **SEC**, size exclusion chromatography

whole spectrum of possible interactions due to their complex composition and structure [5]. These attributes, generally related to proteins, are exploited in commonly used mAb purification platforms, such as HIC and IEX [6]. At the same time, because mAbs also have a high drug potential, there is an ever-growing need for improvements in the present purification methods [7]. With regards to productivity in mAb purification, ion exchangers are more favorable than HIC resins, since the capacity of modern IEX resins is higher. On the other hand, there can be no compromises in product purity and the selectivity of an ion exchanger might not always be sufficient. To address this need, various mixed mode resins have been commercialized, e.g. TOYOPEARL MX-Trp-650M, which contains immobilized tryptophan. The ligand carries a hydrophobic moiety and a carboxylic acid, and functions as a weak cation exchanger entity. Heterocyclic hydrophobic entities are favorable as they benefit from unique hydrophobicity and dissociation properties [8]. Although the transition from a pure ion exchanger to a hydrophobic ion exchanger is gradual, and to some extent a matter of definition, the ion exchange capacity may serve as one criterion for classifying resins into these two groups. Of course, this classification needs to address resins with similar capacities. Well-known factors such as pH and conductivity that influence most interaction-based chromatography modes have an impact on the binding of proteins to, and their elution from, a hydrophobic cation exchanger [9]. For the current approach, these parameters were set to constant values for the different salt mixtures involved in the binding or elution of two humanized immunoglobulins G (IgG). This allowed us to investigate the impact of a particular salt mixture on the dynamic binding capacity and purity for the two model IgGs: mAb A and mAb B. Salt ions in solution can be characterized according to the Hofmeister series, an empirically derived classification system for the potential of different salts to enhance hydrophobic protein binding and precipitation [10, 11]. The solubility of a given protein correlates with the ionic strength of a salt solution [12], which is directly linked with the concentration of a particular salt [13]. In general, low salt concentrations improve protein solubility. For increasing salt concentrations, kosmotropic salts decrease protein solubility, while chaotropic salts continuously contribute to protein solubility [12]. One potential explanation is the preferential binding of salt ions to the protein. Salt ions replace some of the protein-bound water molecules [14]. Thus, in highly concentrated salt solutions these ions destabilize proteins. On the other hand, salts such as sodium sulfate, sodium chloride and sodium acetate cause preferential hydration of proteins [15]. The presence of preferentially bound water may have an impact on the binding behavior of proteins to the immobilized tryptophan ligand. Arakawa et al. showed that binding of the salting-in salt magnesium chloride to tryptophan as a free amino acid is energetically favorable. The opposite is true for magnesium sulfate [16]. In investigations of the capacity, lysozyme was used as a reference protein to confirm the obtained trends. In theory, the binding of basic proteins to a hydrophobic cation exchanger at low pH and moderate salt concentration should be strongly dominated by ionic interactions [17]. For electrostatically driven binding, if an appropriate pH is applied, the ionic strength of the liquid phase plays a major role [18]. The ionic strength of a solution is concentration dependent and thereby related to the conductivity of a solution. In contrast to the binding behavior, elution can be considered to be triggered by a larger number of parameters, including molarity and pH of the liquid phase, but also by the salt type or further chaotropic additives in solution [19, 20], which has often been reported for HIC in the literature [21, 22]. The increasing influence of HIC-related parameters is a result of an increased pH and salt concentration for protein elution, which supports weak hydrophobic interactions [19]. Additional effects for salt mixtures have been described in HIC [23, 24]. Thus, salt mixtures might affect protein elution behavior from hydrophobic cation exchanger resins to some extent.

2 Materials and methods

2.1 Proteins

Two monoclonal humanized IgGs and lysozyme were used. The pI values of mAb A and mAb B ranged from 7.0 to 8.5. The mAbs were produced in Chinese hamster ovary cells. Highly concentrated mAb stock solutions at 16 and 5 g/L were available. Lysozyme was purchased from Sigma Aldrich (Taufkirchen, Germany). The pI of lysozyme is reported to be 11.4 [25].

2.2 Resins

TOYOPEARL MX-Trp-650M (Tosoh Bioscience, Stuttgart, Germany) is a mixed mode resin featuring a carboxylic acid entity and an indolic moiety, naturally belonging to the amino acid tryptophan. The amino acid is coupled via its amino group, preventing positive charging of the ligand. Resin mean particle size is 75 µm, mean pore size is 100 nm. The resin has ion exchange capacities between 0.08 and 0.15 eq/L. Typical binding capacities for γ-globulin are higher than 75 mg/mL resin.

TOYOPEARL GigaCap CM-650M (Tosoh Bioscience) is a weak cation exchanger. Its ligand is a carboxylic acid. Mean particle size is 75 µm. TOYOPEARL GigaCap CM-650M is based on TOYOPEARL HW-65. HW-65 has a mean pore size of 100 nm. Typical adsorption capacities for human IgG are higher than 110 mg/mL resin. The ion exchange capacity of TOYOPEARL GigaCap CM-650M is 0.225±0.055 eq/L. Recommended operational flows for both resins range from 10 to 600 cm/h.

2.3 Buffer systems

Three different buffer systems were used: acetate, citrate and glutamate. Each acid was complemented by its corresponding sodium salt or potassium salt in case of glutamate. Due to low solubility, only a 0.05 M glutamate buffer was used, while 100 mM citrate and acetate buffers were employed. Binding pH was 4.3, elution pH 5.6. Sodium chloride was added until 20 mS/cm for binding and 40 mS/cm for elution were reached. Conductivity was chosen rather than molarity or ionic strength, since conductivity is an online accessible parameter and accounts for ionic mobility, as well as the ion concentration. All chemicals were purchased from Merck, Darmstadt, Germany.

2.4 Solubility measurements

Solubilities of mAb A, mAb B and lysozyme at 1 g/L were investigated by turbidity measurements in 10 mM sodium phosphate buffer, pH 7.0. Optical density was assessed at 680 nm using a Cary 300 spectrophotometer (Varian, Palo Alto, USA). Trisodium citrate, sodium acetate and potassium glutamate were each dissolved to different concentrations in 10 mL of the protein solutions.

2.5 Dynamic binding capacity measurements

Both resins were packed into 2-cm long × 6.6 mm internal diameter (ID) columns (Diba Industries, Cambridge, UK). The mAbs were diluted to 1 mg/mL. Solutions of 1 mg/mL lysozyme in the corresponding buffers were prepared. After bypassing the sample until its maximum absorbance was reached, the sample was loaded onto the column at 150 cm/h. The dynamic binding capacity was measured at 10% breakthrough (DBC_{10}). To regenerate the column, 0.2 M sodium hydroxide (Merck) was used.

2.6 mAb aggregation

Aggregation was induced by acidic incubation at pH 2.7 for 1 h at room temperature. mAbs were titrated with 1.0 M hydrochloric acid (Merck); 0.5 M disodium hydrogen phosphate solution (Merck) was used to neutralize the pH of the solution and to prevent further aggregation.

2.7 Analytical size exclusion chromatography

Aggregate quantification was performed in duplicates or triplicates by analytical size exclusion chromatography (SEC). 20 µL of the mAb samples at a concentration of 1 g/L and 100 µL of the elution fractions were injected onto a TSKgel $G3000SW_{XL}$ 7.8 mm ID × 30 cm (Tosoh Bioscience). The mobile phase consisted of 0.1 M sodium phosphate and 0.1 M sodium sulfate, pH 6.7 (Merck). A flow rate of 1 ml/min was applied. Aggregate contents were calculated by the area under the curve (AUC) from the chromatograms at 280 nm.

2.8 Linear gradient separation of aggregated mAb samples

Linear gradient experiments were conducted on TOYOPEARL GigaCap CM-650M and MX-Trp-650M at 150 cm/h. Columns were packed according to Section 2.5. Aggregated mAb (7 mg) at a concentration of 1 g/L were loaded. Subsequently, the column was washed with 15 column volumes (CV) of loading buffer and a linear gradient over 140 CV was applied for protein elution. This shallow gradient strategy takes into account the short column length and encompasses protein elution for all of the applied buffer systems. The column was regenerated by flushing with 0.2 M sodium hydroxide. Fractions (5 mL) were collected for further analysis.

2.9 Step gradient separations

Conditions were adapted from the linear gradient experiments (Section 2.8). For elution, two steps were introduced: step 1 at 45% B (mAb A) or 60% B (mAb B) for 60 CV, and step 2 at 100% B for 30 CV. Monomer yields were calculated by AUC determination.

3 Results and discussion

3.1 Salting-out properties of the applied buffer salts

The salting-out potentials of acetate, glutamate and citrate are cited in the literature for various proteins: citrate is described as the most kosmotropic, followed by glutamate and acetate [26–28]. Table 1 lists the salting-out molarities at pH 7.0, determined by optical turbidity measurements. The critical salt concentration varied for lysozyme and the two mAbs. The results resemble the expected arrangement for the different salts. Highest salt concentrations could be added in the case of acetate. Glutamate was also tolerated in concentrations higher than 1.0 M. Citrate was the most kosmotropic salt of the tested electrolytes and led to protein precipitation at lowest concentrations.

Table 1. Solubility limits of mAb A, mAb B and lysozyme in solutions of sodium citrate, potassium glutamate and sodium acetate at pH 7.0[a)]

Salt	mAb A [mol/L]	mAb B [mol/L]	lysozyme [mol/L]
Citrate	0.6	0.7	1.2
Glutamate	1.0	1.5	1.9
Acetate	3.3	2.4	4.4

a) Solubility was determined by optical turbidity measurements. Corresponding molarities are listed.

3.2 Dynamic binding capacities

For mAb A, significant deviations in DBC_{10} were observed for the different salt mixtures and resins at a conductivity of 20 mS/cm and pH 4.3. According to previous results, these conditions appeared to be most favorable for acetate buffer and mAb A [29]. Although this pH environment might not be well tolerated by all potential mAb candidates, the molecular integrity of mAbs A and B seemed to be unaffected. Table 2 lists the DBC_{10}s for the two model mAbs and lysozyme and the three different buffers. For lysozyme, the tryptophan capacities at the different salt mixtures were in the range of mAb B. While acetate and sodium chloride led to a capacity of 54 mg/mL resin, the capacity for glutamate and sodium chloride decreased to 51 mg/mL resin and the capacity with citrate and sodium chloride decreased further to 32 mg/mL resin. Lysozyme capacities are typically discussed in context of sulfo type ion exchangers, which achieve higher capacities for lysozyme [30]. Low capacities of tryptophan could be due to the lack of pH or conductivity adjustments, in order to keep up comparability for the liquid phase conditions. Capacities of the weak cation exchanger for lysozyme exceeded 100 mg/mL when applying sodium acetate + sodium chloride or potassium glutamate + sodium chloride. The glutamate mixture achieved a higher capacity than sodium acetate + sodium chloride, but they were still in the same range. The underlying reason for the generally higher capacities might be that lysozyme can benefit more efficiently from the higher ion exchange capacity of the weak cation exchanger than the mAbs. This might cause higher overall capacities than those observed for tryptophan. With the carboxy type resin, no such increase could be observed for the mAbs. If the ligand density is high, mAbs can cover more ligands without necessarily increasing the number of adsorbed molecules. According to the concept of steric mass action for ion exchangers developed by Brooks and Cramer [31], maximum static resin capacity is decreased for an increased shielding factor. On the other hand, the number of adsorbed lysozyme molecules might still be higher if there is tighter packing of lysozyme on the resin surface, based on the smaller size of the molecules. Also, the net charge of lysozyme at the applied pH is higher, which might allow more efficient exploitation of the increased ion exchange capacity of TOYOPEARL GigaCap CM-650M. The highest mAb capacities were achieved for mAb A and the acetate + sodium chloride mixture. This held true for both ligands. Capacities for all of the three proteins were best for this salt combination, except for lysozyme loaded onto TOYOPEARL GigaCap CM-650M. In the other cases, potassium glutamate + sodium chloride led to slightly lower capacities, whereas citrate + sodium chloride showed decreasing capacities compared to the other two salt mixtures. For instance, citrate + sodium chloride led to a capacity of 58 mg mAb A/mL tryptophan resin, but glutamate + sodium chloride to 72 mg/mL tryptophan resin, similar to that for the acetate + sodium chloride mixture, 77 mg/mL tryptophan resin. The capacities for mAb B were generally lower and appeared unaffected by the different salts in the case of TOYOPEARL GigaCap CM-650M. Acetate + sodium chloride led to the highest DBC_{10} on tryptophan, followed by glutamate + sodium chloride and citrate + sodium chloride. Up to 52 mg/mL resin was reached for acetate, while the capacity using citrate + sodium chloride was only 23 mg/mL resin, which is comparable to HIC capacities. An explanation for the observed resistance against salt-specific impacts of the carboxymethyl-type resin may be a different hydrophobic and ionic site distribution, as discussed below. Certainly, 40 mg/mL TOYOPEARL GigaCap CM-650M is beyond the capacities typically achieved for this type of cation exchanger. However, conditions were adopted from mAb A and the salt-tolerant cation exchanger. Although the ion exchange capacity of TOYOPEARL GigaCap CM is higher than for MX-Trp-650M, it is not as salt tolerant, which might explain the low binding capacities. The observed trends in DBC_{10} showed some consistency for both mAbs and the standard protein. Citrate + sodium chloride led to the smallest DBC_{10} of the three tested salt combinations. A more drastic impact on capacity was observed for mAb B, as the DBC_{10} dropped to less than half of the capacity for acetate + sodium chloride. One reason for this might be the kosmotropic character of citrate, which has been described in particular in context of HIC [32]. Kosmotropic salts strongly bind water molecules, while they are excluded from the hydrophobic surface areas of a solvated protein [33]. For traditional ion exchange separations, these effects are usually negligible because the applied salt concentration for protein binding is low. Clearly, elevated salt concentrations enhance this effect in protein solutions. The extent of this stabilizing effect is comparably great for citrate, which stabilizes β-lactoglobulin better against denaturation than phosphate, sulfate or chloride [34]. Assuming that this involves preferential hydration of the protein, the ligand might need to compete against the water molecules, which might act as a capacity damper. Hydrophobic areas on the surface of the mAb are more prone to hydrophobic interactions than with the less kosmotropic salts. In consequence, hydrophobic interactions could play a more dominant role in protein binding to the mixed mode resin if a kosmotropic salt is used. This effect might be extended to the ligand. Hydrophobic interactions and electrostatic interactions address different sites of the protein. Fausnaugh et al. [35] reported changes in the retention of lysozymes from related bird species on hydrophobic stationary phases for amino acid substitutions on the surface of lysozyme opposite the catalytic cleft, which indicates that this is the binding site for the hydrophobic stationary phases. In contrast, sites taking part in ionic interactions seem to be

Table 2. DBC_{10}s for mAb A, mAb B and lysozyme at 10% breakthrough[a)]

Salt	mAb A [mg/mL] TOYOPEARL GigaCapCM	mAb A [mg/mL] tryptophan	mAb B [mg/mL] TOYOPEARL GigaCap CM	mAb B [mg/mL] tryptophan	Lysozyme [mg/mL] TOYOPEARL GigaCap CM	Lysozyme [mg/mL] tryptophan
Citrate + sodium chloride	47	58	44	23	54	32
Glutamate + sodium chloride	31	72	40	42	138	51
Acetate + sodium chloride	90	77	40	52	121	54

a) Different salt mixtures were used at pH 4.3 and 20 mS/cm.

widely spread [36]. If the hydrophobic site interacts primarily with the stationary phase, some of the charged sites are sterically not accessible for the ligands or at least sterically hindered, as their orientation is fixed and, for some sites, opposite from the resin surface. Acetate as a comparably less kosmotropic salt [32] might cause less predominant hydrophobic interactions, which might allow more efficient orientation of the electrostatic sites towards the charged moiety of the ligand. Compared to other hydrophobic ligands such as hexyl, the ring structure of tryptophan is not so hydrophobic that it can adsorb proteins solely based on hydrophobic interactions. In contrast, the ionic interactions seem to be sufficient for protein binding. Protein adsorption can be further enhanced by multipoint attachment via other charged and hydrophobic sites that may interact with the ligand moieties. The relative resistance of the TOYOPEARL GigaCap CM-650M binding of mAb B to salt effects could be explained by a more equal distribution of hydrophobic and ionic sites along the mAb. Weak hydrophobic contributions in mAb B binding of the carboxymethyl ligand are not sufficient to overcome the electrostatic attraction to more closely located ionic sites.

The achieved binding capacities for the mAbs applying acetate and sodium chloride are competitive to capacities of modern ion exchange resins [37]. However, modern ion exchangers, such as TOYOPEARL GigaCap CM or TOYOPEARL GigaCap DEAE, have higher ion exchange capacities than the tryptophan immobilized resin. The ion exchange capacities for these resins range between 0.15 and 0.28 eq/L. The tryptophan immobilized resin has a lower ion exchange capacity but achieves similar binding capacities at higher salt concentrations. This might be further evidence of multipoint attachment that includes hydrophobic interactions. Salt concentrations higher than 1 M led to capacities lower than those typically obtained for HIC resins (data not shown). For this case, electrostatic interactions were clearly prevented by the salt ions, and the enhanced hydrophobic interactions were not capable to overcome this effect. Applying glutamate and sodium chloride, it seems only natural that capacities for the three proteins were in between those for citrate and acetate, as glutamate is generally considered to range between citrate and acetate with regards to its salting-out properties [38]. Differences in the binding behavior of mAb A and mAb B could be explained by the hydrophobicities of the two mAbs. The respective pI values for both mAbs are the same, but the corresponding hydrophobicities were not determined before this study.

3.3 Linear gradient elution

To determine the impact of the different salt mixtures on the resolution of mAb monomers and mAb aggregates, we applied a linear gradient from 20 mS/cm at pH 4.3 to 40 mS/cm at pH 5.6. These conditions were also used for comparison with TOYOPEARL GigaCap CM-650M, a weak cation exchanger. The resulting mixed mode chromatograms for mAb A and mAb B are shown in Figs. 1A and B. Figures 1C and D show the separations on TOYOPEARL GigaCap CM-650M. The mAb A sample contained approximately 30% aggregates, mAb B contained 15% aggregates. Differences in retention for the various salt mixtures and both mAbs and their aggregates showed a similar trend. The highest conductivity and pH was required when applying glutamate buffer, followed by acetate and citrate. Interestingly, the retention for citrate was lower than for the other two salt mixtures. From the Hofmeister series for the salting-out properties, citrate would be expected to impose the highest retention based on hydrophobic interaction. The salting-out behavior for the two mAbs and lysozyme confirm the Hofmeister order obtained from the literature. The effects of different salt mixtures on resin selectivity were not limited to MX-Trp-650M, but were also present for the carboxymethyl cation exchanger. As discussed before, ligand attributes change gradually from a strong cation exchanger to a hydrophobic mixed mode ligand. For this study, a weak cation exchanger was chosen to investigate the contribution of the hydrophobic moiety in mixed mode, rather than a pure strong cation exchanger, such as TOYOPEARL GigaCap S-650M. From a comparison of these two resins we concluded that the indolic group was not the sole factor responding to different salt mixtures. However, the indolic group mediates increased resolution for all separations, compared to TOYOPEARL GigaCap CM-650M. The observed behavior might indicate that the

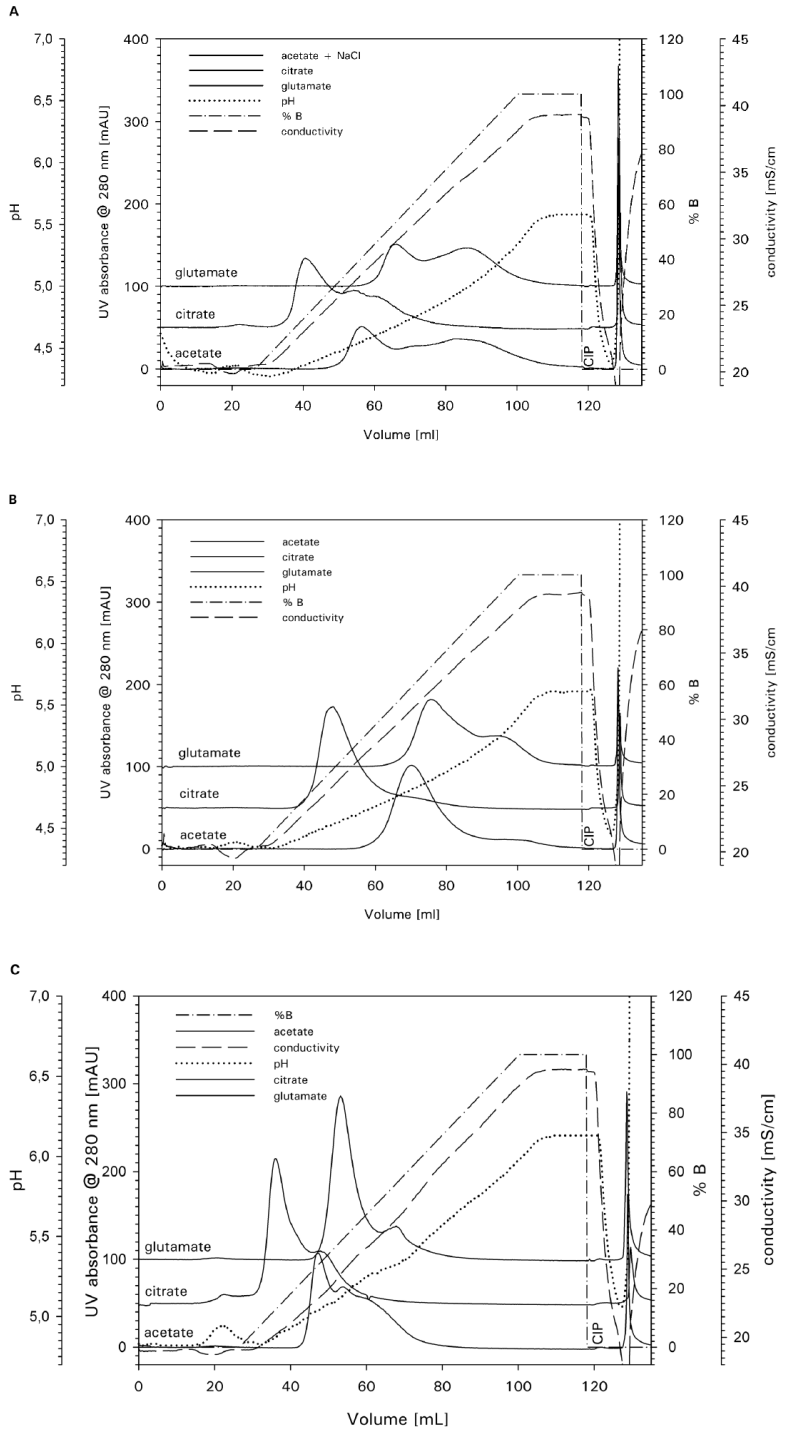

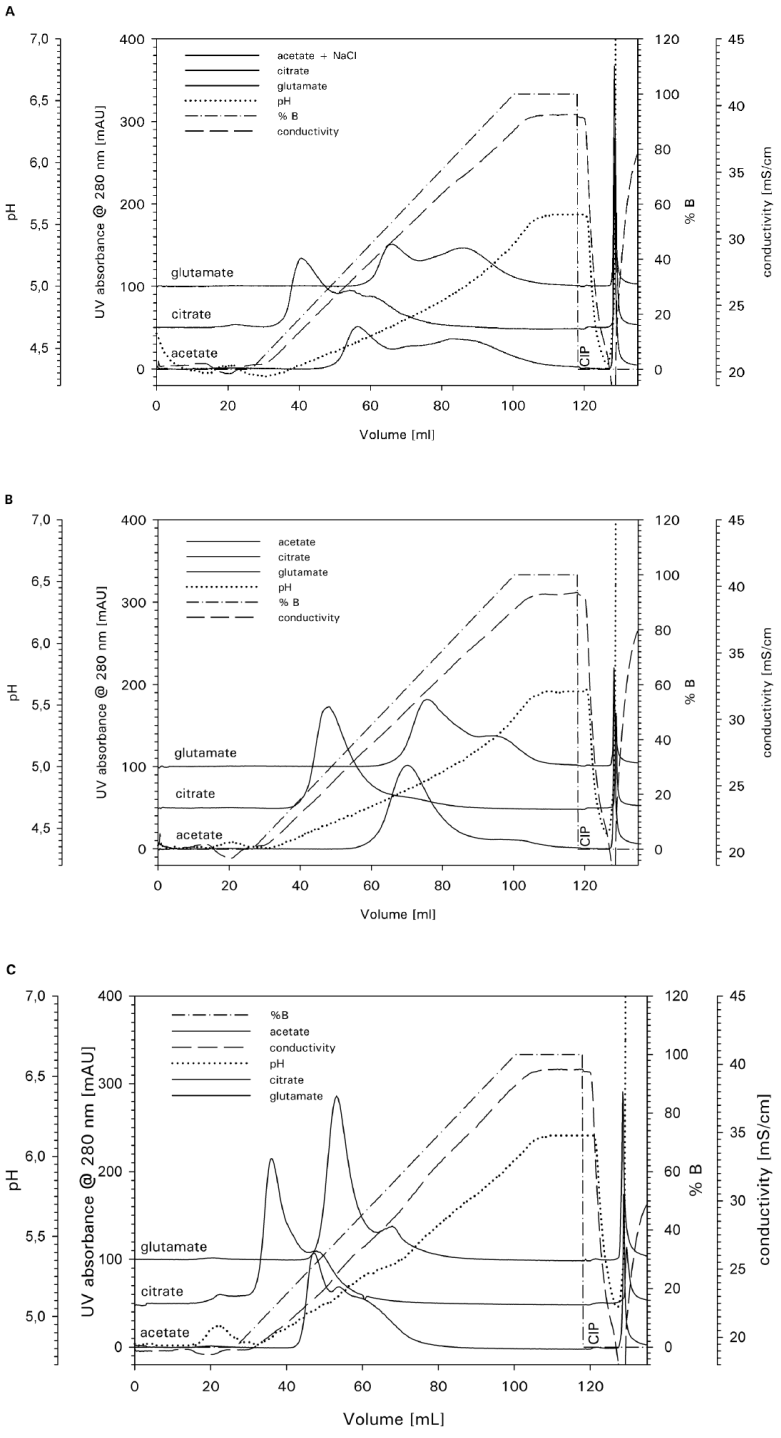

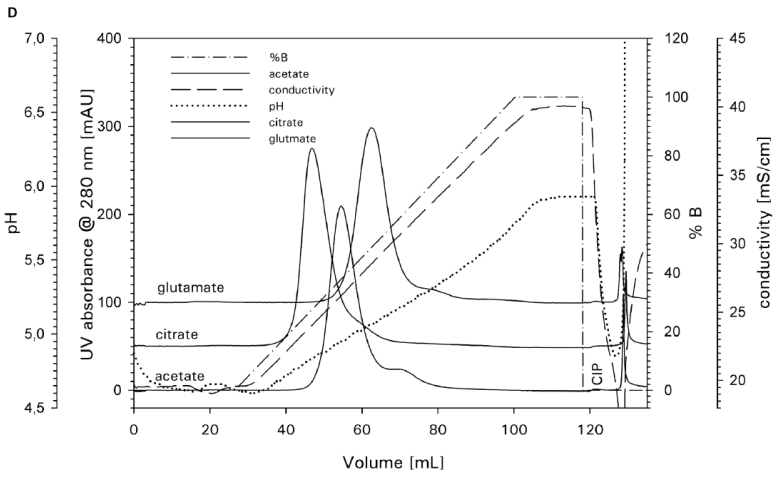

Figure 1. Separation of the aggregated mAbs using a combined salt and pH gradient. Conductivity and pH were kept constant for the three different salt mixtures indicated by the key: sodium acetate + sodium chloride, potassium glutamate + sodium chloride and sodium citrate + sodium Samples were loaded at pH 4.3 and 20 mS/cm. Elution was performed by a 140 CV linear gradient to buffer B at pH 5.6 40 mS/cm. (**A**) mAb A on TOYOPEARL MX-Trp-650M. (**B**) mAb B on TOYOPEARL MX-Trp-650M. (**C**) mAb A on TOYOPEARL GigaCap CM-650M. (**D**) mAb B on TOYOPEARL GigaCap CM-650M. Data are representative of at least two independent experiments with similar results.

balance of ionic interactions and hydrophobic interactions for the elution process differs for the different salt mixtures and that the extent of this effect increases with increasing ligand hydrophobicity. Assuming that hydrophobic interactions only contribute to protein binding if the electrostatic interactions are not strong enough to reorientate a protein, selectivity of the carboxymethyl ligand suffers from a less hydrophobic character. The impact of the chosen salt mixture might also influence the ligand itself. Changes in the hydration shell thickness of tryptophan as a free amino acid in solution have been described in the literature [28]. Depending on the added ion, spherical extension of tryptophan as a free amino acid decreases or increases for elevated molarities. Consequently, the impact of the salt system might not be limited to the protein, but might be extended to the ligand. Table 3 illustrates the impact of different salt mixtures on the resolution of the monomer peak and the aggregates. In general, resolution is higher for the mixed mode separations, except for the mAb B separation using TOYOPEARL GigaCap CM-650M. As previously discussed in context of the dynamic binding capacities, mAb B seems to be less affected by the different salt mixtures when separated by the carboxymethyl ligand. In terms of selectivity for mAb monomers and aggregates, the tryptophan resin outplays the carboxymethyl resin. This underlines the potential of mixed mode resins and how challenging purification tasks could benefit from mixed mode ligands. Although the hydrophobic impact should not play a too dominant role, its presence seems to improve separation of mAb monomers from aggregates. Hydrophobic ion exchangers seem to be a useful extension of ion exchanger resin libraries. Comparing the different salt mixtures, an improvement can be observed for the acetate + sodium chloride mixture compared to the other two mixtures. One reason might be decreased monomer peak tailing for the less kosmotropic salt mixture. We conclude that the mAbs do not rely on kosmotropic salts promoting weak hydrophobic interactions with the tryptophan ligand. Hence, undesired peak tailing might result from a too large contribution of hydrophobic interactions to the retention of the mAbs. Although the adsorption is primarily electrostatically driven, the ligand would still allow more hydrophobic contributions, the more hydrophobic sites are present at a molecule. For mAb monomers and mAb aggregates, this means protein retention based on hydrophobic interactions will be enhanced for the aggregates.

Table 3. mAb monomer dimer resolution of mAb A and mAb B

Salt	mAb A resolution tryptophan	mAb A resolution TOYOPEARL GigaCap CM	mAb B resolution tryptophan	mAb B resolution TOYOPEARL GigaCap CM
Citrate + sodium chloride	0.8	–[a)]	0.9	–[a)]
Glutamate + sodium chloride	0.7	–[b)]	0.7	0.9
Acetate + sodium chloride	1.2	0.4	1.2	0.9

a) Resolutions for citrate buffer could not be calculated since the applied integration criteria led to the detection of a single peak for both monomers and aggregates.
b) Separation of the aggregated mAb A sample with potassium glutamate + sodium chloride is also not sufficient.

3.4 Step gradient elution

In a more practical approach, step gradient elution was used to investigate the suggested concept. Steps at 45 and 60% B were introduced for monomer elution of mAb A and mAb B, respectively. Figures 2A and B present the corresponding chromatograms. Conductivity and pH conditions for monomer elution were chosen from the acetate linear gradient runs for mAb A and mAb B. SEC chromatograms of the elution pools and the loaded samples are shown in Figs. 3A and B. Recoveries and aggregate removal factors are listed in Table 4. For the acetate mixture, the mAb A pool contained 2.1% aggregates. For the mAb B pool, the aggregate content was lower than the limit of detection. Due to the high aggregate content of mAb A before polishing, the resulting aggregate content of mAb A still demonstrates significant aggregate removal. As expected, acetate + sodium chloride perform best with regards to purity. The applied conductivity and pH conditions led to the following purity ranking for the step 1 elution pools: sodium acetate + sodium chloride > potassium glutamate + sodium chloride > sodium citrate + sodium chloride. A lowest purity would be expected for citrate, as the elution occurred earlier for this salt combination and the linear gradient. This is in accordance with yields obtained for this dual salt mixture, as the yield of the citrate run of mAb B is higher than the yield of the acetate + sodium chloride mixture and mAb B. Recovery of mAb A during step 1 is lower, due to the mAb A breakthrough while loading. This breakthrough fraction was not included for yield calculations. On the other hand, following to this hypothesis, purity was sup-

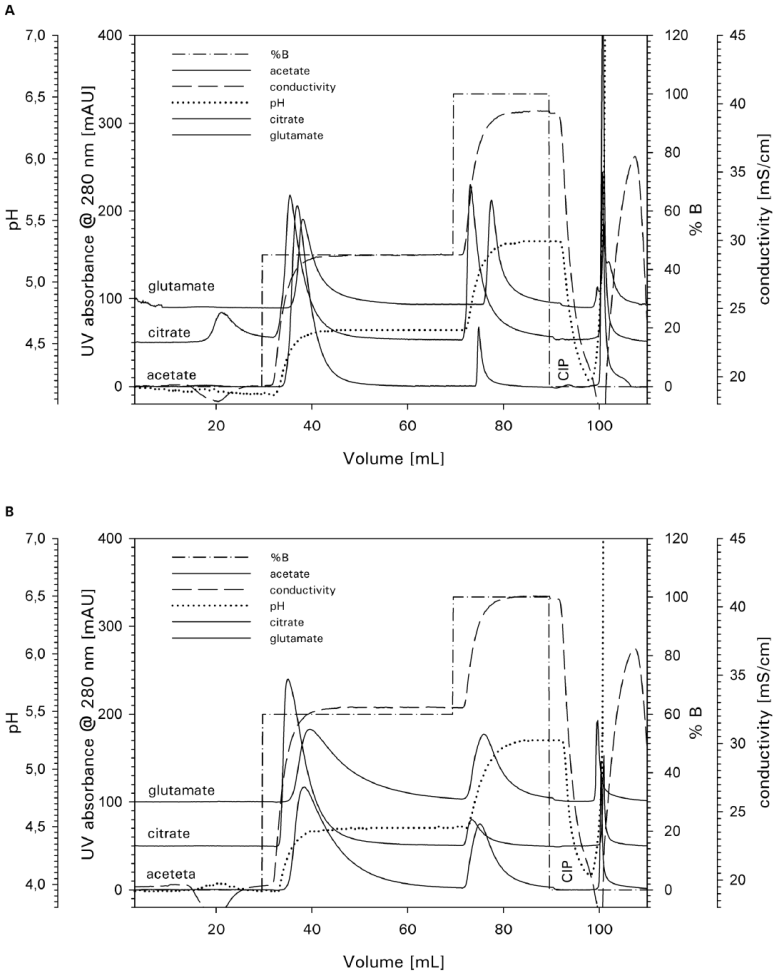

Figure 2. (**A**, **B**) Separation of the aggregated mAb samples on TOYOPEARL MX-Trp-650M by step gradient elution. Step 1 was set to 45% B for mAb A and to 60% B for mAb B. Conditions were chosen from the acetate mixture linear gradient runs presented in Figs. 1A and B. Data are representative of at least two independent experiments with similar results.

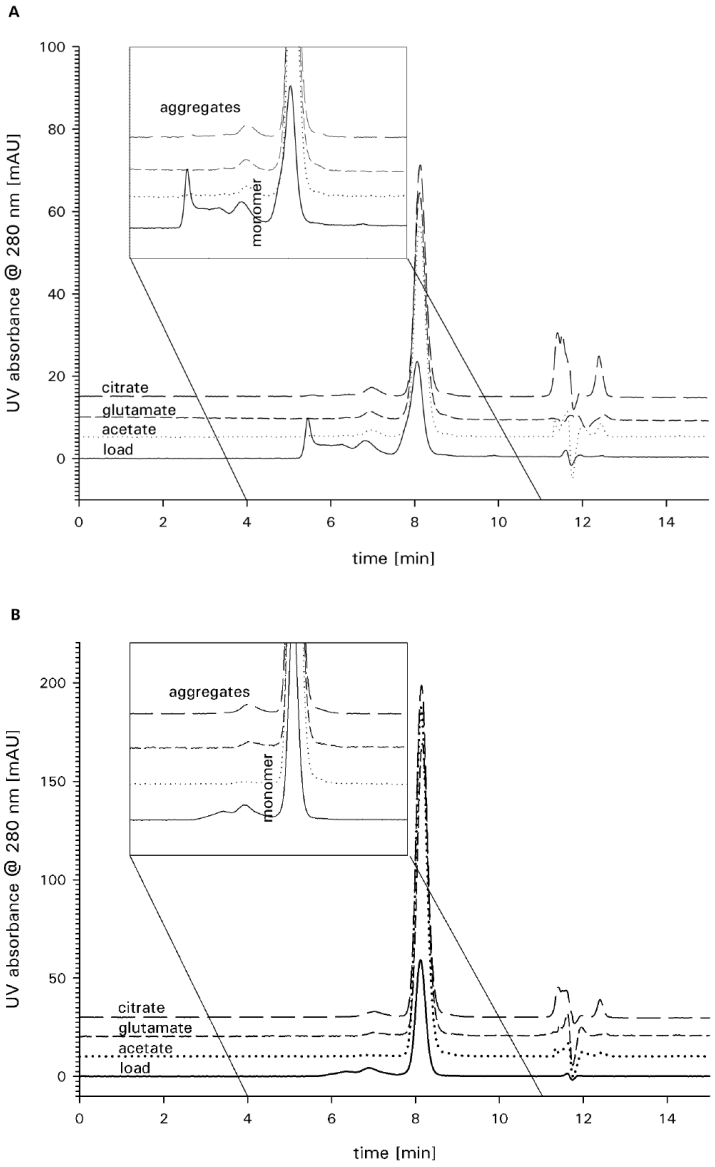

Figure 3. SEC chromatograms using TSKgel G3000SW$_{XL}$ of the pooled elution fractions collected during elution by the first step (dotted lines). The signal heights of the post mixed mode samples are normalized to the elution pool volumes. The load composition is also illustrated. The aggregate content for the elution pools varies for the different salts. (**A**) mAb A contained 30% aggregates before polishing with TOYOPEARL MX-Trp-650M. (**B**) mAb B originally contained 15% aggregates. Data are representative of at least two independent experiments with similar results.

posed to be higher for the glutamate + sodium chloride mixture than for acetate + sodium chloride. In fact, the yield decreased for the glutamate mixture, compared to the sodium acetate + sodium chloride mixture. With regards to purity, the results were not those expected. Monomer purities for the glutamate + sodium chloride mixture were in between those obtained for the other two mixtures. In the light of the Hofmeister series, this behavior is consistent with higher purities and resolution for the less kosmotropic salts. Increasing recoveries for less kosmotropic mixtures are likely to be expected. Combining both effects leads to high yields for acetate + sodium chloride. Considering the assumptions framed for the linear gradient experiments, this could be explained by a varying share of both hydrophobic and ionic interactions. In consequence, the citrate + sodium chloride mixture representing a mixture of a primarily kosmotropic buffer salts and the rather chaotropic salt sodium chloride induces

Table 4. Yield and aggregate removal factor for mAb A and mAb B and the different salt mixtures[a)]

salt	mAb A (30% aggregates)		mAb B (15% aggregates)	
	Yield (%)	Aggregate removal factor	Yield (%)	Aggregate removal factor
Citrate + sodium chloride	40	4.2	90	6.5
Glutamate + sodium chloride	40	8.8	60	30.0
Acetate + sodium chloride	80	11.1	80	> 150

a) Aggregate removal was determined by analytical SEC with TSKgel G3000 SW_{XL}. Yields were calculated from the area under the curve of the tryptophan runs, subtracting the aggregate content determined by analytical SEC.

stronger hydrophobic interactions than the other salt mixtures in order of their arrangement in the Hofmeister series. The decreased DBC_{10}s, lowered resolutions and monomer purities, and the lowered recoveries and purities indicate such a behavior. The comparably decreased conductivity and pH conditions necessary for the elution with the linear gradient when applying the citrate system fit into this picture as the capacity for this mixture is low. For HIC-dominated binding, a much higher salt content would allow competitive binding, but this would lead to pure hydrophobic interaction and all its related drawbacks.

4 Concluding remarks

The behavior of the observed DBC_{10}s does not reflect the behavior of the mAb capacity for HIC resins and dual salt mixtures that we published previously [24]. Mixtures of chaotropic and kosmotropic salts should lead to higher binding capacities than mixtures of two kosmotropic or two chaotropic salt mixtures. However, for this study we do not consider this a problem as, with this particular mixed mode ligand, binding is intended to occur preferably via electrostatic interactions. The applied salt concentrations were too low to reach the solubility limit of the mAbs. Therefore, there was no need to facilitate extended protein solubility with the chaotropic salt as for the salt mixtures in HIC. By choosing a less kosmotropic buffer salt, ionic interactions were predominant in binding, allowing high capacities as typically observed for IEX. Protein adsorption preliminary based on hydrophobic interaction seems to restrict binding site accessibility of the employed proteins. Clearly, the hydrophobic character of the tryptophan is more pronounced for rather hydrophobic molecules. In terms of selectivity, the hydrophobic moiety of the tryptophan resin is advantageous. The linear gradient experiments with the weak cation exchanger TOYOPEARL GigaCap CM-650M showed less resolution compared to the cationic mixed mode resin. The actual separation of mAb monomers and mAb dimers was most successful with the least kosmotropic salt mixture. If the jigsaw of interactions is shifted towards a greater impact of hydrophobic interactions, it appears that the separation will suffer from typical drawbacks related to HIC, such as lower yield and peak tailing. By using more chaotropic mixtures, these effects can be tempered, while there are still weak hydrophobic interactions present, providing altered selectivity compared to traditional IEX media. The degree of hydrophobic retention is adjustable and might need to be enhanced for separations of less hydrophobic components. In contrast to HIC media, the whole range of the lyotropic series is applicable for selectivity modulation using hydrophobic cation exchangers. In HIC, solely chaotropic salts do not allow sufficient capacity. Therefore, hydrophobic ion exchange resins offer the opportunity to modulate hydrophobic interactions to alter selectivity.

This study was supported by Tosoh Bioscience GmbH.

JV and EM are paid employees of Tosoh Bioscience GmbH. EB declares no financial or commercial conflict of interest.

5 References

[1] Gagnon, P., IgG aggregate removal by charged-hydrophobic mixed mode chromatography. *Curr. Pharm. Biotechnol.* 2009, *10*, 434–439.
[2] Chen, J., Tetrault, J., Zhang, Y., Wasserman, A. et al., The distinctive separation attributes of mixed-mode resins and their application in monoclonal antibody downstream purification process. *J. Chromatogr. A* 2010, *1217*, 216–224.
[3] Eriksson, K., Hydrophobic interaction chromatography, in: Janson, J., Rydén, L. (Eds.), *Protein Purification – Principles, High Resolution Methods and Applications*, Wiley-VCH Verlag, Weinheim 1989, pp. 208.
[4] Kennedy, L. A., Kopaciewicz, W., Regnier, F. E., Multimodal liquid chromatography columns for the separation of proteins in either the anion-exchange or hydrophobic-interaction mode. *J. Chromatogr. A* 1986, *359*, 73–84.
[5] Chartrain, M., Lily, C., Development and production of commercial therapeutic monoclonal antibodies in mammalian cell expression systems: An overview of the current upstream technologies. *Curr. Pharm. Biotechnol.* 2008, *9*, 447–467.
[6] Liu, H. F., Ma, J., Winter, C., Bayer, R., Recovery and purification process development for monoclonal antibody production. *mAbs* 2010, *2*, 480–499.
[7] Fontes, N., Advances in technology and process development for industrial-scale monoclonal antibody purification, in: Gottschalk, U. (Ed.), *Process Scale Purification of Antibodies*, Wiley-VCH Verlag, Weinheim 2009, pp. 203.

[8] Zhao, G., Dong, X. Y., Sun, Y., Ligands for mixed-mode protein chromatography: Principles, characteristics and design. *J. Biotechnol.* 2009, *1*, 3–11.
[9] Nfor, B. K., Noverraz, M., Chilamkurthi, S., van der Wielen, L. U. M. et al., High-throughput isotherm determination and thermodynamic modeling of protein adsorption on mixed mode adsorbents. *J. Chromatogr. A* 2010, *1217*, 6829–6850.
[10] Xia, F., Nagrath, D., Garde, S., Cramer, S. M., Evaluation of selectivity changes in HIC systems using a preferential interaction based analysis. *Biotechnol. Bioeng.* 2004, *87*, 354–364.
[11] Hofmeister, F., Zur Lehre von der Wirkung der Salze. *Arch. Exp. Pathol. Pharmakol.* 1888, *24*, 247–260.
[12] Green, A., Studies in the physical chemistry of the proteins: X. The solubility of hemoglobin in solutions of chlorides and sulfates of varying concentration. *J. Biol. Chem.* 1932, *95*, 47–66.
[13] IUPAC. *Compendium of Chemical Terminology, 2nd edn*. Compiled by McNaught, A. D., Wilkinson, A., Blackwell Scientific Publications, Oxford 1997.
[14] Timasheff, S. N., Protein-solvent preferential interactions, protein hydration, and the modulation of biochemical reactions by solvent components. *Proc. Natl. Acad. Sci. USA* 2002, *15*, 9721–9726.
[15] Arakawa, T., Timasheff, S. N., Preferential interactions of proteins with salts in concentrated solutions. *Biochemistry* 1982, *25*, 6545–6552.
[16] Arakawa, T., Ejima, D., Tsumoto, K., Obeyama, N. et al., Suppression of protein interaction by arginine: A proposed mechanism of the arginine effects. *Biophys. Chem.* 2007, *127*, 1–8.
[17] Yang, Y., Geng, X., Mixed-mode chromatography and its applications to biopolymers. *J. Chromatogr. A* 2011, *1218*, 8813–8825.
[18] Chang, C., Lenhoff, A. M., Comparison of protein adsorption isotherms and uptake rates in preparative cation-exchange materials. *J. Chromatogr. A* 1998, *827*, 281–293.
[19] Ghose, S., Jin, M., Liu, J., Hickey, J., Integrated polishing steps for monoclonal antibody purification, in: Gottschalk, U. (Ed.), *Process Scale Purification of Antibodies*, Wiley-VCH Verlag, Weinheim 2009, p 157.
[20] Yang, T., Malmquist, G., Johansson, B. L., Maloisl, J. L. et al., Evaluation of multi-modal high salt binding ion exchange materials. *J. Chromatogr. A* 2007, *1157*, 171–177.
[21] Shukla, A. A., Peterson, J., Sorge, L., Lewis, P. et al., Preparative purification of a recombinant protein by hydrophobic interction chromatography: Modulation of selectivity by the use of chaotropic additives. *Biotechnol. Prog.* 2002, *18*, 556–564.
[22] Tsumoto, K., Ejima, D., Nagase, K., Arakawa, T., Arginine improves protein elution in hydrophobic interaction chromatography: The cases of human interleukin-6 and activin-A. *J. Chromatogr. A* 2007, *1154*, 81–86.
[23] Senczuk, A. M., Klinke, R., Arakawa, T., Vedantham, G. et al., Hydrophobic interaction chromatography in dual salt system increases protein binding capacity. *Biotechnol. Bioeng.* 2009, *103*, 930–935.
[24] Müller, E., Vajda, J., Josic, D., Schröder, T., Mixed electrolytes in hydrophobic interaction chromatography. *J. Sep. Sci.* 2013, *36*, 1327–1334.
[25] Thomas, B. R., Vekilov, P. G., Rosenberger, F., Effets of microheterogeneity in hen egg-white lysozyme crystallization. *Biol. Crystallogr.* 2008, *54*, 226–236.
[26] Yang, Z., Hofmeister effects: An explanation of the impact of ionic liquids on biocatalysis. *J. Biotechnol.* 2009, *144*, 12–22.
[27] Collins, K. D., Ions from the Hofmeister series and osmolytes: Effects on proteins in solution and in crystallization process. *Methods* 2004, *34*, 300–311.
[28] Cacace, M. G., Landau, E. M., Ramsden, J. J., The Hofmeister series: Salt and solvent effects on interfacial phenomena. *Q. Rev. Biophys.* 1997, *30*, 241–277.
[29] Jackewitz, A., Development of a high capacity, mixed-mode resin for high conductivity mAb feedstocks. *BioProcess Int.* 2012, *10*, 82–84.
[30] Staby, A., Jacobsen, J. H., Hansen, R. G., Bruus, U. K. et al., Comparison of chromatographic resins. V. Strong and weak cation exchanger resins. *J. Chromatogr. A* 2006, *118*, 168–179.
[31] Brooks, C. A., Cramer, S. M., Steric mass-action ion exchange: Displacement profiles and induced salt gradients. *AIChE J.*1992, *38*, 1969–1978.
[32] Gagnon, P., Mayes, T., Danielsson, Å., An adaption of hydrophobic interaction chromatography for estimation of protein solubility optima. *J. Pharm. Biomed. Anal.* 1997, *16*, 587–592.
[33] Kalra, A., Tugcu, N., Cramer, S. M., Garde, S., Salting-in and salting-out of hydrophobic solutes in aqueous salt solutions. *J. Phys. Chem. B* 2001, *105*, 6380–6386.
[34] Arakawa, T., Kita, Y., Carpenter, J. F., Protein-solvent interaction in pharmaceutical formulations. *J. Pharm. Res.* 1991, *3*, 285–291.
[35] Fausnaugh, J. L., Regnier, F. E., Solute and mobile phase contributions to retention in hydrophobic interaction chromatography of proteins. *J. Chromatogr. A* 1986, *359*, 131–146.
[36] Fausnaugh-Pollit, J., Thevenon, G., Janis, L., Regnier, F. E., Chromatographic resolution of lysozyme variants. *J. Chromatogr. A* 1988, *443*, 221–228.
[37] Faude, A., Zacher, D., Müller, E., Böttinger, H., Fast deteremination of conditions for maximum dynamic capacity in cation-exchange chromatography of human monoclonal antibodies. *J. Chromatogr. A* 2007, *1161*, 29–35.
[38] Saum, S. H., Müller, V., Regulation of osmoadaptation in the moderate halophile *Halobacillus halophilus*: Chloride, glutamate and switching osmolyte strategies. *Saline Systems* 2008, *4*, 4.

9.3. Cost Estimation for Protein A Chromatography

Autoren: Matthias Franzreb[1], Judith Vajda[2], Egbert Müller[2]

Institutionen:
[1]Karlsruher Institut für Technologie, Institut für Funktionelle Grenzflächen, Hermann-von-Helmholtz-Platz 1, 76344 Eggenstein-Leopoldshafen, Deutschland
[2]Tosoh Bioscience GmbH, Zettachring 6, 70567 Stuttgart, Deutschland

Online veröffentlicht am 16.Oktober 2014

keywords: Design of Experiments (DoE), modeling, cost of goods, response replicates

Cost Estimation for Protein A Chromatography

An In Silico Approach to MAb Purification Strategy

Matthias Franzreb, Egbert Müller, and Judith Vajda

Monoclonal antibody (MAb) production has adopted an accepted technology platform for downstream processing (1). The need for more economic processes has been addressed by increasing MAb titers in fermentation and aiming toward greater bioreactor volumes to increase productivity. Consequently, cost pressures are now passed on to downstream process groups. Membrane and chromatography resin savings are more important for MAb processes than ever before, with highly productive cell cultures generating large volumes of process fluid to purify (2).

Traditionally, protein A resins have a comparably high share among the costs of consumables in MAb processing. Protein A ligands for chromatography need to be alkaline stable, highly discriminating, with low ligand leaching levels, which requires substantial effort in development of these affinity media. Large feed streams also require higher downstream capacities and increase demands on labor and plant equipment, which of course increases the investment.

Debottlenecking the downstream platforms is a current concern in regard to both process capacity and cost. Only after that may manufacturers take full advantage of high titers and large bioreactor volumes. One possible approach to this challenge is to use more efficient resins, and high-capacity protein A resins seem promising.

In silico simulation of a typical MAb process can assist in detailed examination of the particular factors influencing protein A chromatography costs. Applying design of experiments (DoE), Costioli et al. reported (among other things) on the cost-effectiveness of overloading conditions for high-titer cell cultures (3). Such a study is supposed to extend derived results by two factors — resin capacity and the number of protein A runs per fermentation batch — and how they affect the cost of protein A chromatography as a unit operation. That is not linked to protein A resin price alone, but also to the cost of hardware. Identifying important factors that could provide savings in protein A chromatography was a goal of our DoE study.

PRODUCT FOCUS: MONOCLONAL ANTIBODIES

PROCESS FOCUS: DOWNSTREAM PROCESSING

WHO SHOULD READ: ANALYTICAL, PROCESS DEVELOPMENT, MANUFACTURING

KEYWORDS: DESIGN OF EXPERIMENTS (DOE), MODELING, COST OF GOODS, RESPONSE REPLICATES

LEVEL: INTERMEDIATE

MATERIALS AND METHODS

Monoclonal Antibody Process: We simulated several MAb production process scenarios using SuperProDesigner software (version 8.5) from Intelligen, Inc. Although we used in silico modeling rather than actual scale-down experiments, the required computing capacity limited the number of simulations to a reasonable amount, which is why we applied DoE (2). We restricted our example MAb process to 25 unit

operations, eliminating some steps in early inoculum handling and wastewater treatment to yield a less complex process. Nevertheless, we kept the number of annual fermentation batches constant for both process models. We also verified the degree of simplification and how it affects the economics of an entire representative process consisting of 37 unit operations. The original process design was constructed as a average MAb process mostly based on process parameters obtained from literature (4–6).

Design of Experiments: We used MODDE software from Umetrics for our DoE study. The experimental design was optimized according to the "D optimal onion" design, which allows screening for relevant factors with good design-space coverage (7). We built an eight-factorial design based on the following (Table 1):

- protein A resin price
- number of possible cycles
- protein A step yield
- MAb titer
- cycles per fermentation batch
- working capacity
- linear velocity applied in the protein A step
- elution volume of protein A chromatography.

We considered the following responses to have an impact on the process cost: total investment for the production facility, production cost per kilogram of MAb, total operational cost, protein A chromatography step's share of the operational cost, consumables costs' share of the operational cost, and protein A resin cost as part of the consumables' costs.

Calculations are based on average costs and prices in 2013. Further

Table 1: Investigated factors and corresponding levels (chosen according to empirical values) in the D optimal design

Factor	Abbreviation	Unit	Level	Comment
Resin price	Price	€/L	5,000; 7,500; 10,000; 12,000; 14,000	
Number of cycles	cyc	NA	50, 80, 120, 160, 200	Production cycles before resin replacement
Yield	Yield		0.8, 0.85, 0.9, 0.95, 1.0	Yield of protein A step
MAb titer	Titer	g/L	1, 2, 4, 6, 8	MAb titer after fermentation
Cycles/batch	cpb	NA	1,2, 4, 6, 8	Protein A runs per fermentation batch
Working capacity	wq	g/L	20, 30, 40, 50, 60	Working capacity of the protein A resin
Linear velocity	lin	cm/h	100, 150, 200, 400, 600	Linear velocity for operating protein A
Elution pool volume	Pool volume	CV	1, 2, 3, 4, 5	Product pool volume after protein A (in column volumes)

Figure 1: Flow chart of an example MAb process

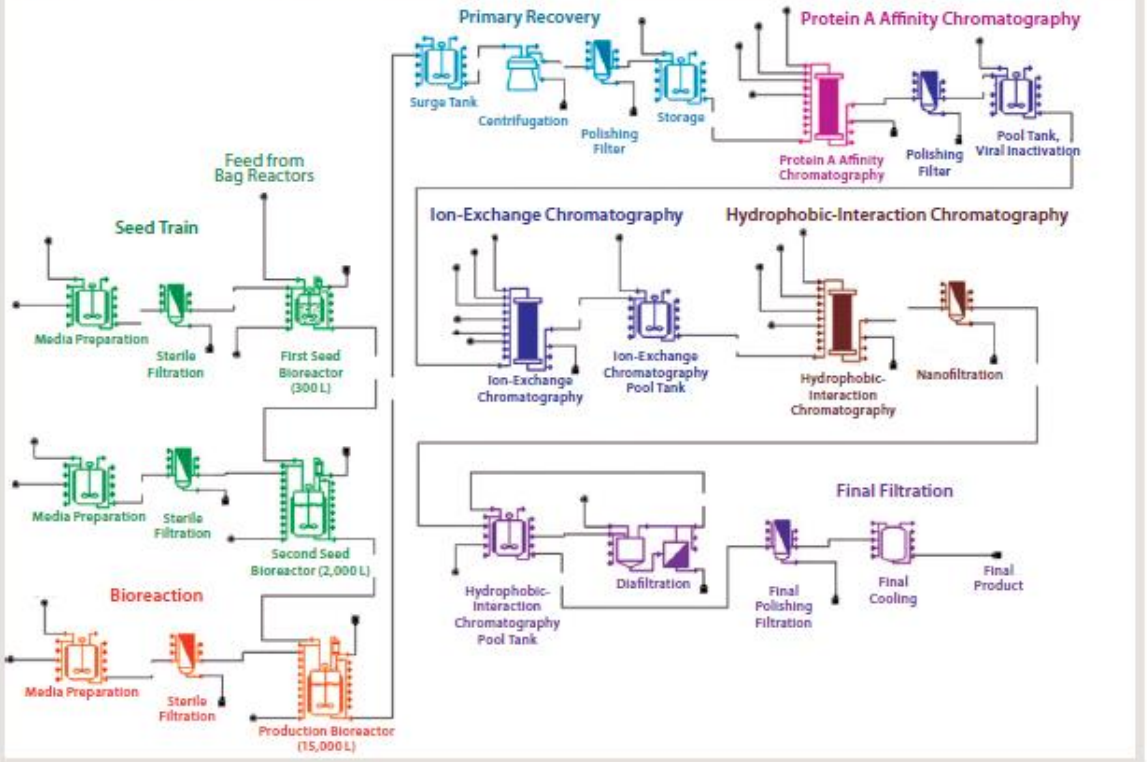

Figure 2: Replicate plots of total investment and unit production costs; experiments 2, 12, and 42 show significant response increases over the other experiment results. These experiments were simulated to include one protein A chromatography run per fermentation batch.

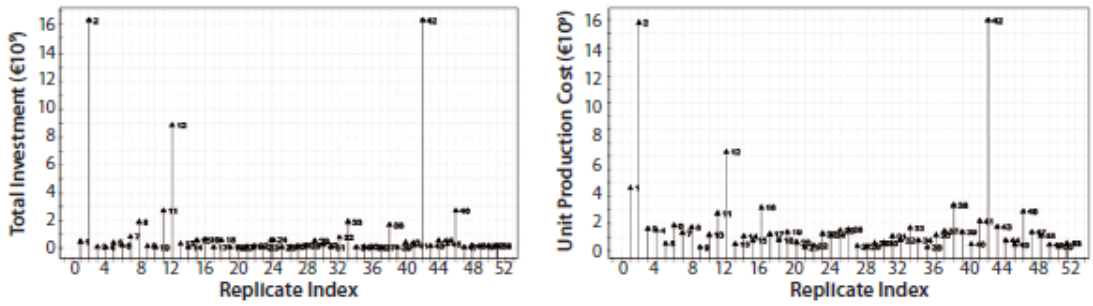

parameters and characteristics of applied unit operations — e.g., realistic sizes and throughput of the single unit operations — were obtained from the modelling program's database. For example, the protein A column size and its corresponding cost are calculated for a given set of levels. If the required volume exceeds a realistic size, then the software automatically incorporates multiple protein A columns in parallel. Optionally, the calculation can be set manually for multiple cycles of protein A on one column.

From MAb process simulations, it appears that REPEATING protein A chromatography for each fermentation batch would be considerably less cost-intense than using a single run per batch.

Results and Discussion

Monoclonal Antibody Process: Figure 1 depicts a simplified, representative MAb process flow scheme with 25 unit operations. Table 2 compares that simplified process with a complete one (37 unit operations) with regards to economic parameters. From the data, you can see that most of the cost for consumables and equipment is reduced in the simplified process. Because that less complex version was applied to all simulations, the error is systematic. We consider it to be negligible in context of a model intended to illustrate trends and qualitative results rather than absolute cost calculations for a single process variant.

Response Replicate Plots: Figure 2 presents replicate plots for exemplary responses from our MAb process simulations. The replicate plots in connection with this process simulation are intended to identify strongly incongruous responses rather than examine experimental correctness. Response plots show increased investment and unit-production costs for experiments 2, 12, and 42. Those three experiments have in common a one-run protein A chromatography step per fermentation batch. For further data plotting, we excluded those extreme response values and their experiments from our analysis.

From simulations of that MAb process, it appears that repeating protein A chromatography for each fermentation batch would be considerably less cost-intense than using a single protein A run per fermentation batch. Required hardware is expensive for columns that can handle large harvest volumes unless a high resin capacity allows for use of a relatively smaller column.

Column hardware volume often is not proportional to hardware pricing because manufacturing big columns is technically difficult. Cranes, extra manpower for handling, and larger machine shops are required for manufacturing columns >1,000 mm in inner diameter (ID). Those special costs exponentially rise for such large columns. The relative price of a 1,000-mm ID column is ~30% of the price for that of a 1,400–mm ID

Table 2: Comparing major economic parameters for less complex and full MAb processes

Parameter	37 unit operations	25 unit operations
Total capital investment	€163,314,000	€153,075,000
Operating cost	€45,829,000/year	€43,858,000/year
Revenues	€189,138,000/year	€188,742,000/year
Cost basis annual rate	307.35 kg MAb/yr	306.71 kg MAb/yr
Unit production cost	€149,109.50/kg MAb	€142,995.64/kg MAb
Unit production revenue	€615,384/kg MAb	€615,384/kg MAb
Gross margin	75.77%	76.76%
Return on investment	66.06%	70.54%

Figure 3: Significant coefficients for total investment; MAb titer has the greatest influence. The number of protein A cycles per batch (cpb) and the protein A resin capacity (wq) also affect total investment.

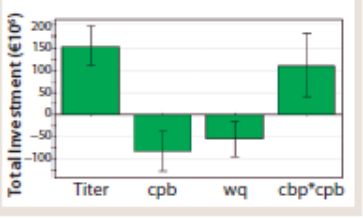

column (8). The software also calculated use of multiple separate protein A columns used in parallel, which also increases the investment but eventually allows for use of columns <1,000-mm ID.

The other main investment in protein A chromatography is the resin itself. Resin capacity does not only have an effect on column hardware cost, but also on the required amount of resin. The importance of resin capacity is also highlighted by our DoE software's data analysis. However, the remaining 43 experiments seem to be significantly less affected, although the amount of resin used further decreases with more protein A runs per fermentation batch. That is because of an opposing effect of decreasing column hardware cost and increasing costs for larger resin volumes.

DoE Model: We used Modde DoE software for our model calculations. The initially calculated model contained 44 regression coefficients for 43 experiments. Obviously, the significance of those different regression coefficients needs to be investigated. With insignificant coefficients removed, the coefficient number dropped below the number of experiments. Then we calculated the coefficient plots including confidence intervals. We applied a 95% confidence level. That provides an individual set of coefficients for each response factor. Figures 3–5 show three exemplary coefficient plots. Figure 3 depicts significant coefficients for the total investment costs for a plant running the average MAb process.

The achieved EXPRESSION TITER during fermentation is the most important factor in determining the necessary total investment for a MAb plant.

As can be expected, the achieved expression titer during fermentation is the most important factor in determining the necessary total investment for a MAb plant. Our simulation always assumes a fixed 15-m^3 fermentation volume. Thus, higher titers provide much more product (and lower cost per kilogram of MAb) but also require clearly higher investment in downstream equipment to process such large product amounts. That relationship is reflected in two additional coefficients: the number of protein A cycles per batch and the protein A resin capacity. The response factor share of the protein A resin cost as a part of the consumables cost (Figure 4) provides more insight into the protein A chromatography step.

It is not surprising that the resin price and the number of cycles before resin replacement are the two most important factors in a protein A affinity unit operation. But working

Figure 4: Coefficient plot for the response protein A resin cost as a part of the total consumables cost; the most important factors are resin price (price), number of possible cycles before resin replacement (cyc), and resin capacity (wq).

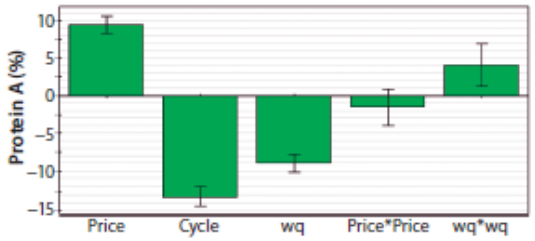

Figure 5: Coefficient plot for the response cost per kg MAb; titer and resin capacity (wq) show greater influence on production cost than does protein A resin price. Further protein A yield and number of protein A runs per fermentation batch also play important roles.

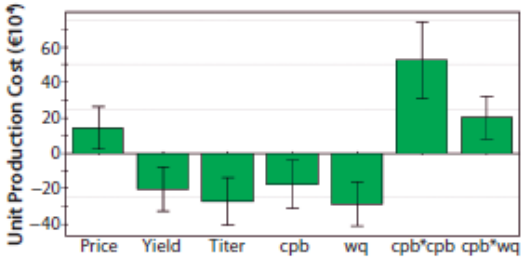

Figure 6: Predicted model dependency for production cost per kg MAb and the number of protein A cycles per fermentation batch showing a minimum for six protein A cycles per fermentation batch

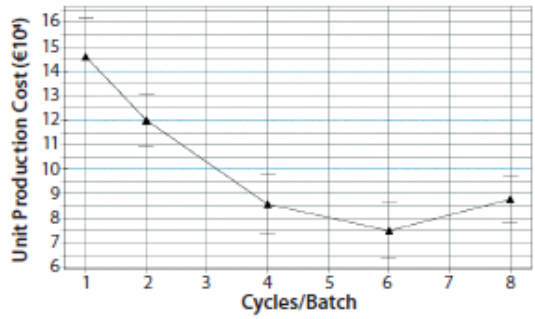

Figure 7: Production cost model for different protein A resin capacities; high-capacity protein A resins decrease unit production cost.

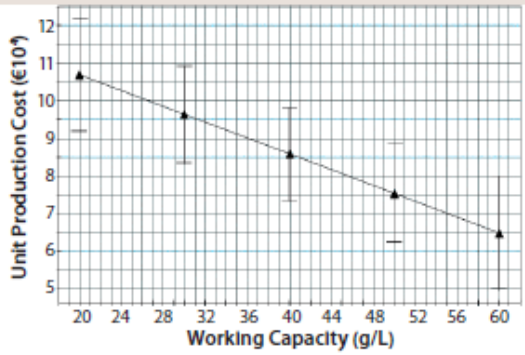

Figure 8: Model predictions for unit production cost dependency from protein A resin price; according to the model, the production cost per kg MAb increases by ~1,500 euros for a protein A resin price increase of €9,000.

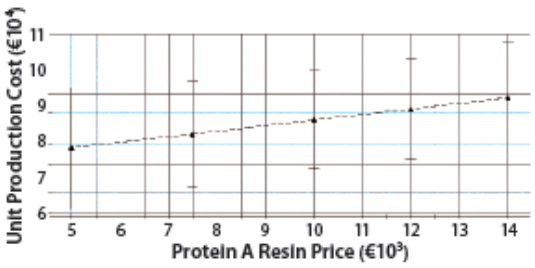

Figure 9: Model predictions for production cost per kg MAb with varying MAb titers; production cost decreases by about a factor of 2 as titer rises from 1 g/L to 8 g/L.

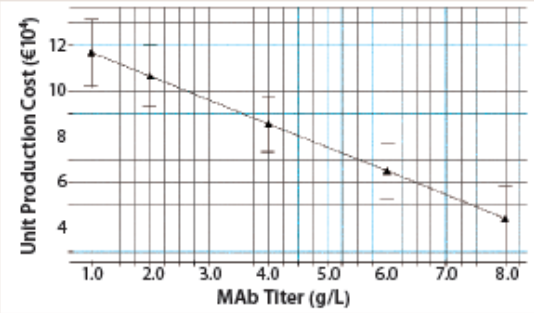

capacity turns out to be important, as well. It is directly linked to resin cost because higher capacities allow for use of smaller resin volumes. That relationship highlights the benefits of high-capacity resins.

The bottom line of all considerations certainly is the production price per kilogram of MAb yielded by the downstream process as a whole. Actual production costs for high-titer MAbs are comparably low, as literature confirms (2). When accepting some assumptions, one dose can be produced and filled for US $12–26, depending on the required substance mass for each dose (6). Importantly, that calculation does not account for research and development, which requires tremendous investment (5). Also, MAb therapy often requires long-term and frequent treatment. For example, Humira (adalimumab) from AbbVie is administered weekly or every two weeks for treatment of rheumatic diseases (9). For that particular MAb, cation-exchange chromatography is applied as a capture step (10). However, the principle of continuous administration holds true for other MAbs (9). So potential savings in drug production remain attractive. Figure 5 shows the significant model coefficients for production cost per kilogram of MAb.

Unexpectedly, protein A resin capacity has a relatively higher influence on production cost per kilogram of MAb than does protein A resin price. Capacity is linked to both plant equipment investment and the number of protein A cycles per batch — the latter being connected with operational cost, which influences labor cost. According to our results, savings for the average MAb process can be achieved using high-capacity resins, which was also reflected in the predicted model. Figure 6 shows a predicted-model response surface plot comparing the production cost per kilogram of MAb with the number of protein A cycles per fermentation batch. For that plot, all other factors were kept constant at their model center-point value.

The production cost minimum is six protein A chromatography cycles per fermentation batch. That is attributable to the effects of increasing resin and hardware costs for fewer cycles and decreasing labor cost. As we expected, our purification model would further be optimized for protein A resins with high capacity (Figure 7). The higher the resin capacity is, the lower the production cost per kilogram of MAb will be.

Other factors affecting the unit production price are protein A resin price (Figure 8) and MAb titer (Figure 9). The unit production cost seems to be more drastically affected by MAb titer and the number of protein A cycles per fermentation batch than by resin price or capacity. Even so, capacity has more influence on the production cost than does resin price. Although our reported values correspond to a average MAb process, the results indicate potential savings when high-capacity protein A media are used. Some high-capacity resins — e.g., Toyopearl AF-rProtein A HC-650F — reach binding capacities of >70 g/L,

exceeding the maximum working capacity applied in our study.

A Useful Model

This DoE study revealed connections between and among different economic parameters in a average MAb process. Protein A chromatography is a major part of downstream processing and thus offers opportunities for improving MAb productivities. Although our results rely on a average MAb process that cannot possibly take into account every single parameter, they do show trends and tendencies. High-capacity protein A resins should be considered for future MAb processes. Potential cost-saving strategies regarding process design also could focus on MAb titer and the number of protein A cycles per fermentation.

References

1 Farid SM. Process Economic Drivers in Industrial Monoclonal Antibody Manufacture. Process Scale Purification of Monoclonal Antibodies. *Process Scale Purification of Monoclonal Antibodies.* John Wiley and Sons: Hoboken USA, 2009; 239–263.

2 Kelley B, Blank G, Lee A. Downstream Processing of Monoclonal Antibodies: Current Practices and future Opportunities. *Process Scale Purification of Monoclonal Antibodies.* John Wiley and Sons: Hoboken, NJ, 2009; 1–23.

3 Costioli M, et al. Cost of Goods Modeling and Quality By Design for Developing Cost-Effective Processes: Combine Cost Analysis with QbD to Improve Operations and Lower Costs. *BioPharm Int.* 23(6) 2010: 26–35.

4 Liu HF, et al. Recovery and Purification Process Development for Monoclonal Antibody Production. *MAbs* 2(5) 2010: 480–499.

5 Chartrain M, Chu L. Development and Production of Commercial Therapeutic Monoclonal Antibodies in Mammalian Cell Expression Systems: An Overview of the Current Upstream Technologies. *Curr. Pharmaceut. Biotechnol.* 9(6) 2008: 447–467.

6 Kelley B. Industrialization of MAb Production Technology: The Bioprocessing Industry at Crossroads. *MAbs* 1(5) 2009: 443–452.

7 Olsson I-E, Gottfries J, Wold S. D-Optimal Onion Designs in Statistical Molecular Design. *J. Chemomet. Intell. Lab. Systems* 3(1) 2004: 37–46.

8 Hoffmann M. Biotechflow Ltd.: Stroud, UK. Personnel communication, October 2013.

9 Zhang N, et al. Therapeutic Antibodies in Clinical Use and Leading Clinical Candidates. *Therapeutic Monoclonal Antibodies: From Bench to Clinic.* John Wiley and Sons: Hoboken, NJ, 2009; 712–745.

10 Lain B, Cacciuttolo MA, Zarbis-Papastoitsis G. Development of a High-Capacity MAb Capture Step Based on Cation-Exchange Chromatography. *BioProcess Int.* 7(5) 2009: 26–34.

*Professor **Matthias Franzreb** is department head at the Karlsruhe Institute of Technology. **Egbert Müller**, PhD, is a private lecturer at the Universities of Darmstadt and Karlsruhe as well as technical director of Tosoh Bioscience GmbH. Corresponding author **Judith Vajda** is senior laboratory specialist at Tosoh Bioscience GmbH, Zettachring 6, 70567 Stuttgart, Germany; 49-71113-2570, fax 49-71113-25789, judth.vajda@tosoh.com, www.tosohbioscience.de.*

9.4. Kinetic plots in aqueous size exclusion chromatography of monoclonal antibodies and virus particles

Autoren: Judith Vajda, Werer Conze, Egbert Müller

Institutionen:
Tosoh Bioscience GmbH, Im Leuschnerpark 4, 64347 Griesheim, Deutschland

Nachdruck mit Genehmigung des Elsevier Verlags
DOI: 10.1016/j.chroma.2015.11.057

keywords: Kinetic plots, Size exclusion chromatography, Monoclonal antibodies, Virions, Particle size

Journal of Chromatography A, 1426 (2015) 118–125

Contents lists available at ScienceDirect

Journal of Chromatography A

journal homepage: www.elsevier.com/locate/chroma

Kinetic plots in aqueous size exclusion chromatography of monoclonal antibodies and virus particles

Judith Vajda*, Werner Conze, Egbert Müller

Tosoh Bioscience GmbH, Im Leuschnerpark 4, Griesheim 64347, Germany

ARTICLE INFO

Article history:
Received 18 September 2015
Received in revised form 5 November 2015
Accepted 17 November 2015
Available online 19 November 2015

Keywords:
Kinetic plots
Size exclusion chromatography
Monoclonal antibodies
Virions
Particle size

ABSTRACT

The growing importance of monoclonal antibodies and virus particles has led to a pressure for faster size exclusion chromatography. In recent years, numerous small particle columns for size exclusion chromatography of biologicals have been introduced. Small particles are a strategy to reduce analysis time. In the following study, opportunities of small particles in size exclusion chromatography of large biomolecules are investigated. Poppe plots reveal that the lower particle size limit depends on the size of the sample molecule. Hydrodynamic radii of monoclonal antibody monomer, aggregates and H1N1 as well as the diffusion coefficients were determined. Considering this sample compound dependency, kinetic plots referring to the resolution of a distinct compound pair instead of the plate number of a single analyte are more meaningful. Plate times were found to be equivalent with 4 and 2 μm particles for a monoclonal antibody aggregate separation at resolutions smaller than 1.8. Quantification of a H1N1 in clarified cell culture can be accomplished with 17 μm and 13 μm particles at equal plate times at resolutions smaller than 2.5. Virus polydispersity is likely to be affected by run times of several hours at room temperature and shear forces resulting from particles smaller than 10 μm. Comparatively high flow rates should be applied in size exclusion chromatography of the 100 nm H1N1 virions.

1. Introduction

Size exclusion chromatography (SEC) is a versatile chromatographic technique for the qualitative and quantitative analysis of biomolecules. Benefits of the method are high reproducibility, straight-forward method development and mild analysis conditions. In recent years, numerous columns and column formats for SEC of biomolecules have been introduced. Smaller particle sizes are promising with regards to resolution and plate numbers. Knox suggested in 1977 the use of 1 to 2 μm particles for economic and efficient liquid chromatography [1,2]. The trend toward smaller particles has originally emerged in reversed phase chromatography. Numerous publications [3,4] describe advantages of the sub 2 μm particles, which include also protein applications of reversed phase chromatography [5]. After years of mostly theoretical considerations, columns with nonporous 2 μm particles made of silica became commercially available in 1996 [2,4]. Smaller particles allow accomplishing given reversed phase separation in shorter analysis times. Popovici and Schoenmakers came to the conclusion that shorter analysis times in SEC can also most likely be realized when using smaller particles, and reduced analysis times are the most important motivation to use small particles in SEC. Smaller particles allow either to reduce the column length or to increase flow rates [6]. Their conclusions were based on results obtained with polystyrenes and packed particle beds. A good tool to compare the separation performance of different columns and column formats are kinetic plots [7]. Various authors have employed different formats of kinetic plots [8–11]. For instance, Poppe plots were employed to compare superficially and fully porous packing material with monoliths in reversed phase chromatography [12]. Separation efficiency of convective media had earlier been evaluated in the light of increasing flow rates by Rodrigues and co-authors [13,14]. However, to our best knowledge the use of monoliths for SEC is yet limited to smaller proteins and has comparatively lower efficiency than SEC columns based on small fully porous particles [15–17]. Superficially porous particles have a lower pore volume than fully porous particles. Since separation in SEC relies on pore volume, superficially porous particles would at the same column volume provide less separation efficiency.

Popovici and Schoenmakers constructed Poppe plots for gel permeation chromatography of high molecular weight polystyrenes [18] based on a reduced van Deemter plot. They found that diffusion of large polystyrenes is not as unfavorable as formerly thought, which is mainly due to the coupling of mass transfer

* Corresponding author. Tel.: +049 6155 7043710; fax: +0049 6155 8357904.
E-mail address: Judith.vajda@tosoh.com (J. Vajda).

http://dx.doi.org/10.1016/j.chroma.2015.11.057

effects and eddy diffusion as introduced by Knox, Parcher and Giddings [19,20]. Poppe plots for small molecules strive asymptotically toward a plate time minimum at high flow rates. According to the results of Popovici and Schoenmakers, this does not hold true for polystyrenes with diffusion coefficients in the range of 10^{-7} cm^2/s [18]. The plate time decreases with decreasing plate numbers even at high flow rates, which means that less challenging separations can be realized at high flow rates and shorter analysis times [18]. This may be a general principle for molecules with similar diffusivity. Diffusion coefficients of typical biopharmaceutical molecules like monoclonal antibodies (mAbs) and virus particles are small compared to small molecules. Typical diffusion coefficients for small molecules in aqueous solution are in the range of 10^{-6} cm^2/s [21]. Diffusion coefficients for IgG molecules are one order of magnitude smaller [22]. This paper intends to discuss the applicability of Poppe plots for SEC of typical biologicals by means of separations with different particle sizes. Practical limits of fast SEC, namely column stability at increased flow, are considered.

2. Theory

SEC discriminates compounds regarding their hydrodynamic radius. The diffusion coefficient is inversely proportional to the hydrodynamic radius of a globular protein by the Stokes Einstein equation [23]. Tanford developed an equation that links the hydrodynamic radius r_h of a globular protein to the cube root of its molecular weight M_W (Eq. (1)) [23,24].

$$r_h \approx 0.081 \cdot \sqrt[3]{M_W} \tag{1}$$

The molecular weight of a protein is logarithmically related to the distribution coefficient K_D of a sample in size exclusion chromatography with k and c as empirical constants [23].

$$K_D = -k \cdot \log M_W + c \tag{2}$$

Eqs. (1) and (2) and the Stokes Einstein equation yield a logarithmic cubic relationship between the diffusion coefficient and the selectivity determining constant K_D in size exclusion chromatography (Eq. (3)).

$$K_D \approx -k \cdot \log\left(\left(\frac{5.7 k_B \cdot T}{6\pi\eta D}\right)^3\right) + c \tag{3}$$

T represents the Temperature, η the dynamic viscosity and k_B the Boltzmann's constant. The diffusion coefficient of H1N1 is smaller than the diffusion coefficient of mAb monomer by one order of magnitude. The diffusions coefficient of mAb may be considered representative for host cell proteins in the virus sample. For a given column and sample type, k and c can be considered constant. Eq. (3) predicts that changes in D will have more impact on K_D if sample diffusivity is low, such as for large molecules. Values between K_D are in the range of 0.0 and 1.0. The impact of K_D and D on H with relation to particle size d_p is given by the following equation [25].

$$H = \frac{2D(1+K_D)}{u} + 2d_p + 0.6u\left(\frac{K_D}{(1+K_D)^2} \cdot \frac{d_p^2}{D}\right) \tag{4}$$

Similar equations correlating *HETP* with sample diffusivity and particle size have been formed by different authors and can be found in literature [17,26]. A more basic correlation of *HETP* and u is given by the van Deemter plot, which is frequently used to construct kinetic plots. Kinetic plots relate the plate time or column void volume to the plate count or the peak capacity [9]. Poppe plots represent a particular kinetic plot, where the plate time t_p, which is the time required to achieve one plate, is plotted on the y-axis. The plate time can be described by the following equation:

$$t_p = \frac{H}{u} \tag{5}$$

The plate time is plotted against the number of plates N required for a given separation. N depends on the column length L and H as can be described by the following equation:

$$N = \frac{L}{H} \tag{6}$$

N and H are related by the Darcy equation (Eq. (7)) at a given flow rate u_1. Plate times of small molecule separations are nearly constant until a critical required plate number is reached. At this threshold value, plate times increase exponentially and strive toward an infinite value at the maximum plate number for a given column and sample. Flow rates or backpressures providing a good compromise between column efficiency (that is plate number) and fast separations can be obtained from Poppe plots and vice versa. A comparative approach allows evaluating different column formats and stationary phases. In the current study, regression of actual $H(u)$ data yields correlations for each sample and column. The Darcy equation can be used to calculate $N(u)$ for a given column, eluent, pressure and flow rate (Eq. (7)).

$$\Delta p = \frac{u\emptyset\eta L}{d_p^2} = \frac{u\emptyset\eta HN}{d_p^2} \tag{7}$$

Δp is the pressure drop across the column and depends on the flow rate. Dynamic viscosity η of water at 298 K is 0.891×10^{-3} kg/(ms) [27]. Flow resistance factors $\emptyset$ are calculated by the Darcy equation (Eq. (7)) at the standard flow rate of every column and the resulting pressure. The Darcy equation is further used to calculate the corresponding Δp at a given flow rate. A pair of variates for N and H/u is calculated for u_0, $u_1 \ldots u_{max}$ and Poppe plots are constructed numerically.

3. Materials and methods

3.1. Samples & standards

p-Amino benzoic acid (pABA) (Sigma Aldrich, Taufkirchen, Germany) was used for TSKgel SW column performance tests. A solution of 5% acetone (Sigma Aldrich) in water was used to test performance of TSKgel PW SEC columns. A mAb from Chinese hamster ovary cell culture was purified by preparative Protein A chromatography with TOYOPEARL AF-rProtein A-HC 650F. The mAb was eluted from Protein A with 100 mM sodium acetate buffer at pH 3.5. pH of the post-Protein A pool was elevated to pH 6.5 by addition of 0.5 M disodium hydrogen phosphate. The solution was diluted to 0.71 g/L and stored at 2–8 °C.

A pandemic influenza type A H1N1 virus was produced in adherent Madin-Darby Bovine Kidney bioreactor cell culture. This feedstream was kindly provided by IDT Biologika GmbH, Dessau-Rosslau, Germany. The feedstream was concentrated 20-fold volumetrically and contained 4.11 log hemagglutination units/100 μL. Inactivation was accomplished with β-propriolactone. The applied hemagglutination assay protocol by Kalbfuß [28] was adapted from Mahy and Kagro [29].

3.2. Protein size exclusion chromatography columns

TSKgel SW columns were chosen for mAb analysis. Packing material of these columns is based on diol bonded silica particles. Pore size of the TSKgel SW columns used in this study was 250 Å. TSKgel SuperSW3000 and TSKgel UP-SW3000 (all Tosoh Bioscience GmbH, Griesheim, Germany) are available in 4.6 mm ID × 30 cm L.

Corresponding particle sizes are 4 μm and 2 μm. Particle sizes are mean values and were determined with a Coulter counter. Custom made columns with the same pore size and 5 μm as well as 10 μm particles were used in 4.6 mm ID × 30 cm L hardware.

3.3. H1N1 size exclusion chromatography columns

TSKgel G6000PW, TSKgel G6000PWxl and TSKgel G-DNA PW (all Tosoh Bioscience) are based on highly crosslinked hydroxylated polymethacrylate particles. Corresponding mean particle sizes are 17 μm, 13 μm and 10 μm and were determined with a Coulter counter. Pore size of all particles is >1000 Å. TSKgel G6000PW particles are packed into a 7.5 mm ID × 30 cm L format. Column hardware dimensions of TSKgel G6000PWxl and G-DNA PW is 7.8 mm ID × 30 cm L.

3.4. Hydrodynamic radius and diffusion coefficient measurements

Hydrodynamic radii and diffusion coefficients of the samples were determined with a DelsaMax Pro dynamic light scattering (DLS) instrument (Beckman, Pasadena, USA). Each DLS measurement consisted of 30 individual measurements and was determined in triplicates. MAb monomer and dimer were purified by semi-preparative SEC using TSKgel G3000SW (7.5 mm ID × 30 cm L). 1 mL post-Protein A pool was injected per run. The separation was accomplished in 100 mM sodium phosphate buffer + 100 mM sodium sulfate, pH 6.7 at 0.5 mL/min. Dimers and monomers were collected separately and manually injected into the DLS device. Separation of H1N1 from host cell proteins was accomplished by preparative SEC using TOYOPEARL HW-65F. The stationary phase was packed into a 26 mm inner diameter glass column (GE Healthcare, Uppsala, Sweden) to a bed height of 22 cm. 5 mL of the H1N1 feedstock were injected per run. 100 mM sodium phosphate buffer, pH 7.0 was used for preparative SEC. The linear flow was 135 cm/h. H1N1 eluate was collected and analyzed by DLS.

3.5. Analytical size exclusion chromatography

The protein SEC buffer consisted of 100 mM sodium phosphate, 100 mM sodium sulfate, pH 6.7 and 0.05% sodium azide. Analytical H1N1 SEC was accomplished in 100 mM sodium phosphate, 200 mM sodium chloride, pH 7.0. All chemicals were purchased from Merck Millipore, Darmstadt Germany. Buffers were filtered through 0.1 μm membranes from Merck Millipore. Columns were connected to a Dionex UHPLC Ultimate 3000 RS system (Thermo Fisher, Dreieich, Germany). UV absorbance was detected at 280 nm. The lowest applied flow rate was 0.05 mL/min. The volumetric flow was accelerated gradually by 0.05 mL/min until the standard test procedure revealed column deterioration. Standard tests were interlaced at every flow rate increase by 0.2 mL/min. Once a test revealed column deterioration, flow rates equal or higher to the previously tested ones were excluded from kinetic plot construction. Conditions for column testing were chosen according to the inspection data sheet. Samples were injected at least in duplets. Height equivalent of a theoretical plate (HETP) values were determined by automated software integration for best reproducibility.

4. Results and discussion

4.1. Hydrodynamic radii and diffusion coefficients

Diffusion coefficients and hydrodynamic radii of mAb monomer, mAb dimer and H1N1 determined by DLS are presented in Table 1. The hydrodynamic radii of mAb monomer and dimer are 5.2 and 6.8 nm. H1N1 has a hydrodynamic radius of 108.3 nm. Diffusion coefficients of mAb are greater than the diffusion coefficient of

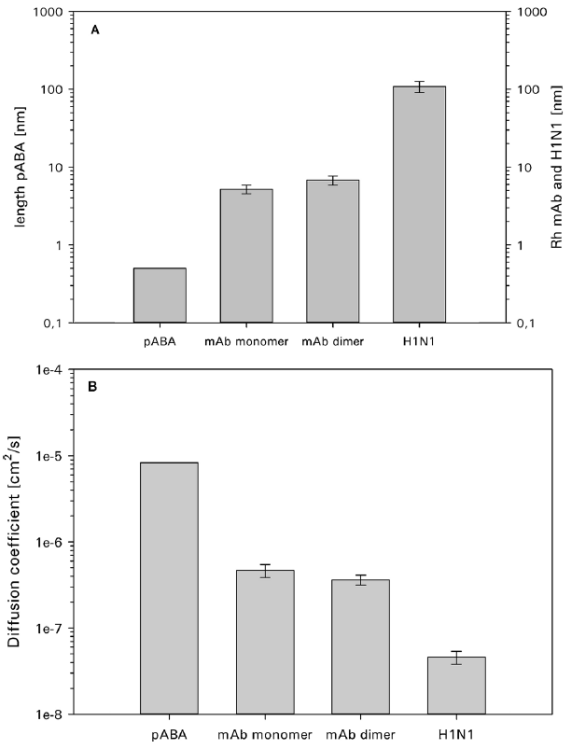

Fig. 1. Diffusion coefficients and sizes of the sample molecules. (A): Hydrodynamic radii of H1N1, mAb monomer and mAb dimer determined by DLS and the lengthwise size of pABA are plotted. (B): Diffusion coefficients of pABA, mAb monomer, mAb dimer and H1N1. Corresponding data of pABA was obtained from the literature.

H1N1 by one order of magnitude. Diffusion coefficients of small molecules, such as pABA are greater than the ones determined for mAb or H1N1. The lengthwise extension of pABA is approximately 0.5 nm [30]. The diffusion coefficient of pABA is 8.43×10^{-6} cm^2/s [41]. Results and corresponding standard deviations are displayed in Fig. 1A and B. Diffusion coefficients and sizes of the molecules correlate inversely, which is expected. From this data, it could be concluded that normalizing H(u) relationships to the diffusion coefficient will allow straight-forward access to kinetic plots for a given sample molecule provided the diffusion coefficient is known. This has been demonstrated for SEC of polystyrenes [18]. However, polystyrenes are more uniform than large biomolecules and no shift in diffusivity due to changes in the analyte conformation is expected.

4.2. Poppe plots

Exemplary chromatograms of the mAb and virus sample at different flow rates are shown in Fig. 2. Unsurprisingly, mAb aggregates are better resolved at slow flow rates and monomer peaks are more efficiently separated. In contrast, the virus particle peak is broader at slow flow rates. Poppe plots based on actual H(u) relations are constructed for mAb, mAb aggregates and H1N1 (Fig. 4). Regression functions of the van Deemter plots (Fig. 3A–C) and the Darcy equation were used. Van Deemter curves of mAb can be described by linear regression, which is expected for biopolymers like proteins. Due to the lower diffusivity of virions, linear $H(u)$ correlations are as well expected in case of H1N1. However, it can be seen in Fig. 3C that an additional hyperbolic term is required to

Table 1
Diffusion coefficients and hydrodynamic radii determined by DLS.

Sample	Diffusion coefficient [m²/s]	Hydrodynamic radius [nm]	Buffer system
mAb monomer	4.66E – 11	5.2	100 mM sodium phosphate + 100 mM sodium sulfate pH 6.7
mAb dimer	3.63E – 11	6.8	100 mM sodium phosphate + 100 mM sodium sulfate pH 6.7
H1N1	4.58E – 12	108.3	100 mM sodium phosphate pH 7.0

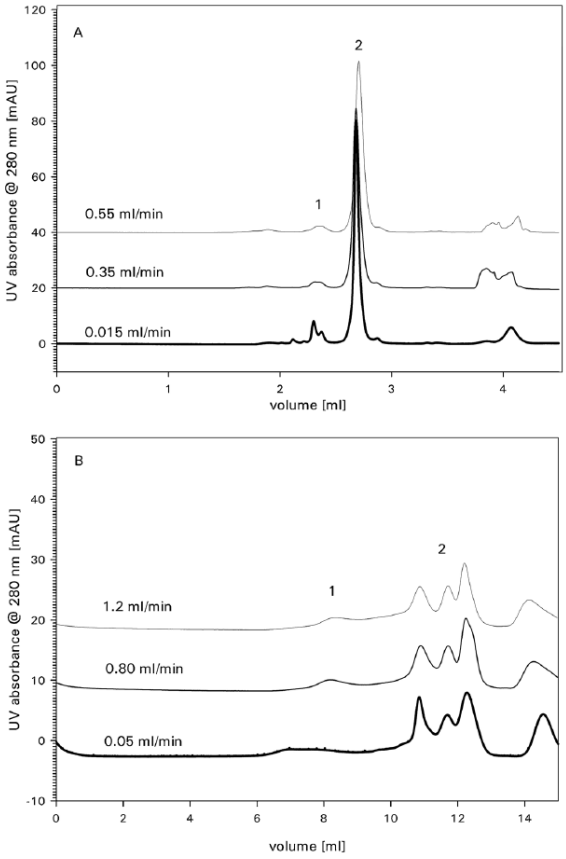

Fig. 2. SEC chromatograms of the mAb sample (A) on 2 μm particles and the virus sample (B) on 10 μm particles at different flow rates as indicated in the chromatograms. In figure (A), peak 1 and 2 correspond to aggregates and monomers, respectively. Peak 1 represents the virion in figure (B) and the second group of peaks corresponds to host cell proteins.

approximate $H(u)$ relationships. Although the reduced plate height equation as introduced by Giddings [31] contains the inverse B term, it seems that it still has limited applicability to large fragile biological samples. Different biological compounds cannot be normalized using the diffusion coefficient. The decay of HETP with increasing flow rate is probably due to virus particle instability and not due to strong longitudinal diffusion. The applied low flow rates result in analysis times as long as 6 h. Virus feedstock samples seem to degrade when eluting through a chromatography column at room temperature for such a long time. Additionally, it has been shown that band broadening in SEC is particularly great close to the total exclusion volume of a column but smaller as expected at high flow rates [20]. H1N1 virus particles elute close to the exclusion volume of the tested columns. These concerting effects seem to balance the HETP increase at higher flow rates due to mass transfer problems. Another point to consider is that large pores may contribute to improved mass transfer characteristics of porous particles. Afeyan et al. attributed coupling of diffusive mass transport and convective flow to particles with mesopores in the range of 6000 to 8000 Å [32]. They could show that reduced plate heights of such packing materials are nearly independent from the applied flow rates. Potential secondary interactions should be similar with all of the columns tested with virus particles, since they are all based on the same backbone chemistry. Secondary interactions with a low mass transfer may influence separations of virus particles at very low flow rates. Such additional interactions could partly be responsible for the broadened peaks. The presence of such interactions prohibits the use of Poppe plots constructed from reduced van Deemter curves. A comparative approach with experimental H(u) relations however seems still useful to obtain optimum flow conditions. C-terms of the constructed van Deemter curves are smaller for smaller packing material particles, which is in accordance with results published in literature [4,17,33] and is described by equation 4. Shape, steepness and ordinate of van Deemter curves are reflected in the different Poppe plots, which are shown in Fig. 4A–C. Constructed Poppe plots account for the actual experimental space, which is limited by column stability and possible automatic software integration. The constructed plots do not resemble conventional Poppe plots for small molecules. The horizontal part of the plot is not reached, due to pressure constraints. This holds true for mAb monomers, dimers and H1N1. MAb monomer and dimer plots strive toward maximum plate numbers for a given particle size at very low flow rates. Highest plate numbers and resolution are achieved with the smallest applied particle size. Similar results have been reported for the separation of mAb light and heavy chains with various SEC particles sizes ranging from 5 to 10 μm [17,34]. In another publication, Diederich et al. compare columns with particle sizes ranging from 1.7 μm to 5 μm for mAb aggregate detection [17,35]. However, in this particular case pore size of the tested columns was not equivalent. Required plate times to reach the maximum plate number of the herein acquired data decrease with smaller particles. It can be seen from the plots that small particles allow to accomplish a given plate number at significantly shorter plate times, but the maximum plate number does not increase strongly at very low flow rates. The offset in *y*-direction of the curves is greater than the *x*-wise shift. Reduction of analysis time could be accomplished for a given plate number by reducing the column length of a small particle column. Poppe plots for H1N1 are less typically shaped. A relation between increasing plate times and increasing plate numbers is only valid for the lower part of the Poppe plots and 13 μm as well as 17 μm particles. Data generated for 10 μm particles, which are the smallest particles used with H1N1 does not show this trend. Instead, highest plate numbers are achieved at fastest flow rates. This is also true when exceeding the point of return of the curves prepared from 17 and 13 μm particle data. Mathematically, this is because the H(u) relations extrapolated from the van Deemter plots of H1N1 (Fig. 3C) contain a comparatively strong hyperbolic term. One conclusion to be drawn from the H1N1 Poppe plots (Fig. 4C) is the apparent maximum plate number achieved for a particular plate time. The corresponding plate time is approximately 0.45 s in case of the 13 and 17 μm particles. This means that flow rates in SEC of very large and sensitive samples should not only be considered

in the light of analysis time counteracting to column performance. Sample degradation may lead to greater polydispersity, which in turn does result in an increased HETP. HA activity (data not shown) decreases after 24 h at 4 °C and the samples start to turn turbid. It can be assumed that the integrity of virus particles is affected. Low flow rates and analysis times of several hours at room temperature are likely to introduce similar effects. Any conditions that could potentially modify sample composition should be avoided to ensure data generated by SEC is reflecting the actual sample polydispersity. $H(u)$ correlations such as equation 4 do not account for sample stability and cannot serve as an theoretical and exclusive tool to determine optimum flow conditions.

If the Poppe data of all compounds were normalized against particle size, variance was obtained for each compound. Maximum plate numbers for all samples increase to a higher degree if particle size is halved from 10 to 5 μm (decreased from 17 μm to 13 μm for H1N1) as in case of a particle size reduction from 4 to 2 μm (decreased from 13 μm to 10 μm for H1N1). The extent to which reducing stationary phase particle size increases plate numbers decrements. It seems like critical particle size becomes the greater the larger sample molecules are. Particle size limits in column chromatography have previously been described in literature. Gregg suggests that the minimum particles size is 1–10 μm, because smaller particles will lead to elongated run times provided backpressure is a limiting factor [26,36]. Almost 25 years later, Halász et al. concluded on a 1 μm stationary phase particle size limit in reversed phase high pressure liquid chromatography (HPLC) with small molecules. In HPLC, or another 35 years after invention of UHPLC, pressure limits of the chromatographic equipment are not an issue anymore. Column pressure drops still imply a 1 μm limit on particle size. One reason for this is that frictional heating causes viscosity gradients inside a column [26]. The temperature increase of water per 100 atm is 2.43 °C [26]. Temperature sensitive and large samples like proteins and virus particles may be affected with regards to sample integrity and diffusivity. Additionally, thermal conductivity of 1 μm silica particles is poorer compared to sand powders with particle sizes in the range of 75 to 250 μm [37], which means that smaller particle sizes support thermal gradients inside of a chromatography column.

Packing material particle size is in the range of 10^{-6} m and obtained diffusion coefficients are in the range of 10^{-11} m^2/s. According to equation 4, d_p gains impact on *HETP* for small *D* and small particles are thought to be especially beneficial for SEC of large particles. However, this approximation does not account for fragile compounds prone to sample degradation due to shear forces, frictional heating or influences from hydrodynamic chromatography. Smaller particles lead to greater shear forces stressing sample molecules in the column [38]. It can be speculated, that shear forces imply a particle size limit of approximately 10 μm to SEC of influenza virus particles with the herein tested polymethacrylate resin. Analysis of the comparatively more robust mAbs does benefit from 2 μm particles. This observation leads to some further conclusions: The purpose of SEC of proteins and virions is often to quantify these biologics and potentially present contaminants, such as aggregates, fragments or host cell proteins. This is an important difference to SEC of large polymers like polystyrene. One goal of

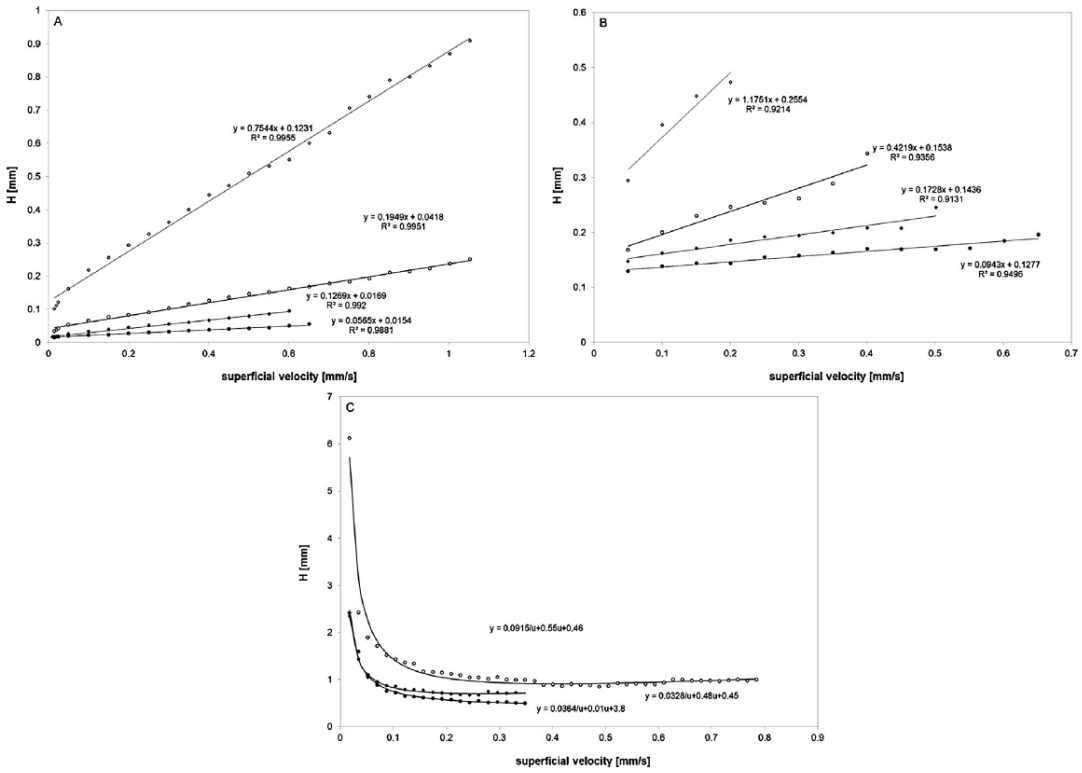

Fig. 3. van Deemter plots of mAb monomer (A), mAb aggregates (B), H1N1 (C). Particle sizes in (A) and (B) are 2 μm (bold dot), 4 μm (bold rhomb), 5 μm (circle) and 10 μm (hollow rhomb). Particle sizes in (C) are 10 μm (bold dot), 13 μm (bold rhomb) and 17 μm (circle). Regression curves and corresponding functions are displayed for every data set.

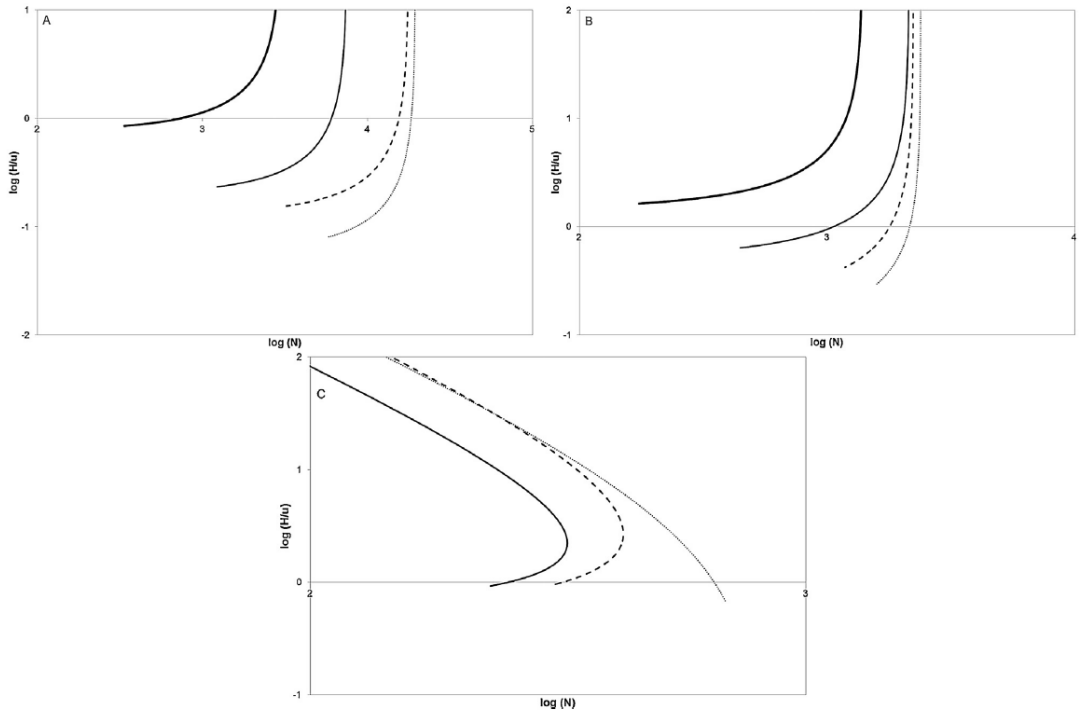

Fig. 4. Poppe plots of mAb monomer (A), mAb aggregates (B) and H1N1 (C). Particle sizes in (A) and (B) are 2 μm (dotted line), 4 μm (dashed line), 5 μm (thin line) and 10 μm (thick line). Particle sizes in (C) are 10 μm (dotted line), 13 μm (dashed line) and 17 μm (continuous line).

the latter is to determine the polydispersity index of a sample [20]. In contrast, sample compounds and impurities in SEC of biologicals are rather distinct compared to large polymer samples and baseline separation is desirable. Resolution is an important parameter to distinguish between target component and impurities. This means it is important to look at both molecules of a given separation problem. For instance, when aiming to determine mAb aggregate contents or virion purity from host cell proteins and degradation products. According to these results, Poppe plots have limited applicability to real conditions in SEC of biopharmaceuticals. Poppe plots mind plate numbers and HETP of only one substance. The comparison of different stationary phase particle sizes for different sample molecules has shown that the optimum particles size is different for molecules with different diffusion coefficients. Kinetic plots based on resolution could be a good tool to include diffusivity of both molecules to be separated by SEC. For instance, the lower particle size limit for a mAb aggregate and mAb fragment separation seem to be not identical.

4.3. Resolution plots

Plotting the plate time against the resolution of a given separation allows comparing column performance for a given pair of compounds. According to the Poppe plots for mAb monomer, mAb aggregates and H1N1, optimum particle size depends on the compound size. Resolution plots are presented in Fig. 5A and B. At low resolutions, plate times are nearly constant. At higher resolutions, plate time increases and the increment of this increase seems to depend on particle size. Not surprisingly, smallest particles provide highest overall resolution and the plate time will start to increase comparatively later. For instance, plate time can only be reduced by using a 2 μm particle column, in case a mAb separation requires a resolution greater than 1.8. Any application requiring less resolution can be accomplished at equal plate times with a 4 μm particle. Resolution with a 10 μm particle does only allow baseline separation of mAb aggregates and monomers at plate times close to 10. This suggests that 4 μm or 3 μm particles are a good choice for routine applications. The resulting lower pressure of this particle size is less challenging for the employed instrumentation. DiCesare et al. found that particle sizes smaller than 5 μm require bypassing loops in the autosampler valve to reduce a pressure pulse and therewith related column lifetime issues [39]. Column deterioration by column clogging is another issue that occurs more likely with small particle columns, due to their increased surface area [40]. Column packings of greater particles are less prone to pressure and or flow deterioration, as can be seen from the van Deemter curves (Fig. 3). Displayed graphs do only include data points from columns passing the interlaced standard test. MAb monomer and H1N1 data suggests that packings of greater particles tolerate higher flow rates, although applied flow rates exceed the specified range for all columns. Automated software integration of mAb aggregate data with greater particles was not possible at higher flow rates, since peaks were too broad. Nevertheless, sophisticated applications take advantage of smaller particle sizes. Plate times remain comparatively short even if resolution needs to be higher than 3.0 or 4.0. This general trend is also true for the separation of H1N1 particles from host cell proteins. Although plate times are nearly constant until a resolution of 2.5 is exceeded. Plate times of the 17 μm particle increase with negative slope. This holds true for the curves of 13 and 10 μm particles when a resolution of 3.5 is exceeded. The negative slope can be interpreted as a result of the stability problems of H1N1 at very low flow rates. Working at flow rates resulting in plate times greater than 5 is not to be recommended, since sample stability is questionable. Resolution of H1N1 and host cell proteins

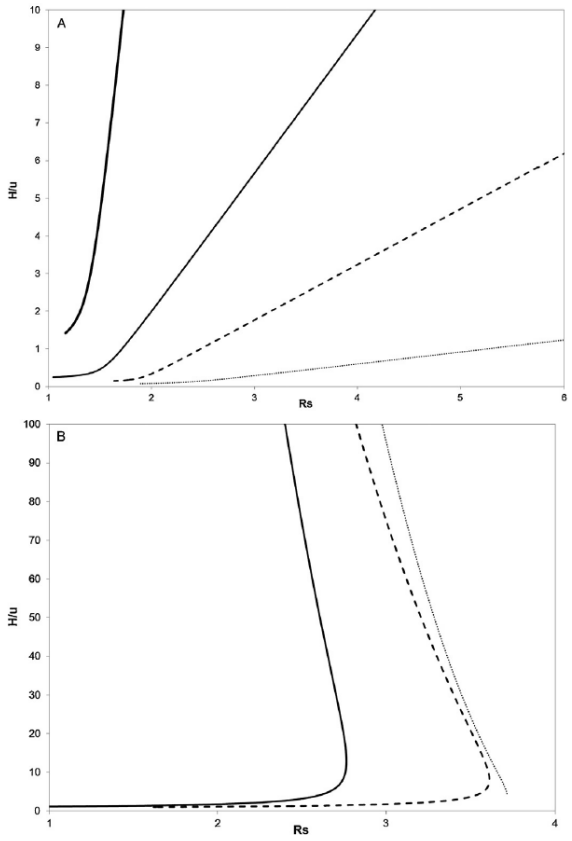

Fig. 5. Resolution plots of mAb aggregate separation (A) and H1N1 separation from host cell proteins (B). Particle sizes in (A) are 2 μm (dotted line), 4 μm (dashed line), 5 μm thin line and 10 μm (thick line). Particle sizes in (B) are 10 μm (dotted line), 13 μm (dashed line) and 17 μm (continuous line).

is comparatively high for all tested columns. 17 μm particles are a good choice in case pressure related degradation of a virus particle may occur and resolutions of up to 2.5 are sufficient. Alternatively, shorter columns with smaller particles may be a good option to reduce analysis time.

5. Conclusions

Poppe plots for mAb, mAb aggregates and H1N1 were constructed from data accomplished with various different particle sizes. From the Poppe plots it can be concluded that small particles lead to much shorter plate times for a given plate number. Small particles are a convenient tool when aiming for fast SEC separations. However, the horizontal part of the Poppe plots is of less practical significance, since very high flow rates lead to column deterioration, in particular when using small particles. Relative benefits of small particles for the maximum plate number decrease with decreasing diffusivity of the sample (increasing r_h). This correlation implies that column performance should be discussed in context of both compounds to be separated from each other. The herein presented resolution plots may serve as kinetic plot to evaluate SEC separations biologicals. Conclusions on the particle size of choice can be drawn from these plots. It seems economically reasonable to use medium particle size for standard applications that require resolutions ranging from 1.5 to 2.5. Superior performance of smaller particles will show advantage if a resolution greater than 2.5 is required. Plate times for such separations are significantly shorter using 2 μm particles or smaller. Benefits of small particles are becoming more important the greater the required resolution is. Further progress in SEC aiming for even shorter analysis times may focus on improved pressure flow characteristics and column packing. It seems like limits postulated decades ago sustain, but are individual for a particular sample and column type.

Acknowledgements

This work was supported by funding of the German Federal Ministry of Education and Research, Grant 0315640D, and is part of the research project “Optimization of an industrial process for the production of cell-culture-based seasonal and pandemic influenza vaccines”.

References

[1] J.H. Knox, Practical aspects of LC theory, J. Chromatogr. Sci. 15 (1977) 352–364, http://dx.doi.org/10.1093/chromsci/15.9.352.
[2] D.T.T. Nguyen, D. Guillarme, S. Rudaz, J.-L. Veuthey, Fast analysis in liquid chromatography using small particle size and high pressure, J. Sep. Sci. 29 (2006) 1836–1848, ⟨http://www.ncbi.nlm.nih.gov/pubmed/16970187⟩ (accessed September 3, 2015).
[3] J.J. Kirkland, Ultrafast reversed-phase high-performance liquid chromatographic separations: an overview, J. Chromatogr. Sci. 38 (2000) 535–544.
[4] R.E. Majors, Fast and ultrafast HPLC on sub-2 μm porous particles—where do we go from here? LC GC 19 (6.) (2006), ⟨http://www.chromatographyonline.com/fast-and-ultrafast-hplc-sub-2-m-porous-particles-where-do-we-go-here-0⟩.
[5] K.K. Unger, O. Jilge, J.N. Kinkel, M.T.W. Hearn, Evaluation of advanced silica packings for the separation of biopolymers by high-performance liquid chromatography II. Performance of non-porous monodisperse 1.5-μm Silica beads in the separation of proteins by reversed-phase gradient elution high-perform, J. Chromatogr. 359 (1986) 61–72, http://dx.doi.org/10.1016/0021-9673(86)80062-0.
[6] S.T. Popovici, P.J. Schoenmakers, Fast size-exclusion chromatography—theoretical and practical considerations, J. Chromatogr. A 1099 (2005) 92–102, http://dx.doi.org/10.1016/j.chroma.2005.08.071.
[7] U.D. Neue, Kinetic Plots Made Easy, LC GC, North Am., 2009, ⟨http://www.chromatographyonline.com/kinetic-plots-made-easy-1⟩.
[8] T.J. Causon, K. Broeckhoven, E.F. Hilder, R.A. Shellie, G. Desmet, S. Eeltink, Kinetic performance optimisation for liquid chromatography: principles and practice, J. Sep. Sci. 34 (2011) 877–887, http://dx.doi.org/10.1002/jssc.201000904.
[9] G. Kahsay, K. Broeckhoven, E. Adams, G. Desmet, D. Cabooter, Kinetic performance comparison of fully and superficially porous particles with a particle size of 5 μm: intrinsic evaluation and application to the impurity analysis of griseofulvin, Talanta 122 (2014) 122–129, http://dx.doi.org/10.1016/j.talanta.2014.01.050.
[10] M. D'Hondt, F. Verbeke, S. Stalmans, B. Gevaert, E. Wynendaele, B. De Spiegeleer, Derringer desirability and kinetic plot LC-column comparison approach for MS-compatible lipopeptide analysis, J. Pharm. Anal. 4 (2014) 173–182, http://dx.doi.org/10.1016/j.jpha.2013.09.001.
[11] Y. Vanderheyden, D. Cabooter, G. Desmet, K. Broeckhoven, Isocratic and gradient impedance plot analysis and comparison of some recently introduced large size core-shell and fully porous particles, J. Chromatogr. A 1312 (2013) 80–86, http://dx.doi.org/10.1016/j.chroma.2013.09.009.
[12] F. Gritti, Fast analytical chromatography and the role of the design of new stationary phases, Am. Pharm. Rev. (2011), ⟨http://www.americanpharmaceuticalreview.com/Featured-Articles/37012-Fast-Analytical-Chromatography-and-the-Role-of-the-Design-of-New-Stationary-Phases/⟩.
[13] A.E. Rodrigues, C. Chenou, M. Renduelles de la Vega, Protein separation by liquid chromatography using permeable POROS Q/M particles, Chem. Eng. J. Biochem. Eng. J. 61 (1996) 191–201, http://dx.doi.org/10.1016/0923-0467(95)03045-X.
[14] M. Zabka, P.S. Gomes, A.E. Rodrigues, Performance of simulated moving bed with conventional and monolith columns, Sep. Purif. Technol. 63 (2008) 324–333, http://dx.doi.org/10.1016/j.seppur.2008.05.018.
[15] Y. Li, H.D. Tolley, M.L. Lee, Preparation of polymer monoliths that exhibit size exclusion properties for proteins and peptides, Anal. Chem. 81 (2009) 4406–4413, http://dx.doi.org/10.1021/ac900364d.
[16] Y. Li, H.D. Tolley, M.L. Lee, Size-exclusion separation of proteins using a biocompatible polymeric monolithic capillary column with mesoporosity, J. Chromatogr. A. 1217 (2010) 8181–8185, http://dx.doi.org/10.1016/j.chroma.2010.10.067.

[17] P. Hong, S. Koza, E.S.P. Bouvier, Size-exclusion chromatography for the analysis of protein biotherapeutics and their aggregates, J. Liq. Chromatogr. Relat. Technol. 35 (2012) 2923–2950, http://dx.doi.org/10.1080/10826076.2012.743724.
[18] S.T. Popovici, P.J. Schoenmakers, Poppe plots for size-exclusion chromatography, J. Chromatogr. A. 1073 (2005) 87–91, http://dx.doi.org/10.1016/j.chroma.2004.12.024.
[19] J.H. Knox, J.F. Parcher, Effect of the column to particle diameter ratio on the dispersion of unsorbed solutes in chromatography, Anal. Chem. 41 (1969) 1599–1606, http://dx.doi.org/10.1021/ac60281a009.
[20] S.T. Popovici, W.T. Kok, P.J. Schoenmakers, Band broadening in size-exclusion chromatography of polydisperse samples, J. Chromatogr. A 1060 (2004) 237–252, http://dx.doi.org/10.1016/j.chroma.2004.05.099.
[21] J.R. Hazel, B.D. Sidell, A method for the determination of diffusion coefficients for small molecules in aqueous solution, Anal. Biochem. 166 (1987) 335–341, http://dx.doi.org/10.1016/0003-2697(87)90582-3.
[22] B. Pokrić, Z. Pucar, The two-cross immunodiffusion technique: diffusion coefficients and precipitating titers of IgG in human serum and rabbit serum antibodies, Anal. Biochem. 93 (1979) 103–114, ⟨http://www.ncbi.nlm.nih.gov/pubmed/107826⟩ (accessed September 3, 2015).
[23] G. Carta, A. Jungbauer, Protein Chromatography: Process Development and Scale-Up, Wiley-VCH Verlag, Weinheim, 2010.
[24] Y. Nozaki, N.M. Schechter, J.A. Reynolds, C. Tanford, Use of gel chromatography for the determination of the Stokes radii of proteins in the presence and absence of detergents. A reexamination, Biochemistry 15 (1976) 3884–3890, ⟨http://www.ncbi.nlm.nih.gov/pubmed/952891⟩ (accessed September 3, 2015).
[25] U.D. Neue, Waters columns for size exclusion chromatography, in: C. Wu (Ed.), Column Handb. Size Exclusion Chromatogr, Academic Press, London, 1999, p. 332.
[26] I. Halász, R. Endele, J. Asshauer, Ultimate limits in high-pressure liquid chromatography, J. Chromatogr. 112 (1975) 37–60, http://dx.doi.org/10.1016/S0021-9673(00)99941-2.
[27] P. Atkins, J. De Paula, Atkin's Physical Chemistry, Oxford University Press, Oxford, 2006.
[28] B. Kalbfuß, Downstream Processing of Influenza Whole-Virions for Vaccine Production, Otto-von-Guericke Universität Magdeburg, 2009.
[29] B.W.J. Mahy, H.O. Kangro (Eds.), Virology Methods Manual, Academic Press, London, 1996.
[30] P. Kochersperger, Metabolic Characterization of Folate Precursor pABA Uncovers its Folate Independent Activity on Root Growth of Arabidopsis Thaliana, Albert-Ludwigs-Universität Freiburg im Breisgau, 2011.
[31] J. Giddings, Dynamics of Chromatography, in: Part1 Princ. Theory, Marcel Dekker Inc, New York, NY, 1965.
[32] N.B. Afeyan, N.F. Gordon, I. Mazsaroff, L. Varady, S.P. Fulton, Y.B. Yang, et al., Flow-through particles for the high-performance liquid chromatographic separation of biomolecules: perfusion chromatography, J. Chromatogr. 519 (1990) 1–29, http://dx.doi.org/10.1016/0021-9673(90)85132-F.
[33] R.D. Ricker, L.A. Sandoval, Fast, reproducible size-exclusion chromatography of biological macromolecules, J. Chromatogr. A 743 (1996) 43–50, ⟨http://www.ncbi.nlm.nih.gov/pubmed/8817873⟩ (accessed September 3, 2015).
[34] H. Liu, G. Gaza-Bulseco, C. Chumsae, Analysis of reduced monoclonal antibodies using size exclusion chromatography coupled with mass spectrometry, J. Am. Soc. Mass Spectrom. 20 (2009) 2258–2264, http://dx.doi.org/10.1016/j.jasms.2009.08.015.
[35] P. Diederich, S.K. Hansen, S.A. Oelmeier, B. Stolzenberger, J. Hubbuch, A sub-two minutes method for monoclonal antibody-aggregate quantification using parallel interlaced size exclusion high performance liquid chromatography, J. Chromatogr. A 1218 (2011) 9010–9018, http://dx.doi.org/10.1016/j.chroma.2011.09.086.
[36] S.J. Gregg, The Surface Chemistry of Solids, first ed., London, Chapman and Hall, 1951.
[37] V.D. Chari, D.V.S.G.K. Sharma, P.S.R. Prasad, S.R. Murthy, Dependence of thermal conductivity in micro to nano silica, Bull. Mater. Sci. 36 (2013) 517–520, http://dx.doi.org/10.1007/s12034-013-0519-3.
[38] C. Wu, Handbook of Size Exclusion Chromatography and Related Techniques, Revised and Expanded, second ed., CRC Press, Boca Raton, FL, 2003.
[39] J.L. DiCesare, M.W. Dong, J.R. Gant, Influence of injector bypass on lifetime of small-particle liquid chromatographic columns, Chromatographia 15 (1982) 595–598, http://dx.doi.org/10.1007/BF02280381.
[40] K. Rowe, M. Armstrong, D. Cullimore, Particle size and clogging of granular media permeated with leachate, J. Geotech. Geoenviron. Eng. 126 (9) (2000) 775–786.
[41] P.D. Edmonds, Ultrasonics Methods of Experimetal Physics, vol. 19, Academic Press, New York, 1981.

9.5. Routes to improve binding capacities of affinity resins demonstrated for Protein A chromatography

Autoren: Egbert Müller, Judith Vajda

Institutionen:
Tosoh Bioscience GmbH, Im Leuschnerpark 4, 64347 Griesheim, Deutschland

Nachdruck mit Genehmigung des Elsevier Verlags
DOI: 10.1016/j.jchromb.2016.01.036

Online veröffentlicht am 22.Januar 2016

keywords: Protein A chromatography; Dynamic binding capacity; Ligand coupling; Spacer technology; mAb adsorption

Journal of Chromatography B, 1021 (2016) 159–168

Contents lists available at ScienceDirect

Journal of Chromatography B

journal homepage: www.elsevier.com/locate/chromb

Routes to improve binding capacities of affinity resins demonstrated for Protein A chromatography

Egbert Müller*, Judith Vajda

Tosoh Bioscience GmbH, Im Leuschnerpark 4, 64347 Griesheim, Germany

ARTICLE INFO

Article history:
Received 28 August 2015
Received in revised form
19 December 2015
Accepted 19 January 2016
Available online 22 January 2016

Keywords:
Protein A chromatography
Dynamic binding capacity
Ligand coupling
Spacer technology
mAb adsorption

ABSTRACT

Protein A chromatography is a well-established platform in downstream purification of monoclonal antibodies. Dynamic binding capacities are continuously increasing with almost every newly launched Protein A resin. Nevertheless, binding capacities of affinity chromatography resins cannot compete with binding capacities obtained with modern ion exchange media. Capacities of affinity resins are roughly 50% lower. High binding capacities of ion exchange media are supported by spacer technologies. In this article, we review existing spacer technologies of affinity chromatography resins. A yet known effective approach to increase the dynamic binding capacity of Protein A resins is oligomerization of the particular Protein A motifs. This resembles the tentacle technology used in ion exchange chromatography. Dynamic binding capacities of a hexameric ligand are roughly twice as high compared to capacities obtained with a tetrameric ligand. Further capacity increases up to 130 mg/ml can be realized with the hexamer ligand, if the sodium phosphate buffer concentration is increased from 20 to 100 mM. Equilibrium isotherms revealed a BET shape for the hexamer ligand at monoclonal antibody liquid phase concentrations higher than 9 mg/ml. The apparent multilayer formation may be due to hydrophobic forces. Other quality attributes such as recovery, aggregate content, and overall purity of the captured monoclonal antibody are not affected.

1. Introduction

Affinity chromatography is usually described as the most selective chromatographic mode. The nature of interactions in affinity chromatography is complex and multimodal, which is different from ion exchange chromatography (IEX), hydrophobic interaction chromatography (HIC), and size exclusion chromatography (SEC). A combination of ionic interactions, hydrophobic interactions, hydrogen bonding and steric effects leads to cooperative adsorption of the target molecule with superior selectivity. Affinity resins may be classified according to their selectivity into mono-specific and group-specific affinity chromatography [1]. In mono-specific affinity chromatography, purification factors are often very high and higher than in other chromatographic modes like IEX or HIC. These resins allow for purification of a single substance. Typical mono-specific affinity ligands are macromolecular substances, such as enzymes, polynucleotides, or antibodies (immune-affinity chromatography). Group specific affinity chromatography ligands are less selective. Their specificity is restricted to a motif that is common in a whole group of target molecules, such as the Fc part of immunoglobulin G (IgG) 1. Low molecular weight ligands are frequently used. The most important group specific affinity resins are:

1. Immobilized metal chelate chromatography (IMAC) [2].
2. Dye chromatography and derived biomimetic ligands [3].
3. Resins with immobilized heparin [4].
4. Immobilized lectins [5].
5. Protein A, Protein G and Protein L chromatography [6].

In IMAC, proteins with surface standing histidine moieties or proteins with a histidine tail can efficiently be purified by resins with complex-bound metal ions [2]. In dye chromatography, chemically modified reactive dyes are immobilized on the resin and undergo specific interaction with several groups of proteins. For instance, enzymes with attached co-factors are purified with immobilized blue or red dyes [7]. Immobilized heparin is mainly used for the purification of plasma proteins, especially Antithrombine III [4]. Immobilized lectins and especially resins carrying Concanavalin A are useful for the fractionation of glycoproteins and glycans [8].

The most important group specific affinity resins in biopharmaceutical production today are resins with immobilized Protein

* Corresponding author.
E-mail addresses: Egbert.mueller@tosoh.com (E. Müller), Judith.vajda@tosoh.com (J. Vajda).

http://dx.doi.org/10.1016/j.jchromb.2016.01.036
1570-0232/

A. Protein A is a wall protein from *Staphylococus aureus* bacteria and has high affinity to a variety of immunoglobulins [6,9]. Mainly hydrophobic interactions, salt bridges and hydrogen bonding co-interact in binding of Protein A to the hinge region of IgG1 and IgG2 [10]. IgG4 is bound with lower affinity and binding to IgG3 is negligible. When Protein A ligands were still derived from natural Protein A, protein A affinity media played a minor role. Only after the development of recombinant Protein A ligands and the appearance of monoclonal antibodies (mAb) as important biotherapeutics, Protein A resins received outstanding importance in downstream processing [11]. The use of affinity resins other than Protein A in production of biopharmaceuticals is marginal. It is estimated that the up-to-date share of Protein A cost among the total revenue of the biotechnology resin market is greater than 50% [12]. However, the success story of Protein A chromatography was clouded in its early days, because of lacking chemical stability, low binding capacity, and high acquisition cost. There were and is still a continuous effort to find alternatives to Protein A. Especially the chemical stability against caustics was an argument for new ligands [13]. Among them, the most important types are designer dyes [10], peptides [14], aptamers [15], library derived cameloid antibodies [16], or hydrophobic charge induced chromatography ligands [17]. Despite the performance of these ligands is getting close to the properties of Protein A, they have not been able to replace Protein A, yet [18]. Since the first Protein A media was made commercially available in 1975, they have improved, as well. One major economic drawback is the comparatively low binding capacity [19], which has been addressed in development of the recent generation of Protein A resins. Eshmuno® A [20], MabSelect Sure LX [21], ProSep®-vA High Capacity [22], Amsphere™ Protein A JWT203 [23] and Toyopearl AF rProtein A HC-650F [24] have high binding capacities. Thus, this paper is mainly focusing on binding capacity of Protein A resins. All other affinity resins have less economic significance. Dynamic binding capacity of a Protein A resin in production is one of the most important selection criteria and there is a continuous competition among vendors to increase dynamic binding capacities. High dynamic binding capacities at short residence times and high feed concentrations have become more important, since progress in upstream processing has led to higher mAb titers and an increase of the throughput of the harvested cell culture fluid [25]. The increased binding capacity of the most recent generation of alkaline stable Protein A resins is one of the main reasons why the development of biomimetic ligands other than Protein A has lost attractiveness.

Nevertheless, high protein binding capacity is not the only quality criteria for affinity media. There are several other objectives to be achieved, such as maintaining protein activity, high recovery, host cell protein removal, and low protein aggregation [26,27]. Increasing protein binding capacity of an affinity resin and sustaining the other product quality parameters can be challenging. This paper intends to investigate effects of increased dynamic binding capacity on other quality attributes. Two commercialized Protein A resins that are derived from the same domain of Protein A are compared. The high capacity version carries a hexameric ligand and the conventional version a tetrameric ligand. Binding capacities were determined at different conditions. In a second step, both resins were used to purify a monoclonal IgG1 from chinese hamster ovary (CHO) supernatant. Purity, protein recovery and host cell protein (HCP) removal were determined in a design of experiments (DoE) based approach.

1.1. Binding capacities of affinity resins for biochromatography

Resin capacities specified by the supplier provide a first overview; although these are usually referring to standard proteins. Binding capacities for other proteins and conditions can deviate significantly. For instance, kosmotropic salts increase static and dynamic binding capacity of a Protein A resin by more than 100% [28]. Some selected binding capacities of affinity resins are summarized in Table 1. Capacities were obtained from literature [29–33,15,34]. Binding capacities of IEX resins are more than twofold higher than typical capacities of affinity or HIC resins. This difference cannot be explained by lower affinity constants. Affinity resins have similar or higher binding constants than ion exchange resins. Another important prerequisite to realize high binding capacities is good ligand accessibility [35]. Batch capacity determinations (as an equilibrium value) and the dynamic binding capacity can be compared to distinguish well accessible and hardly accessible ligands. Small differences in static and dynamic capacity indicate good ligand accessibility and favorable isotherm shape [36]. In this case, pore-surface, film diffusion, and reaction limitations, or in other words mass transfer resistances, are minimized. However, this ideal situation is rarely accomplished in affinity chromatography. Especially in Protein A chromatography, decreasing residence times will lead to decreasing dynamic binding capacities [37]. Major principles for the construction of affinity resins will be discussed in the next paragraphs, focusing on minimized mass transfer resistance.

1.2. Design and preparation of chromatographic resins

The preparation of a resin for biochromatography is a multistage process consisting of [38]:

1. Preparation of a hydrophilic base matrix by polymerization.
2. Activation of the base matrix by a bi-functional ligand.
3. Ligand selection.
4. Ligand coupling.

Particle size is one of the most important parameters of classical bead based media. Small particles provide high resolutions and high dynamic binding capacities because of faster mass transfer [39]. Hahn et al. demonstrated the influence of particle size and pore size on dynamic binding capacities of Protein A resins. Smaller particles benefit from fast mass transfer and high dynamic binding capacities [40]. One major drawback is the comparatively higher backpressure. Pore size is another important factor, which has a big impact on mass transfer. Mass transfer properties of adsorptive media can also be improved by surface modifications. Significant increases in dynamic binding capacities have been demonstrated for such media [41,42]. Different kinds of surface modifications are discussed in the next paragraph.

1.3. Immobilization and spacer technologies—ways to increase protein binding capacities of chromatographic resins

Epoxy immobilization is one of the most popular ligand coupling methods, since it generates a chemically stable covalent coupling of the ligand to the chromatographic support. Coupling of amino groups requires a comparatively high pH environment. This method may not be suitable for coupling of less robust ligands. However, epoxy coupling via sulfhydryl groups of a protein at moderate pH can be realized, since thiol groups are more nucleophilic. This technology is used for immobilization of r-Protein A ligands [43]. Interactions with the backbone polymer and greater ligand accessibility can be achieved by introducing a spacer between resin backbone and ligand. Especially accessibility of low molecular weight ligands seems to benefit from immobilization via a spacer [44]. However, large protein ligands do still take advantage of spacers, since they gain flexibility and in turn accessibility [45]. Thus, most ligand immobilization chemistries use a spacer. Polymeric modifications, such as tentacle arrangements or cross linked

Table 1
Properties and binding capacities of some selected group specific affinity resins.

Ligand type	Supplier	Name	Binding capacity
Immobilized reactive dyes [29]	Tosoh Bioscience GmbH	Toyopearl AF Blue HC-650M	18 mg/ml HSA
Metal chelate chromatography [30]	GE healthcare	Chelating sepharose fast flow	12 mg/ml for His tagged protein
Concanvalin resin [31]	GE healthcare	Con A sepharose 4B	20–45 mg/ml porcine thyroglobuline
Mimetic Protein A adsorbents [32]	Prometic life sciences	MabSorbent	20–30 mg mAb/ml resin
Cameloid antibody derived capture protein [33]	Life technologies	CaptureSelect™ IgG-CH1 affinity matrix	>15 g of IgG/l of matrix
Aptamer [15]	Non commercialized	–	30 mg/ml IgG
Protein A [34]	GE healthcare	MabSelect SuRe LX	Approximately 60 mg/ml IgG

polymers are an alternative to single point spacers [46]. Spacers can improve binding capacity. On the other hand, they are prone to nonspecific interactions, especially if long alkyl chain ligands are used. There are also activated affinity resins on the market bearing polymeric epoxy groups (e.g., Fractogel® EMD Epoxy, [47]), but the advantage of such grafted affinity resins remains to be proven [48].

As previously described in Section 1, Protein A media are the most important affinity resins. Surface modification technology that could lead to increased dynamic binding capacities of these resins is of great importance for the mAb producing industry [49]. Several possibilities to connect the recombinant Protein A ligand to an activated matrix exist. Site directed immobilization via a terminal cysteine residue of the recombinantly expressed Protein A seems to be the most efficient concept [43,50]. Binding capacity of such resins is higher compared to random immobilization methods. However, Ghose et al. [50] described steric hindrance problems of current Protein A resins. Increasing ligand densities will only increase binding capacity until a threshold value is reached. Improved steric accessibility of the protein A ligand is likely to increase binding capacity. Freiherr von Roman and Berensmeier [51] coupled repeated units of r-Protein A binding domain B motifs onto Profinity Epoxide® (BioRad Laboratories) beads. Oligomers were expressed in *Escherichia coli* strains DH5α. The expression vector was pET28a. Ligand polymerization was achieved using the enzymes XbaI and SpeI. They describe the influence of the degree of oligomerization, as well as the site-specific ligand immobilization, on static and dynamic binding capacities (Table 2). A 4-fold increase in static binding capacity was observed from dimer to octamer. The affinity constants are all in the range of 10^{-7}–10^{-8} M. However, the dynamic binding capacity increases by 2.7 times, comparing dimer and octamer. No further increase was observed for the nonamer compared to octamer. Site-specific immobilization resulted in further capacity increases. The octamer material showed a very high static binding capacity of 87 mg/ml and a dynamic binding capacity of more than 68 mg/ml at residence times of 4.8 min.

Similar results were reported by Johansson and Palmgren [52]. They found a binding capacity increase of about 30% for a hexamer compared to a tetramer. The polymerized B motifs serve as a genuine spacer to increase the number of interaction sites. This behaves quite similar to a tentacle arrangement of ionic groups used in ion exchange chromatography.

Protein A ligands with higher molecular weight than single binding domains, have found application in various commercialized Protein A resins. Recombinantly produced, native Protein A [53] motifs are being used. E, D, A, B, and C motifs exclude the cell wall domains [54]. An optimized, alkaline stable ligand is derived from the B motif of natural Protein A (Z-ligand) [55]. The use of several binding motifs per ligand is based on an increase in binding ratio of Protein A to IgG. Important properties of selected commercialized Protein A resins are summarized in Table 3 [56,21,57,22,58,59,24,34,43].

Listed binding capacities are widely spread. All ligands were immobilized by proprietary immobilization protocols and resin evaluation was accomplished at different conditions. It is difficult to discuss the influence of the Protein A spacer length on the binding capacity on this basis. Affinity constants are all in the range of 10^{-8} M [60]. Highest binding capacities are exceeding 60 mg/ml. Another strategy has been approached by PolyBatics. A new expression platform technology in *E. coli* has been developed that produces multiple copies of Z-ligands, which are already cross-linked to polyester beads. This PolyBind Z resin is produced in a single step platform. Multiple copies are displayed in the same orientation at the resin surface This allows for better accessibility than random chemical immobilization of Protein A ligands [61].

An interesting possibility for the evaluation of the spacer ability of oligomeric Protein A motifs is provided by Protein A resins from Tosoh. Either a tetramer or a hexamer ligand are immobilized on a methacrylate matrix. A significantly higher binding capacity can be found with the hexamer ligand. This could be due to the elongated ligand, serving as a spacer and by increasing the IgG/ligand ratio.

However and as previously discussed, a spacer can be a potential source of additional specific and non-specific interactions. Recently, two different groups reported conformational changes of IgG upon adsorption to and desorption from Protein A. Gagnon et al. showed that the hydrodynamic radius of IgG1 is halved after elution from Protein A [62]. Mazzer et al. found that IgG4 incubated in Protein A elution buffers are less affected by aggregation than IgG4 eluted from Protein A [63]. Such specific and additional non-specific interactions may affect the overall purification result, despite and in particular the spacer is the ligand itself. Naturally, polymeric protein ligands with polar and hydrophobic patches are more prone to a variety of less specific interactions than defined polymeric, grafted ligands of IEX resins. Interactions with the spacer may torpedo other requirements in Protein A chromatography. Such requirements are:

1. Log reduction of host cell proteins in the range of 2–3.
2. Sufficient removal of DNA, cell culture media components and virus particles.
3. Elution pHs greater than 3.0.
4. Recoveries greater than 85%.
5. Life times greater than 200 cycles.

These properties are desired to remain unaffected by increasing the number of r-Protein A binding domains. The influence of improved binding capacity on purity, aggregate removal and recovery are investigated in the following.

2. Experimental

2.1. Reagents

Different reagents a were prepared from citric acid monohydrate (Th. Geyer GmbH & Co. KG, Renningen Germany), di-Sodium hydrogen phosphate (Merck KGaA, Darmstadt Germany), sodium acetate trihydrate (Merck KGaA), sodium chloride (VWR, Darmstadt Germany), Acetone (Sigma–Aldrich Taufkirchen Germany). A humanized monoclonal IgG1 with an isoelectric point of 7.5 and a ten-fold concentrated cell culture fluid concentrate were used

Table 2
Overview of static and dynamic IgG binding capacities (t_{res} = 4.8 min) of r-Protein A binding B motifs coated Profinity Epoxide® materials (Prof-BX). BX ligands have an increasing number of B-domains (X = 2–9). For comparison rSpA ligand contains the native E, D, A, B, C motif without cell wall domains. $B6_{cys}$ and $B8_{cys}$ ligands were site-specific coupled by using a high reactive C-terminal cysteine residue [51].

Number of Protein B oligomer Units	Name and molecular weight [Da]	Static binding capacity [mg/m]	K_D value [M]	Dynamic binding capacity [mg/ml]
	Prof-B2	22.9 ± 1.7	8×10^{-7}	20.9
	Prof-B3	32.2 ± 3.2	3.53×10^{-7}	–
	Prof-B4	44.1 ± 3.4	6.26×10^{-7}	–
Natural Protein A	Prof-rSpA	35.3 ± 0.4	1.93×10^{-7}	–
	Prof-B6	61.1 ± 4.7	1.26×10^{-7}	40.7
	Prof-B8	80.1 ± 8.4	3.7×10^{-7}	57.5
	Prof-B9	77.8 ± 7.6	4.8×10^{-7}	52.3

Table 3
Overview about some selected commercial available Protein A resins.

Resin	Supplier	Base material	Particle size [μm]	Ligand type	Binding capacity	Affinity constants	References
CaptivA PriMab	Repligen	Cross linked agarose	45–165	Recombinant native Protein A (pentamer)	>40 mg/ml static binding capacity	n.s.	[78]
MabSelect Sure	GE healthcare	Highly cross-linked agarose	85	Tetramer of Z-type ligands (from B motif derived), alkaline tolerant	35 mg/ml human IgG (dynamic binding capacity)	3.9×10^{-8}–9.55×10^{-7} M	[21,79]
Prosep-va ultra	Merck-Millipore	Porous glass	100	Native Protein A	56 mg/ml static binding capacity	5×10^{-7} M	[22]
rmp Protein A sepharose	GE healthcare	Cross-linked agarose	90	Recombinant native Protein A (Pentamer)	> 22 mg/ml human IgG (dynamic binding capacity)	n.s.	[80]
Toyopearl AF-rProtein A-650F	Tosoh corp.	Methacrylate	45	Tetramer of Y type ligands (from C-motif derived), alkaline tolerant	30 mg/ml human IgG (dynamic binding capacity)	n.s.	[81]
Toyopearl AF-rProtein A HC-650F	Tosoh corp.	Methacrylate	30–60	Hexamer of Y type ligands (from C-motif derived), alkaline tolerant	65 mg/ml human IgG (dynamic binding capacity)	n.s.	[24]
MabSelect Sure LX	GE healthcare	Rigid, highly cross-linked agarose	85	MabSelect Sure ligand, (from B motif derived), alkaline tolerant	60 mg/ml human IgG (dynamic binding capacity	n.s.	[33]
Polybind-Z	PolyBatics	Biopolyester beads displaying a range of ligands		Multiple copies of Z-domain	100 mg/g drained beads	n.s.	[60]

to simulate different feedstreams. TOYOPEARL AF-rProtein A-650F and TOYOPEARL AF-rProtein A HC-650F were supplied from Tosoh Bioscience GmbH, Griesheim Germany. TOYOPEARL AF-rProtein A HC-650F is a high capacity Protein A resin with a hexameric ligand, a mean pore size of 100 nm and a mean particle size of 45 μm. TOYOPEARL AF-rProtein A-650F is a conventional Protein A resin, carrying a tetrameric ligand coupled to a backbone with the same pore size and particle size characteristics. Both Protein A resins are based on polymethacrylate beads.

2.2. Instruments

Lab scale experiments were conducted on an Äkta Explorer system (GE Healthcare Life Science, Uppsala Sweden). A NanoDrop 2000c spectrophotometer (VWR) was used for protein concentration determinations. A TECAN Freedom Evo 150 liquid handling system (TECAN Trading GmbH) for high through put testing was equipped with eight fixed pipetting tips, ChromStation, a plate moving arm and an integrated Infinite M200 UV plate spectrometer. Analytical size exclusion chromatography with TSKgel SuperSW mAb HR 4 μm, 7.8 × 300 mm (Tosoh Bioscience GmbH) was performed using a Dionex Ultimate 3000 RS UHPLC system (ThermoFisher, Dreieich Germany).

Lab scale chromatography runs were conducted on Omnifit chromatography glass columns with a volume of 0.7 ml and an inner diameter of 6.6 mm (Diba Industries Ltd., Cambridge UK). Columns were packed according to procedure defined by the resin supplier [64].

MediaScout RoboColumns were used in robotic screening experiments were purchased from Atoll (Weingarten, Germany). The column volume was 200 μl at an inner diameter of 5 mm.

3. Methods

3.1. Determination of the dynamic binding capacity of Protein A

Columns were equilibrated with the appropriate buffer solution. MAb loading concentration was determined externally by UV absorbance at 280 nm using the NanoDrop2000c spectrophotometer. Dynamic binding capacities were determined in breakthrough experiments. Capacities at 10% breakthrough were calculated according to Eq. (1),

$$\mathrm{DBC}\left[\frac{\mathrm{mg}}{\mathrm{mL}}\right] = \frac{V_{10\%} \times c_{\mathrm{protein}}}{V_{\mathrm{col}}} \quad (1)$$

$V_{10\%}$ was determined from the UV signal at 280 nm [ml] and c_{protein} was determined externally using NanoDrop 2000c [mg/ml]. V_{col} is the geometric total volume of the column [ml]. MAb concentrations were set to 1 g/l, 5 g/l and 10 g/l.

Table 4
Factor range of the DOE.

Factor	Name	Units	Minimum	Maximum	−1 actual	+1 actual	Center mid point
A	pH		2.25	4.25	2.75	3.75	3.25
B	Load	mg/ml resin	10	50	20	40	30
C	Titer	g/l	0.25	9.25	2.50	7.00	4.75
D	CHOP concentration	μg/ml	100	500	200	400	300

Table 5
Dynamic binding capacities of Toyopearl AF-rProtein A-650F (r Protein A) and Toyopearl AF-rProtein A HC-650F (r Protein A HC).

Binding Buffer		20 mM phosphate buffer				100 mM phosphate buffer			
Resin		r Protein A		r Protein A HC		r Protein A		r Protein A HC	
Residence time [min]		1	5	1	5	1	5	1	5
mAb concentration [mg/ml]	1	20.6	36.8	40	70.2	26.4	44	32.9	66.8
	5	22.1	34.4	38.5	71.9	34.2	44.4	76.5	98.3
	10	23.5	33.6	43	73	38.1	52.8	107.8	137.4

3.2. Isotherm determination

2 ml antibody solution in phosphate buffer, pH 7.0 were shaken with 500 μl 12.5% resin slurry in phosphate buffer, pH 7.0. Phosphate buffer and mAb concentrations were adjusted according to the individual experiment. The adsorbed mAb concentration was calculated from absorbance measurements after 3 h. Static binding capacities were determined at least in duplets, every measurement was repeated three times.

3.3. Chromatographic method for MediaScout® RoboColumns and Tecan Freedom Evo

The system was equilibrated with 20CV of 100 mM phosphate buffer, pH 6.5. Flow was set to 150 cm/h for equilibration. The sample was loaded onto the column at 2 min residence time. Loading volume and concentration was varied for the different experiments according to the DoE.

Subsequently, a washing step with equilibration buffer (100 mM phosphate buffer pH 6.5) for 20CV at 150 cm/h was applied. Total elution pool was 4 ml.

Elution buffers were 100 mM sodium citrate or sodium acetate. The elution pH ranged between 2.25 and 4.25. Collected elution pools were further analyzed.

3.4. DoE method

The applied central composite design resulted in 30 experiments per resin and elution buffer. The software package Design of Experts version 9.0 (comp.Stat.Ease, Inc.) was used for the central composite experimental design. The graphic presentations of the experimental data with contour plots were performed by using the program SigmaPlot version 13.0 from the comp.Systat Software Inc. Four factors were investigated: elution pH, load, mAb titer and CHOP content. Corresponding levels of the central composite design for all factors are listed in Table 4. Elution pH was varied within a process relevant range of pH 2.25–4.25. For column loading, a range from 10 mg/ml to 50 mg/ml was chosen, since TOYOPEARL AF-rProtein A-650F exhibits optimal binding capacities within this range. In comparison, TOYOPEARL AF-rProtein A HC-650F provides binding capacities exceeding this range. The maximum evaluated titer was 9.25 g/l. Investigated response factors were protein recovery, CHOP log reduction, and mAb aggregate content.

3.5. Determination of antibody aggregate content and protein recovery

Aggregate and monomer contents were quantified with analytical size exclusion chromatography (SEC). 100 μl post-Protein A sample were analyzed at a flow rate of 1.0 ml/min. 0.1 M sodium phosphate buffer containing 0.2 M sodium sulfate and 0.05% sodium azide, pH 6.5 was used. Run time was set to 15 min, which corresponds to approximately one column volume. Antibody monomers eluted after 7.65 min. Aggregated antibodies eluted earlier. Protein A recovery was determined by integration of the areas under the curve (AUC) using Chromeleon software version 7.1.2.1514 (Thermo Fisher Scientific). Calculated areas were converted into the elution pool volume concentration by a standard calibration curve for this mAb.

3.6. CHOP ELISA

CHOP contents were determined using the CHO HCP 3rd Generation ELISA kit from Cygnus Technologies. The procedure was performed according to the manufacturer's specifications.

4. Results and discussion

4.1. Dynamic MAb binding capacities of the Protein A resins

Dynamic binding capacities were determined in 20 mM and 100 mM sodium phosphate buffers, pH 7.0. Capacities were determined at 1 min and 5 min residence time. Current antibody processes are frequently set to 3 min residence time. 1 min residence time may represent conditions of future processes with a higher throughput. 5 min residence time is close to the equilibrium binding capacity. Results are summarized in Table 5.

Dynamic binding capacities of Toyopearl AF-rProtein A-650F (tetramer ligand) and Toyopearl AF-rProtein A HC-650F (hexamer Protein A ligand) in 20 mM phosphate buffer, pH 7.0, are summarized in Fig. 1. Binding capacities observed for the Protein A resin with the tetramer ligand are about half as high as for TOYOPEARL AF-rProtein A HC-650F. At 5 min residence time, 35 mg/ml IgG bind to the tetrameric ligand and 70 mg/ml are adsorbed by the hexameric ligand. This capacity increase becomes smaller at shorter residence times. DBC of TOYOPEARL AF-rProtein A-650F increases by 80% if increasing from 1 min to 5 min residence time. DBC of the hexamer ligand increases by 100% when elongating the residence time from 1 to 5 min. This is most likely the result of mass transfer limitations. A comparatively small dependency on the feed concentrations can be observed in 20 mM phosphate buffer. Differences in binding capacities between the Protein A resin with the tetramer

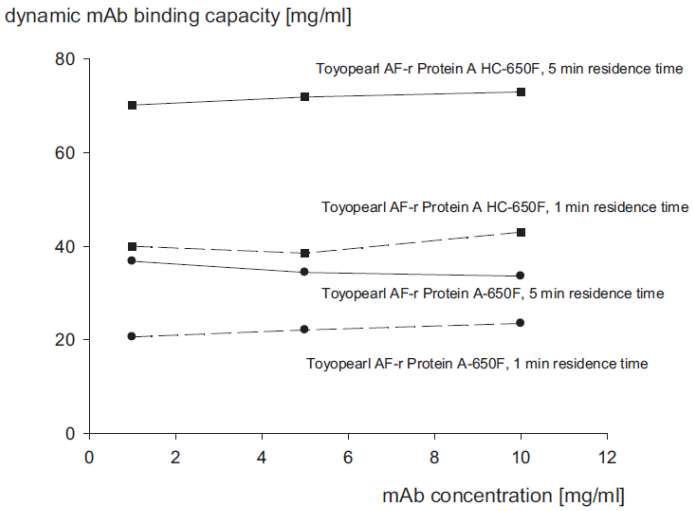

Fig. 1. Dynamic binding capacities of Toyopearl AF-rProtein A-650F (round markers) and Toyopearl AF-rProtein A HC-650F (square markers) at 20 mM phosphate buffer concentration pH 7 and 1 min and 5 min residence time as a function of load concentration.

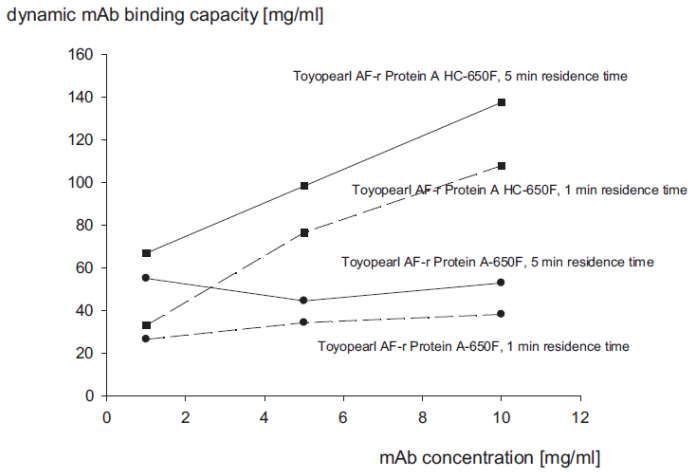

Fig. 2. Dynamic binding capacities of Toyopearl AF-rProtein A-650F (round markers) and Toyopearl AF-rProtein A HC-650F (square markers) at 100 mM phosphate buffer concentration pH 7 and 1 min and 5 min residence time as a function of load concentration.

ligand and the resin with the hexamer ligand are similar to those reported by Freiherr von Roman and Berensmeier [51].

Binding capacities at 100 mM phosphate buffer concentration are different from the results obtained in 20 mM phosphate buffer, although both were determined at pH 7.0. Results are presented in Fig. 2. An increase in dynamic binding capacity of Protein A at increasing concentrations of a cosmotropic salt has been described by Chen et al. [28]. Dynamic binding capacities of both resins were increased (by about 50% in case of Toyopearl AF-rProtein A-650F and doubled in case of Toyopearl AF-rProtein A HC-650F) when changing the buffer concentration from 20 to 100 mM sodium phosphate. Although this refers to a particular mAb, the magnitude of these mAb binding capacities is remarkable and is similar to capacities obtained for ion exchange resins with a polymeric surface. This further capacity increase of the hexameric ligand at mAb concentration of 10 mg/ml in 100 mM phosphate buffer can hardly be explained by hydrophobic interactions. The applied sodium phosphate concentration is not comparable to salt concentrations used in HIC. Ngo described an increase in yield by adding kosmotropic buffer additives [65]. The strong increase in binding capacity between the resin with the tetramer ligand and the hexamer ligand is difficult to explain. Isotherms were determined to clarify the binding behaviour of the two different Protein A resins at different mAb and sodium phosphate concentrations.

4.2. Isotherm measurements

Isotherms of both Protein A resins are plotted in Fig. 3. The isotherm of Toyopearl AF-r Protein A HC-650F in 100 mM phosphate buffer pH 7.0 shows an increase of bound mAb at a concentration of more than 8 mg/ml mAb. This leads to a BET shaped isotherm. A multilayer arrangement of the mAb molecules on the resin surface seems possible. Multilayer phenomena have previously been observed in chromatography. Multilayer adsorptions

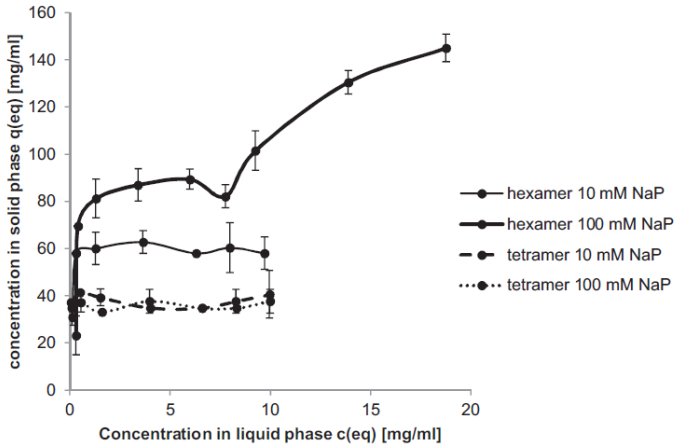

Fig. 3. Isotherms Toyopearl AF-rProtein A-650F and Toyopearl AF-rProtein A HC-650F recorded at 20 mM and 100 mM phosphate buffer concentration, pH 7.

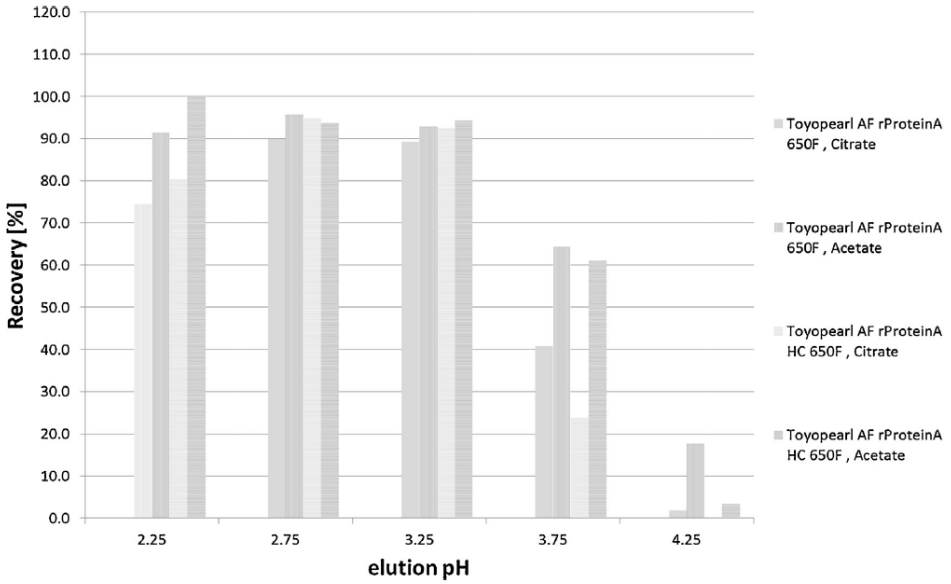

Fig. 4. Recovery dependency of the elution pH for TOYOPEARL AF-rProtein A-650F and TOYOPEARL AF-rProtein A HC-650F in different buffers.

of mAb have been described for Protein A modified membranes by Castilho et al. [66]. However, the effective capacity increase relatively low, since mAb concentrations did not exceed 5 mg/ml. Others have described multilayer arrangement in context of grafted ion exchanger membranes and particles [42]. BET shaped isotherms have yet only been confirmed for membranes. So far and to our knowledge, BET shaped isotherms have not been reported for Protein A resins.

As previously discussed, hydrophobic interactions between mAb and Protein A oligomers may be responsible for the multilayer arrangement. Sodium phosphate is a kosmotropic salt. Greater binding capacities at increasing salt concentrations may be based on additional hydrophobic interactions. It can further be deduced that the higher overall surface area of the hexamer ligand compared to the tetramer ligand leads to a greater number of hydrophobic patches. Greater flexibility of larger ligands may contribute, as well. This could explain the general increase of binding capacity of the hexamer ligand in 100 mM sodium phosphate. No such difference in binding capacity at different sodium phosphate concentrations can be obtained for the tetramer.

With this provided, purity and aggregate content should be negatively affected in a real purification process. Chen et al. reported that CHOP clearance is decreased by more than one order of magnitude if 1 ammonium sulfate is applied for mAb adsorption [28].

4.3. Protein A chromatography DoE at a phosphate buffer concentration of 100 mM

Experiments of the DoE were accomplished using parallel chromatography. Loading, titer and elution pH varies according to the schedule. Response factors are recovery, aggregate content, and

Table 6
Cumulative CHO log reduction values of Toyopearl AF-rProtein A-650F and Toyopearl AF-rProtein A HC-650F in the DOE.

Resin	Elution buffer citrate	Elution buffer acetate
TOYOPEARL AF-rProtein A-650F	LRV 3.0	LRV 3.0
TOYOPEARL AF-rProtein A HC-650F	LRV 2.9	LRV 2.7

host cell protein removal. Sodium acetate and sodium citrate were both used for elution.

MAb recovery is plotted against the applied elution pH (Fig. 4). MAb recoveries of more than 90% were achieved at pH 2.75 and 3.25. At pH 2.25, recovery of TOYOPEARL AF-rProtein A HC-650F is about 10% higher compared to TOYOPEARL AF-rProtein A-650F resin. Recoveries of acetate buffer at pH 3.25 are greater compared to sodium citrate. This is in contrast to previously reported results. Ngo described an increase in yield by adding kosmotropic buffer additives [65]. Sodium citrate is more kosmotropic than sodium acetate [67]. Recovery decreases at pH 3.75 and is closed to zero at pH 4.25. The overall functional relationship between elution pH and mAb recovery of both Protein A resins appears to be similar and independent from the height of binding capacity or the number of oligomers.

This is also true for mAb aggregate contents of the post-Protein A pool. The mAb shows equally low aggregation behavior for both resins under the chosen conditions. Fig. 5a–d displays the aggregate content in %, which is generated during elution with low pH using sodium citrate or sodium acetate. The pH dependency is plotted against protein loading. The initial aggregate content of the applied mAb is 1%. All other factors of the experimental schedule are kept constant during evaluation at the center point of the design. The corresponding mAb titer is 4.75 g/l and the CHO spiking is 300 μg/ml.

As expected, mAb aggregate contents increase at lower pH. Low pH values can induce conformational changes [68]. Acetate buffer causes less aggregation than citrate. This can be observed best at pH 2.5 for TOYOPEARL AF-rProtein A-650F, where citrate buffer leads to 4% aggregates and acetate to 3%. This may be due to the more kosmotropic salt. Overall, none of the selected factors have significant influence on aggregation. Only. Low aggregate contents are a result of the exceptional stability of this particular mAb and reflect that the robustness of a mAb is crucial for efficient and high yielding Protein A steps. Consequently high capacity resins do not necessarily cause aggregation due to a more concentrated product elution.

Host cell proteins are process-related impurities that need to be removed during Protein A chromatography. Fig. 6 illustrates the reduction of CHO proteins during purification with Protein A. CHOP contents were determined by ELISA. Mean log reduction values are given in Table 6. The reduction of CHO proteins reaches for both resins a mean of about 3 log steps, which is equal to factor 1000. Clearance can be considered acceptable, since these values are comparable to literature. For instance, Shukla et al. reached a LRV of 2.3 in a spiking approach with Protein A columns [69]. The log reduction factor of TOYOPEARL AF-rProtein A HC-650F is lower compared TOYOPEARL AF-rProtein A-650F. Similarly, lower LRVs have been observed for other new generation resins with high binding capacity, such as MabSelect Sure LX and JSR Amsphere Protein A. This effect may be based on greater resin hydrophobicity, due to higher ligand densities and molecular weights of the ligands [70]. In this context, it was observed that citrate buffer leads to slightly better CHOP reduction than acetate buffer. There is great diversity among host cell proteins with regards charge, size, and hydrophobicity. This allows for non-specific binding to the ligand, ligand mAb complex or to the matrix at neutral pH. Subsequently, remaining

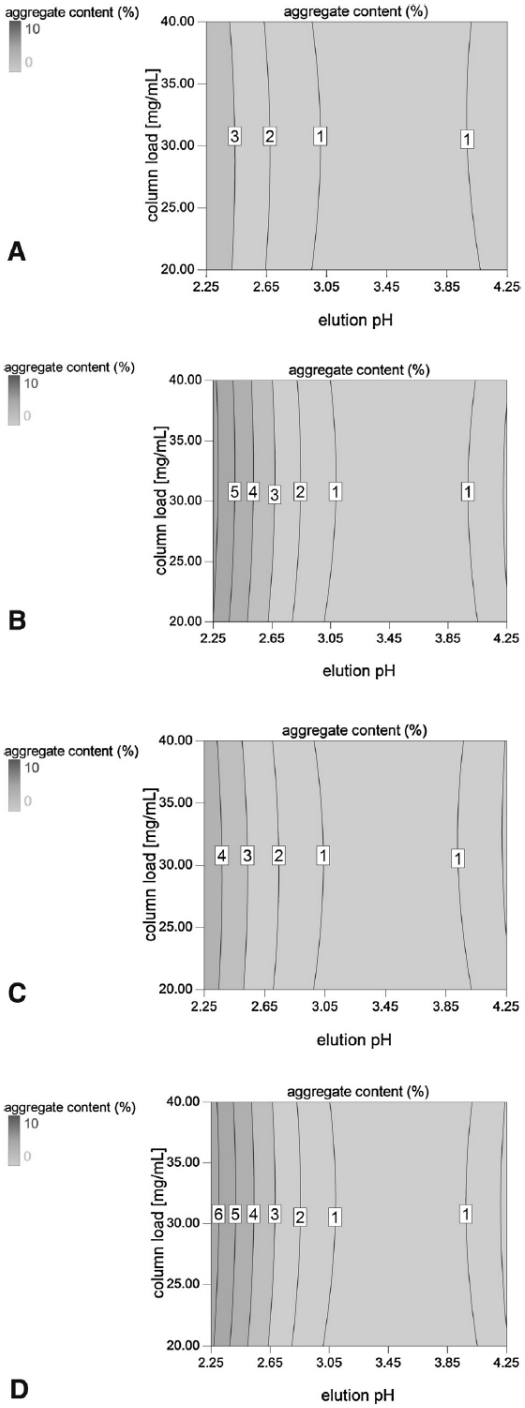

Fig. 5. Aggregate content generated during elution using citrate or acetate as elution buffer for TOYOPEARL AF-rProtein A-650F and TOYOPEARL AF-rProtein A HC-650F. The other factors of the experimental schedule are maintained constant during evaluation at the center point of the design at a titer of 4.75 g/l and at a CHO spiking of 300 μg/ml. (A) TOYOPEARL AF-rProtein A-650F acetate elution, (B) TOYOPEARL AF-rProtein A-650F citrate elution, (C) TOYOPEARL AF-rProtein A HC-650F acetate elution, (D) TOYOPEARL AF-rProtein A HC-650F citrate elution.

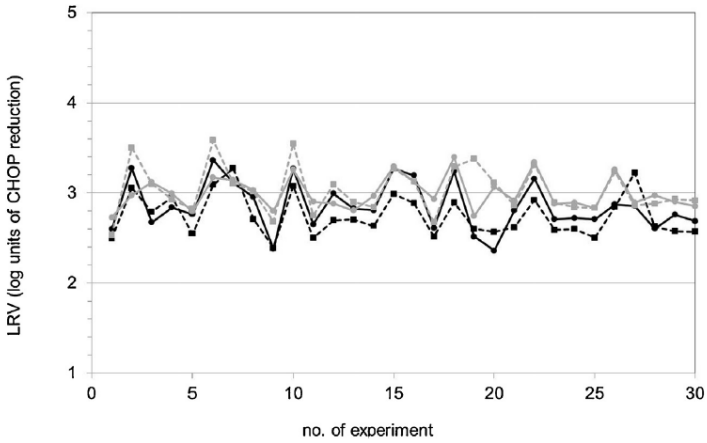

Fig. 6. HCP log reduction values (LRV) for TOYOPEARL AF-rProtein A-650F (grey) and TOYOPEARL AF-rProtein A HC-650F (black). Continuous traces correspond to citrate buffer, discontinued traces to acetate buffer. LRVs of all 30 experimental conditions from the DoE are presented.

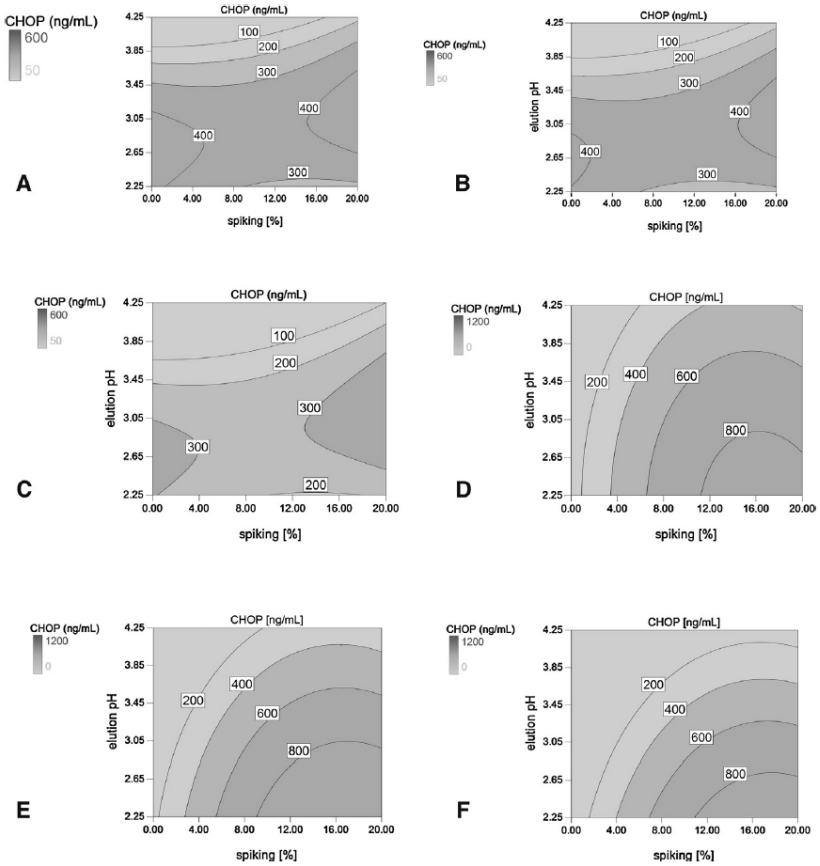

Fig. 7. CHOP content [ng/ml] in dependency of the feed antibody titer that was set to its low design point of 2.5 g/l, the center point of 4.75 g/l, and its highest design point of 7 g/l. Data for all of the tested Protein A resins is shown. The remaining parameter set was kept constant at the center point. (A) TOYOPEARL AF-rProtein A-650F, antibody titer 2.5 g/l, (B) TOYOPEARL AF-rProtein A-650F, antibody titer 4.75 g/l, (C) TOYOPEARL AF-rProtein A-650F, antibody titer 7 g/l, (D) TOYOPEARL AF-rProtein A HC-650F, antibody titer 2.5 g/l, (E) TOYOPEARL AF-rProtein A-650F, antibody titer 4.75 g/L, (F) TOYOPEARL AF-rProtein A-650F, antibody titer 7 g/l.

host cell proteins and the mAb are eluted under acidic conditions. According to our results, non-specifically bound CHO proteins are washed off the resin more efficiently when applying acetate buffer for elution. Impurities bound by hydrophobic interactions might remain bound to the resin when using citrate buffer for elution. CHOPs attached to mAbs will co-elute and equally reduce purity of the eluate.

Another interesting point is that CHOP contents are significantly influenced by the feed titer. The higher the titer, the less CHOP could be detected (Fig. 7a–f). Purity is improved from almost 400 ng/ml to 200 ng/ml for Toyopearl AF-rProtein A-650F at pH 3.0 and 15% CHOP spiking and from 800 ng/ml to 600 ng/ml for Toyopearl AF-rProtein A HC-650F. A possible explanation could be that sites for unspecific binding a covered by bound mAb. If mAb is present in low concentrations in the feed, more binding sites are unoccupied. It may occur that CHO proteins are adsorbed to the resin and are not displaced by antibody molecules. Since the antibody shows affine binding to Protein A, it potentially displaces non-specifically bound proteins from the binding sites. The concentration gradient between adsorbed and free mAb is smaller at low mAb concentrations compared to high titer feedstreams.

5. Conclusion

Binding capacity of Protein A affinity resins can be improved by the immobilization of longer rProtein A linear oligomer ligands. Depending on the conditions, dynamic binding capacity of a hexameric ligand is twice as high as a tetrameric ligand with the same binding motif. The maximum dynamic binding capacity of Toyopearl AF-rProtein A-650F in this study is higher than 50 mg/ml. The highest obtained dynamic binding capacity of Toyopearl AF rProtein A HC-650F is higher than 130 mg/ml. A strong mAb concentration independent increase of binding capacity was observed for the hexameric ligand at 100 mM sodium phosphate. This effect could not be found for Toyopearl AF-rProtein A-650F and is not the result of an increased ligand density. The corresponding isotherm of the Toyopearl AF-rProtein A HC-650F is BET shaped. An increase in the bound mAb concentration was determined at mAb concentrations higher than 8 mg/ml. This behavior indicates multilayer arrangement and is likely the result of the increased spacer length. The reason for multilayer formation is not yet clear and will be subject to future investigations. An increase in spacer length often results in an increase of non-specific interactions leading to a loss in purity and productivity. However, a DoE based approach confirmed that recovery, aggregate contents, and host cell protein removal are not significantly affected by the use of hexameric instead of tetrameric ligands.

References

[1] G. Carta, A. Jungbauer, Chromatography Media, Wiley-VCH Verlag, Weinheim, 2010.
[2] E. Sulkowski, Trends Biotechnol. 3 (1985) 1–7.
[3] R.S. Beissner, F.B. Rudolph, Arch. Biochem. Biophys. 189 (1978) 76–80.
[4] T. Burnouf, M. Radosevich, J. Biochem. Biophys. Methods 49 (2001) 575–586.
[5] A. Monzo, G.K. Bonn, A. Guttman, TrAC Trends Anal. Chem. 26 (2007) 423–432.
[6] J. Nilvebrant, S. Hober, T. Boström, in: Rizwan Ahmad (Ed.), Purification Systems Based on Bacterial Surface Proteins, Protein Purification, inTech, 2016, http://dx.doi.org/10.5772/29947, ISBN:978-953-307-831-1, Available from: http://www.intechopen.com/books/protein-purification.
[7] N. Labrou, in: P. Bailan, G.K. Ehrlich, W.J. Fung, W. Berthold (Eds.), Methods Mol. Biol., vol. 147, Humana Press Totowa, 2000, 2016, pp. 129–139.
[8] J. Hirabayashi, K. Kasai, J. Chromatogr. B Anal. Technol. Biomed. Life Sci. 771 (2002) 67–87.
[9] S. Vunnum, G. Vedantham, B. Hubbard, in: U. Gottschalk (Ed.), Process Scale Purif. Antibodies, John Wiley & Sons, Hoboken, 2009, pp. 79–99.
[10] R. Li, V. Dowd, D.J. Stewart, S.J. Burton, C.R. Lowe, Nat. Biotechnol. 16 (1998) 190–195.
[11] J. Curling, in: U. Gottschalk (Ed.), Process Scale Purif. Antibodies, John Wiley & Sons, Hoboken, 2009, pp. 25–32.
[12] Www.chromatan.com (2014).
[13] D. Baines, S. Wiliams, S. Burton, Euro Biotech News (2009) 217–228.
[14] J.M. Billakanti, C.J. Fee, A.D. Naik, R.G. Carbonell, Food Bioprod. Process. 92 (2014) 199–207.
[15] S. Miyakawa, Y. Nomura, T. Sakamoto, Y. Yamaguchi, K. Kato, S. Yamazaki, Y. Nakamura, RNA 14 (2008) 1154–1163.
[16] A. Cheung, S. Ghose, J. Hickey, J.L. Liu, BioPharm Int. (2009) 1–5.
[17] S. Burton, D.R. Harding, J. Chromatogr. A 814 (1998) 71–81.
[18] S. Ghose, B. Hubbard, S.M. Cramer, J. Chromatogr. A 1122 (2006) 144–152.
[19] D. Low, R. O'Leary, N.S. Pujar, J. Chromatogr. B Anal. Technol. Biomed. Life Sci. 848 (2007) 48–63.
[20] Www.merckmillipore.com (2015).
[21] Www.gelifescience.com (2015).
[22] Www.merckmillipore.com (2015).
[23] Www.jsrmicro.com (2014).
[24] Www.separations.eu.tosohbioscience.com (n.d.).
[25] P. Gronemeyer, R. Ditz, J. Strube, Bioengineering 1 (2014) 188–212.
[26] F.B. Anspach, D. Petsch, W.D. Deckwer, Bioseparation 6 (1996) 165–184.
[27] T.R. Mccaw, E.K. Koepf, L. Conley, Biotechnol. Prog. 203 (2014).
[28] W. Chen, S., Lacy, R. Huelsman, Novel purification of human, humanized, or chimeric antibodies using protein a affinity (51), Chromatography, US 2013/0336957 A1 (2013).
[29] Www.separations.eu.tosohbioscience.com (n.d.).
[30] http://www.gelifesciences.com/file_source/GELS/Service%20and%20Support/Documents%20and%20Downloads/Handbooks/Affinity_chromatography_handbook.pdf (2007) 88–96.
[31] https://www.gelifesciences.com/gehcls_images/GELS/Related%20Content/Files/1314823637792/litdoc71707700AG_20110901000046.pdf (n.d.) 3.
[32] Http://www.prometic.com (2004) 1–4.
[33] Https://tools.thermofisher.com (2014) 1–4.
[34] https://www.gelifesciences.com/gehcls_images/GELS/Related%20Content/Files/1314823637792/litdoc71707700AG_20110901000046.pdf (2011) 1–6.
[35] F. Anspach, Chromatography, Elsevier Science, Amsterdam, 2004, pp. 139–161.
[36] R. Hahn, Engineering of Industrial Chromatography, Universität für Bodenkultur Wien, 2008, 2016.
[37] R. Hahn, P. Bauerhansl, K. Shimahara, C. Wizniewski, A. Tscheliessnig, A. Jungbauer, J. Chromatogr. A 1093 (2005) 98–110.
[38] J. Carlsson, J.-C. Janson, M. Sparrman, Protein Purif., VCH, New York, 1989, pp. 285–292.
[39] G. Hagel, Handb. Process Chromatogr., Academic Press London, 2008, 2016, pp. 237–267.
[40] R. Hahn, R. Schlegel, A. Jungbauer, J. Chromatogr. B Anal. Technol. Biomed. Life Sci. 790 (2003) 35–51.
[41] E. Müller, J. Chromatogr. A 1006 (2003) 229–240.
[42] A.M. Lenhoff, J. Chromatogr. A 1218 (2011) 8748–8759.
[43] B. Lain, BioProcess Int. 11 (8) (2013) 29–38.
[44] E. Müller, Polymere Oberflächenbeschichtungen—Eine Methode Zur Herstellung von Trägermaterialien Für Die Biochromatographie, Otto-von-Guericke Universität Magdeburg, 2003, 2016.
[45] P. Cuatrecasas, Nature 228 (1970) 1327–1328.
[46] E. Müller, Chem. Eng. Technol. 28 (2005) 1295–1305.
[47] Www.wolfson.huji.ac.il (n.d.) 1.
[48] R. Hahn, E. Berger, K. Pflegerl, A. Jungbauer, Anal. Chem. 75 (2003) 543–548.
[49] M. Franzreb, E. Müller, J. Vajda 4 (4) (2014) 52.
[50] S. Ghose, B. Hubbard, S.M. Cramer, Biotechnol. Bioeng. 96 (2007) 768–779.
[51] M. Freiherr von Roman, S. Berensmeier, J. Chromatogr. A 1347 (2014) 80–86.
[52] H.J. Johansson, R. Palmgren, Affinity Chromatogr. Matrix (2013), WO2013081540 A1.
[53] P.M. Hammond, K.A. Philip, R.J. Hinton, G.W. Jack, Ann. N. Y. Acad. Sci. 613 (1990) 863–867.
[54] J.J. Langone, Adv. Immunol. 32 (1982) 157–252.
[55] C. Ljungquist, B. Jansson, T. Moks, M. Uhlén, Eur. J. Biochem. 186 (1989) 557–561.
[56] http://www.repligen.com/sites/default/files/bioprocessing/library/captiva_primab_rsf1003-01_05_18_10.pdf (2010) 1–72.
[57] B. Sheth, Characterisation of Chromatography Adsorbents for Antibody Bioprocessing, University College London, 2009.
[58] https://www.gelifesciences.com/gehcls_images/GELS/Related%20Content/Files/1314716762536/litdoc18114134_20150323220338.pdf (2015) 1–4.
[59] http://www.separations.eu.tosohbioscience.com/NR/rdonlyres/299AA93F-33BA-4274-8653-49C8927B3A0A/0/F10P11B_ProteinA.pdf (n.d.) 1–4.
[60] S. Hober, K. Nord, M. Linhult, J. Chromatogr. B Anal. Technol. Biomed. Life Sci. 848 (2007) 40–47.
[61] M. Plassmeyer, T. Thompson, B. Rehm, BioPharm Int. 24 (5) (2011).
[62] P. Gagnon, R. Nian, D. Leong, A. Hoi, J. Chromatogr. A 1395 (2015) 136–142.
[63] A.R. Mazzer, X. Perraud, J. Halley, J.O. Hara, D.G. Bracewell, J. Chromatogr. A 1415 (2015) 83–90.
[64] Toyopearl Instr. Man. (n.d.) 1–20.
[65] T.T. Ngo, D. Narinesingh, J. Immunoassay Immunochem. 29 (2008) 105–115.
[66] L.R. Castilho, W.-D. Deckwer, F.B. Anspach, J. Membr. Sci. 172 (2000) 269–277.
[67] S.O. Ugwu, P.A. Shireesh, Pharm. Technol. (2004) 83–113.
[68] D. Ejima, K. Tsumoto, H. Fukada, R. Yumioka, K. Nagase, T. Arakawa, J.S. Philo, Proteins 66 (2007) 954–962.
[69] A.A. Shukla, C. Jiang, J. Ma, M. Rubacha, L. Flansburg, S.S. Lee, Biotechnol. Prog. 24 (2016) 615–622.
[70] P. Thillaivinayagalingam, K. Reidy, A. Lindeberg, A.R. Newcombe, BioPharm Int. 10 (3) (2012) 36–39.

9.6. Mono- and polyprotic buffer systems in anion exchange chromatography of influenza virus particles

Autoren: Judith Vajda[1], Dennis Weber[2], Sabine Stefaniak[3], Boris Hundt[3], Tanja Rathfelder[4], Egbert Müller[1]

Institutionen:
[1]Tosoh Bioscience GmbH, Im Leuschnerpark 4, 64347 Griesheim, Deutschland
[2]Karlsruher Institut für Technologie, Institut für Bio- und Lebensmitteltechnik, Bereich IV: Molekulare Aufarbeitung von Bioprodukten, Engler-Bunte Ring 3, 76131 Karlsruhe, Deutschland
[3]IDT Biologika GmbH, Am Pharmapark, 06861 Dessau-Roßlau, Deutschland
[4]Hochschule Mannheim, Institut für Biochemie, Paul-Wittsack- Str. 10, 68163 Mannheim

DOI: 10.1016/j.chroma.2016.04.047

keywords: Pandemic influenza virus; Multimodal chromatography; Anion exchange chromatography; Polyprotic acids; Whole virus particle capturing; Pseudo affinity chromatography

Journal of Chromatography A, 1448 (2016) 73–80

Contents lists available at ScienceDirect

Journal of Chromatography A

journal homepage: www.elsevier.com/locate/chroma

Mono- and polyprotic buffer systems in anion exchange chromatography of influenza virus particles

Judith Vajda[a,*], Dennis Weber[b], Sabine Stefaniak[c], Boris Hundt[c], Tanja Rathfelder[d], Egbert Müller[a]

[a] Tosoh Bioscience GmbH, Im Leuschnerpark 4, 64347 Griesheim, Germany
[b] Karlsruher Institut für Technologie, Institut für Bio- und Lebensmitteltechnik, Engler-Bunte Ring 3, 76131 Karlsruhe, Germany
[c] IDT Biologika GmbH, Am Pharmapark, 06861 Dessau-Roßlau, Germany
[d] University of Applied Sciences Mannheim, Institut für Biochemie, Paul-Wittsack-Str. 10, 68163 Mannheim, Germany

ARTICLE INFO

Article history:
Received 23 February 2016
Received in revised form 14 April 2016
Accepted 18 April 2016
Available online 21 April 2016

Keywords:
Pandemic influenza virus
Multimodal chromatography
Anion exchange chromatography
Polyprotic acids
Whole virus particle capturing
Pseudo affinity chromatography

ABSTRACT

Different ions typically used in downstream processing of biologicals are evaluated for their potential in anion exchange chromatography of an industrially produced, pandemic influenza H1N1 virus. Capacity, selectivity and recovery are investigated based on single step elution parallel chromatography experiments. The inactivated H1N1 feedstream is produced in Madin-Darby Bovine Kidney cells. Interesting effects are found for sodium phosphate and sodium citrate. Both anions are triprotic kosmotropes. Anion exchange chromatography generally offers high scalability to satisfy sudden demands for vaccines, which may occur in case of an emerging influenza outbreak. Appropriate pH conditions for H1N1 adsorption are determined by Zeta potential measurements. The dynamic binding capacity of a salt tolerant polyamine-type resin is up to 6.4 times greater than the capacity of a grafted Q-type resin. Pseudo-affinity interactions of polyamines with the M2 protein of influenza may contribute to the obtained capacity increase. Both resins achieve greater capacity in sodium phosphate buffer compared to Tris/HCl. A recovery of 67% and DNA clearance close to 100% without DNAse treatment are achieved for the Q-type resin. Recovery of the virus from the salt tolerant resin requires the use of polyprotic acids in the elution buffer. 85% of the DNA and 60% of the proteins can be removed by the salt tolerant resin. The presence of sodium phosphate during anion exchange chromatography seems to support stability of the H1N1 particles in presence of hydrophobic cations.

1. Introduction

Recently, the use of anion exchange chromatography for influenza particle purification has become more attractive. In 2007, the first influenza vaccine propagated in cell culture has been approved by the European Medicines Agency [1]. Seamlessly scalable production of virions in cell culture requires efficient and flexible downstream purification strategies. Column chromatography is a well-established technology that meets these requirements. Ion exchange chromatography in particular provides high productivity, due to its comparatively high capacity. Anion exchange chromatography based on Q-Sepharose after preparative size exclusion chromatography removes high base pair host cell DNA, which may also be associated to virus particles [2]. Chromatographic strategies based on size exclusion chromatography for primary purification and subsequent polishing by ion exchange chromatography are comparatively less efficient. Ion exchange chromatography as a first step and size exclusion chromatography of reduced pre-purified volumes are more productive. Anion exchange chromatography in flow-through mode is part of a three step purification scheme including, DNase treatment, and flow-through chromatography with restricted access media [3]. However, non-capturing purification trains are often less efficient, since water for injection represents volume-wise the largest impurity. In flow-through chromatography, the product is diluted during downstream processing. Hence, development of a chromatographic capturing step on the basis of anion exchange chromatography could help to improve process efficiency and process scalability in case of a pandemic outbreak of viral diseases. Crucial factors in ion exchange chromatography are pH and salt

* Corresponding author.
E-mail addresses: Judith.Vajda@tosoh.com (J. Vajda), dennis.weber2@student.kit.edu (D. Weber), Sabine.Stefaniak@idt-biologika.de (S. Stefaniak), Boris.Hundt@idt.biologika.de (B. Hundt), TanjaRathfelder@gmx.de (T. Rathfelder), Egbert.mueller@tosoh.com (E. Müller).

http://dx.doi.org/10.1016/j.chroma.2016.04.047

concentration. However, virus stability sets tight bonds to the applicable operational window [4,5], which impede conditions typically used in ion exchange chromatography of proteins. Trilisky and Lenhoff have studied the adsorption behavior of adenovirus type 5 to strong anion exchangers with quaternary ammonium ligands. The corresponding maximum capacity is reached at 0.2 mM sodium chloride, determined by optical density measurements [6]. Several other studies show that the adsorption of viruses to soils of the same charge is supported by introducing moderate salt concentrations. Further, multivalent ions like Ca^{2+} support aggregation of phage MS2 [7]. Cations carrying two or three charges at concentrations in the range of 10–30 mM appear to be especially useful [8–12]. Taylor et al. suggest that this is due to the shielding of surface charges and a reduction of the electric double layer [12]. In turn, van der Waals interactions become more dominant, which according to the Derjaguin–Landau–Verwey–Overbeek–Lifshitz theory supports coagulation and sorption processes [12–14]. In case of matrices with different charge, charge shielding is expected to reduce binding of virus particles. Based on these findings, salt tolerant resins may lead to productivity improvements in anion exchange chromatography of influenza particles. High salt concentrations lead to dissociation of protein-DNA complexes and a salt tolerant ion exchange chromatography step could potentially benefit from this effect with regards to capacity and product purity [15–22]. Salt tolerance of ion exchange resins is often supported by an additional hydrophobic moiety of the ligand. This strategy seems less promising for adsorption of influenza particles. Hydrophobic cations induce inactivation, structural damage and release of RNA from the influenza virus particle [23]. Such effects may be anticipated by the use of stabilizing electrolytes. Calcium ions support thermal stability of neuraminidase 1 [24]. The effectiveness of a variety of additives during downstream processing of biopharmaceuticals is widely recognized. For instance, arginine improves recovery of monoclonal antibody (mAb) from Protein A [25] and generally prevents non-specific interactions [26,27]. Another example is polyethylene glycol 10,000. Addition of 1% of this modifier to the liquid phase increases ion exchange chromatography recovery of hepatitis B virus surface antigen from 55% to 80% [28]. To our best knowledge, effects of different electrolytes on influenza purity, recovery and sorption efficiency have not yet been investigated. The herein employed influenza strain is an industrially produced virus for use in vaccines and originates from pandemic H1N1.

2. Materials and methods

2.1. H1N1

Inactivated H1N1 feedstream was provided by courtesy of IDT Biologika GmbH, Dessau-Rosslau, Germany and was used in all experiments of this study. The H1N1 is a pandemic influenza A vaccine strain, which is produced in an industrial process in Madin-Darby Canine Kidney bioreactor cell culture according to the process established by Hundt et al. [29]. The virus particles were harvested, 20-fold concentrated, and inactivated by treatment with β-propriolactone.

2.2. Resins

Two methacrylate based strong anion exchange resins named TOYOPEARL GigaCap Q-650M, and TOYOPEARL NH2-750F were used in this study. Both resins were supplied by Tosoh Bioscience GmbH (Griesheim, Germany). GigaCap Q-650M is a grafted resin with a particle size of 65 μm and a pore size of 100 nm of the base matrix. Mean particle size of NH2-750F is 45 μm and pore size is greater than 100 nm. Functionality of NH2-750F is based on a proprietary polyamine ligand Primary amine groups have strong anion exchange functionality. The ligand backbone allows for hydrogen bonding. GigaCap Q-650M is a classical quaternary amine-type stationary phase. Ion exchange capacity of GigaCap Q-650M is 0.15 ± 0.05 meq/ml, whereas ion exchange capacity of NH2-750F is 0.1 ± 0.03 meq/ml. Sorption of anionic proteins, e.g. bovine serum albumin (BSA), to NH2-750F is salt tolerant.

2.3. Zeta potential measurements

The zeta potential of the inactivated virus particles and the protein nanoparticles was assessed by electrophoretic light scattering with the DelsaMax Pro according to the model of Smoluchowski. An electric field with amplitude of 2.5 V alternated at 10 Hz. Buffer exchange and removal of the majority of host cell proteins or remaining reaction educts were accomplished with preparative size exclusion chromatography using TOYOPEARL HW-65F. The zeta potential was measured in 100 mM sodium acetate buffer at pH 4.0, 4.5, 5.0, 5.5, 100 mM sodium phosphate at pH 6.0, 6.5, 7.0, 8.0. Zeta potential measurements were performed at least in triplets.

2.4. Hemagglutination assay

The hemagglutination activity was determined with Tecan Freedom Evo 150. Chicken erythrocyte preparations in Alsever solution were purchased from preclinics GmbH (Potsdam, Germany). 4 ml of the erythrocyte preparation were diluted with 40 ml phosphate buffered saline (PBS): 1.54 mM potassium dihydrogen phosphate, 8.10 mM disodium hydrogen phosphate, 2.68 mM potassium chloride and 137 mM sodium chloride, pH 7.5 at 25 °C. All chemicals were purchased from Merck (Darmstadt, Germany), unless indicated otherwise. Pelleted erythrocytes were resuspended in 40 ml of cold PBS. Erythrocyte concentration was determined with a Fuchs-Rosenthal cytometer, and adjusted to $2 \times 10^7 \pm 0.1 \times 10^7$ cells per ml. 100 μl of the H1N1 containing samples were transferred into every second row of the first two columns of U-bottom 96 well plates. A $1{:}2^{0.5}$ dilution of the samples was pipetted into the first two wells of the remaining rows. Serial 1:2 dilutions of all samples in phosphate buffered saline within every row were completed. 100 μl of the erythrocyte solution were added to all wells and plates were incubated for one hour at room temperature. Results were evaluated by absorbance readings at 700 nm. Results were double-checked manually and experiments were repeated in the rare case of inconsistency.

2.5. Dynamic binding capacities

Dynamic binding capacities (DBC) at 10% breakthrough were determined with a Tecan Freedom Evo 150 (Männerdorf, Switzerland) system equipped with a TeChrom Station, and a Tecan infinite 200 PRO UV reader. 200 μl RoboColumns packed with TOYOPEARL GigaCap Q-650M, and TOYOPEARL NH2-750F were purchased from Atoll (Weingarten, Germany). Virus feedstream was dialyzed through 24 Å pores into loading buffer overnight at 4 °C and loaded at 150 cm/h. 200 μl fractions of the flow-through were collected into U-bottom 96 well plates (Greiner Bio-One, Frickenhausen, Germany). Breakthrough was determined by an adapted hemagglutination assay of the collected fractions and the feed solution. The hemagglutination assay titer of the feed diluted 1:10 in PBS was identified. Collected fractions were then diluted to the least concentration, at which the prior hemagglutination assay of the 1:10 sample dilution turns positive. 100 μl of the dilution and 100 μl of the prepared erythrocytes were then pipetted into U-bottom 96 well microplate and incubated for 1 h at room temperature. If the assay turned positive, 10% of the virus

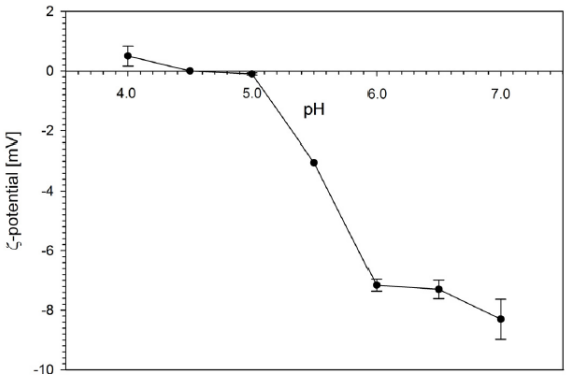

Fig. 1. Zeta Potential of inactivated H1N1 at different pHs. The isoinic point is in the range of pH 4.5–5.0. Virus samples are buffered in 100 mM sodium acetate or sodium phosphate.

would be detected in the eluate fraction. DBC of both resins for BSA were determined in the same instrument, except breakthrough was determined by absorbance readings at 280 nm. 50 and 100 mM sodium phosphate and Tris/HCl buffer, respectively, were tested for column loading at pH 7.0 and 8.0. Columns were cleaned with 0.5 M sodium hydroxide and 0.5 M chlorous acid prior to re-equilibration. Capacities were determined at least in duplicates.

2.6. Elution buffer screening

Screening of suitable elution buffers was performed in 600 μl RoboColumn format using the previously described Tecan system. Various different elution buffers or additives were tested: 1 M sodium chloride, 1 M calcium chloride, 0.5 M sodium phosphate, 0.5 M sodium citrate, 1 M arginine/HCl. Electrolytes were solved in 50 mM Tris/HCl or sodium phosphate, pH 6.0, 7.0, and 8.0.

2.7. Size exclusion chromatography

Size Exclusion Chromatography was used for qualitative and quantitative analysis of the H1N1 samples. A polymethacrylate based TSKgel G6000PWxl (Tosoh Bioscience GmbH) with pores greater than 100 nm was connected to a Shimadzu LC Prominence system (Shimadzu, Tokyo, Japan) equipped with a MiniDawn Treos (Wyatt Technology, Santa Barbara, USA). 100 mM sodium phosphate buffer at pH 7.0 containing 200 mM sodium chloride was used at a flow rate of 1.0 ml/min. UV absorbance was monitored at 214 nm. 100 μl of the samples were injected and analysis was performed at least in duplicates.

2.8. DNA quantification

DNA contents in load, flow-through and elute fractions of anion exchange chromatography were determined with a fluorescence based assay. The applied Quant-iT ds DNA HS assay (Invitrogen, Carlsbad, USA) was conducted according to the instructions of the manufacturer. The lower limit of detection of this assay is 0.2 ng/ml.

3. Results and discussion

3.1. Zeta potential

Zeta potential of H1N1 particles purified by size exclusion chromatography was determined at different pHs. Results are shown in Fig. 1. The isoionic point of the inactivated H1N1 is in the range of 4.5–5.0. This corresponds to findings obtained with other influenza strains, published in literature. Miller et al. report an isoelectric point of 5.3 [30]. Zhilinskaya et al. determine it as 5.0 [31]. Interestingly, hemagglutination activity of another H1N1 virus has a minimum at pH 5.0 [2]. The zeta potential of H1N1 decreases to −8 mV at pH 8.0. 100 nm protein nanoparticles prepared from BSA have a zeta potential of −15 mV at 8.0 [32]. Zeta potential of BSA in 100 mM solutions of different salts range from −5 to −20 mV [33]. The value of the zeta potential of H1N1 is comparatively lower. Contributions of interactions other than ion exchange might become more important. Nevertheless, H1N1 is still anionic in a neutral pH environment. Hence, pH 8.0 should support binding of H1N1 particles through electrostatic interactions.

3.2. Dynamic binding capacities

DBCs for H1N1 in 50 mM Tris/HCl and sodium phosphate at pH 7.0 and 8.0 are shown in Table 1. The DBCs of NH2-750F for the virus are higher compared to the capacities of GigaCap Q-650M. NH2-750F has smaller particles. The surface available for adsorption of the virions is greater, compared to GigaCap Q-650M. Pore size may also contribute to a greater capacity, since the virions may have access to the comparatively larger pores of this resin. Although the pore size is only slightly greater than the virions itself, good coverage of the resin outer particle surface may induce osmotic pressure to accelerate diffusion of the virions into the pores. Resin specific effects may extend to binding kinetics of virion particles during anion exchange chromatography. Yu et al. report a decrease in k_D and an increase in q_{max} for increasing ligand densities of DEAE resins [34]. In contrast, Opitz et al. find no direct correlation of lectin ligand density and binding efficiency of H1N1 inactivated virions [35]. However, this comparison includes ligand densities and different backbones, such as agarose, cellulose or glass particles. The employed ligand densities are in the range of several mg/ml resin, which ensures an excess of ligand. Ion exchange capacity of GigaCap Q-650M is 50% higher than ion exchange capacity of NH2-750F. Based on the ion exchange capacities, one would expect that virus capacity of GigaCap Q-650M is higher or equivalent to the capacity of NH2-750F. However, the opposite is true (Table 1). One potential explanation for higher capacities of the polyamine type resin refers to specific effects of the polyamine. The influenza ion channel protein M2 has a high affinity binding site for polyamines [36]. Polyamines, such as spermidine bind to M2 and block the ion channel. Adamantanes are antiviral drugs that make use of this mechanism [36]. Pseudo affinity interactions may contribute to the binding of the polyamine ligand to the influenza particles. Adsorption of other enveloped viruses may be supported, as well. For instance, HIV has ion channels similar to M2 [37]. These ion channels are a drug target for polymeric adamantan analogues [38]. In presence of physiological sodium or potassium concentrations, the minimum inhibitory concentration of polyamines for influenza is 100 μM. Inhibitory polyamine concentrations decline by two to three orders of magnitude in absence of sodium ions. This could lead to smaller k_D values of the polyamine ligand. Lin et al. further suggest that polyamines bind to negatively charged lipid head groups with lower affinity [36]. Other interactions, i.e. hydrophobic or van der Waals interactions may contribute as well. The Zeta potential of H1N1 in buffered solutions is low. Further evidence for non-electrostatic interactions during H1N1 adsorption is provided by a comparison of capacities in different binding buffers. Binding capacities in sodium phosphate are higher, compared to Tris/HCl. This applies to both resins (Table 1). However, capacity increases of NH2-750F are comparatively greater: NH2-750F binds 6.4-fold more H1N1 than GigaCap Q-650M in 50 mM sodium phosphate buffer, pH 8.0. Higher resin capacity due to binding in sodium phosphate buffer is unexpected in anion exchange

Table 1
Dynamic binding capacity of NH2-750F and GigaCap Q-650M for H1N1. Capacities were determined at pH 7.0 and 8.0 in sodium phosphate and Tris/HCl buffer. Depending on the individual conditions, NH2-750F binds up to 6.4 times more H1N1 than GigaCap Q-650M.

Resin	buffer	fraction volume [μL]	HA Titer load [HAU × 100 μl^{-1}]	breakthrough fraction	DBC_{10} [HAU/ml-resin]
NH2-750F	50 mM Tris pH 7.0	200	128	48	6.14E+04
	50 mM Tris pH 8.0	200	45	62	2.79E+04
	50 mM NaP_i pH 7.0	200	288	>45	>1.30E+05
	50 mM NaP_i pH 8.0	200	341	>45	>1.53E+05
GigaCap Q-650M	50 mM Tris pH 7.0	200	362	6	2.17E+04
	50 mM Tris pH 8.0	200	362	3.75	1.36E+04
	50 mM NaP_i pH 7.0	200	288	9.50	2.74E+04
	50 mM NaP_i pH 8.0	200	341	7.00	2.39E+04

chromatography. If an anion exchanger is equilibrated in phosphate buffer, phosphate will adsorb to the stationary phase. If Tris/HCl buffer is used instead, comparatively smaller chloride ions will adsorb to the chromatography matrix. Smaller ions are thought to be displaced faster by proteins or virions. Further, a considerable portion of phosphate ions carry two charges at the applied pH conditions. It binds with higher avidity to the anion exchange resin. Hence, it neutralizes charges of the anion exchange resin. Simultaneously, the buffer concentration and capacity of the mobile phase is decreased. Changing the eluent may lead to pH waves, due to buffer ion adsorption or desorption [39,40]. This effect is particularly important in context of weak (cation) ion exchangers. The employed resins are strong anion exchangers. However, different phosphate buffers stabilize influenza vaccines [41,42]. For this reason the presence of phosphate during chromatography seems beneficial. Higher virus binding capacities in phosphate buffer might be due to greater van der Waals forces. The capacity increase due to sodium phosphate does not hold true for BSA and both resins. Fig. 2 shows DBCs of BSA in sodium phosphate and Tris/HCl. BSA capacities in Tris/HCl are roughly three times higher for GigaCap Q-650M and ten times higher for NH2-750F, compared to sodium phosphate. Electrostatic interactions may play a comparatively minor role in binding of virus particles, compared to proteins. Instead, van der Waals interactions may become more important for adsorption to NH2-750F. The Debye length decreases with increasing ionic strength [43]. The latter is a sum of the molal concentration and valence of the ions in solution. In turn, sodium phosphate supports additional van der Waals interactions. Citrate and phosphate buffer form pseudo-polyampholytes with polyethylenimin [44]. The presence of phosphate ions may decrease net charge of the polyamine ligand. Entropic effects due to the release of a greater number of salt ions in close vicinity of the virus particles may contribute as well. Highly branched polyethylenimin ligands retain amino acids and other polar biocompounds through hydrophilic interactions [45]. Hydration of the virus and the polyamine ligand might be affected by the presence of phosphate. Similarly hydrated molecules of opposite charge preferably interact [46].

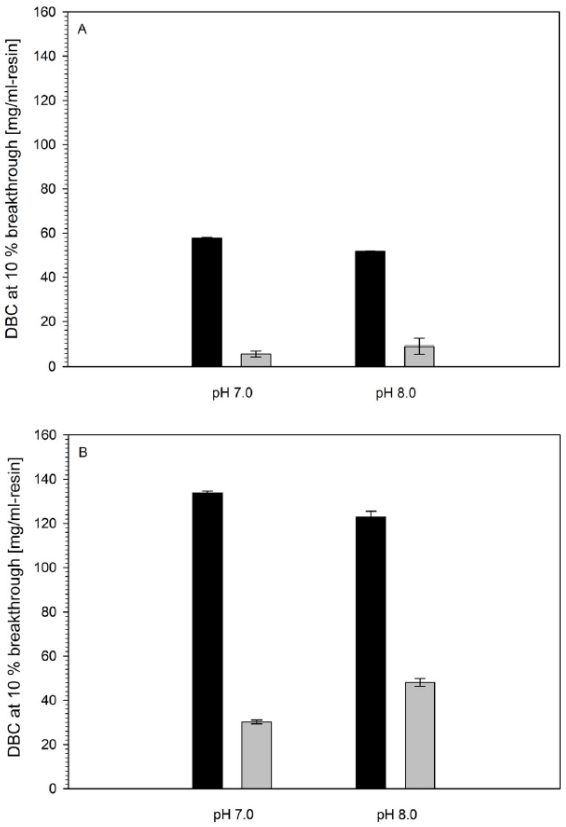

Fig. 2. DBC of NH2-750F (A) and GigaCap Q-650M (B) for BSA. Capacities were determined at pH 7.0 and 8.0 in sodium phosphate (light grey) and Tris/HCl (black) buffer at a protein concentration of 10 g/L. Capacities in Tris/HCl are higher compared to sodium phosphate buffer.

3.3. Recovery

Recovery was determined by analytical size exclusion chromatography and the hemagglutination assay. Results are listed in Tables 2 and 3. Calcium mediated hemagglutination is described in literature [47]. Yet calcium chloride elution buffers interfere with the hemagglutination activity and lead to false positive results in the assay (Fig. 3). Hence, two analytical methods were applied to determine recoveries. Recoveries determined by size exclusion chromatography are roughly 50% lower compared to recoveries determined by the hemagglutination assay. This may be due to broken virus particles with remaining hemagglutination activity. Such debris co-elutes with protein impurities and is not recognized as recovered virus in size exclusion chromatography. Recoveries and purities obtained at pH 7.0 and pH 8.0 are consistent.

Table 2 shows results obtained with monovalent anions and zwitterions. H1N1 cannot be recovered from NH2-750F with the applied monovalent anions or zwitterions. This may indicate great binding avidity and insufficient displacement of the virus by monovalent ions. Alternatively, this could be explained by an insufficient sodium concentration to weaken the suggested affinity-like interactions with the M2 protein.

Recoveries from TOYOPEARL GigaCap Q-650M with monovalent anions or zwitterions are higher, compared to recoveries of NH2-750F. Recoveries determined by analytical size exclusion

Table 2
H1N1 recovery, DNA removal, and protein clearance of NH2-750F and GigaCap Q-650M. The pools were eluted with sodium chloride, calcium chloride, arginine, and lysine. Recoveries based on the hemagglutination activity are roughly twice as high as recoveries determined by size exclusion chromatography. Protein removal could not be determined in salts with high UV absorbance at 214 nm, i.e. lysine, arginine. Whole H1N1 particles cannot be recovered from NH2-750F with the applied elution buffers. DNA removal is 99% except in case of sodium chloride elution from GigaCap Q-650M.

load buffer	elute buffer [M]	resin	pH	DNA removal [%]	recovery by HA [%]	recovery by SEC [%]	protein removal [%]
50 mM Tris/HCl	1.0 sodium chloride	NH2-750F	7.0	99.80	0.00	0.62	71.96
			8.0	100.00	0.00	0.92	57.85
		GigaCap Q-650M	7.0	70.77	192.12	60.54	14.09
			8.0	55.12	251.56	66.80	−0.20
	1.0 lysine	NH2-750F	7.0	99.89	0.00	0.60	n/a
			8.0	100.30	0.00	1.07	n/a
		GigaCap Q-650M	7.0	42.37	177.85	67.87	n/a
			8.0	64.86	184.57	41.67	n/a
	1.0 arginine	NH2-750F	7.0	99.95	0.00	0.64	n/a
			8.0	99.39	0.00	0.00	n/a
		GigaCap Q-650M	7.0	42.35	114.13	58.13	n/a
			8.0	40.16	123.05	49.43	n/a
	1.0 calcium chloride	NH2-750F	7.0	99.71	n/a	0.85	n/a
			8.0	99.19	n/a	4.56	n/a
		GigaCap Q-650M	7.0	99.47	n/a	26.47	n/a
			8.0	99.13	n/a	2.18	n/a
50 mM sodium phosphate	0.5 sodium chloride	NH2-750F	7.0	100.00	4.10	1.69	83.18
			8.0	100.00	0.00	0.30	90.00
		GigaCap Q-650M	7.0	98.68	77.25	41.00	57.98

Table 3
H1N1 recovery, DNA removal, and protein clearance of NH2-750F and GigaCap Q-650M. The pools were eluted with sodium phosphate and sodium citrate. Citrate containing elution buffers did not allow determining the protein content. 50 or 30% (depending on the method used for quantification) of the applied H1N1 can be recovered from NH2-750F using sodium phosphate or sodium citrate for elution. 60% of the proteins are removed if sodium phosphate is used during chromatography. DNA clearance rates range from 65 to 100%.

laod buffer	elute buffer [M]	resin	pH	DNA removal [%]	recovery by HA [%]	recovery by SEC [%]	protein removal [%]
50 mM Tris/HCl	0.5 sodium phosphate	NH2-750F	7.0	91.69	15.22	6.82	−5.23
			8.0	86.84	11.62	9.91	1.50
		GigaCap Q-650M	7.0	98.81	66.58	35.69	23.28
			8.0	99.51	31.39	17.61	44.39
	0.5 sodium citrate	NH2-750F	7.0	76.31	33.89	4.65	n/a
			8.0	80.36	34.38	2.31	n/a
		GigaCap Q-650M	7.0	98.08	61.06	39.62	n/a
			8.0	95.64	52.88	40.31	n/a
50 mM sodium phosphate	0.5 sodium phosphate	NH2-750F	7.0	84.94	36.79	30.07	61.16
			8.0	87.05	16.92	32.70	60.24
		GigaCap Q-650M	7.0	99.50	36.57	30.57	33.53
	0.5 sodium citrate	NH2-750F	7.0	86.52	50.00	26.21	n/a
			8.0	75.01	39.14	20.92	n/a
		GigaCap Q-650M	7.0	65.47	58.89	18.42	n/a
			8.0	100.40	54.81	41.00	n/a
	0.5 sodium phosphate + 0.5 sodium citrate	NH2-750F	7.0	76.31	33.89	9.20	n/a
			8.0	80.36	34.38	9.13	n/a
		GigaCap Q-650M	7.0	98.08	61.06	9.40	n/a
			8.0	95.64	52.88	21.46	n/a

chromatography range from 40 to 70%, except for calcium chloride. Calcium chloride recoveries range between 2 and 26%. Recoveries determined through hemagglutination activity exceed 100%. Naturally, this must be an artifact. The standard deviation of the hemagglutination assay is comparatively high. Although the assay was run on a pipetting robot, other factors, such as the elution buffer composition and aging of the erythrocytes continue to impair assay reproducibility. Further, virus particle fragmentation leading to a greater number of debris molecules with remaining hemagglutination activity may lead to false positive results. The comparatively low recovery of H1N1 from GigaCap Q-650M by calcium chloride elution may be explained by the Schulze–Hardy rule. The concentrations of counterions required to induce colloid flocculation decreases with higher valency of the counterions [48]. Together with a comparatively low zeta potential, this may support unspecific adsorption of the virus particles to the resin. Recoveries of the other monovalent anions and zwitterions are similar. This can be expected, provided the adsorption can be described by the stoichiometric exchange of charges. According to these results, H1N1 adsorption to GigaCap Q-650M seems to be governed by ion exchange interactions.

Table 3 shows H1N1 recoveries obtained from NH2-750F and GigaCap Q-650M with polyprotic acids. Citrate and phosphate support elution of H1N1 from NH2-750F. Recoveries determined by size exclusion chromatography range from 0 to more than 40%. Recoveries determined by the hemagglutination assay reach more than 60%. Recoveries from GigaCap Q-650M are higher compared to recoveries from NH2-750F, except if sodium phosphate is applied for loading and elution. Hydrophobicity seems to play a minor role in binding of H1N1 particles to the NH2-750F resin. Sodium citrate and sodium phosphate are both kosmotropic. Hence, hydrophobic interactions will be strengthened at increasing concentrations and would prevent H1N1 elution. Roughly 10% (according to analytical size exclusion chromatography) of the virus can be recovered by elution in 0.5 M sodium phosphate for NH2-750F. This recovery supporting effect may be attributed to the valency of these ions.

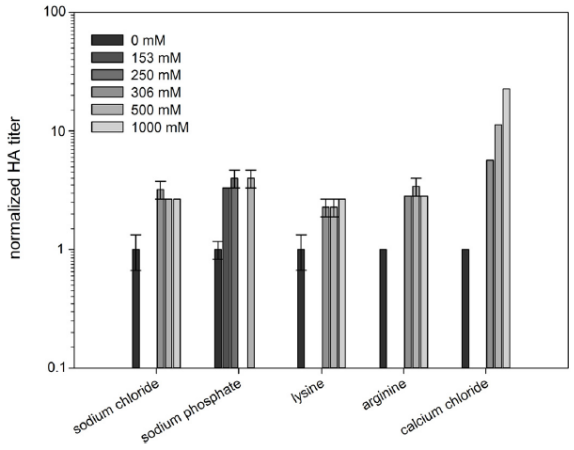

Fig. 3. Impact of different electrolytes on hemagglutination at pH 7.0. Results are normalized against the hemagglutination activity in 5 mM Tris/HCl without further addition of salt (0 mM, black). Grey tones of the bars indicate different concentrations of the corresponding electrolyte concentrations. Effects of sodium chloride, sodium phosphate, lysine, and arginine are negligible. Hemagglutination activity correlates proportionally with the calcium chloride concentration.

Such effects can be expected for polyamine ligands. The avidity of polyprotic acids to the polyamine ligands of NH2-750F is higher than in case of monovalent ions. Increasing concentrations of citrate and phosphate may lead to the formation of polyampholytes with increasing negative net charge. This would lead to charge induced repulsion of adsorbed virus particles. Changing the charge density of the polyamine ligand affects its hydration. Thus, hydrophobic interactions will be affected, as well. Further, every mole sodium citrate or sodium phosphate contains three times the amount of sodium ions, compared to sodium chloride. Benefits of polyprotic acids may not be limited to the stoichiometric exchange of counter ions and avidity. The polyamine binding sites in the M2 protein are usually occupied by sodium ions [36]. Greater sodium concentrations may displace the polyamine ligand from the M2 protein. Inhibitory polyamine concentrations increase by two to three orders of magnitude in the presence of physiological sodium concentrations [36]. Hence, affinity-like interactions should be weakened by increasing sodium concentrations.

Comparing virus recoveries of samples eluted with sodium phosphate, loading with 50 mM sodium phosphate instead of 50 mM Tris/HCl increases recovery from the polyamine type resin to more than 30%. This may be due to the present sodium ions. The M2 protein regulates the proton flux across the virus membrane. Mutations in the M2 protein have been shown to increase the expression levels of the low pH-form of hemagglutinin [49]. The binding of polyamines to M2 and blockage of the ion channel in absence of competitive sodium ions seem to induce breakup of the membrane at the chromatographic stationary phase. Hydrophobic poly-cations, such as the polyamine ligand, have been described to inactivate influenza virus particles [23]. The addition of 0.1 M phosphate to saline solutions of influenza virus particles maintains activity of the virus [41]. A mixture of sucrose, phosphate, and glutamate increases stability of influenza vaccine formulations against temperature [42]. The suggested mechanism involves adherence and shearing of the virus particle, as well as release of the incorporated RNA. This effect is independent from the nature of the surface to which the hydrophobic poly-cation is immobilized. Polyprotic acids present during virus adsorption may shield some of the charges of the poly-cation and remain bound, based on their greater avidity. This would inhibit shearing, spreading and destruction of virus particles. Due to the smaller number of ionic interactions, this would support virus recovery. Further, sodium ions may prevent from inhibition of all M2 proton channels, thus stabilizing the virus particle. Virus recovery from GigaCap Q-650M is not affected by the different load buffers. Recoveries from GigaCap Q-650M with sodium citrate and sodium phosphate are lower compared to monovalent anions and zwitterions. Citrate and phosphate are kosmotropic ions, and hydrophobic interactions could prevent higher recoveries.

3.4. DNA clearance

The applied experimental setup with a step elution does not allow complete separation of virus particles from DNA in all cases. Nevertheless, different electrolytes seem to affect DNA clearance. DNA clearance results of the various parallel chromatography runs are shown in Tables 2 and 3. DNA clearance of the NH2-750F resin is close to 100%, except from elution with polyprotic acids. DNA is a poly-anion. Binding of DNA to the poly-cationic ligand is like a zipper. Replacement may only be accomplished by ions with multi charged structure. DNA removal of NH2-750F in combination with sodium phosphate and sodium citrate elution still exceeds 75%. It is in most cases roughly 85%. DNA removal of GigaCap Q-650M ranges from 40 to 100%. The valency of the applied salt ions has no significant impact. However, lysine and arginine support DNA co-elution with the virus. Lysine elution led to a DNA reduction by 40%. Sodium phosphate leads to almost complete DNA removal with GigaCap Q-650M. No such effect can be observed with NH2-750F. The capabilities of arginine to prevent from non-specific interactions have been described for various applications in protein chromatography, such as size exclusion chromatography and protein A chromatography [50]. The limiting DNA concentration in human whole virion influenza vaccines is 10 ng per dose and the required amount of hemagglutination assay antigen is 15 μg of each of the 3 strains per dose [51]. The detection limit of the applied DNA assay is not sufficient to confirm compliance with these guidelines.

3.5. Total protein content

Protein contents were determined by analytical size exclusion chromatography. A Bradford assay calibrated against BSA led to negative protein concentrations in several cases (results not shown). Size exclusion chromatography allows differentiating between virus proteins arranged in whole virus particles and host cell proteins, as well as virus proteins from virus particle debris. Representative size exclusion chromatograms of the virus sample and anion exchange elute pools are shown in Fig. 4A and B. Elution buffers containing citrate, arginine, or lysine were excluded from the evaluation. The background signal of these salts interferes with the protein peaks. Protein removal of 1 M NaCl is negligible for both resins. Gradient experiments are required for further evaluation of the selectivity provided by sodium chloride. However, other electrolytes applied in this study achieve protein removal. GigaCap Q-650M removes one third of the feedstream proteins if sodium phosphate is applied for sorption and desorption. NH2-750F achieves removal of 60% of the initial protein content. This may be due to the salt tolerant binding characteristics of NH2-750F. Retention of anionic proteins is greater and proteins are not eluted from the resin. NH2-750F binds proteins at their isoelectric point. This allows for a greater efficiency in protein binding. Protein removal of sodium chloride elution and sodium phosphate elution should be compared with caution. The limiting solubility of sodium phosphate in aqueous solution implies to use lower concentrations of phosphate, compared to sodium chloride. Given a stoichiometric exchange of ions is required for protein elution with no preferential effects present, higher salt concentrations lead to lower protein

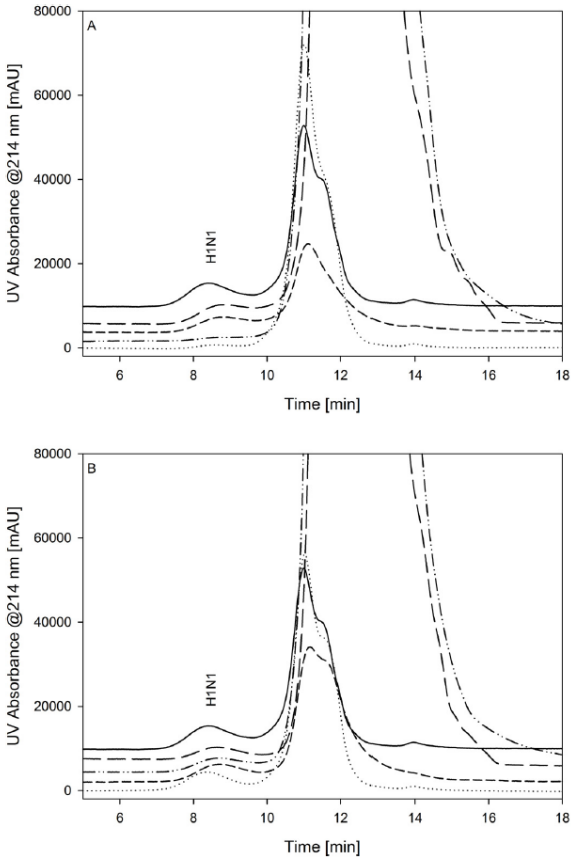

Fig. 4. Size exclusion chromatograms of the virus samples eluted from TOYOPEARL NH2-750F (A) and TOYOPEARL GigaCap Q-650M (B). The Anion exchange chromatography feedstream (continuous line) is shown as a reference. H1N1 recovery from NH2-750F is low if the sample is loaded in Tris/HCl and eluted with sodium phosphate (dotted line) or sodium citrate (dot-dashed line). H1N1 Recovery from NH2-750F increases if the sample is loaded in sodium phosphate and eluted in sodium phosphate (short dashes) or sodium citrate (long dashes). Recovery from GigaCap Q-650M is not affected by different load buffers.

removal. However, resin specific effects of sodium phosphate can still be observed.

The buffer applied during adsorption of the virus particles seems to play a role, as well. Virus samples eluted from NH2-750F contain comparatively more protein impurities, if Tris/HCl was used during adsorption. A reduction by 60% is achieved if sodium phosphate is applied for sample adsorption and desorption. Adsorption in Tris/HCl and desorption in sodium phosphate does not reduce the proteins determined by analytical size exclusion chromatography (Fig. 4). Considering the lower virus recoveries achieved after sorption in Tris/HCl, this may indicate virus particle destruction. Greater total protein contents in the anion exchange elute pools could be due to virus particle debris. Greater protein capacities of the resins in presence of Tris/HCl buffer during adsorption (Fig. 2) may contribute to lower protein purities, as well.

4. Conclusions

Capturing of H1N1 by anion exchange chromatography seems to be a promising approach to increase efficiency and flexibility of influenza purification. This is especially important for the production of vaccines against pandemic viruses, such as the herein investigated H1N1. A salt tolerant polyamine-type and a grafted Q-type anion exchanger were tested and both resins have their benefits and drawbacks. The Q-type resin allows for high DNA clearance rates. Remaining DNA levels are close to the limit of detection of the applied fluorescence assay without DNAse treatment. Comparatively higher recoveries are obtained with TOYOPEARL GigaCap Q-650M. The salt tolerant polyamine type resin provides mostly lower DNA removal, up to 6.4-fold higher capacities and higher protein clearance. Pseudo-affinity interactions of the polyamine ligand to the M2 influenza protein may contribute to this capacity increase. Virus recovery from the polyamine type resin requires polyprotic buffers, such as sodium citrate and sodium phosphate. Low concentrations of phosphate seem to support stability of the virus particles during chromatography. Inactivation of the influenza particles is attributed to hydrophobic poly-cations. This effect is inhibited in presence of sodium phosphate buffer. Based on these findings, gradient chromatography will be developed as a next step to further exploit anion exchange chromatography for influenza capturing. The presented results were obtained with an industrially relevant virus strain, which is part of a pandemic H1N1 vaccine.

Acknowledgments

This work was supported by funding of the German Federal Ministry of Education and Research, Grant 0315640D, and is part of the research project “Optimization of an industrial process for the production of cell-culture-based seasonal and pandemic influenza vaccines”.

References

[1] A. Doroshenko, S.A. Halperin, Trivalent MDCK cell culture-derived influenza vaccine optaflu (Novartis Vaccines), Expert Rev. Vaccines 8 (2009) 679–688, http://dx.doi.org/10.1586/erv.09.31.
[2] B. Kalbfuss, M. Wolff, R. Morenweiser, U. Reichl, Purification of cell culture-derived human influenza A virus by size-exclusion and anion-exchange chromatography, Biotechnol. Bioeng. 96 (2007) 932–944, http://dx.doi.org/10.1002/bit.
[3] T. Weigel, T. Solomaier, A. Peuker, T. Pathapati, M.W. Wolff, U. Reichl, A flow-through chromatography process for influenza A and B virus purification, J. Virol. Methods 207 (2014) 45–53, http://dx.doi.org/10.1016/j.jviromet.2014.06.019.
[4] G.L. Miller, Influence of pH and of certain other conditons on the stability of the infectivity and red cell agglutinating activity fo influenza virus, J. Exp. Med. 80 (1944) 507–520.
[5] H.-J. Choi, C.F. Ebersbacher, M.-C. Kim, S.-M. Kang, C.D. Montemagno, A mechanistic study on the destabilization of whole inactivated influenza virus vaccine in gastric environment, PLoS One 8 (2013) e66316, http://dx.doi.org/10.1371/journal.pone.0066316.
[6] E.I. Trilisky, M.A. Lenhoff, Sorption processes in ion-exchange chromatography of viruses, J. Chromatogr. A 1142 (2007) 2–12, http://dx.doi.org/10.1016/j.chroma.2006.12.094.
[7] S.E. Mylon, C.I. Rinciog, N. Schmidt, L. Gutierrez, G.C.L. Wong, T.H. Nguyen, Influence of salts and natural organic matter on the stability of bacteriophage MS2, Langmuir 26 (2010) 1035–1042, http://dx.doi.org/10.1021/la902290t.
[8] G. Bitton, Adsorption of viruses onto surfaces in soil and water, Water Res. 9 (1975) 473–484, http://dx.doi.org/10.1016/0043-1354(75)90071-8.
[9] G.F. Carlson, F.E. Woodard, D.F. Wentworth, O.J. Sproul, Virus inactivation on clay particles in natural waters, J. Water Pollut. Control Fed. 40 (1968) R89–R106, accessed 16.10.15 http://www.ncbi.nlm.nih.gov/pubmed/4297609.
[10] W.A. Drewry, R. Eliassen, Virus movement in groundwater on JSTOR, Water Pollut. Control Fed. 40 (1968) R257–R271, accessed 16.10.15 http://www.jstor.org/stable/25036093?seq=1#page_scan_tab_contents.
[11] C.P. Gerba, J.L. Melnick, C. Wallis, Fate of wastewater bacteria and viruses in soil, J. Irrig. Drain. Div. 101 (2016) 157–174, accessed 16.10.15 http://cedb.asce.org/cgi/WWWdisplay.cgi?6199.
[12] D.H. Taylor, R.S. Moore, L.S. Sturman, Influence of pH and electrolyte composition on adsorption of poliovirus by soils and minerals, Appl. Environ. Microbiol. 42 (1981) 976–984.
[13] J.P. Murray, Physical Chemistry of Virus Adsorption and Degradation on Inorganic Surfaces: Its Relation to Wastewater Treatment| US EPA report EPA-600/2-80-136, 1980, accessed 16.10.15 http://yosemite.epa.gov/water/

owrcCatalog.nsf/065ca07e299b464685256ce50075c11a/3d5894335c5acb2385256ffd00774438!OpenDocument.
[14] James P. Murray, G.A. Parks, Poliovirus Adsorption on Oxide Surfaces Correspondence with the DLVO-Lifshitz Theory of Colloid Stability, American Chemical Society, Washington D.C, 1980, http://dx.doi.org/10.1021/ba-1980-0189.
[15] G.K. Sofer, L.-E. Nyström, Process Chromatography: A Guide to Validation, Academic Press, London, 1991.
[16] D. Nau, The role of hydrophobic interaction chromatography in antibody purification-optimization of mobile phase conditions, Biochromatography 5 (1990) 62–73.
[17] D. Nau, in: B. Swaminathan, G. Prakash (Eds.), Nucleic Acid Monoclon. Antib. Probes—Appl. Diagnostic Microbiol., Marcel Dekker Inc., New York, 1982, p. 383.
[18] M. Belew, Y. Zhou, S. Wang, L.E. Nyström, J.C. Janson, Purification of recombinant human granulocyte-macrophage colony-stimulating factor from the inclusion bodies produced by transformed *Escherichia coli* cells, J. Chromatogr. A 679 (1994) 67–83, http://dx.doi.org/10.1016/0021-9673(94)80312-9.
[19] R.F. Steiner, Reversible association processes of globular proteins. II. Electrostatic complexes of plasma albumin and lysozyme, Arch. Biochem. Biophys. 47 (1953) 56–75, http://dx.doi.org/10.1016/0003-9861(53)90437-8.
[20] R.F. Steiner, Reversible association processes of globular proteins. IV. Fluorescence methods in studying protein interactions, Arch. Biochem. Biophys. 46 (1953) 291–311, http://dx.doi.org/10.1016/0003-9861(53)90202-1.
[21] P. Gagnon, Special Weapons and Tactics for removal of Product-Bound DNA, in: BioEast, Washington D.C., 1996. p. slide presentation.
[22] P. Gagnon, Hydrophobic interaction chromatography, in: Purif Tools Monoclon. Antibodies, 1st ed., Validated Biosystems Inc., Tucson, 1996, pp. 103–126.
[23] B.B. Hsu, S. Yinn Wong, P.T. Hammond, J. Chen, A.M. Klibanov, Mechanism of inactivation of influenza viruses by immobilized hydrophobic polycations, Proc. Natl. Acad. Sci. U. S. A. 108 (2011) 61–66, http://dx.doi.org/10.1073/pnas.1017012108.
[24] W.P. Burmeister, S. Cusack, R.W. Ruigrok, Calcium is needed for the thermostability of influenza B virus neuraminidase, J. Gen. Virol. 75 (Pt. 2) (1994) 381–388, accessed 3.09.15 http://www.ncbi.nlm.nih.gov/pubmed/8113759.
[25] T. Arakawa, J.S. Philo, K. Tsumoto, R. Yumioka, D. Ejima, Elution of antibodies from a Protein-A column by aqueous arginine solutions, Protein Expr. Purif. 36 (2004) 244–248, http://dx.doi.org/10.1016/j.pep.2004.04.009.
[26] T. Arakawa, K. Tsumoto, K. Nagase, D. Ejima, The effects of arginine on protein binding and elution in hydrophobic interaction and ion-exchange chromatography, Protein Expr. Purif. 54 (2007) 110–116, http://dx.doi.org/10.1016/j.pep.2007.02.010.
[27] R. Yumioka, H. Sato, H. Tomizawa, Y. Yamasaki, D. Ejima, Mobile phase containing arginine provides more reliable SEC condition for aggregation analysis, J. Pharm. Sci. 99 (2010) 618–620, http://dx.doi.org/10.1002/jps.21857.
[28] W. Zhou, J. Bi, J.-C. Janson, A. Dong, Y. Li, Y. Zhang, et al., Ion-exchange chromatography of hepatitis B virus surface antigen from a recombinant Chinese hamster ovary cell line, J. Chromatogr. A 1095 (2005) 119–125, http://dx.doi.org/10.1016/j.chroma.2005.08.006.
[29] B. Hundt, N. Mölle, S. Stefaniak, R. Dürrwald, J. Weyand, Large pilot scale cultivation process study of adherent MDBK cells for porcine Influenza A virus propagation using a novel disposable stirred-tank bioreactor, BMC Proc. 5 (2011) P128, http://dx.doi.org/10.1186/1753-6561-5-s8-p128.
[30] G.L. Miller, Electrophoretic studies on PR8 influenza virus, J. Exp. Med. 80 (1944) 549–559, accessed 12.01.16 http://jem.rupress.org/cgi/content/long/80/6/549.
[31] I.N. Zhilinskaya, L.H. el-Saed, N.A. Ivanova, D.E. Golubev, N.N. Sokolov, Isolation of A2-Singapore-57 influenza virus V and S antigens by isoelectric focusing, Acta Virol. 16 (1972) 436–439, accessed 12.01.16 http://www.ncbi.nlm.nih.gov/pubmed/4404653.
[32] J.Y. Jun, H.H. Nguyen, S.Y.R. Paik, H.S. Chun, B.C. Kang, S. Ko, Preparation of size-controlled bovine serum albumin (BSA) nanoparticles by a modified desolvation method, Food Chem. 127 (2011) 1892–1898, http://dx.doi.org/10.1016/j.foodchem.2011.02.040.
[33] S. Salgin, U. Salgin, S. Bahadir, Zeta potentials and isoelectric points of biomolecules: the effects of ion types and ionic strengths, Int. J. Electrochem. Sci. 7 (2012) 12404–12414.
[34] M. Yu, S. Zhang, Y. Zhang, Y. Yang, G. Ma, Z. Su, Microcalorimetric study of adsorption and disassembling of virus-like particles on anion exchange chromatography media, J. Chromatogr. A 1388 (2015) 195–206, http://dx.doi.org/10.1016/j.chroma.2015.02.048.
[35] L. Opitz, S. Lehmann, A. Zimmermann, U. Reichl, M.W. Wolff, Impact of adsorbents selection on capture efficiency of cell culture derived human influenza viruses, J. Biotechnol. 131 (2007) 309–317, http://dx.doi.org/10.1016/j.jbiotec.2007.07.723.
[36] T.I. Lin, H. Heider, C. Schroeder, Different modes of inhibition by adamantane amine derivatives and natural polyamines of the functionally reconstituted influenza virus M2 proton channel protein, J. Gen. Virol. 78 (Pt. 4) (1997) 767–774, http://dx.doi.org/10.1099/0022-1317-78-4-767.
[37] W.B. Fischer, M.S.P. Sansom, Viral ion channels: structure and function, Biochim. Biophys. Acta—Biomembr. 1561 (2002) 27–45, http://dx.doi.org/10.1016/S0304-4157(01)00009-0.
[38] A.G. Boukrinskaia, A.V. Serbin, O.P. Bogdan, L.L. Stotskaya, I.V. Alymova, Y.N. Klimochkin, Polymeric adamantane analogues US5880154A, 1999, accessed 31.03.16 http://www.google.com/patents/US5880154?hl=de.
[39] T.M. Pabst, G. Carta, pH transitions in cation exchange chromatographic columns containing weak acid groups, J. Chromatogr. A 1142 (2007) 19–31, http://dx.doi.org/10.1016/j.chroma.2006.08.066.
[40] A. Jungbauer, R. Hahn, Methods in enzymology—ion exchange chromatography, in: R.R. Burgess, M.P. Deutscher (Eds.), Guid. to Protein Purif., 2nd ed., Academic Press, San Diego, 2009, pp. 349–370, accessed 30.03.16 https://books.google.com/books?id=f6Lp4yna4hoC&pgis=1.
[41] C.A. Knight, The stability of influenza virus in the presence of salts, J. Exp. Med. 79 (1944) 285–290, http://dx.doi.org/10.1084/jem.79.3.285, accessed 30.03.16 https://books.google.com/books?id=f6Lp4yna4hoC&pgis=1.
[42] D.A. Yannarell, K.M. Goldberg, R.N. Hjorth, Stabilizing cold-adapted influenza virus vaccine under various storage conditions, J. Virol. Methods 102 (2002) 15–25, accessed 13.01.16 http://www.ncbi.nlm.nih.gov/pubmed/11879689.
[43] C. Pfeiffer, C. Rehbock, D. Hu, C. Carrillo-carrion, D.J. De Aberasturi, V. Merk, et al., Interaction of colloidal nanoparticles with their local environment: the (ionic) nanoenvironment around nanoparticles is different from bulk and determines the physico-chemical properties of the nanoparticles, J. R. Soc. Interfaces 11 (2014) 1–13, http://dx.doi.org/10.1098/rsif.2013.0931.
[44] A. Manzur, D. Spelzini, B. Farruggia, D. Romanini, G. Picó, Polyethyleneimine phosphate and citrate systems act like pseudo polyampholytes as a starting method to isolate pepsin, J. Chromatogr. B Anal. Technol. Biomed. Life Sci. 860 (2007) 63–68, http://dx.doi.org/10.1016/j.jchromb.2007.10.013.
[45] Y. Peng, Y. Hou, F. Zhang, G. Shen, B. Yang, A hyperbranched polyethylenimine functionalized stationary phase for hydrophilic interaction liquid chromatography, Anal. Bioanal. Chem. (2016), http://dx.doi.org/10.1007/s00216-016-9446-7.
[46] K.D. Collins, Ions from the Hofmeister series and osmolytes: effects on proteins in solution and in the crystallization process, Methods 34 (2004) 300–311, http://dx.doi.org/10.1016/j.ymeth.2004.03.021.
[47] H. Hamazaki, Calcium-mediated hemagglutination by serum amyloid P component and the inhibition by specific glycosaminoglycans, Biochem. Biophys. Res. Commun. 150 (1988) 212–218, accessed 12.01.16 http://www.sciencedirect.com/science/article/pii/0006291x88905074.
[48] J.D. Seader, E.J. Henley, K.D. Roper, Separation Process Principles—Chemical and Biochemical Operations, John Wiley & Sons, Hoboken, 2011.
[49] S. Grambas, M.S. Bennett, A.J. Hay, Influence of amantadine resistance mutations on the pH regulatory function of the M2 protein of influenza A viruses, Virology 191 (1992) 541–549, http://dx.doi.org/10.1016/0042-6822(92)90229-I.
[50] Improved Column Chromatography Performance Using Arginine | American Laboratory, (n.d.), 2016, accessed 19.01.16 http://www.americanlaboratory.com/913-Technical-Articles/18995-Improved-Column-Chromatography-Performance-Using-Arginine/.
[51] L. Opitz, J. Salaklang, H. Büttner, U. Reichl, M.W. Wolff, Lectin-affinity chromatography for downstream processing of MDCK cell culture derived human influenza A viruses, Vaccine 25 (2007) 939–947, http://dx.doi.org/10.1016/j.vaccine.2006.08.043.

9.7. Size distribution analysis of influenza virus particles using size exclusion chromatography

Autoren: Judith Vajda[1], Dennis Weber[2], Dominik Brekel[2], Boris Hundt[3], Egbert Müller[1]

Institutionen:
[1]Tosoh Bioscience GmbH, Im Leuschnerpark 4, 64347 Griesheim, Deutschland
[2]Karlsruher Institut für Technologie, Institut für Bio- und Lebensmitteltechnik, Bereich IV: Molekulare Aufarbeitung von Bioprodukten, Engler-Bunte Ring 3, 76131 Karlsruhe, Deutschland
[3]IDT Biologika GmbH, Am Pharmapark, 06861 Dessau-Roßlau, Deutschland

Eingereicht und zur externen Prüfung angenommen beim Journal of Chromatography A des Elsevier Verlags.

keywords: analytical size exclusion chromatography, pandemic H1N1, hemagglutination assay, fragmentation, process analytical technique

SIZE DISTRIBUTION ANALYSIS OF INFLUENZA VIRUS PARTICLES USING SIZE EXCLUSION CHROMATOGRAPHY

Judith Vajda[1], Dennis Weber[2], Dominik Brekel[2], Boris Hundt[3], Egbert Müller[1]

[1]Tosoh Bioscience GmbH, Im Leuschnerpark 4, 64347 Griesheim, Germany

[2]Karlsruher Institut für Technologie, Institut für Bio- und Lebensmitteltechnik, Engler-Bunte Ring 3, 76131 Karlsruhe, Germany

[3]IDT Biologika GmbH, Am Pharmapark, 06861 Dessau-Roßlau, Germany

ABSTRACT

Size exclusion chromatography is a standard method in quality control of biopharmaceutical proteins. In contrast, vaccine analysis is often based on activity assays. The hemagglutination assay is a widely accepted influenza quantification method in research, development, and for the release of animal vaccines. However, it provides no insight in the size distribution of virus particles. Capabilities of size exclusion chromatography to complement the hemagglutination assay are investigated. Quantitative elution of the virus preparations from size exclusion chromatography is confirmed by balancing the corresponding hemagglutination activity. The universal applicability is demonstrated with three different influenza virus samples, including an industrially produced, pandemic vaccine strain. The size distribution of the pandemic H1N1v 5258, H1N1 PR/8/34, and H3N2 Aichi/2/68 preparations spreads across a wide elution range. Hemagglutination activity was found in all fractions from size exclusion chromatography. Thus, virus particle debris seems to induce hemagglutination. Fragments generated by Triton™ X-100 treatment or heat incubation do not generally increase hemagglutination activity. In a semi-preparative approach, size exclusion chromatography can be coupled with activity assays. Components of the sample matrix that are potentially interfering with hemagglutination are exchanged during size exclusion chromatography. The presented method seems especially valuable if qualitative and quantitative analysis of influenza preparations is to be accomplished in different buffers and electrolyte solutions.

Keywords: analytical size exclusion chromatography; pandemic H1N1; hemagglutination assay; fragmentation; process analytical techniques

INTRODUCTION

Vaccination is an effective cure against the pandemic outbreak of influenza. Various influenza vaccines from different manufacturers are based on inactivated whole virus particles. Influenza virus particles have a size of 80-120 nm. Hemagglutinin (HA) and neuraminidase are the two most abundant proteins on the surface of Influenza A virus particles. Currently, 17 different HA and 10 different neuraminidases have been characterized and give name to the different influenza A subtypes [1]. The amount of HA in an influenza vaccine is a crucial parameter for release of the biopharmaceutical. Guidelines by the European Pharmacopoeia require 15 μg of HA antigen for each of the present virus strains in a trivalent human vaccine [2]. HA can be quantified based on hemagglutination of erythrocytes [3]. Dilutions of the investigated virus sample are incubated with a chicken erythrocyte preparation. In case sufficient virus particles are present to induce hemagglutination, erythrocytes will float carpet-like in solution. Virus particle concentrations are estimated assuming hemagglutination requires one virus particle per erythrocyte. This assay dates back to the 1940s and is currently still accepted in research, development, quality control testing and the release of animal vaccines. Drawbacks of this method are the lack of standardization, its discrete format, deviations due to erythrocyte aging [4], secondary interactions of pH, buffer ions [5] and other compounds in complex virus samples. Virus inactivation agents have been shown to specifically affect HA activity of different strains [6][7]. Jonges et al. evaluated the use of different conditions and agents for viral inactivation. Heat and β-propiolactone lead to a decreased HA-titer. Comparatively smaller losses of the HA-titer can be observed after formalin treatment. Triton™ X-100 concentrations exceeding 0.2 % lead to a complete loss of hemagglutination activity of H3N2. However, the determined HA-titer of H7N3 increases above the initial value after treatment with 1 % Triton™ X-100 [7]. The influence on HA activity extends to inorganic ions typically used during downstream processing. Calcium ions have been shown to mediate hemagglutination in presence of amyloid proteins [8]. During the last years, enhanced process understanding and control has been pushed by the authorities [9]. This can be accomplished through process analytical technologies that are applicable to a wide design space of conditions potentially being used during the manufacturing process. The single radial immune diffusion (SRID) assay represents an alternative assay relying on antigen binding and is the gold standard for release of human vaccines [10]. Both methods are generally recognized and are being applied in research and development of purification processes. Kalbfuss et al. use the HA assay for mass-balancing of filtration. They conclude that roughly 40 % of the HA activity is deposited on or inside the membrane, since it could neither be recovered in the permeate fraction nor in the retentate. They further suggest that this may represent cell debris [11]. Changes in HA activity due to fragmentation of initially spherical virus particles and aggregation might contribute as well. Thus, comparing the efficiency of different purification schemes based on HA activity may lead to an incomplete picture. This is in particular important when comparing data obtained with different virus feedstreams. Non-closing mass balances and reproducibility issues are addressed by another manuscript by Kalbfuss et al., where they suggest the use of a continuous HA assay format [12]. Undoubtedly, this assay format leads to a general improvement of the assay. However, matrix interference remains a problem. Consequently, buffer exchange steps might be necessary to quantify samples from process development. Public institutions, such as the European Medicine Agency (EMA), encourage research in the field

to complement the SRID assay [13]. Investigation of size, content, and immunogenicity of aggregates in the drug product or substance is recommended [13]. Numerous other techniques to either quantify influenza virus particles or the activity have been published. These include, but are not limited to: electron microscopy [14][15], surface plasmon resonance [16][17], enzyme linked immunosorbent assay (ELISA) [18], and reversed phase high pressure liquid chromatography [10]. Electron microcopy and surface plasmon resonance are comparatively expensive. Surface plasmon resonance further suffers from the same constraint as the SRID, since it requires an appropriate set of antibodies for new influenza strains. This holds true for most ELISAs. Reversed phase liquid chromatography is sample destructive and strong interference with β-propiolactone [4] limits its versatility. Except for electron microscopy, none of the previously listed methods allows to investigate the aggregate or fragment content of virus preparations. Alternative techniques to investigate the size distribution of virus samples are dynamic light scattering or differential centrifugal sedimentation [19]. These methods do not allow sampling the different size fractions of the virus preparations for further activity analysis. Analytical size exclusion chromatography (SEC) is a mild technique that has been used for decades to analyze the aggregate and fragment content of therapeutic proteins [20]. Recently, several approaches to apply SEC to the aggregate analysis of virus and virus like particle samples have been published [21][22][23][24]. Earlier approaches in SEC of viruses did not pay much attention to this aspect [25]. Complex samples can be fractionated preparatively and subsequently analyzed in an activity assay. Considering the great number of parameters interfering with the HA assay, SEC is two in one: sample preparation step and analysis. Due to their size, analysis of influenza virus particles requires pore sizes exceeding 100 nm. Herein, we present a complimentary analytical SEC method. The current study includes 3 different influenza A virus strains. The pandemic H1N1 vaccine strain 5258 is industrially produced in mammalian cells. Influenza A H1N1 PR/8/34 and H3N2 Aichi/2/68 originate from embryonated chicken cells.

MATERIAL AND METHODS

INFLUENZA SAMPLES

The pandemic H1N1 vaccine strain (5258) was produced in adherent Madin Darby Bovine Kidney (MDBK) cells at IDT Biologika GmbH (Dessau-Roßlau, Germany). A reference process has been published by Hundt et. al [26]. The H1N1v 5258 virus sample was inactivated by β-propiolactone treatment. The feedstream was volumetrically concentrated by a factor of 20. Feedstream for ion exchange chromatography was dialyzed into 50 mM Tris/HCl, pH 7.0. Samples for analytical experiments were pre-purified by preparative SEC. TOYOPEARL HW-65F (Tosoh Bioscience GmbH, Griesheim, Germany) was packed to a bed height of 22 cm. 100 mM sodium phosphate, pH 7.0 containing 200 mM sodium chloride was used as mobile phase at a flow rate of 150 cm/h. All chemicals were purchased from Sigma Aldrich/Merck KGaA (Darmstadt, Germany), unless otherwise stated.

Influenza A H1N1 PR/8/34 and H3N2 Aichi/2/68 were purchased from Charles River Avian Vaccine Services (North Franklin, USA). Both viruses were produced in embryonated

chicken eggs and inactivated by formalin treatment. The virus samples were purified and concentrated to 2 mg/mL by density gradient centrifugation.

MERCURY POROSIMETRY

Mercury porosity of the TSKgel G6000PWxl stationary phase was accomplished with a PoreMaster 60-GT (Quantachrome, Odelzhausen, Germany). Porosimetry experiments were conducted according to the instructions of the instrument supplier. The resin was freeze-dryed with a Zirbus VaCo 2 (Bad Grund, Germany) lyophilizer prior to the porosimetry experiments.

ANALYTICAL SIZE EXCLUSION CHROMATOGRAPHY

TSKgel G6000PWxl (7.8 mm ID x 30 cm L) columns were used for analytical SEC (Tosoh Bioscience GmbH). Low densities of residual anionic groups on the surface of the 13 μm polymethacrylate beads prevent from ionic interactions with anions. The UV signals were traced at 214 nm or 215 nm. The applied flow rate was 1.0 mL/min. 100 μL of the samples were injected in analytical experiments. The column was overloaded in semi-preparative SEC experiments. 1 mL of the virus samples was injected. The pre-purified and concentrated H1N1 PR/8/32 and H3N2 Aichi/2/68 samples were 3-fold diluted prior to injection. 1 mL fractions were collected. All samples were analyzed in duplets or triplets.

ANION EXCHANGE CHROMATOGRAPHY

TOYOPEARL GigaCap Q-650M (Tosoh Bioscience GmbH) was used for anion exchange chromatography. The grafted Q-type resin is based on a polymethacrylate backbone. The base beads have a pore size of 100 nm and a mean particle size of 65 μm. Samples were loaded in 50 mM Tris/HCl, pH 7.0. The adsorption buffer was substituted with different electrolytes to recover the virus: 1 M sodium chloride, 1 M arginine, 1 M lysine, 0.5 M sodium phosphate, 0.5 M sodium citrate. 600 μL RoboColumns (Atoll, Weingarten, Germany) were used in a parallel chromatography approach with a Tecan Freedom Evo 150 equipped with a ChromStation (Tecan Group Ltd., Männerdorf, Switzerland).

HEMAGGLUTINATION ASSAY

The hemagglutination activity was determined using a Tecan Freedom Evo 150. Chicken erythrocyte preparations in Alsever solution were purchased from preclinics (Potsdam, Germany). 4 mL of the erythrocyte preparation were diluted with 40 mL phosphate buffered saline (PBS): 1.54 mM potassium dihydrogen phosphate, 8.10 mM disodium hydrogen phosphate, 2.68 mM potassium chloride and 137 mM sodium chloride, pH 7.5 at 25 °C. Pelleted erythrocytes were resuspended in 40 mL cold PBS. Erythrocyte concentration was determined with a Fuchs-Rosenthal cytometer and adjusted to 2 x 10^7 cells per mL. 100 μL of the H1N1 containing samples were transferred into every second row of the first column of U-bottom 96 well plates. A $1{:}2^{0.5}$ dilution of the samples was pipetted into the first well of the remaining rows. Serial 1:2 dilutions of all samples in phosphate buffered saline were completed. 100 μL of the erythrocyte solution were added

to all wells and plates were incubated for one hour at room temperature. Results were evaluated manually and by absorbance readings at 700 nm.

VIRUS PARTICLE FRAGMENTATION

Fragmentation of pre-purified H1N1v 5258 was accomplished through treatment with Triton™ X-100 or heat incubation according to the protocol from Jonges et al. [7]. 1 mL aliquots of the pre-purified virus sample were incubated for 1 h with 0.0, 0.2, 0.5, and 1.0 % (v/v) Triton™ X-100 at room temperature. Samples were dialyzed into 100 mM sodium phosphate buffer, pH 7.0 containing 200 mM sodium chloride at 4 °C to remove the detergent. Alternatively, 1 mL samples were incubated for 30 min at 20, 40, 50, 60, and 70 °C. Experiments were performed at least in duplets.

RESULTS AND DISCUSSION

PORE SIZE MEASUREMENTS

The pore size of TSKgel G6000PWxl was determined using mercury porosimetry. The resulting pore size distribution ranges from 100 nm to 1000 nm (Fig. 1). The mean pore size is roughly 250 nm. The results suggest that virus particle aggregates are not completely excluded from the pore volume of this column. Virus particle monomers should have access to a considerable ratio of the pore volume. The column is used for the subsequent analytical and semi-preparative SEC experiments.

ANION EXCHANGE CHROMATOGRAPHY

The impact of different elution buffers on virus recovery from ion exchange chromatography is shown in Figure 2. Recoveries determined by HA are greater than recoveries determined by analytical SEC. Recoveries of samples eluted with sodium chloride, lysine, and arginine deviate by more than 100 % from the recoveries determined by analytical SEC. HA activity of the elution pools recovered with sodium chloride and lysine is roughly doubled compared to the initial HA activity. The variation among the recoveries determined by HA using different elution buffers is comparatively great. Recoveries determined by analytical SEC in different buffers are roughly 50 %. There is a general trend of higher recoveries in sodium chloride, arginine, and lysine, compared to sodium phosphate and sodium citrate. However, the magnitude of this trend is greater in case of HA activity. This may be attributed to buffer exchange during the analysis and a comparatively lower susceptibility to interference of the applied buffer ions. Nevertheless, interference of the herein applied ions with the HA assay may not account to full extent for the observed deviations. Previously published data from our group [27] indicates that the impact of sodium chloride, sodium phosphate, lysine, and arginine on the HA activity is comparatively low. The employed robotic system allows reducing the standard deviation to a reasonable level. Recoveries well exceeding 100 % suggest an increase of HA activity during chromatography. This may be due to virus particle fragmentation. Fragmentation of virus particles leads to a molar increase of the hemagglutination inducing molecules. Such

fragments are separated from the whole virus particles in SEC and are excluded from quantification. Hemagglutination activity of different size fractions and preparations of influenza virus particles is evaluated in the following paragraphs.

HEMAGGLUTININ ACTIVITY OF SIZE EXCLUSION CHROMATOGRAPHY FRACTIONS

Semi-preparative SEC chromatograms of H1N1v 5258, H1N1 PR/8/34, and H3N2 Aichi/2/68 on TSKgel G6000PWxl are shown in Figure 3. The HA activity of the collected fractions is plotted on the right y-axis. The higher system dead volume of the preparative system and the great injection volume have a negative impact on chromatographic performance. Fractions corresponding to the peak eluting between 8 and 10 minutes have the highest HA activity. Fractions eluting after the main virus peak contain HA activity, as well. Roughly 50 % of the total HA activity elutes in the peaks of comparatively lower molecular weight. Hemagglutination is considered a cross-linking reaction. It appears reasonable that the hemagglutination inducing molecules must not have a minimum size, but at least two functional sites. Thus, virus particle debris most likely mediates hemagglutination. This means virus particle fragmentation can lead to higher HA activity, compared to whole virus particles, since the total number of HA mediating molecules increases. This has important implications on the use of HA activity as a measure for virus particle quantification. Virus particle quantification based on activity measurements can lead to significantly overestimated virus particle contents. On the other hand, it explains the appearance of virus recoveries in anion exchange chromatography greater than 100 %. Different degrees of virus fragmentation may also contribute to the high standard deviation of the HA assay.

Summed HA activities of all fractions are in good agreement with the initial HA activity of the sample prior to SEC. 3.9 log of the H1N1v 5852 sample were loaded in Figure 3 A. The HA activity of all fractions normalized against the volume is 4.1 log HAU. The initially injected HA activity of H1N1 PR/8/34 is 5.4 log HAU (Fig. 3 B). The recovered HA activity of this sample sums up to 5.2 log HAU. A comparatively greater, but still acceptable loss appears for the fractions of H3N2 Aichi/2/68 (Fig. 3 C). 4.8 log HAU of the loaded 5.4 log HAU can be recovered from TSKgel G6000PWxl. Considering SEC is a diluting method, HA activity of the fractions framing the virus particle peaks might be lower than the limit of detection of the HA assay. Further, the HA assay uses a discrete format. Precision of the assay could be enhanced by a greater number of erythrocyte dilutions. Thus, the applied buffer conditions can be considered suitable to quantitatively recover influenza virus samples.

HEMAGGLUTINATION OF DIFFERENT VIRUS PARTICLE FRAGMENTS

The previously reported results suggest that virus fragments increase the total HA activity of a sample. Different virus inactivation methods lead to decreasing or increasing HA activity. Jonges et al. evaluated the impact of different inactivation agents on hemagglutination activity [7]. The experiments revealed that HA activity of some influenza

strains increases after treatment with the membrane solubilizing detergent Triton™ X-100. In contrast, they found a decrease in HA activity in response to heat treatment. HA activity of H1N1v 5258 after heat incubation or Triton™ X-100 treatment is shown in Figure 4 A & B. Incubation at 50 °C or higher leads to a loss of HA activity. In contrast, HA activity is increasing after treatment with 0.2 and 0.5 % Triton™ X-100, but declines again after treatment with 1 % Triton™ X-100. Jonges et al. found no such decrease after passing a maximum HA activity. However, the general trend observed with H1N1v 5258 corresponds to their study. Analytical SEC chromatograms of the pre-purified and treated samples are shown in Figure 5 A & B. Increasing concentrations of the membrane solubilizing detergent increase the fragment peaks. Increasing the incubation temperature leads to an increase of the low molecular weight peak, as well. It appears fragments do not necessarily increase the HA activity of a sample. The activity of the HA protein seems unaffected by low concentrations of Triton™ X-100. The enveloping virus membrane is presumably affected, though. Higher concentrations of the detergent may lead to protein unfolding and subsequent activity loss. Inactivation by heat treatment seems to immediately affect functionality of HA.

CONCLUSIONS

TSKgel 6000PWxl has a mean pore size of 250 nm and allows discriminating different influenza A virus particle monomers and fragments. The pore size distribution suggests that potential virus particle aggregates can be separated, as well. Retention of particles from the H1N1 vaccine strain and the two strains propagated in embryonated chicken eggs are similar, which confirms the ubiquitousness of this approach. The recovered hemagglutination activity corresponds to the hemagglutination activity prior to SEC. More than 50 % of the HA activity of the samples is attributed to low molecular weight variants, which is most probably virus particle debris. SEC adds valuable data regarding the size distribution of influenza virus samples to the commonly used HA assay for the quantification of influenza viruses. Alternatively, the method could be combined with SRID. Future purification processes may benefit from a more detailed picture of the virus size distribution and how it is affected during the different steps of downstream processing.

ACKNOWLEDGEMENTS

This work was supported by funding of the German Federal Ministry of Education and Research, Grant 0315640D, and is part of the research project “Optimization of an industrial process for the production of cell-culture-based seasonal and pandemic influenza vaccines”.

REFERENCES

[1] C.M. Mair, K. Ludwig, A. Herrmann, C. Sieben, Biochim. Biophys. Acta 1838 (2014) 1153–68.

[2] L. Opitz, J. Salaklang, H. Büttner, U. Reichl, M.W. Wolff, Vaccine 25 (2007) 939–47.

[3] G.K. Hirst, J. Exp. Med. 75 (1942) 49–64.

[4] C.M. Thompson, E. Petiot, A. Lennaertz, O. Henry, A. a Kamen, Virol. J. 10 (2013) 141.

[5] G.L. Miller, J. Exp. Med. 80 (1944) 507–520.

[6] P. Bonnafous, M.C. Nicolaï, J.C. Taveau, M. Chevalier, F. Barrière, J. Medina, O. Le Bihan, O. Adam, F. Ronzon, O. Lambert, Biochim. Biophys. Acta - Biomembr. 1838 (2014) 355–363.

[7] M. Jonges, W.M. Liu, E. van der Vries, R. Jacobi, I. Pronk, C. Boog, M. Koopmans, A. Meijer, E. Soethout, J. Clin. Microbiol. 48 (2010) 928–40.

[8] H. Hamazaki, Biochem. Biophys. Res. Commun. 150 (1988) 212–218.

[9] J.O. Josefsberg, B. Buckland, Biotechnol. Bioeng. 109 (2012) 1443–1460.

[10] J. Transfiguracion, A.P. Manceur, E. Petiot, C.M. Thompson, A. a Kamen, Vaccine 33 (2015) 78–84.

[11] B. Kalbfuss, Y. Genzel, M. Wolff, A. Zimmermann, R. Morenweiser, U. Reichl, Biotechnol. Bioeng. 97 (2007) 73–85.

[12] B. Kalbfuss, A. Knöchlein, T. Kröber, U. Reichl, Biologicals 36 (2008) 145–161.

[13] European Medicines Agency, Guideline on Influenza Vaccines – Quality Module, 2014.

[14] T. Noda, Front. Microbiol. 2 (2011) 269.

[15] S.M. Dumitrescu, C.N. Zaharia, I. Samuel, F. Bârnaure, N. Manolescu, Virologie 32 289–92.

[16] D.K. Takemoto, J.J. Skehel, D.C. Wiley, Virology 217 (1996) 452–8.

[17] C.-F. Mandenius, R. Wang, A. Aldén, G. Bergström, S. Thébault, C. Lutsch, S. Ohlson, Anal. Chim. Acta 623 (2008) 66–75.

[18] S. Chun, C. Li, G. Van Domselaar, J. Wang, A. Farnsworth, X. Cui, H. Rode, T.D. Cyr, R. He, X. Li, Vaccine 26 (2008) 6068–76.

[19] M.M. Pieler, A.R. Fortuna, U. Reichl, M.W. Wolff, Chemie Ing. Tech. 86 (2014) 1588–1588.

[20] P. Hong, S. Koza, E.S.P. Bouvier, J. Liq. Chromatogr. Relat. Technol. 35 (2012) 2923–2950.

[21] Z. Wei, M. Mcevoy, V. Razinkov, A. Polozova, E. Li, J. Casas-Finet, G.I. Tous, P. Balu, A.A. Pan, H. Mehta, M.A. Schenerman, J. Virol. Methods 144 (2007) 122–132.

[22] Y. Yang, H. Li, Z. Li, Y. Zhang, S. Zhang, Y. Chen, M. Yu, G. Ma, Z. Su, Vaccine 33 (2015) 1143–50.

[23] M. Havlik, M. Marchetti-Deschmann, G. Friedbacher, P. Messner, W. Winkler, L. Perez-Burgos, C. Tauer, G. Allmaier, Analyst 139 (2014) 1412–9.

[24] C. Ladd Effio, S.A. Oelmeier, J. Hubbuch, Vaccine 34 (2016) 1259–67.

[25] M. Potschka, Macromolecules 24 (1991) 5023–5039.

[26] B. Hundt, N. Mölle, S. Stefaniak, R. Dürrwald, J. Weyand, BMC Proc. 5 (2011) P128.

[27] J. Vajda, D. Weber, S. Stefaniak, B. Hundt, T. Rathfelder, E. Müller, J. Chromatogr. A 1448 (2016) 73–80.

FIGURES

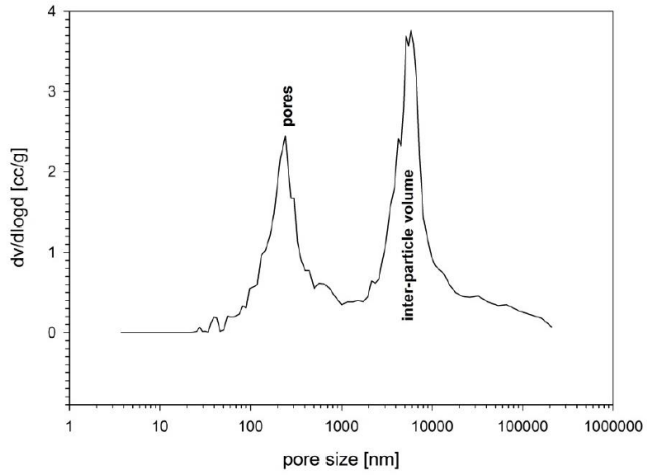

Figure 1: Mercury porosimetry data for the TSKgel G6000PWxl resin. The mean pore size of the resin is 250 nm. The pore size distribution ranges from 100 nm to 1000 nm. The peak ranging from 2 μm to 20 μm corresponds to the inter-particle volume.

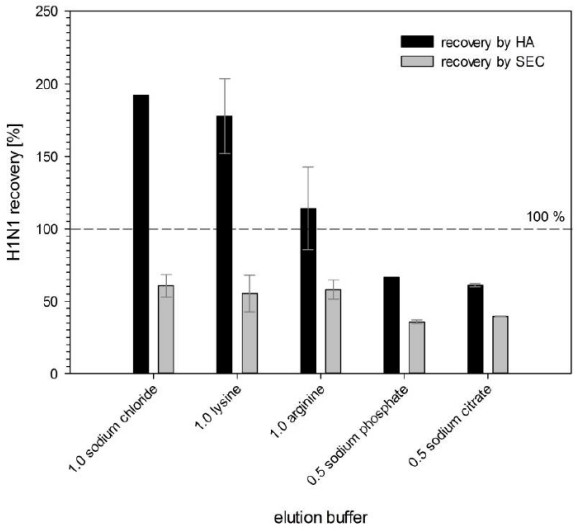

Figure 2: Recoveries of H1N1v 5258 from TOYOPEARL GigaCap Q-650M. The different elution buffers applied for virus recovery are indicated in the graph. Recoveries determined by HA (black bars) and analytical SEC (grey bars) deviate. Recoveries of H1N1 in sodium chloride and lysine approach 200 %.

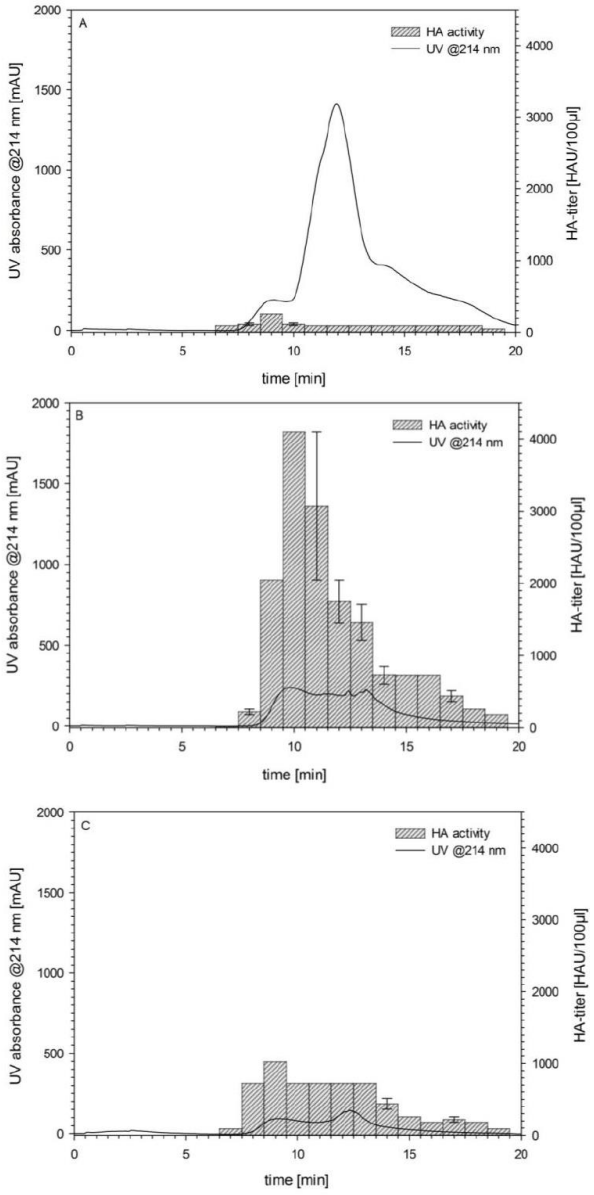

Figure 3: SEC chromatograms of H1N1v 5258 (A), H1N1 PR/8/34 (B), H3N2 Aichi/2/68 (C) on TSKgel G6000PWxl. The HA activity of the corresponding SEC fractions is plotted in the graph. HA activity is not restricted to the whole virus particle peak eluting between 8 and 10 min. Fractions from the lower molecular weight range have HA activity.

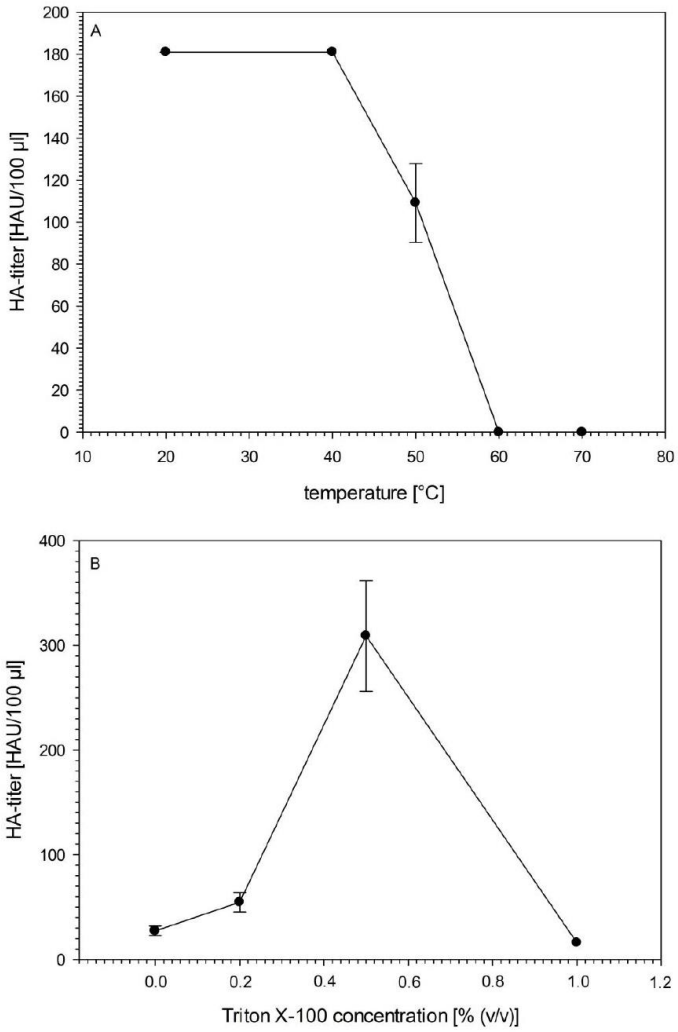

Figure 4: Hemagglutination activity of SEC pre-purified H1N1v 5258 in HAU per 100 μL after heat incubation (A) and Triton™ X-100 treatment (B). HA activity of the Triton reference sample is comparatively lower, due to an additional dialysis step. Temperatures and Triton concentrations are indicated in the corresponding graphs. HA activity decreases with increasing incubation temperature. 0.2 % and 0.5 % (v/v) Triton lead to an increase in HA activity. Treatment with 1 % Triton decreases HA activity.

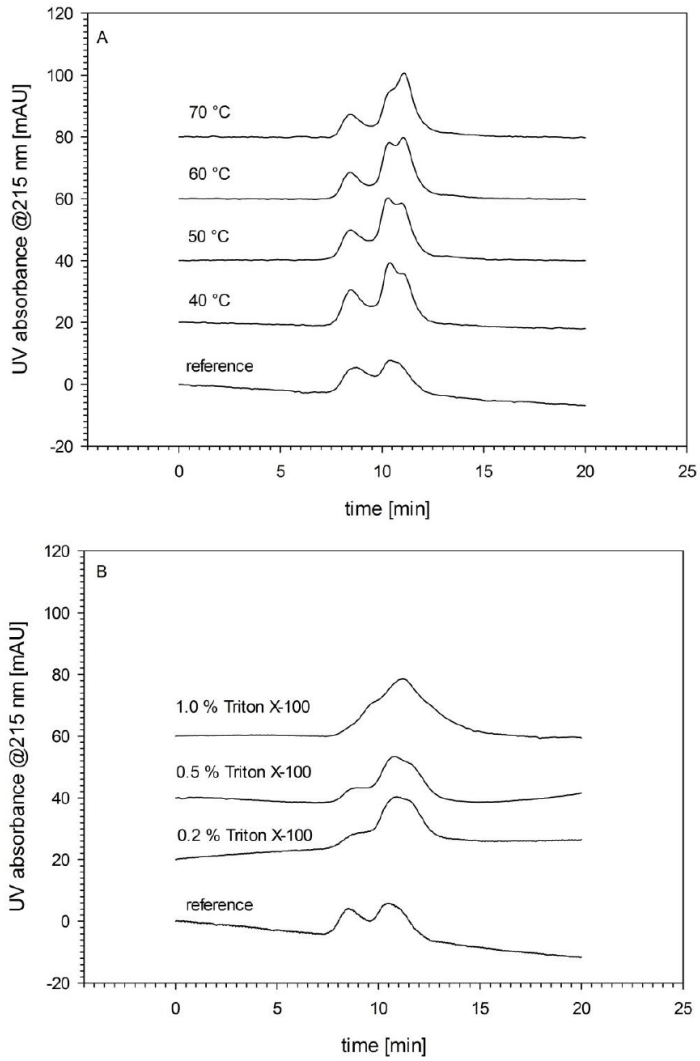

Figure 5: SEC chromatograms of H1N1v 5258 after heat incubation (A) or Triton™ X-100 treatment (B) on TSKgel G6000PWxl. Temperatures and detergent concentrations are indicated in the graph. The whole virus particle peak eluting at 9 min decreases with increasing temperature or detergent concentration. Fragment peaks increase.

10. Erklärung

Judith Vajda

Erklärung

Ich erkläre hiermit, dass ich meine Dissertation selbstständig und nur mit den angegebenen Hilfsmitteln verfasst habe.

Darmstadt, 01.07.2016 _____

Judith Vajda

Judith Vajda

Erklärung

Ich erkläre hiermit noch keinen Promotionsversuch unternommen zu haben.

Darmstadt, 01.07.2016 _____

Judith Vajda

11. Curriculum Vitae

Dipl. Biol. (t.o.) Judith Vajda

Wissenschaftlicher Werdegang

Seit März 2013	**Promotion** am Clemens-Schöpf-Institut für Organische Chemie und Biochemie der Technischen Universität Darmstadt und bei Tosoh Bioscience GmbH, Griesheim unter Betreuung von PD Dr. Egbert Müller und Prof. Dr. Harald Kolmar.
Seit April 2013	**Senior Application Specialist** bei Tosoh Bioscience GmbH Entwicklung von präparativen und analytischen Chromatographieverfahren für monoklonale Antikörper und strukturverwandte Moleküle. Prototyptestung in Kooperation mit R&D Aufarbeitung und Präsentation relevanter Daten im internationalen, wissenschaftlichen Umfeld und im Produkt Management Kontext. Betreuung und Anleitung diverser Bachelor- und Masterstudenten Technische Kundenbetreuung im pre-Sales und after-Sales Bereich (EMEA)
Oktober 2010 – April 2013	**Technical Specialist** bei Tosoh Bioscience GmbH Applikationsentwicklung Technische Kundenbetreuung vor Ort, via Telefon und Email (EMEA)
Oktober 2006-März 2012	**Diplomstudium der Technischen Biologie** an der Universität Stuttgart. Thema der Diplomarbeit: „Gemischte Elektrolyte in der HIC zur mAb Aufreinigung“. Abschluss mit der Gesamtnote „mit Auszeichnung bestanden“.
April 2009 – Mai 2010	**Wissenschaftliche Hilfskraft** bei Tosoh Bioscience GmbH Unterstützung der technischen Abteilung bei Applikationsaufgaben und der Testung von reklamierten Produkten
November 2008 – Dezember 2008	**Wissenschaftliche Hilfskraft** am Institut für Zoologie der Universität Stuttgart. Filtration von Protozoen Kulturen und Herstellung von Medien.

Schulbildung

1997-2006	Besuch des Max-Planck-Gymnasiums Böblingen mit Abschluss des Abiturs (Note 1,2). Preise der Gesellschaft Deutscher Chemiker und der Scheffel Stiftung für Literatur
1991-1997	Besuch der Johann-Bruecker Grundschule Schönaich

Sprachen

Deutsch (Muttersprache)

Englisch (verhandlungssicher)
Französisch (Grundkenntnisse)
Spanisch (Grundkenntnisse)

Darmstadt, 01.07.2016

Judith Vajda